Universidade do Minho
Escola de Engenharia

Marina Inês Martins Santos

Cellular Aproaches and Tailor-Made 3D Starch-Based Scaffolds for Improved Vascularization in Bone Tissue Engineering Strategies

Janeiro de 2009

Cellular Aproaches and Tailor-Made 3D Starch-Based Scaffolds for Improved Vascularization in Bone Tissue Engineering Strategies

Marina Inês Martins Santos

UMinho | 2009

Universidade do Minho
Escola de Engenharia

Marina Inês Martins Santos

Cellular Aproaches and Tailor-Made 3D Starch-Based Scaffolds for Improved Vascularization in Bone Tissue Engineering Strategies

Tese de Doutoramento em Engenharia Biológica

Trabalho efectuado sob a orientação do
Professor Rui L. Reis
e do
Professor C. James Kirpaprick

Janeiro de 2009

Universidade do Minho, ___/___/_____

Assinatura: _____

To my parents

ACKNOWLEDGMENTS

I would like to start by acknowledging my supervisor Prof. Rui Reis for believing in me and my capability to pursue such an exciting project. Also, I am thankful for his vision of a PhD course as a period that should not be limited to learning new techniques or acquiring and analysing data but as a time to widen skills, broaden our horizons and to find ourselves. In sum, thank you for preparing me for the future and for providing me with the weapons to fight in the scientific arena.

I am deeply grateful to Prof. Kirkpatrick for accepting to be my co-supervisor and for the warm way he received and integrated me in his team. His positive attitude and enthusiasm were crucial to keep me grounded and focused during this journey.

To Ron, my friend and mentor, I want to express my gratitude for the enjoyable scientific discussions and for the support all these years. Be sure that whenever I plan an experiment I will always keep in mind your advice “baby steps”.

I am grateful to the Portuguese Foundation for Science and Technology for the financial support through a PhD grant (SFRH/BD/13428/2003).

Thank you Kadrus for your friendship and for the great teacher that you are. In the lab you taught me how it is possible to make a perfect match between creativity and science and in life your lessons of strength and determination were a source of inspiration that marked me profoundly.

To my dear friend Gabi who since the very first day of this PhD course has always been able to put me on track. Regardless of the geographic distance and time zone she was always present with her advices, encouragement words and tireless listening. Thank you for keeping my motivation and balance during the most important moments.

To my colleagues in 3B's my word of appreciation for sharing all these 5 years their knowledge, space and time with me. To MT team who always found room to assist me whenever I needed, though they were confined to a few square meters.

To Ana Martins, Simone and Jonny my friends from the times where 3B's was still a nano lab (i.e. with less than 20 researchers) thanks for accompanying me on this journey. To Iva I am thankful for your warm words in crisis moments, and for accompanying me in a short but profitable journey into the deepness of the chemistry underworld. To Rui Amandi and Ana Leite I want to acknowledge their friendship and encouragement. A very special word of appreciation to José Vitor who although speaks a different language always finds a way to support and help me.

To my colleagues in Mainz, I would like to acknowledge all their efforts to make me feel at home. To Frau Müller, Meyer and Molter thank you for your excellent technical support in TEM and SEM. A special thanks to Anne and Barbara for the great teachers and friends they are and for their endless patience to answer all my questions. Mädchen, vielen dank für alle!

My stay in Mainz was also extremely precious due to the friends that I made. To Roman, Susana, Vitor, Hwei Ling, Despina, Massimo, Nuno, Despina and Andrea I acknowledge all the moments we shared. I am also particularly thankful to Sérgio for the immense generosity with which he opened the doors of his house to me.

To my old friends Marta, Filipe, Ana Lúcia and Luís who have always been by my side. To Nuno, who along these 24 years of friendship has celebrated with me my achievements and gave me strength in the hardest moments. Thank you for your unconditional and timeless friendship.

Last, but definitely not least I want to acknowledge my parents. Just saying that they believed and bet in me would not be fair. In fact, they made much more, they made the impossible, and they made me believe in myself.

CELLULAR APPROACHES AND TAILOR-MADE 3D STARCH-BASED SCAFFOLDS FOR IMPROVED VASCULARIZATION IN BONE TISSUE ENGINEERING STRATEGIES

ABSTRACT

The establishment of a vascular supply in bone grafts is presently identified as the main pitfall in bone tissue engineering and the major hurdle for the clinical application of the engineered constructs. Granted the importance of intraosseous vasculature in bone physiological processes, the existence of a microcirculation is not only essential to assure cell survival in strategies that involve cell seeding but also on all the other approaches aimed at bone tissue formation. This is particularly critical in the regeneration of large bone defects because in these cases diffusion can not assure the metabolic demands of the cells and post-implantation vascularization is a slow and insufficient process to assure the success of the implant. The recognition of the aforementioned problem urged the development of strategies to induce and accelerate the formation of a blood vessel network to simultaneously supply the implant and functionally connect to the host vasculature.

The research work described in this thesis addresses strategies to augment vascularization on different formulations of starch poly(ε-caprolactone) (SPCL) fiber-mesh scaffold, a biodegradable material previously proposed for bone regeneration.

Endothelial cells (ECs) are the key element in angiogenesis. Vascularization strategies either directly or indirectly target this cell type. Thus, the first part of this thesis aimed to build a body of evidence regarding the compatibility of ECs and SPCL fiber-mesh scaffolds and the effect of surface and architectural modifications on ECs' biology. In chapter III, ECs derived from the macro- and microvasculature are shown to adhere and proliferate on SPCL fiber-mesh scaffolds. Furthermore, seeded cells not only expressed the most typical endothelial marker von Willebrand factor (vWF) but also maintained cell-cell contact through the expression of Platelet/Endothelial Cell Adhesion Molecule 1 (PECAM-1). ECs are also known to participate in inflammatory response and regarding this role, cells on scaffolding material were sensitive to a pro-inflammatory stimulus, as shown by the induction of the expression of the cell adhesion molecules. Despite the fact that these results indicate a good interaction between cell and substrate, the adhesion of ECs to the scaffold material was dependent on a pre-coating with fibronectin.

Chapter IV consisted in the development of strategies for the surface modification of SPCL fiber-mesh scaffold in order to promote the adhesion of ECs independently of protein coating of the scaffold. Argon (Ar) plasma revealed itself to be a very effective methodology for the proposed task. Hence, plasma modified scaffolds could successfully sustain ECs' growth, proliferation, maintenance of endothelial monolayer integrity and the expression of endothelial markers. This

improved overall biological outcome was the reflex of the novel surface properties and their interaction with adsorbed adhesive proteins that ultimately modulated cell behaviour.

The next two chapters V and VI focused on the innovative designs of SPCL fiber-mesh scaffolds inspired in the extracellular matrix (ECM). This was achieved by means of combining in the same 3D structure a nano-network with a micro-fiber mesh. It was hypothesized that the nano-network on nano/micro fiber-combined scaffold might favour the 3D guidance and distribution of ECs and might thus accelerate vascularization of the implanted constructs. In chapter V it was observed that addition of nano-fibers to the structure improved the spatial distribution of ECs in the bulk structure of the scaffold. This finding, together with the formation of microcapillary-like structures in an angiogenic environment, provided evidence of the ability of these structures to provide the structural and organizational stability necessary for ECs migration.

Chapter VI described the development and characterization of collagen-nano and SPCL-micro fiber-combined scaffold, a structure similar to the one described in the previous chapter but with a built-in nano-network made of type I collagen. This combined structure incorporating the major structural protein of bone matrix was developed by a two-step methodology consisting in wet-spinning followed by type I collagen electrospinning. The structural merit of this scaffolding material was evaluated by monocultures of osteoblast-like cells (SaOs-2) and human umbilical vein ECs (HUVECs). In the case of SaOs-2 it was observed increased proliferation and a different rearrangement of cell cytoskeleton on the nano-fibers, whereas HUVECs exhibited a peculiar organization in circular structures resembling the shape of microcapillary-like structures.

The last chapter (chapter VII) presents the outcome of a complex cellular strategy consisting in the simultaneous culture of primary human osteoblasts (hOBs) with ECs derived from the microvasculature (HDMECs). It was successfully demonstrated that co-culturing hOBs with HDMEC on SPCL fiber-mesh scaffold resulted in the formation of microcapillary-like structures. The existence of branching, lumen and type IV collagen positive-staining in the perivascular region attested the complexity of the formed vascular structures. The mechanisms that supported and orchestrated this system comprised the dense matrix of type I collagen deposited by hOBs that provided the physical and chemical cues for migrating HDMECs; and the HDMEC:hOBs communication though the soluble factor vascular endothelial growth factor (VEGF) and by direct contact through the expression of the gap junction protein connexin43.

In summary, the results reported in this thesis provide insights that can be used in the successful establishment of a vascular network in 3D starch-based scaffolding materials aimed at bone regeneration.

ESTRATÉGIAS CELULARES E ADEQUAÇÃO DE SUPORTES 3D À BASE DE AMIDO PARA A MELHORIA DA VASCULARIZAÇÃO EM ENGENHARIA DE TECIDOS ÓSSEOS

RESUMO

Actualmente é reconhecido que o principal obstáculo em engenharia de tecidos ósseos e à aplicação clínica dos seus produtos é o suprimento vascular dos implantes ósseos. Dada a importância da vasculatura intraóssea nos processos fisiológicos do osso, a existência de uma microcirculação é não só essencial para garantir a sobrevivência das células em estratégias que envolvam o seu cultivo, como em qualquer outra que vise a formação deste tipo de tecido. Esta questão é principalmente importante na regeneração de grandes defeitos ósseos, uma vez que nestes casos a difusão não consegue assegurar as necessidades metabólicas das células e a vascularização pós-implantação é um processo lento e insuficiente para garantir a viabilidade do implante. O reconhecimento deste problema levou ao desenvolvimento de estratégias para induzir e acelerar a formação de uma rede de vasos sanguíneos, que simultaneamente abasteça o implante e que garanta a ligação funcional à vasculatura do paciente.

O trabalho descrito nesta tese reporta a estratégias para aumentar a vascularização em diferentes formulações de um suporte à base de fibras de amido/policaprolactona (SPCL), um material biodegradável previamente proposto para regeneração óssea.

As células endoteliais são o elemento chave no processo de angiogénese. As estratégias de vascularização têm directa ou indirectamente este tipo celular como alvo. Assim, a primeira parte desta tese teve como objectivo reunir um conjunto de elementos relativos à compatibilidade das células endoteliais com o suporte de SPCL e o efeito das modificações superficiais e arquitectónicas na biologia destas mesmas células. No capítulo III prova-se que as células endoteliais originadas da micro- e macrovasculaturas aderem e proliferam nos suportes de SPCL. Para além desta evidência as células não só expressaram o marcador endotelial mais típico (factor von Willebrand, vWF), como também expressaram a molécula de adesão PECAM-1, sinónimo de coesão celular. As células endoteliais também são conhecidas pela sua participação na resposta inflamatória, e relativamente a esta função as células no suporte tridimensional revelaram-se sensíveis a um estímulo pró-inflamatório, como observado pela indução da expressão das moléculas de adesão celular. Apesar destes resultados indicarem uma interacção células-substrato favorável, a adesão das células endoteliais ao material polimérico estava dependente de um pré-revestimento com fibronectina.

O capítulo IV consistiu na modificação superficial do suporte de SPCL com o intuito de promover a adesão das células endoteliais independentemente do revestimento proteico. O plasma de árgon (Ar) provou ser uma metodologia eficaz para evitar esta dependência. Assim sendo, os

suportes 3D modificados por plasma puderam suportar eficientemente o crescimento celular das células endoteliais, proliferação, a manutenção da integridade da monocamada endotelial e a expressão dos respectivos marcadores. Este resultado foi o reflexo das novas propriedades de superfície e da sua interacção com as proteínas adesivas adsorvidas, que, por sua vez modulam o comportamento celular.

Os dois capítulos seguintes incidiram nos designs inovadores dos suportes de SPCL, inspirados na matrix extracelular (ECM). Estes resultaram da combinação na mesma estrutura 3D de uma rede-nano com uma malha de micro-fibras. Foi sugerido que esta rede-nano poderia favorecer a orientação 3D e a distribuição das células endoteliais e desta forma acelerar a vascularização do implante. No capítulo V, observou-se que a adição das nano-fibras à estrutura 3D melhorou a distribuição espacial das células endoteliais dentro do suporte polimérico. Este facto, juntamente com a formação em ambiente angiogénico de estruturas similares a microcapilares, forneceu a prova da capacidade deste tipo de estruturas poliméricas em proporcionar a estabilidade estrutural e organizacional para a migração das células endoteliais.

O capítulo VI descreveu o desenvolvimento e caracterização de um suporte combinando nano-fibras de colagénio com uma malha de micro-fibras SPCL. Esta estrutura é similar à descrita no capítulo anterior (capítulo V), mas em que a rede-nano incorporada é composta por colagénio tipo I. Esta estrutura combinada, incorporando a principal proteína da matriz óssea foi conseguida por uma metodologia de dois passos consistindo em "wet-spinning" seguido de "eletrospinning" de colagénio. O desempenho deste material foi avaliado com monoculturas de osteoblastos (SaOs-2) e células endoteliais isoladas da veia do cordão umbilical (HUVEC). Nas células SaOs-2 verificou-se o aumento da proliferação e um rearranjo diferente do citoesqueleto nas nano-fibras, enquanto que as HUVECs curiosamente exibiram uma organização em estruturas circulares semelhantes à forma das estruturas microcapilares.

O último capítulo (capítulo VII) apresenta o resultado de uma estratégia celular complexa consistindo na cultura simultânea de osteoblastos humanos (hOBs) com células endoteliais derivadas da microvasculatura (HDMECs). Provou-se com sucesso que o co-cultivo de hOBs com HDMECs nos suportes de SPCL resultou na formação de estruturas microcapilares. A existência de ramificação, lúmen e da marcação positiva para colagénio tipo IV na região perivascular confirmou a complexidade das estruturas vasculares formadas. Os mecanismos que suportaram e orquestraram este sistema incluem a densa matriz de colagénio tipo I depositada pelos hOBs e que providenciou o suporte físico-químico para a migração das HDMECs; e a comunicação HDMEC:hOBs através do factor de crescimento do endotélio vascular (VEGF) e pelo contacto directo através da expressão da proteína de junção connexina-43.

Em suma, os resultados apresentados nesta tese fornecem elementos importantes que poderão ser usados na implementação de uma rede vascular em estruturas 3D à base de amido usadas na regeneração óssea.

TABLE OF CONTENTS

LIST OF ABBREVIATIONS

2D	Two dimensional
2PP	Two-photon polymerization
3D	three dimensional
AFM	Atomic force microscopy
ALP	Alkaline phosphatase
Ar	argon
BMP-2	Bone morphogenic protein-2
BMP7	Bone morphogenic protein 7
BMU	Bone multicellular units
CAD/CAM	Computer-aided design/computer aided manufacturing
CLSM	Confocal laser scanning microscopy
Connexin-43	Cx43
DAB	3,3'-diaminobenzidine
DMF	dimethylformamide
ECGS	Endothelial cell growth supplement
ECM	Extracellular matrix
ECs	endothelial cells
ELISA	Enzye-linked immunosorbent assay
EPCs	Endothelial progenitor cells
ET-1	Endothelin-1
FCS	Fetal calf serum
FGF	Fibroblast growth factor
FGF-2	Fibroblast growth factor -2
Fn	Fibronectin
GAPDH	glyceraldehyde-3-phosphate dehydrogenase
HA	hydroxyapatite
hBMSCs	Human bone marrow mesenchymal stem cells
HDMEC	Human dermal microvascular endothelial cell
HFP	1,1,1,3,3,3-hexafluoro-2-propanol
HIF-1	Hypoxia-inducible factor-1
hOBs	Primary human osteoblasts
HUVEC	Human umbilical vein endothelial cell
ICAM-1	Intercellular adhesion molecule-1
IGF	Insulin growth factor
LPS	lipopolysaccharide
MMP-2	Matrix metalloproteinase-2
MMP-8	Matrix metalloproteinase-8
MSCs	Mesenchymal stem cells

MTS	3-(4,5-dimethylthiazol-2-yl)-5-(3-carboxymetyhoxyphenyl)-2(4-sulfophenyl)- 2H tetrazolium
NADPH	**nicotinamide adenosine dinucleotide phosphate**
OECs	**Outgrowth endothelial cells**
PBS	**Phosphate buffered saline**
PCL	polycaprolactone
PCL-HA	Polycaprolactone-hyroxiapatite
PCR	Polymerase chain reaction
PDGF-BB	Platelet-derived growth factor BB
PDMS	Poly(dimethyl siloxane)
PECAM-1	Platelet/endothelial cell adhesion molecule-1
Pen/strep	Penicillin/streptomycin
PGA	Polyglycolic acid
PGA-PLLA	polyglycolic acid-poly-L-lactic acid
PGS	Poly(glycerol sebacate)
PIPAAm	Poly(N-isopropylacrylamide)
PLGA	Poly(lactide-co-glycolide)
RANKL	**Receptor activator for nuclear factor kappa B ligand**
RT	Room temperature
S1P	**Sphingosine 1-phosphate**
SEM	Scanning electron microscopy
SMCs	Smooth muscle cells
SPCL	Blend of corn starch/poly(ε-caprolactone)
SU8	Epoxy-based polymer
TCP	**Tissue culture polystyrene**
TEM	Transmission electron microscopy
TGF	Transforming growth factor
TGF-β1	Transforming growth factor β1
TOF-SIMS	Time-of-flight secondary ion mass spectroscopy
UA	**Poly(urethane acrylate)**
VCAM	**Vascular cell adhesion molecule**
VE-cadherin	Vascular endothelial-cadherin
VEGF	Vascular endothelial growth factor
VEGFR1	vascular endothelial growth factor receptor 1
VEGFR2	vascular endothelial growth factor receptor 2
Vn	Vitronectin
VSI	Vertical scanning interferometry
vWF	Von Willebrand factor
XPS	**X-ray photoelectron spectroscopy**
μCT	**Micro computed tomography**

LIST OF FIGURES

CHAPTER I.

Vascularization in Bone Tissue Engineering: Hurdles, Physiology, Strategies and Future Challenges

CHAPTER III.

Response of micro- and macrovascular endothelial cells to starch-based fiber meshes for bone tissue engineering

CHAPTER IV.

Surface-Modified 3D Starch-based Scaffold for Improved Endothelialization for Bone Tissue Engineering

CHAPTER V.

Endothelial Cell Colonization and Angiogenic Potential of Combined Nano- and Micro-fibrous Scaffolds for Bone Tissue Engineering

CHAPTER VI.

Design of Nano- and Micro-fiber Combined Scaffolds by Electrospinning of Collagen onto Starch-based Fiber Meshes: A Man-made Equivalent of Natural ECM

CHAPTER VII.

Cellular Crosstalk on Biomaterials as a Strategy for Bone Vascularization: Co-culture of Human Endothelial cells and Osteoblasts on a Starch-based Scaffold

LIST OF TABLES

CHAPTER I.

Vascularization in Bone Tissue Engineering: Hurdles, Physiology, Strategies and Future Challenges

CHAPTER II.

Materials and Methods

CHAPTER III.

Response of micro- and macrovascular endothelial cells to starch-based fiber meshes for bone tissue engineering

CHAPTER IV.

Surface-Modified 3D Starch-based Scaffold for Improved Endothelialization for Bone Tissue Engineering

CHAPTER VII.

Cellular Crosstalk on Biomaterials as a Strategy for Bone Vascularization: Co-culture of Human Endothelial cells and Osteoblasts on a Starch-based Scaffold

SHORT *CURRICULUM VITAE*

Marina Santos was born in 1980 in Miragaia, Portugal. She has been a researcher at the 3B's Research Group - Biomaterials, Biodegradables and Biomimetics, since June 2003.

Regarding her background she has a BSc in Applied Biology from University of Minho. During these 5 years in 3B's Research Group she has been working in a new research line devoted to the development of strategies to augment vascularization in bone tissue-engineered constructs. The research work was developed in collaboration with the Institute of Pathology, Johannes-Gutenberg University, Germany, under the supervision of Prof. C.J. Kirkpatrick. A total period of 2 years was spent in this institution, which is also one of the partners of the European STREP Project HIPPOCRATES (FP6).
Furthermore, during PhD course she also integrated interdisciplinary teams involved in writing proposals for the 6th and 7th Framework Programme. Of special remark was the project "*Bio-inspired 3rd generation highly porous scaffolds and hydrogels to produce vascularized engineer bone*" (call NMP-2007-2.3-1) where she was informally involved in leading the team responsible for the proposal preparation.

As a result of her research work, Marina Santos has attended the most relevant conferences in her research field. Presently, she is the author of 9 papers in international refereed journals (4 submitted, 2 *in press* and 3 published), 2 book chapters and 18 abstracts in international conference proceedings.

.

LIST OF PUBLICATIONS

This thesis is based on the following publications:

PAPERS IN INTERNATIONAL REFEREED JOURNALS:

1. **M.I. Santos**, R.L. Reis. "Vascularization in Bone Tissue Engineering: Physiology, Current Strategies, Major Hurdles and Future Challenges". (2008), review paper, *submitted.*

2. **M.I. Santos**, R.E. Unger, R.A. Sousa, R.L. Reis, C.J. Kirkpatrick. "Cellular Crosstalk on Biomaterials as a Strategy for Bone Vascularization: Co-culture on a Starch-based Scaffold", (2008), *submitted*.

3. K. Tuzlakoglu*, **M.I. Santos***, Nuno Neves, R. L. Reis**.** "Design of Nano- and Micro-fiber Combined Scaffolds by Electrospinning of Collagen onto Starch-based Fiber Meshes: A Man-made Equivalent of Natural ECM", (2008), *submitted.* (* the authors contributed equally to this work)

4. **M.I. Santos**, I. Pashkuleva, C. Alves, M.E. Gomes, S. Fuchs, R.E. Unger, R.L. Reis, C.J. Kirkpatrick. "Tailoring the Surface of a 3D Starch-based Scaffold for Improved Endothelialization in Bone Tissue Engineering", (2008), *submitted*

5. **M.I. Santos**, K. Tuzlakoglu, S. Fuchs, M.E. Gomes, K. Peters, R.E. Unger, E. Piskin, R.L Reis, C.J. Kirkpatrick. "Nano- and Micro-fiber Combined Scaffolds: An Innovative Design for Improving Endothelial Cell Colonization and Angiogenic Potential in Bone Tissue Engineering Applications", Biomaterials (2008), 29, 4306-4313.

6. M.I. Santos, S. Fuchs, M.E. Gomes, R.E. Unger, R.L. Reis, C.J. Kirkpatrick, "Response of Micro- and Macrovascular Endothelial Cells to Starch-based Fiber Meshes for Bone Tissue Regeneration", Biomaterials (2007), 28, 240-248.

BOOK CHAPTERS

M.I. Santos, R.L. Reis, 2008, "Vascularization strategies in tissue engineering", In Natural-based polymers for biomedical applications, eds. RL Reis, J Mano, N Neves, H Azevedo , AP Marques, ME Gomes, Cambridge, United Kingdom, 761-780.

CONFERENCE PROCEEDINGS

M.I. Santos, R. Unger, R.A. Sousa, R.L. Reis, C.J. Kirkpatrick, "Co-culture system of osteoblasts and endothelial cells, an *in vitro* strategy to enhance vascularization in bone regeneration", Tissue Engineering: Part A, 14: 712.

COMMUNICATIONS IN INTERNATIONAL CONFERENCES

1. M.I. Santos, RE Unger, R.A. Sousa, R.L. Reis, C.J. Kirkpatrick, "Co-culture system of osteoblasts *in vitro* strategy to enhance vascularization in bone regeneration", TERMIS-EU Annual Meeting, Porto, Portugal, June 2008, *oral*

2. K. Tuzlakoglu, **M.I. Santos**, N.M. Neves and R.L. Reis, "A New Scaffod Design Approach to Mimic the Physical and Chemical Structure of Natural Extracellular Matrix", 4th European Symposium on Biopolymers, Kusadasi, Turkey, October 2007, *oral.*

3. K. Tuzlakoglu, **M.I. Santos** , R.A. Sousa, N.M. Neves and R.L. Reis, "Design of nano- and micro-fiber combined scaffolds by electrospinning of collagen onto starch-based

fiber meshes" , 1st Summer School of TERMIS EU, Madeira, Portugal, June 2007, *oral.*

4. K. Tuzlakoglu, **M.I. Santos** , R.A. Sousa, N.M. Neves and R.L. Reis, "Design of nano- and micro-fiber combined scaffolds by electrospinning of collagen onto starch-based fiber meshes", 3rd Marie Curie Cutting-Edge Conference(Biomineralisation of polymeric materials, bioactive biomaterials and biomimetic methodologies). 1st Summer School of TERMIS – EU, Funchal, Madeira, Portugal, June 2007, *oral.*

5. M.I. Santos , I. Pashkuleva, M.E. Gomes, S. Fuchs, R.E. Unger, R.L. Reis and C.J. Kirkpatrick, "Tailoring the Surface of a 3D Starch-based Scaffold for Improved Endothelialization for Bone Tissue Engineering", Annual TERMIS-EU Meeting, Rotterdam, Netherlands, October 2006, *oral.*

6. M.I. Santos , K. Tuzlakoglu, S. Fuchs, K. Peters, R.E. Unger, E. Piskin, R.L. Reis and C.J. Kirkpatrick, "Nano- and Micro-fiber combined Scaffolds: An Architecture Tailored Toward Improving Endothelial Cell Migration in Bone Tissue Engineering Constructs", ESF-EMBO Symposium – Stem Cells in Tissue Engineering, Sant Feliu de Guixols, Spain, October 2006, *oral.*

7. M.I. Santos , K. Tuzlakoglu, M.E. Gomes, S. Fuchs, K. Peters, R.E. Unger, R.L. Reis and C.J. Kirkpatrick, "Nano- and Micro-fiber combined Scaffolds: An Architecture Tailored Toward Improving Endothelial Cell Migration in Bone Tissue Engineering Constructs", Gordon Conference – Endothelial Cell Phenotypes in Health & Disease, Biddford, United States of America, July 2006, *oral.*

8. M.I. Santos , K. Tuzlakoglu, M.E. Gomes, S. Fuchs, R.E. Unger, R.L. Reis and C.J. Kirkpatrick, "Nano- and Micro-fiber Combined Scaffolds: An Innovative Design for Improving Endothelial Cell Migration in Bone Tissue Engineering Approaches", 8th Annual Meeting of Tissue Engineering Society International, (TESI), Shanghai, China, October 2005, *oral.*

9. M.I. Santos , A.M. Martins, S. Fuchs, R.E. Unger, R.L. Reis and C.J. Kirkpatrick, "Endothelialization of Chitosan/Starch Scaffolds with in situ Forming Ability as a New Approach for Bone Tissue Engineering Applications", 19th European Conference of Biomaterials, (ESB), Sorrento, Italy, September 2005, *oral.*

10. M.I. Santos , M.E. Gomes, S. Fuchs, R.E. Unger, O.P. Coutinho, R.L. Reis and C.J. Kirkpatrick, "Assessment of Endothelial Cells Response to Starch-based Fiber-Meshes for Bone Tissue Regeneration", 30th Annual Meeting & Exposition -Society for Biomaterials(SFB), Memphis, United States of America, April 2005, *oral.*

11. M.I. Santos , M.E. Gomes, S. Fuchs, R.E. Unger, O.P. Coutinho, R.L. Reis and C.J. Kirkpatrick, "Response of Human Endothelial Cells to Starch-Based Fiber Meshes", Joint Meeting of the Tissue Engineering Society International and the European Tissue Engineering Society (TESI-ETES), Lausanne, Switzerland, October 2004, *poster*.

CHAPTER I

Vascularization in Bone Tissue Engineering: Physiology, Current Strategies, Major Hurdles and Future Challenges

CHAPTER I

Vascularization in Bone Tissue Engineering: Physiology, Current Strategies, Major Hurdles and Future Challenges *

ABSTRACT

The lack of a functional vascular supply has hampered to a large extent an all range of clinical applications of laboratory "successful" bone tissue engineering strategies. Until now implanted grafts were dependent on post-implant vascularization but this is either a slow process or the formed capillaries are rather unstable, thus jeopardizing graft integration and often leading to its failure. Therefore, it became a major goal for tissue engineering research community the development of strategies that could effectively induce the establishment of a microcirculation in the engineered constructs that is connected to the host supply and on time to assure the survival of seeded cells. Only in this way it might be possible to meet the metabolic demands of the construct and assure a successful post-implantation performance.

In bone physiology angiogenesis is an omnipresent phenomenon that is relevant in every process from bone development, to remodeling and repair. Furthermore, the intimate connection that exists between angiogenesis and osteogenesis gives important clues to the design of bone vascularization strategies. This review addresses the importance and role of vasculature in a bone construct and on bone biology. Moreover, up-to-date research approaches to optimize vascularization outcomes, their principles, limitations and the identification of future challenges in the field are also emphasized.

* This chapter is based on the following publication:

Santos M. I., Reis R.L. Vascularization in Bone Tissue Engineering: Physiology, Current Strategies, Major Hurdles and Future Challenges, review paper, *Submitted.* (2008).

1. VASCULARIZATION: THE HURDLE IN REGENERATION OF ENGINEERED BONE

One of the most explored tissue engineering approaches used for the repair and regeneration of bone defects has been the *in vitro* culture of a three dimensional (3D) scaffolding material seeded with autologous cells, followed by the implantation in the patient from which the cells have been harvest. Despite the enormous potential, this regenerative strategy is generally associated with a major pitfall. When the engineered tissue construct is implanted seeded cells will have limited access to substrate molecules (oxygen, glucose and amino acids) and clearance of products of metabolism (CO_2, lactate and urea) thus impairing cell viability to an extent that limits the utility and success of the engineered tissue [1, 2]. The lack of a functional microvasculature connected to the host blood supply is identified as the culprit for implant failure and currently recognized as the major challenge [3-6] in tissue engineering.

Bone is a metabolically active tissue supplied by an intraosseous vasculature with osteocytes distancing no more than 100 μm from an intact capillary [2, 7, 8]. In the absence of a vascular supply nutrients transport is mainly assured by diffusion, a transport mechanism only efficient over short distances or for tissues with low metabolic activity (e.g. cartilage). Theoretical modeling predicts [2] that a cm thick scaffold without a vascular supply can support 280,000 cells/cm^3 without central necrosis, whereas in native autogenous cancellous bone this value is 1000-fold higher. Diffusion constrains of engineered constructs are already patent during *in vitro* culture in which nutrient transport is only assured to cells on the superficial areas of the scaffold, while those deeper in the construct face nutrient deprivation and ultimately cell death [9, 10]. Therefore, mass transfer in a graft, defined as the in and out movement of molecules, is a phenomenon highly impaired by the thickness of the implant [11]. From the clinical point of view this is an important aspect because the most critical cases in orthopedics, such as those resultant from resection of bone tumors or trauma, originate large skeletal defects. *In vitro* delivery of nutrients to engineered constructs can be further improved with dynamic culture using bioreactor systems [12, 13] however this will in most cases only postpone the problem of mass transfer to the *in vivo* situation.

Upon graft implantation, angiogenesis, i.e., the formation of new blood vessels from pre-existing ones, will occur spontaneously. This vascular response induced by inflammation is part of the wound-healing generated by the host as a response to the ischemia-reperfusion injury formed during surgery [3, 4, 14]. However, capillary networks induced by inflammatory processes are relatively transient in nature and will regress within few weeks [1, 15, 16]. Apart from capillary networks formed during wound healing, neovascularization of the scaffold will occur. Nonetheless, the slow infiltration rate of blood vessels into the scaffold (<1 mm per day) [4, 17] makes it an unsuitable process to vascularize tissues of clinically relevant size.

The challenge following the development of microcirculation in the engineered construct is to connect it to the recipient's systemic circulation, a phenomenon designated as inosculation or anastomose [18]. Inosculation between the recipient and construct vasculature is not an immediate process and may take up to 8 days, leading to ischemia and a hostile environment [19]. Consequently, the spontaneous postimplantation neovascularization from the host is not sufficient to assure implant integration. This generates a need to design new strategies envisioning acceleration of neovascularization.

The focus of the current review is vascularization in the context of bone tissue engineering. It aims to cover the intricate connection between vascularization and bone, starting with the development, moving through remodeling and ending with repair. Furthermore, we will be herein reviewing the most recent strategies proposing to accelerate the establishment of a fully functional vascular network within bone engineered constructs.

2. INTRAOSSEOUS VASCULATURE IN BONE FORMATION, REMODELING AND FRACTURE REPAIR

2.1. Intramembranous and endochondral ossification

Aside from assuring the nutrient transport and removal of waste products, intraosseous vasculature accomplishes other important functions that range from

bone development, to remodeling and fracture repair. Depending on their origin, bone is formed by two distinct modes of ossification: by intramembranous ossification, characteristic of flat bones such as those from skull and clavicle; and by endochondral ossification which is involved in the development of bones from load bearing joints [20, 21]. Despite the differences, the two types of ossification have as a common denominator the pre-requisite of vascularization [22-24]. In intramembranous bone formation there is an invasion of capillaries transporting mesenchymal stem cells that differentiate directly into osteoblasts which deposit bone matrix [21]. Alternatively, in endochondral ossification mesenchymal stem cells differentiate into cartilage, which provides a template for bone morphogenesis [25]. Then, the hypertrophic chondrocytes in the mineralized cartilaginous matrix secret angiogenic growth factors, that promote the invasion of blood vessels bringing along a number of highly specialized cells that will replace the cartilage mold by bone and bone marrow [21, 23]. Vasculature also orchestrates bone formation through the production of growth factors that control the recruitment, proliferation, differentiation, function and/or survival of various cell including bone-forming osteoblasts and bone-resorbing osteoclasts [24]. These bioactive factors are secreted by endothelial cells (ECs), the cell type that forms the inner linning of blood vessels [26-28]. Therefore, angiogenesis not only precedes osteogenesis but is also required for its occurrence [29], and this is accomplished by a combination of factors, including adequate oxygen tension, compression forces, nutrients and growth factors [30].

2.2. Vascular organization of bone

Adult long bone is supplied by four arterial inputs, named according to their location: nutrient artery or diaphyseal, periosteal arteries, metaphyseal arteries and epiphyseal arteries. Nutrient artery, is the largest vessel and responsible for more than 50 % of total blood supply of the long bones [31, 32]. As suggested by the name, periosteal arteries supply periosteum, the membrane that covers the exterior of bones and a rich source of stem cells that has been explored in several

regenerative strategies [29, 33]. Arteries enter the bone trough the respective foramina, transverse the cortex, reach the medullary cavity and then branch to supply the cortical and marrow microcirculations. In cortical bone vessels branch to feed the capillaries in Havers's and Volkmann's canals [34], whereas in marrow, arterial capillaries drain into sinusoids that are low-pressure vascular channels surrounded by a single layer of fenestrated endothelium [35, 36]. Venous blood is drained to the venous central sinus that runs along the middle of the diaphysis and leaves the bone through veins that accompany arteries [32, 34].

2.3. Bone remodeling

Cortical and cancellous bone undergo ceaseless remodeling starting in the 6th week of gestation and continuing along adulthood [8, 34]. Bone remodeling comprises two phases, resorption of pre-existing bone tissue by the osteoclasts, followed by *de novo* bone formation by the osteoblasts [37, 38]. Osteoblasts have a tight control on osteoclast activity thus balancing resorption and bone deposition. When metabolically active, osteoblasts secret osteoprotegerin, an inhibitor of osteoclast activity; whereas the mature osteoblasts loose the ability to produce this molecule and become vulnerable to osteoclast resorption [39]. Blood vessels direct osteoclast precursors to specific areas of bone, i.e., to bone multicellular units (BMU) [20]. These are small compartments composed by osteoblasts, osteoclasts and blood vessels where remodeling takes place [40]. In BMU resorption is initiated when the receptor activator for nuclear factor kappa B ligand (RANKL), secreted by osteoblast, binds to RANK receptors on the osteoclast cell membrane [39, 41]. Meanwhile, bone vessels start the second phase of the process by trafficking osteoprogenitor cells into BMU for the deposition of new bone [38]. The invading vasculature therefore serves as both a reservoir and conduit for the recruitment of essential cell types involved in bone resorption and deposition and it regulates the functional activities of such cells and provides key signals necessary for bone morphogenesis [30]. In summary, alterations of the micro-vascular supply network will ultimately affect the tightly

regulated resorption sequence resulting in a decrease in bone formation, regeneration and repair [20].

2.4. Fracture repair

One of the hallmarks of bone is, upon injury, its capacity to truly regenerate [14], in contrast to soft tissue that heals by forming scar tissue [25]. Fracture repair is a complex regenerative mechanism as evidenced by the distinguishable processes that it involves, such as the immediate response to injury, intramembranous bone formation, endochondral bone formation and bone remodeling [42]. When bone is injured not only skeletal integrity is compromised at the fracture site, but intraosseous vasculature is clearly disrupted [20]. First a hematoma is formed and due to the disruption of oxygen supply the fracture milieu becomes hypoxic. Hypoxia is an important physiological signal in bone repair because it regulates osteoblast production of key modulators that influence ECs proliferation [30], directs cellular differentiation [43] and induces ECs to secret osteogenic growth factors [44, 45]. In the hematoma phase, the first out of four overlapping phases that characterize bone repair, a normal healing response is triggered [46, 47]. The inflammatory response and the hypoxic environment are associated with the release of several growth factors and cytokines that trigger ECs migration and the formation of new capillaries [24, 46]. In fact, reconstruction of intraosseous circulation is one of the earliest events during bone repair [47, 48]. Meanwhile, the hypoxic microenvironment supports the differentiation of mesenchymal stem cells (MSCs) into chondrocytes that stabilize the fracture by cartilage formation, known as internal callus [14]. Then, the periosteum directly undergoes intramembranous bone formation leading to the formation of an external callus. In the next phase, hard callus formation, the internal callus becomes mineralized and forms a hard callus of woven bone. Finally, in the remodeling phase callus is replaced by lamellar bone [46].

External factors such as biomechanical environment also influence bone regenerative process by affecting angiogenesis and consequently cell differentiation [49, 50] . In a fixed fracture the vascular network is rapidly reestablished and healing occurs mainly by intramembranous ossification [49, 50]. Conversely, in an unstable

mechanical environment the spreading capillaries are disrupted and the hypoxic environment promotes the differentiation of chondrocytes that stabilize the fracture by cartilage formation [14]. The lack of angiogenesis is pointed out [49] as one of the main reasons for non-healing bone. For instance, using a rat distraction osteogenesis model Fang et al [51] have shown that the administration of an anti-angiogenic drug prevented normal osteogenesis, which resulted in a fibrous nonunion.

2.5. Heterotypic communication between osteoblasts and endothelial cells

Considering the intricate connection between angiogenesis and osteogenesis processes is not surprising that communication between osteoblasts and ECs is one of the most important cellular interactions orchestrating bone [30, 52]. The cross-talk between osteoblasts and ECs occurs at two levels, by indirect cell contact [53, 54] trough the release of soluble factors with paracrine and autocrine action and by direct cell-cell contact [55] mediated by proteins at gap junctions. One of the most studied growth factors is vascular endothelial growth factor (VEGF) [47, 56, 57], a potent and specific angiogenic cytokine produced at the fracture site by numerous cell types, including osteoblasts. Besides being an EC-specific mitogen, VEGF also induces increased vascular permeability and monocyte migration through endothelial layers [58]. The action of VEGF it is not limited to ECs and there are some studies reporting that osteoblasts also respond to members of VEGF family [59-61]. However a recent study [22] has shed some light on the cellular and molecular mechanisms responsible for controlling VEGF-dependent osteoblast-ECs crosstalk by confirming that VEGF is released predominantly by human osteoblasts and its primary action is via ECs. Another angiogenic growth factor, fibroblast growth factor (FGF) is also produced by osteoblasts among other cell types [62, 63]. FGF functions as a paracrine factor stimulating ECs proliferation and migration [63] and as an autocrine factor inducing the proliferation and differentiation of osteoblasts [20]. Furthermore, FGF-2 exerts its angiogenic effect indirectly by modulating VEGF expression through osteoblasts [64]. Once the crosstalk between ECs and osteoblasts is bidirectional, ECs also secret numerous regulatory molecules which exert major effects in

controlling the differentiation and activity of bone-forming cells [30]. Bone morphogenic protein-2 (BMP-2) and endothelin-1 (ET-1) are two of the growth factors produced by ECs that promote osteoblastic proliferation and differentiation [65-67]. In addition, platelet-derived growth factor BB (PDGF-BB) released at the fracture site by several cell types including EC, has a mitogenic and chemotatic effect over osteoblasts [68, 69]. Osteogenic growth factors produced by ECs (BMP-2, PDGF-BB) and by osteoblasts (insulin-like growth factor, IGF and transforming growth factor, TGF) also have an angiogenic effect by inducing VEGF mRNA expression in osteoblasts [68, 70-72]. Nevertheless, Veillette et al [73] proposed an inhibitory role of ET-1 on VEGF synthesis in osteoblastic cells as a feedback mechanism in the temporal and spatial coupling of angiogenesis to bone formation and resorption.

External factors such as the hypoxic microenvironment of fracture healing stimulate the expression of a variety of cytokines from inflammatory cells, ECs, osteoblasts and fibroblasts [74]. ECs and osteoblasts respond to hypoxia by upregulating the expression of numerous osteogenic factors (ET-1, PDGF-BB, BMP-2, IGF-II and TGF-β1) and of the angiogenic growth factor VEGF [66, 74-78]. The mechanism underlying cells' response to the hypoxic microenvironment is primarily mediated through genes whose expression contain a hypoxia-inducible factor-1 (HIF-1) binding site [79, 80]. Nevertheless, it has been reported [74, 77, 81] that this environment of low oxygen tension has no effect on the expression of growth factors such as FGF-2 and members of IGF and TGF families.

The fact that hypoxia is a driving factor to the creation of a growth factor rich milieu inspired researchers to exploit its potential benefits in engineered tissues. Several studies have addressed oxygen tension as an important variable in optimizing *in vitro* conditions for stem differentiation [82-85], while others [43] have hypothesized that adapting the graft to hypoxia prior to engraftment might induce angiogenesis after implantation. It is obvious that in order to avoid the noxious effects of low oxygen tension culture conditions must be well balanced. While on one hand 48 hours of culture do not have a significant effect on cell death [86], on the other hand long-term cultures will have an inhibitory effect on bone formation partly due to decreased osteoblast proliferation [87].

3. STRATEGIES TO INCREMENT VASCULARIZATION

In order to accelerate the establishment of a functional vascular network in bone engineered tissues several strategies have been proposed (Fig. I.1). The following sections will review the main approaches, their principles, outcomes and limitations.

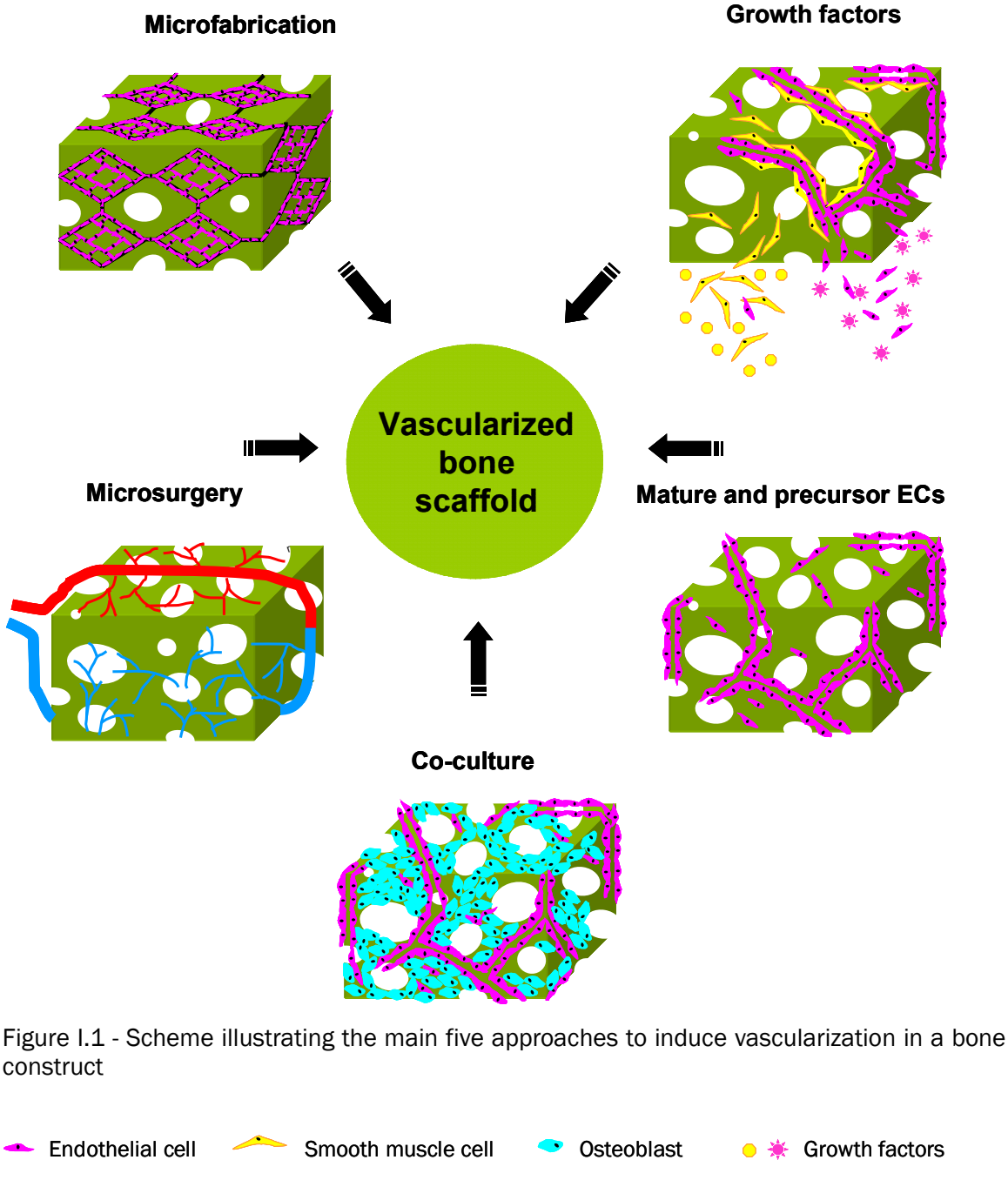

Figure I.1 - Scheme illustrating the main five approaches to induce vascularization in a bone construct

3.1. Scaffolds architecture and microfabrication

Resection of tumors [88, 89], congenital deficiency, trauma or infection [90] are the main pathologies responsible for the loss of large bone segments. Engineering bone must assure the mechanical stability of the osseous defect, while simultaneously stimulating the healing capacity of the tissue. Therefore the vast majority of bone regeneration strategies have been centered on the scaffold material. However, within the last few years a conceptual shift has been taking place in the development of scaffolds for bone engineering, from considering only the role of supporting bone-forming cells to a scaffold that homes a vascular network. On what concerns to the bulk properties of a scaffolding material, porosity has been one of the most discussed issues [91-93] but mainly focusing on osteoblast proliferation, matrix deposition and calcification rather than in penetration of vasculature. Recent work from Narayan et al [94] evaluated the effect of pore size and interpore distance on ECs growth on 3D polymeric scaffolds and found that cell growth was enhanced by smaller pore size (5-20 μm) and lower interpore distance. A similar behaviour was also reported for osteoblasts where *in vitro* lower porosity stimulates osteogenesis by suppressing cell proliferation and forcing cell aggregation [93]. However, the *in vivo* scenario is completely different and higher porosity and pore size result in greater bone ingrowth and vascularization [93, 95]. This is explained by the fact that when implanted scaffolds with smaller pores tend to be hypoxic and this environment will favor chondrogenesis, whether in constructs with larger pores the higher oxygen tension promotes the differentiation of mesenchymal stem cells into osteoblast lineage.

The design and architecture of the scaffold are other features of paramount importance. One example of an innovative architecture is the nano/micro fiber-combined scaffold [96] (Fig. I.2a). This scaffold made from a blend of starch with polycaprolactone (SPCL) [13, 92, 97-99] combines in the same structure micro- and nano-fibers to simultaneously provide the mechanical support for bone repair and to mimic the physical structure of extracellular matrix (ECM). As it will be described later in greater detail, strategies that include seeding ECs on biomaterials and promoting their adhesion, migration and functionality might be a solution for the formation of

vascularized bone. Therefore, the nano-network resembling ECM physical structure on SPCL nano/micro fiber-combined scaffolds was designed with the aim at promoting cell migration, namely ECs, and consequently the establishment of vascular network. Under pro-angiogenic conditions *in vitro*, this nano-network provided the structural and organizational stability for ECs' migration and organization into capillary-like structures [100]. The architecture of nano/micro-fiber-combined scaffolds elicited and guided the 3D distribution of ECs without compromising the structural requirements of a scaffold for bone regeneration. Our group further explored the concept of combined structures and developed a scaffold comprising type I collagen nano-fibers on SPCL fiber-mesh structure [101] (2b). Besides being one of the main constituents of ECM, type I collagen provides chemotactic and haptotactic signals to migrating ECs [102]. Thus, by providing both physical and chemical cues to enhance ECs motility, collagen-nano and SPCL-micro fiber-combined structure might lead to an increase of angiogenic activity.

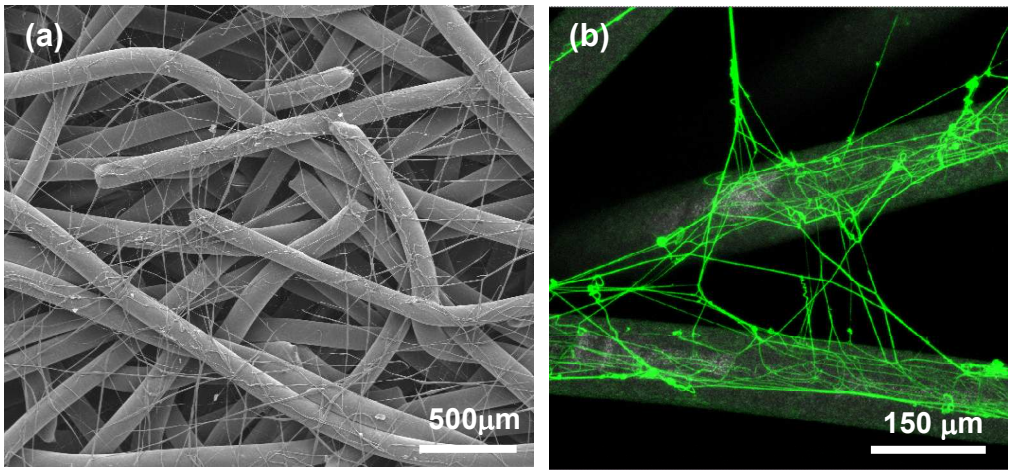

Figure I.2 - The architecture of nano/micro combined structures. These scaffolds comprise two structures: a micro-fiber-mesh to give the mechanical support required during bone repair and a nano-network mimicking ECM that can be made from SPCL (a) or collage I (b). Scanning electron microscopy (SEM) of SPCL nano/micro fiber-combined scaffold (a). Confocal laser scanning microscopy (CLSM) of collagen-nano and SPCL-micro fiber-combined scaffold stained with type I collagen where nano-fibers are depicted in green fluorescence (b).

Another interesting concept is the inclusion of a network with a vascular geometry in a biocompatible polymer. This is achieved for instance by means of using microfabrication techniques that comprise a full range of processes and tools originally developed for applications in the microelectronics, automotive, aerospace and defense fields [103]. Photolitography, a process based on semiconductor waffer technologies has been gathering some attention. This methodology is a two-step process where a mould is first produced, generally made of silica, with an imprinted pattern. Then, by replica-molding the pattern is printed in a biocompatible polymer where the cells will be cultured [104]. The microfabricated pattern can go from aligned microgrooves to a network with vascular geometry and can be incorporated into a biodegradable or non-biodegradable material (table I.1). In order to achieve the best hydrodynamic performance the imprinted network should be made up of multi branches with no more than two vertical nodes in individual branch [105]. Fidkowski et al [106] engineered a microvascular network made of poly(glycerol sebacate) (PGS), a biodegradable and functional *in vivo* elastomer with mechanical properties similar to veins. For that, a capillary network pattern was imprinted in PGS using microfabricated silicon wafers as molds. Then, by seeding the imprinted capillary networks with ECs and perfusing them with culture medium it was possible to obtain a bioengineered microvascular network *in vitro*. Moreover, combining fabrication with the principle of thermoresponsive surfaces it is possible to take the fabrication of artificial networks to a whole new level. By imprinting the capillary pattern in a thermoresponsive poymer it is possible to harvest an EC tubular network that can then be used in the fabrication of 3D vascularized tissue grafts [107]. Unfortunatelly, a drawback of photolitopgraphy is that it is not very effective at creating 3D arquitectures. Recently, a novel Computer-Aided Design/Computer-Aided Manufacturing (CAD/CAM) technology named tow-photon polymerization (2PP) has emerged that allows the fabrication of any computer-designed 3D structure with a structural resolution down to 100 nm from a photosensitive polymer material [108]. 2PP was applied to a photosensitive polymer to successfully produce a microstructure with a shape of microcapillaries [109]. The flexibility of this technology and the ability to precisely define 3D construct geometry holds a great potential to address issues associated with the establishment an intrinsic microcapillary network.

Another CAD/CAM technique used for scaffold production is rapid prototyping [88, 110]. For example, Moroni et al [111] developed 3D fiber deposition, a rapid prototyping tool to create 3D scaffolds with a hollow fiber architecture. Due to their hollow structure these fibers can potentially provide the physical support within the 3D matrice for the formation of a compartimentalized vasculature.

A general remark regarding microfabrication is that these technologies are being mainly applied to the establishment of complex branching vascular tree in soft organs. A hard tissue such as bone has an increased level of complexicity, which demands microfabrication methodologies to be adapted in order to address simultaneously design and mechanical issues. For an excellent review about microfabrication in the context of tissue engineering the readers should for example refer to Borenstein et al [103].

Table I.1. Microfabrication techniques used to engineer structures with vascular geometry. Compiled from references [104, 106-108].

Microfabricated Structure	Substrate	Processing methodology	*In vitro*	Ref
Network with vascular geometry	PGS	Litography	Lumens endothelialized under flow perfusion after 14 days	[106]
Network with vascular geometry	PDMS	Silicon microfabrication and polymer replica molding	HMEC-1 reached confluency after 4 days	[104]
Aligned topographical microridges and microgrooves	UA grafted with PIPAAm	Photolithography and soft lithography	ECs reach confluency within 7 days of culture and at longer (2-3 weeks) form capillary-like tube formation	[107]
Microcapillary structure	SU8	Two-photon polymerization	n.a.	[109]

Abbreviations:

PGS - Poly(glycerol sebacate)

PDMS - Poly(dimethyl siloxane)

UA - Poly(urethane acrylate)

PIPAAm - poly(N-isopropylacrylamide)

SU8 - epoxy-based polymer (photosensitive)

3.2. Angiogenic growth factors

Due to the close association between angiogenesis and osteogenesis angiogenic growth factors are not only implicated in neovascularization but also in endochondral ossification, thus being an important therapeutic agent for bone regeneration [57, 112]. For instance, VEGF the main angiogenic growth factor involved in bone healing has an important role in bone repair by promoting angiogenesis and by stimulating major skeletal cell populations, chondrocytes, osteoblasts and osteoclasts [113]. Current approaches to therapeutic angiogenesis focus on localized and sustained delivery of growth factors [114, 115] rather than on local and systemic bolus injection [116]. Delivery systems permit prolonged exposure of regenerating tissue to low and localized doses of angiogenic factors [114, 115] and thus are superior over bolus injection that are characterized by lack of control over growth factor availability. A great variety of natural [117-123], synthetic [124] and composite materials [125, 126] have been used as delivery matrices for angiogenic growth factors. The localized and sustained delivery of VEGF from a macroporous of biomineralized poly(lactide-co-glycolide) (PLGA) led to simultaneous regeneration of both vascular and bone tissue in a cranium critical defect [126]. A particular case where angiogenic therapy can be applied but with a certain restraint is in defects resulting from the resection of carcinomas that failed to be eliminated with radiation therapy [90]. In these cases not only there is a large segmental loss of bone but also the regenerative capacity of the adjacent tissue is impaired due to vasculature damage by radiation treatment [90, 127]. The work of Kaigler and co-workers [124] addressed this problem by delivering VEGF from PLGA scaffolds in irradiated osseous defects. Although this revealed to be an effective strategy to augment neovascularization and bone regeneration, the use of growth factors in cancer patients might come near to the tenuous line that separates the therapeutic and pathological effects of angiogenic growth factors.

The advances in molecular biology and drug delivery permitted the localized delivery of the gene that codes for the angiogenic molecule of interest. For instance, Tarkka and collaborators [113] have used a first-generation adenoviral vector to deliver

VEGF in a mouse femur defect and reported that the gene transfer induced angiogenesis, improved bone healing and bone mineral content. Another alternative way to promote fracture healing by means of VEGF gene transfer consists in transfecting cells with the gene of interest and thus using them as vectors. When fibroblasts transfected with VEGF were applied to bone defects it was observed complete bridging of new bone, whereas in control (fibroblasts alone) the defects were fibrous and sparsely ossified [128].

One of the most critical and important aspects when designing an angiogenic therapy is the dose of angiogenic growth factor delivered [115, 129]. For instance, blood vessels formed by exposure to high doses of VEGF tend to be malformed and leaky [115]. In addition, one can not disregard that angiogenesis is associated to several pathologic processes such as tumor development, atheroscleosis, and proliferative retinophaties, so there is the risk that a treatment with angiogenic growth factor might exacerbate these processes [130]. Experiments performed by Davies and co-workers [129] shed some more light into the effect of the continued delivery of VEGF concentrations on scaffold vascularization. They reported that the administration of 150 ng/day led to a constant increase in vascularization, even after the cessation of delivery, whereas a 10 time higher concentration induced a transient vessel growth into the porous scaffold.

Recently other molecules with dual action have also been explored. For example, sphingosine 1-phosphate (S1P) is a bioactive phospholipid affecting the proliferation and migration of ECs, smooth muscle cells (SMCs) and osteoblast-like cells. Due to its multiple cellular targets, S1P is an attractive molecule for bone repair and Sefcik et al [131] have evaluated the sustained release of S1P-loaded microsphere-based scaffold in a critical-size cranial defect. Their findings have showed that the sustained delivery of S1P significantly stimulated new bone formation and increased vasculature in the defect site.

Considering that angiogenesis is a multifactor processes involving the interplay of several factors, a way to induce the formation of mature and stable blood vessels includes the administration of multiple growth factors. Kilian et al [132, 133] have explored the potential of enrichment with a non-defined cocktail mixture of growth factors isolated from the platelet fraction aimed to stimulate the formation of new

blood vessels in osseous defects. Using nanoparticulate hydroxyapatite (HA), a neovasculature was formed in the defects independently of the delivery of platelet growth factors. The low affinity of the cytokines to the HA might be a reason to the lack of angiogenic effect of this growth factor cocktail. On the other hand, another work [134] have tested the combined addition of both FGF-2 and VEGF to a collagen-heparin scaffold and have reported the establishment of an early mature vasculature. Growth factors with angiogenic properties can also be part of other multifactorial delivery systems. For instance, the concerted delivery of VEGF, BMP-4 and human bone marrow mesenchymal stem cells (hBMSCs) from biodegradable scaffolds proved to be more effective at promoting bone formation when compared with any single or combination of two factors [135].

However the real turning point in delivery systems from a single growth factor to a dual growth factor delivery technology came with the landmark paper from Richardson and Money et al [136]. They reported a polymeric system that allows the delivery of two or more growth factors with controlled dose and rate of delivery. With the coordinated spatial and temporal presentation of VEGF and PDGF it was possible to obtain a rapid and mature vascular structure [136]. PDGF is the key factor for vessel stabilization because it is responsible for the recruitment of SMCs and pericytes [114, 136]. In sum, an effective and safe angiogenic therapy is not only dependent on the right combination of growth factors delivered but also on a temporal and dose controlled release.

3.3. Mature and precursor endothelial cells

Regardless of the approach adopted to accelerate vascularization all of the strategies will involve ECs directly or indirectly. Hence, in light of the critical role of ECs in the angiogenic process, a necessary step to evaluate and properly predict the vascularization potential of biomaterials is to assess the interaction of ECs with the respective substrate [137-139]. Accordingly, a great number of works have examined different aspects of ECs such as cell attachment, viability, growth and phenotypic/ genotypic expression on different bone substitutes: collagen [140], silk fibroin [141],

polyethersulfone [139], polycaprolactone (PCL) [142], and PLGA [137]. SPCL, a fiber-mesh scaffold a material proposed by our group for bone regeneration [13, 92, 97-99], also revealed to be compatible and a rather good substrate for ECs [138]. However, similar to what was observed in a large number of other polymeric substrates [143-145], in order to sustain ECs adhesion and endothelialization the surface of SPCL fiber-mesh scaffolds required a pre-coating with an adhesive protein [138]. Protein coating has several drawbacks namely the difficulty to control it and its stability over time [146]. In order to overcome this step and to render the surface compatible for ECs, the scaffold was modified with argon (Ar) plasma [147]. The Ar modified scaffolds had a performance comparable with the fibronectin-coated substrate, i.e., the proliferation profile of cultured ECs were similar and the expression of the endothelial markers maintained. Further investigation revealed that the treatment by Ar plasma changed the chemical and physical properties of the substrate and consequently changed the adsorption pattern of the adhesive protein vitronectin.

Alternatively, ECs can be used to engineer a vascular network, in an approach based on the principle that transplanted ECs will interact with host ECs and vasculature, thus establishing a vascular supply much faster. The first line of evidence of construct vascularization due to ECs transplantation came from the work of Holder et al [148]. Polyglycolic acid (PGA) porous matrices seeded with aortic ECs demonstrated organized and unorganized ECs within the matrix and increased numbers of capillaries and lymphatic-like structures relatively to the controls with SMCs and skeletal muscle cells. The feasibility of engineering microvascular network *in vivo* has later been confirmed with ECs derived from the macro- and micro vasculatures [149, 150]. However, Koike et al [6] have shown that in order to obtain stable and durable vascular networks, ECs require co-implantation with perivascular cells. These findings highlight that although mature ECs have the required proliferative and angiogenic activity to create vascular networks *in vivo*, the cooperation between ECs and perivascular cells is fundamental for vascular maturation.

Mature ECs can be isolated from a great variety of sources such as the umbilical cord, skin, fat tissue and saphenous vein but the low availability and proliferation

capacity are the major drawbacks of these cells [151, 152]. There are also other problems associated with mature ECs. On one hand, the senescent state of ECs on larger vessels that can lead to the existence of defective signaling pathways and thus decrease the ability to properly respond to angiogenic growth factors [4, 28]. On the other hand, mature ECs display remarkable phenotypic and genotypic heterogeneity in different tissues and these differences might generate different responses depending on the tissue from where the cells were isolated [27, 28, 153].

An alternative source of autologous ECs to support pro-angiogenic therapies in tissue engineering are endothelial progenitor cells (EPCs). These cells indentified trough the expression of three cell markers (CD133, CD34 and vascular endothelial growth factor receptor 2, VEGFR2) are present in bone marrow, fat tissue and peripheral blood, are able to differentiate into mature ECs and participate in both angiogenesis and vasculogenesis [154, 155]. EPCs occur in low number but when expanded in culture can undergo more than 1000 population doublings, in stark contrast to mature ECs that senesce after 30 population doublings [156].

EPCs are a heterogenous population composed by two cell sub-populations: early-EPC [157] and late-EPCs [157, 158]. As suggested by their name, early-EPCs are the first to appear in culture generally within 4-7 days, share some endothelial but also monocytic characteristics and exhibit a restricted capacity of expansion [157]. In contrast, late-EPCs also known as blood outgrowth ECs (OECs) develop after 2-3 weeks of culture, exhibit cobblestone-like morphology and long term proliferative potential [157, 158]. Regarding the differences and relevance of the different populations of EPCs on vascularization, the work from Yoon et al [159] has highlighted the synergism between EPCs populations during neovascularization. In this work it was shown that the injection of early EPCs ($CD14^+$) and OECs resulted in superior neovascularization *in vivo* relatively to any single-cell-type transplantation. It was suggested that this synergy between EPCs population might be to different contributions, early EPCs may contribute to neovascularization by secretion of cytokines and matrix metalloproteinase-8 (MMP-8), whereas OECs participate by providing building blocks and secreting MMP-2.

The phenotypic stability in culture that characterize OECs [158], has also been demonstrated in 3D matrices. OECs have been used in combination with fibroin silk

fiber meshes for application in tissue engineering and the results showed endothelialization of fibroin silk fiber meshes, maintaining their endothelial characteristics and functions [160]. Furthermore, when embebbed in a wound-healing matrix, OECs migrated from the fibroin scaffolds and formed a microvessel-like network *in vitro*.

EPCs have already been successfully applied in the treatment of fracture healing. Matsumoto and co-workers [161] demonstrated that transplantation of EPCs can be a successful strategy for the treatment of delayed unions. Briefly, EPCs were systemically transplanted and recruited to the osseous fracture by factors present in the healing environment. Once within the fracture site, the transplanted cells enhanced vasculogenesis/angiogenesis and osteogenesis, thus leading to the recovery of the fracture. However, in order to avoid large systemic doses of EPCs and potential side effects [162], later on the same group refined the strategy [163]. For that, EPCs were seeded in the femoral non-union site and mobilized by local delivery of granulocyte colony stimulating factor, hence promoting fracture union.

Similarly, as reported for mature cells, for EPCs to form stable and long-lasting microcapillary structures the construct requires a perivascular component [164, 165]. For instance, it has been found that seeding EPCs in polyglycolic acid-poly-L-lactic acid (PGA-PLLA) preserved the endothelial phenotype but the formation of microvessels *in vitro* was only observed when SMCs were added to the culture [156]. In the same research line, it was reported the formation of functional microvascular beds in immunodeficient mice by co-implantation of EPCs and mesenchymal progenitor cells isolated from blood and bone marrow, respectively [166].

3.4. Co-culture systems

Bone is a complex tissue and this is well present in the multitude of cell populations that make up this tissue. Hence, it is expected that co-culture of heterogenous cell types recreate more closely the *in vivo* environment than single-cell cultures [142, 167]. As previously described, one of the most important heterotypic cross-talks in fracture is the one between ECs and osteoblasts. Many researchers [168-170] have

explored this relationship and have designed strategies to regenerate a vascularized bone construct based on the simultaneous culture of these two cell types. Co-cultures may be applicable to a prevascularization strategy for biomaterials prior to implantation [170] or to a vascularization strategy post-implantation. The co-culture system of ECs and osteoblasts can be used in several ways such in scaffold-free approaches (e.g. spheroids) [168, 171] or in conjunction with 3D scaffolds [172, 173] (table I.2). Furthermore, fully differentiated mature or progenitor cells isolated from several sources can make-up the co-culture system. Although normally ECs and osteoblasts are isolated from different sources, from the clinical point of view it is more practical to obtain the two cell populations from a common cell source as it has being described for adipose tissue and bone marrow [173, 174].

Table I.2 – Co-culture systems for vascularization of bone constructs. Compiled from the references [168-170, 172-179].

Components of co-culture system		Substrate	*In vivo*	Ref
HUVEC	hOBs	Tutobone®	Recruitment of mural cells and anastomose with host vasculature	[175]
HUVEC	hOBs	Polyurethane scaffolds	n.a.	[172]
Cell line HBMEC-60	Bone marrow fibroblasts	PCL scaffold	n.a.	[142]
HDMEC	hOBs or MG-63	Several 3D bone materials	n.a.	[170]
HDMEC	hOBs	SPCL fiber-mesh scaffolds	n.a.	[177]
HUVEC	hOBs	Collagen gel	n.a.	[178]
OECs	hOBs or MG-63	Scaffold-free approach	n.a.	[171]
HUVEC	hMSCs	Scaffold-free approach	Limited anastomose with host vasculature	[168]
Kidney vascular ECs	MSCs	PLGA scaffolds	Neovasculature and bone formation	[179]
EPCs	hOBs	PCL-HA scaffolds	Establishment of capillary network and osteoid formation	[173]
Adipose tissue stromal cells		Porous HA ceramic scaffolds	Formation of ectopic bone tissue and blood vessels connected to host vasculature	[174]

Abbreviations:
Tutobone® – processed bovine cancellous bone
hOBs – primary human osteoblasts
hMSCs – human mesenchymal stem cells
HUVEC – human umbilical vein endothelial cells
HDMEC – human dermal microvascular endothelial cells
EPCs – endothelial progenitor cells
PCL-HA – polycaprolactone-hydroxiapatite

It has been reported by several authors [170, 172, 177] that ECs co-cultured with osteoblasts are able to establish microcapillary-like structures in a 3D scaffold and that these vascular structures are stable in *in vitro* culture for up to 42 days. Furthermore, the complexity of these structures formed by ECs was confirmed by the presence of a patent lumen and by the expression in the perivascular region of type IV collagen, the major constituent of endothelial basement membrane. The great

advantage of this strategy is its self-sustainability, i.e., the interaction between the two cell populations recreates the physical and chemical environment favorable for the formation of vascular-like structures, thus obviating the exogenous supply of angiogenic stimuli. Regarding the mechanisms and factors underlying the cross-talk communication between ECs and osteoblasts it has been shown [170, 177, 180] that osteoblasts in co-culture released higher amounts of the pro-angiogenic factor VEGF than in monoculture. However, not only soluble factors [170] but also molecules from ECM [177, 181] play an important role in the orchestration of co-culture. In agreement with other studies of 2D co-culture [53], our group has shown that co-culture of human dermal microvascular ECs (HDMECs) with osteoblasts on SPCL fiber-mesh scaffold triggered collagen type I mRNA and protein synthesis [177] (Fig. I.3). Hence, collagen type I is a key molecule and modulator in the co-culture system by providing chemical and physical cues for migration and proliferation of ECs. On the other hand, ECs also influence osteoblasts' activity and the up-regulation of alkaline phosphatase expression (ALP) is an indicator of the effect of ECs on osteogenic differentiation [168, 182]. Another major issue in co-culture is the direct cell-cell contact. Interestingly, when conditioned medium from osteoblast was added to ECs or when the two cell types were co-cultured physically separated by a filter, no formation of microcapillary-like structure was observed [170]. Also in support of these findings it has been reported that changes in the expression of several genes in both cell populations were dependent on cell to cell contact and that were not seen in conditioned supernatants [182, 183]. Connexin-43 (Cx43) is pointed out as the gap junction protein that mediates the intracellular exchanges of regulatory ions and small molecules between ECs and osteoblasts [54, 55]. Studies from Villars and co-workers [55] have confirmed the role of this gap junction in this heterotypic communication by showing that its inhibition decreased the effect of human umbilical vein endothelial cell (HUVEC) co-cultures on hBMSC differentiation.

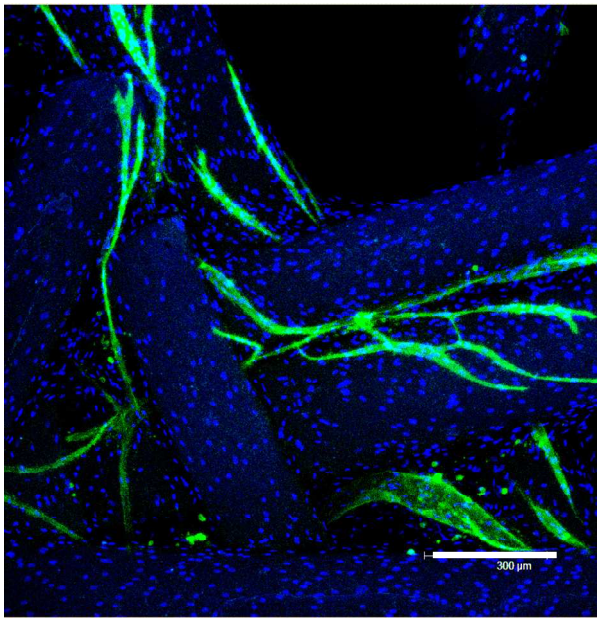

Figure I.3 - Co-culture system of HDMEC and primary osteoblasts on SPCL fiber-mesh scaffold. After 21 days of culture HDMEC organized into microcapillary-like structures with linear and branched forms. In order to distinguish between the two cell populations the sample was stained for CD31 (green fluorescence, endothelial-specific) and nuclei (blue fluorescence, both osteoblasts and HDMECs). The value of the scale bar is 300 µm.

In vitro co-culturing for long-term holds the promise that *in vitro* pre-vascularization might accelerate the establishment of a vascular supply within the implanted scaffold but it remains to be determined whether these pre-formed microcapillary-like structures in the biomaterials are able to link up with the host microvasculature. Another alternative to the *in vitro* establishment of a microcapillary network is to co-culture ECs and osteoblasts in the scaffolding material for short time (hours to few days) followed by implantation. This approach takes advantage of the *in vivo* environment to orchestrate the cellular interaction for the establishment of a functional vasculature. In the work of Yu and co-workers [173] implanted co-culture of EPCs and bone marrow-derived osteoblasts on porous PCL not only improved osteogenesis but also enhanced vascularization that consequently prevented the ischemic necrosis at the center of the graft. In contrast, when the same scaffolding material was seeded with osteoblasts alone impaired osteogenesis accompanied with progressive necrosis of the graft were observed. Steffens et al [175] also reported the formation of vasculature after implanting sub-cutaneously into

immunodificient mice a co-culture of mature ECs and osteoblasts on bovine cancellous bone. Specially worth mentioning was the fact that vasculature was stabilized by recruited mural cells and that the newly vascular networks anatomoed with mouse vasculature.

3.5. Microsurgery strategies

A vascularized graft can be obtained from a hybrid approach combining microsurgery approaches with bone tissue engineering concepts. Biomaterials, osteogenic cells and osteoinductive growth factors have been used for the creation of vascularized bone tissues in combination with the microsurgery approaches: flap fabrication and arteriovenous loop [184]. In flap fabrication the engineered structure relies on extrinsic blood supply, in which vascular ingrowth occurs from the surrounding tissues [185]. It basically consists of a two-stage surgical procedure, where in the first stage the scaffolding material loaded with cells and/or growth factors is implanted into a site of rich vascularization, usually a muscle or the forearm fascia [18, 186]. Capillary ingrowth from recipient site vascularizes the scaffold, and in the second stage the graft is transferred as free bone flap to the defect and by microvascular surgery the vascular pedicle is anastomosed with vessels at the recipient site. Many researchers have tried to develop and explore this concept [187-189]. For instance, the clinical studies performed by Warnke et al [88] took the concept of combining tissue engineering with flap fabrication to a new level. They accomplish mandible reconstruction putting together custom scaffold with bone morphogenetic protein 7 (BMP-7) and patient's bone marrow. Then, the construct was implanted into the lastissimus dorsi muscle for 7 weeks and transferred as a free bone-muscle flap to repair the mandibular defect. The mandible replacement remarkable improved patient's quality of life and retained its function over 13 months, until the death of patient from cardiac arrest [89]. Despite the successful outcome of this approach one can not disregard its drawbacks such as the inconvenience of two surgical interventions and donor-site morbidity in sacrificing the attached muscle [185].

Vascularization of porous matrices can also be accomplished by means of implanting an arteriovenous loop around the construct. The advantages over flap fabrication is that the arteriovenous loop accomplishes vascular growth with minimal fibrosis [186], the construct acquires an inherent perfusion and thus does not need to rely on favorable local conditions [184]. Kneser et al [190] reported the induction of axial vascularization in a processed bovine cancellous bone matrix by means of a microsurgically constructed arteriovenous loop. Additionally, the induction of vascularization in scaffolding material prior to cell injection may help to increase the initial survival and engraftment of transplanted cells and may consecutively optimize bone formation in bioartificial osteogenic bone tissues [191]. The work of Lokmic and co-workers [192] explored this concept and developed a model where an arteriovenous loop is placed in a noncollapsible space protected by a polycarbonate chamber aimed to provide a proper vascularized environment for a successful cell transplantation. They hypothesized that the optimal time point for exogenous cell seeding would be in the period of intense angiogenesis, i.e., 7 to 10 days after implantation. However, there are some drawbacks associated to arteriovenous loop. On one hand there is the technical challenge of loop fabrication and on the other hand the donor site morbidity caused by removal of donor vein graft [3, 19].

4. CONCLUSIONS AND FUTURE CHALLENGES

In the last few years we have observed a shift in the paradigm of bone tissue engineering. The major players have always been osteoblasts and the osteoconductive and/or inductive properties of the biomaterials, and bone vasculature was typically relegated to a secondary and less relevant role. Lately, this scenario has changed when it became clear that the successful clinical outcome of the implanted cell-constructs was dependent on the establishment of a functional tissue. Furthermore, a large body of evidence emerged to highlight the crucial role of intraosseous vasculature in bone development, repair and remodeling. The intricate relation between angiogenesis and osteogenesis has been unveiled and the cross-talk between osteoblasts and ECs was identified as one of the most important

cellular interactions orchestrating bone processes. Several strategies for the acceleration of neovascularization either *in vivo* or *in vitro* have been proposed and explored. As revised in this work, it is possible to establish capillary networks by several approaches: by adding angiogenic growth factors that elicit an angiogenic response *in vivo*; through the seeding of mature and progenitor ECs; by incorporating microcapillary-like structures into the scaffold design that could provide the necessary physical cues for ECs; by exploring the unique relation between ECs and osteoblasts through co-culture systems; and by combining microsurgery techniques with tissue engineering concepts.

Although this great first achievement of establishment of capillary structures on bone constructs, these vascular structures revealed to be unstable and prone to regression. Hence, at the present moment, efforts are mainly centered on stabilizing neovasculature and thus on promoting the formation of long-lasting blood vessels. Perivascular cells such as pericytes and SMCs contribute to the remodeling and maturation of the primitive vascular network and are therefore targets for the construction of durable engineered vasculature. In this line of thought the strategy of dual growth factor delivery encompasses the release of growth factors to promote ECs activity and the recruitment of perivascular cells in separate phases. In addition, it is also expected that the complexity of co-culture systems will be upgraded and tri-cultures encompassing the triad osteoblasts, ECs and mural cells will be the adopted system.

An issue equally important to the establishment of microcirculation in the engineered construct is its anastomose with host circulation. If this connection to recipient's site is not accomplished the all vascularization strategy will be jeopardized. Until now, the existing technology allows the connection to host vasculature of vessels with a minimum diameter of 1mm. The solution is either the establishment of vessels with bigger caliber or the improvement of vascular surgery techniques.

The reconstruction of lesions that involve both vascular and avascular tissue, such as osteochondral defects, raises a new challenge. The regeneration of osteochondral defects implies not only the development of biphasic systems that meet the distinct mechanical/metabolic requirements of bone and cartilage, but also an integrated system that compartimentalizes and limits vascularization to the bone phase.

The take home message is that bone is a multicomponent system and any successful vascularization strategy of bone engineered-construct must be able to recreate all these elements and the intricate network of connections between them. All bone tissue engineering strategies must take that into relevant account or they will be always prone to fail.

REFERENCES

1. Sieminski AL, Gooch KJ. Biomaterial-microvasculature interactions. Biomaterials. 2000; 21(22):2232-41.

2. Muschler GF, Nakamoto C, Griffith LG. Engineering principles of clinical cell-based tissue engineering. J Bone Joint Surg Am. 2004; 86-A(7):1541-58.

3. Cassell OC, Hofer SO, Morrison WA, Knight KR. Vascularisation of tissue-engineered grafts: the regulation of angiogenesis in reconstructive surgery and in disease states. Br J Plast Surg. 2002; 55(8):603-10.

4. Nomi M, Atala A, Coppi PD, Soker S. Principals of neovascularization for tissue engineering. Mol Aspects Med. 2002; 23(6):463-83.

5. Yu H, VandeVord PJ, Mao L, Matthew HW, Wooley PH, Yang SY. Improved tissue-engineered bone regeneration by endothelial cell mediated vascularization. Biomaterials. 2009; 30(4):508-17.

6. Koike N, Fukumura D, Gralla O, Au P, Schechner JS, Jain RK. Tissue engineering: creation of long-lasting blood vessels. Nature. 2004; 428(6979):138-9.

7. Lee SH, Coger RN, Clemens MG. Antioxidant functionality in hepatocytes using the enhanced collagen extracellular matrix under different oxygen tensions. Tissue Engineering. 2006; 12(10):2825-34.

8. Davies JE. Mechanisms of endosseous integration. International Journal of Prosthodontics. 1998; 11(5):391-401.

9. Landman KA, Cai AQ. Cell proliferation and oxygen diffusion in a vascularising scaffold. Bull Math Biol. 2007; 69(7):2405-28.

10. Sachlos E, Czernuszka JT. Making tissue engineering scaffolds work. Review: the application of solid freeform fabrication technology to the production of tissue engineering scaffolds. Eur Cell Mater. 2003; 5:29-39; discussion -40.

11. Oh SH, Ward CL, Atala A, Yoo JJ, Harrison BS. Oxygen generating scaffolds for enhancing engineered tissue survival. Biomaterials. 2009; 30(5):757-62.

12. Volkmer E, Drosse I, Otto S, Stangelmayer A, Stengele M, Kallukalam BC, et al. Hypoxia in static and dynamic 3D culture systems for tissue engineering of bone. Tissue Eng Part A. 2008; 14(8):1331-40.

13. Gomes ME, Sikavitsas VI, Behravesh E, Reis RL, Mikos AG. Effect of flow perfusion on the osteogenic differentiation of bone marrow stromal cells cultured on starch-based three-dimensional scaffolds. J Biomed Mater Res. 2003; 67A(1):87-95.

14. Probst A, Spiegel HU. Cellular mechanisms of bone repair. J Invest Surg. 1997; 10(3):77-86.

15. Greisler HP. Induction of endothelialization of tissue engineered cardiovascular constructs via in vivo angiogenesis in post-implant remodelling. Atherosclerosis Supplements. 2003; 4(2):265-.

16. Arnold F, West DC. Angiogenesis in wound healing. Pharmacol Ther. 1991; 52(3):407-22.

17. Mikos AG, Sarakinos G, Lyman MD, Ingber DE, Vacanti JP, Langer R. Prevascularization of Porous Biodegradable Polymers. Biotechnol Bioeng. 1993; 42(6):716-23.

18. Scheufler O, Schaefer DJ, Jaquiery C, Braccini A, Wendt DJ, Gasser JA, et al. Spatial and temporal patterns of bone formation in ectopically pre-fabricated, autologous cell-based engineered bone flaps in rabbits. Journal of Cellular and Molecular Medicine. 2008; 12(4):1238-49.

19. Lokmic ZM, G. Engineering the Microcirculation. Tissue Engineering: Part B. 2008; 14(1):87-103.

20. Kanczler JM, Oreffo RO. Osteogenesis and angiogenesis: the potential for engineering bone. Eur Cell Mater. 2008; 15:100-14.

21. Chung UI, Kawaguchi H, Takato T, Nakamura K. Distinct osteogenic mechanisms of bones of distinct origins. J Orthop Sci. 2004; 9(4):410-4.

22. Clarkin CE, Emery RJ, Pitsillides AA, Wheeler-Jones CP. Evaluation of VEGF-mediated signaling in primary human cells reveals a paracrine action for VEGF in osteoblast-mediated crosstalk to endothelial cells. J Cell Physiol. 2008; 214(2):537-44.

23. Gerber HP, Ferrara N. Angiogenesis and bone growth. Trends Cardiovasc Med. 2000; 10(5):223-8.

24. Collin-Osdoby P. Role of vascular endothelial cells in bone biology. J Cell Biochem. 1994; 55(3):304-9.

25. Ortega N, Behonick DJ, Werb Z. Matrix remodeling during endochondral ossification. Trends Cell Biol. 2004; 14(2):86-93.

26. Red-Horse K, Crawford Y, Shojaei F, Ferrara N. Endothelium-microenvironment interactions in the developing embryo and in the adult. Dev Cell. 2007; 12(2):181-94.

27. Sumpio BE, Riley JT, Dardik A. Cells in focus: endothelial cell. Int J Biochem Cell Biol. 2002; 34(12):1508-12.

28. Garlanda C, Dejana E. Heterogeneity of endothelial cells. Specific markers. Arterioscler Thromb Vasc Biol. 1997; 17(7):1193-202.

29. McCarthy I. The physiology of bone blood flow: a review. J Bone Joint Surg Am. 2006; 88 Suppl 3:4-9.

30. Brandi ML, Collin-Osdoby P. Vascular biology and the skeleton. J Bone Miner Res. 2006; 21(2):183-92.

31. Trueta J. The Role of the Vessels in Osteogenesis. Journal of Bone and Joint Surgery-British Volume. 1963; 45(2):402-18.

32. Johnson EO, Soultanis K, Soucacos PN. Vascular anatomy and microcirculation of skeletal zones vulnerable to osteonecrosis: vascularization of the femoral head. Orthop Clin North Am. 2004; 35(3):285-91, viii.

33. Hutmacher DW, Sittinger M. Periosteal cells in bone tissue engineering. Tissue Eng. 2003; 9 Suppl 1:S45-64.

34. Laroche M. Intraosseous circulation from physiology to disease. Joint Bone Spine. 2002; 69(3):262-9.

35. Draenert K, Draenert Y. The vascular system of bone marrow. Scan Electron Microsc. 1980; (4):113-22.

36. Wilson A, Trumpp A. Bone-marrow haematopoietic-stem-cell niches. Nat Rev Immunol. 2006; 6(2):93-106.

37. Karsenty G. How many factors are required to remodel bone? Nat Med. 2000; 6(9):970-1.

38. Barou O, Mekraldi S, Vico L, Boivin G, Alexandre C, Lafage-Proust MH. Relationships between trabecular bone remodeling and bone vascularization: A quantitative study. Bone. 2002; 30(4):604-12.

39. Marx RE. Bone and bone graft healing. Oral Maxillofac Surg Clin North Am. 2007; 19(4):455-66, v.

40. Migliorati CA, Casiglia J, Epstein J, Jacobsen PL, Siegel MA, Woo SB. Managing the care of patients with bisphosphonate-associated osteonecrosis: an American Academy of Oral Medicine position paper. J Am Dent Assoc. 2005; 136(12):1658-68.

41. Martin TJ, Seeman E. Bone remodelling: its local regulation and the emergence of bone fragility. Best Pract Res Clin Endocrinol Metab. 2008; 22(5):701-22.

42. Barnes GL, Kostenuik PJ, Gerstenfeld LC, Einhorn TA. Growth factor regulation of fracture repair. J Bone Miner Res. 1999; 14(11):1805-15.

43. Malda J, Klein TJ, Upton Z. The roles of hypoxia in the in vitro engineering of tissues. Tissue Eng. 2007; 13(9):2153-62.

44. Faller DV. Endothelial cell responses to hypoxic stress. Clin Exp Pharmacol Physiol. 1999; 26(1):74-84.

45. Kourembanas S, Hannan RL, Faller DV. Oxygen tension regulates the expression of the platelet-derived growth factor-B chain gene in human endothelial cells. J Clin Invest. 1990; 86(2):670-4.

46. Carano RA, Filvaroff EH. Angiogenesis and bone repair. Drug Discov Today. 2003; 8(21):980-9.

47. Schindeler A, McDonald MM, Bokko P, Little DG. Bone remodeling during fracture repair: The cellular picture. Semin Cell Dev Biol. 2008; 19(5):459-66.

48. Hansen-Algenstaedt N, Joscheck C, Wolfram L, Schaefer C, Muller I, Bottcher A, et al. Sequential changes in vessel formation and microvascular function during bone repair. Acta Orthopaedica. 2006; 77(3):429-39.

49. Ferguson C, Alpern E, Miclau T, Helms JA. Does adult fracture repair recapitulate embryonic skeletal formation? Mechanisms of Development. 1999; 87(1-2):57-66.

50. Le AX, Miclau T, Hu D, Helms JA. Molecular aspects of healing in stabilized and non-stabilized fractures. J Orthop Res. 2001; 19(1):78-84.

51. Fang TD, Salim A, Xia W, Nacamuli RP, Guccione S, Song HM, et al. Angiogenesis is required for successful bone induction during distraction osteogenesis. Journal of Bone and Mineral Research. 2005; 20(7):1114-24.

52. Choi IH, Chung CY, Cho TJ, Yoo WJ. Angiogenesis and mineralization during distraction osteogenesis. J Korean Med Sci. 2002; 17(4):435-47.

53. Villars F, Bordenave L, Bareille R, Amedee J. Effect of human endothelial cells on human bone marrow stromal cell phenotype: role of VEGF? J Cell Biochem. 2000; 79(4):672-85.

54. Guillotin B, Bourget C, Remy-Zolgadri M, Bareille R, Fernandez P, Conrad V, et al. Human primary endothelial cells stimulate human osteoprogenitor cell differentiation. Cell Physiol Biochem. 2004; 14(4-6):325-32.

55. Villars F, Guillotin B, Amedee T, Dutoya S, Bordenave L, Bareille R, et al. Effect of HUVEC on human osteoprogenitor cell differentiation needs heterotypic gap junction communication. Am J Physiol Cell Physiol. 2002; 282(4):C775-85.

56. Spector JA, Mehrara BJ, Greenwald JA, Saadeh PB, Steinbrech DS, Bouletreau PJ, et al. Osteoblast expression of vascular endothelial growth factor is modulated by the extracellular microenvironment. American Journal of Physiology-Cell Physiology. 2001; 280(1):C72-C80.

57. Street J, Bao M, deGuzman L, Bunting S, Peale FV, Jr., Ferrara N, et al. Vascular endothelial growth factor stimulates bone repair by promoting angiogenesis and bone turnover. Proc Natl Acad Sci U S A. 2002; 99(15):9656-61.

58. Stavri GT, Zachary IC, Baskerville PA, Martin JF, Erusalimsky JD. Basic fibroblast growth factor upregulates the expression of vascular endothelial growth factor in vascular smooth muscle cells. Synergistic interaction with hypoxia. Circulation. 1995; 92(1):11-4.

59. Mayr-Wohlfart U, Waltenberger J, Hausser H, Kessler S, Gunther KP, Dehio C, et al. Vascular endothelial growth factor stimulates chemotactic migration of primary human osteoblasts. Bone. 2002; 30(3):472-7.

60. Midy V, Plouet J. Vasculotropin/vascular endothelial growth factor induces differentiation in cultured osteoblasts. Biochem Biophys Res Commun. 1994; 199(1):380-6.

61. Deckers MML, Karperien M, van der Bent C, Yamashita T, Papapoulos SE, Lowik CWGM. Expression of Vascular Endothelial Growth Factors and Their Receptors during Osteoblast Differentiation. Endocrinology. 2000; 141(5):1667-74.

62. Tokuda H, Hirade K, Wang X, Oiso Y, Kozawa O. Involvement of SAPK/JNK in basic fibroblast growth factor-induced vascular endothelial growth factor release in osteoblasts. Journal of Endocrinology. 2003; 177(1):101-7.

63. Collin-Osdoby P, Rothe L, Bekker S, Anderson F, Huang Y, Osdoby P. Basic fibroblast growth factor stimulates osteoclast recruitment, development, and bone pit resorption in association with angiogenesis in vivo on the chick chorioallantoic membrane and activates isolated avian osteoclast resorption in vitro. J Bone Miner Res. 2002; 17(10):1859-71.

64. Saadeh PB, Mehrara BJ, Steinbrech DS, Spector JA, Greenwald JA, Chin GS, et al. Mechanisms of fibroblast growth factor-2 modulation of vascular endothelial growth factor expression by osteoblastic cells. Endocrinology. 2000; 141(6):2075-83.

65. von Schroeder HP, Veillette CJ, Payandeh J, Qureshi A, Heersche JN. Endothelin-1 promotes osteoprogenitor proliferation and differentiation in fetal rat calvarial cell cultures. Bone. 2003; 33(4):673-84.

66. Bouletreau PJ, Warren SM, Spector JA, Peled ZM, Gerrets RP, Greenwald JA, et al. Hypoxia and VEGF up-regulate BMP-2 mRNA and protein expression in microvascular endothelial cells: implications for fracture healing. Plast Reconstr Surg. 2002; 109(7):2384-97.

67. Yamaguchi A, Ishizuya T, Kintou N, Wada Y, Katagiri T, Wozney JM, et al. Effects of BMP-2, BMP-4, and BMP-6 on osteoblastic differentiation of bone marrow-derived stromal cell lines, ST2 and MC3T3-G2/PA6. Biochem Biophys Res Commun. 1996; 220(2):366-71.

68. Bouletreau PJ, Warren SM, Spector JA, Steinbrech DS, Mehrara BJ, Longaker MT. Factors in the fracture microenvironment induce primary osteoblast angiogenic cytokine production. Plastic and Reconstructive Surgery. 2002; 110(1):139-48.

69. Hollinger JO, Hart CE, Hirsch SN, Lynch S, Friedlaender GE. Recombinant human platelet-derived growth factor: biology and clinical applications. J Bone Joint Surg Am. 2008; 90 Suppl 1:48-54.

70. Goad DL, Rubin J, Wang H, Tashjian AH, Jr., Patterson C. Enhanced expression of vascular endothelial growth factor in human SaOS-2 osteoblast-like cells and murine osteoblasts induced by insulin-like growth factor I. Endocrinology. 1996; 137(6):2262-8.

71. Deckers MML, van Bezooijen RL, van der Horst G, Hoogendam J, van der Bent C, Papapoulos SE, et al. Bone Morphogenetic Proteins Stimulate Angiogenesis through Osteoblast-Derived Vascular Endothelial Growth Factor A. Endocrinology. 2002; 143(4):1545-53.

72. Saadeh PB, Mehrara BJ, Steinbrech DS, Dudziak ME, Greenwald JA, Luchs JS, et al. Transforming growth factor-beta 1 modulates the expression of vascular endothelial growth factor by osteoblasts. Am J Physiol Cell Physiol. 1999; 277(4):C628-37.

73. Veillette CJH, von Schroeder HP. Endothelin-1 down-regulates the expression of vascular endothelial growth factor-A associated with osteoprogenitor proliferation and differentiation. Bone. 2004; 34(2):288-96.

74. Warren SM, Steinbrech DS, Mehrara BJ, Saadeh PB, Greenwald JA, Spector JA, et al. Hypoxia regulates osteoblast gene expression. J Surg Res. 2001; 99(1):147-55.

75. Kourembanas S, Marsden PA, McQuillan LP, Faller DV. Hypoxia induces endothelin gene expression and secretion in cultured human endothelium. J Clin Invest. 1991; 88(3):1054-7.

76. Humar R, Kiefer FN, Berns H, Resink TJ, Battegay EJ. Hypoxia enhances vascular cell proliferation and angiogenesis in vitro via rapamycin (mTOR)-dependent signaling. Faseb J. 2002; 16(8):771-80.

77. Steinbrech DS, Mehrara BJ, Saadeh PB, Greenwald JA, Spector JA, Gittes GK, et al. Hypoxia increases insulinlike growth factor gene expression in rat osteoblasts. Ann Plast Surg. 2000; 44(5):529-34; discussion 34-5.

78. Steinbrech DS, Mehrara BJ, Saadeh PB, Chin G, Dudziak ME, Gerrets RP, et al. Hypoxia regulates VEGF expression and cellular proliferation by osteoblasts in vitro. Plast Reconstr Surg. 1999; 104(3):738-47.

79. Minchenko A, Caro J. Regulation of endothelin-1 gene expression in human microvascular endothelial cells by hypoxia and cobalt: role of hypoxia responsive element. Mol Cell Biochem. 2000; 208(1-2):53-62.

80. Peters K, Schmidt H, Unger RE, Kamp G, Prols F, Berger BJ, et al. Paradoxical effects of hypoxia-mimicking divalent cobalt ions in human endothelial cells in vitro. Mol Cell Biochem. 2005; 270(1-2):157-66.

81. Brogi E, Wu T, Namiki A, Isner JM. Indirect angiogenic cytokines upregulate VEGF and bFGF gene expression in vascular smooth muscle cells, whereas hypoxia upregulates VEGF expression only. Circulation. 1994; 90(2):649-52.

82. Xu Y, Malladi P, Chiou M, Bekerman E, Giaccia AJ, Longaker MT. In vitro expansion of adipose-derived adult stromal cells in hypoxia enhances early chondrogenesis. Tissue Eng. 2007; 13(12):2981-93.

83. Hung SC, Pochampally RR, Hsu SC, Sanchez C, Chen SC, Spees J, et al. Short-term exposure of multipotent stromal cells to low oxygen increases their expression of CX3CR1 and CXCR4 and their engraftment in vivo. PLoS ONE. 2007; 2(5):e416.

84. Khan WS, Adesida AB, Hardingham TE. Hypoxic conditions increase hypoxia-inducible transcription factor 2alpha and enhance chondrogenesis in stem cells from the infrapatellar fat pad of osteoarthritis patients. Arthritis Res Ther. 2007; 9(3):R55.

85. Villarruel SM, Boehm CA, Pennington M, Bryan JA, Powell KA, Muschler GF. The effect of oxygen tension on the in vitro assay of human osteoblastic connective tissue progenitor cells. J Orthop Res. 2008; 26(10):1390-7.

86. Potier E, Ferreira E, Meunier A, Sedel L, Logeart-Avramoglou D, Petite H. Prolonged hypoxia concomitant with serum deprivation induces massive human mesenchymal stem cell death. Tissue Eng. 2007; 13(6):1325-31.

87. Utting JC, Robins SP, Brandao-Burch A, Orriss IR, Behar J, Arnett TR. Hypoxia inhibits the growth, differentiation and bone-forming capacity of rat osteoblasts. Exp Cell Res. 2006; 312(10):1693-702.

88. Warnke PH, Springer IN, Wiltfang J, Acil Y, Eufinger H, Wehmoller M, et al. Growth and transplantation of a custom vascularised bone graft in a man. Lancet. 2004; 364(9436):766-70.

89. Warnke PH, Wiltfang J, Springer I, Acil Y, Bolte H, Kosmahl M, et al. Man as living bioreactor: Fate of an exogenously prepared customized tissue-engineered mandible. Biomaterials. 2006; 27(17):3163-7.

90. Bishop AT, Pelzer M. Vascularized bone allotransplantation: current state and implications for future reconstructive surgery. Orthop Clin North Am. 2007; 38(1):109-22, vii.

91. Martins AM, Santos MI, Azevedo HS, Malafaya PB, Reis RL. Natural origin scaffolds with in situ pore forming capability for bone tissue engineering applications. Acta Biomater. 2008.

92. Gomes ME, Holtorf HL, Reis RL, Mikos AG. Influence of the porosity of starch-based fiber mesh scaffolds on the proliferation and osteogenic differentiation of bone marrow stromal cells cultured in a flow perfusion bioreactor. Tissue Eng. 2006; 12(4):801-9.

93. Karageorgiou V, Kaplan D. Porosity of 3D biornaterial scaffolds and osteogenesis. Biomaterials. 2005; 26(27):5474-91.

94. Narayan D, Venkatraman SS. Effect of pore size and interpore distance on endothelial cell growth on polymers. J Biomed Mater Res A. 2008.

95. Bonfield W. Designing porous scaffolds for tissue engineering. Philos Transact A Math Phys Eng Sci. 2006; 364(1838):227-32.

96. Tuzlakoglu K, Bolgen N, Salgado AJ, Gomes ME, Piskin E, Reis RL. Nano- and micro-fiber combined scaffolds: a new architecture for bone tissue engineering. J Mater Sci Mater Med. 2005; 16(12):1099-104.

97. Gomes ME, Azevedo HS, Moreira AR, Ella V, Kellomaki M, Reis RL. Starch-poly(epsilon-caprolactone) and starch-poly(lactic acid) fibre-mesh scaffolds for bone tissue engineering applications: structure, mechanical properties and degradation behaviour. J Tissue Eng Regen Med. 2008; 2(5):243-52.

98. Gomes ME, Bossano CM, Johnston CM, Reis RL, Mikos AG. In vitro localization of bone growth factors in constructs of biodegradable scaffolds seeded with marrow stromal cells and cultured in a flow perfusion bioreactor. Tissue Eng. 2006; 12(1):177-88.

99. Pavlov MP, Mano JF, Neves NM, Reis RL. Fibers and 3D mesh scaffolds from biodegradable starch-based blends: production and characterization. Macromol Biosci. 2004; 4(8):776-84.

100. Santos MI, Tuzlakoglu K, Fuchs S, Gomes ME, Peters K, Unger RE, et al. Endothelial cell colonization and angiogenic potential of combined nano- and micro-fibrous scaffolds for bone tissue engineering. Biomaterials. 2008.

101. Tuzlakoglu K. SMI, Neves N, Reis R. L. Design of Nano- and Micro-fiber Combined Scaffolds by Electrospinning of Collagen onto Starch-based Fiber Meshes: A Man-made Equivalent of Natural ECM. Advanced Functional Materials. 2008; Submitted.

102. Davis GE, Senger DR. Endothelial extracellular matrix: biosynthesis, remodeling, and functions during vascular morphogenesis and neovessel stabilization. Circ Res. 2005; 97(11):1093-107.

103. Borenstein JT, Weinberg EJ, Orrick BK, Sundback C, Kaazempur-Mofrad MR, Vacanti JP. Microfabrication of three-dimensional engineered scaffolds. Tissue Eng. 2007; 13(8):1837-44.

104. Shin M, Matsuda K, Ishii O, Terai H, Kaazempur-Mofrad M, Borenstein J, et al. Endothelialized networks with a vascular geometry in microfabricated poly(dimethyl siloxane). Biomed Microdevices. 2004; 6(4):269-78.

105. Wang GJ, Hsu YF. Structure optimization of microvascular scaffolds. Biomed Microdevices. 2006; 8(1):51-8.

106. Fidkowski C, Kaazempur-Mofrad MR, Borenstein J, Vacanti JP, Langer R, Wang Y. Endothelialized microvasculature based on a biodegradable elastomer. Tissue Eng. 2005; 11(1-2):302-9.

107. Tsuda Y, Yamato M, Kikuchi A, Watanabe M, Chen GP, Takahashi Y, et al. Thermoresponsive microtextured culture surfaces facilitate fabrication of capillary networks. Advanced Materials. 2007; 19(21):3633-+.

108. Ovsianikov A, Ostendorf A, Chichkov BN. Three-dimensional photofabrication with femtosecond lasers for applications in photonics and biomedicine. Applied Surface Science. 2007; 253(15):6599-602.

109. Ovsianikov A, Schlie S, Ngezahayo A, Haverich A, Chichkov BN. Two-photon polymerization technique for microfabrication of CAD-designed 3D scaffolds from commercially available photosensitive materials. J Tissue Eng Regen Med. 2007; 1(6):443-9.

110. Ciocca L, De Crescenzio F, Fantini M, Scotti R. CAD/CAM and rapid prototyped scaffold construction for bone regenerative medicine and surgical transfer of virtual planning: a pilot study. Comput Med Imaging Graph. 2009; 33(1):58-62.

111. Moroni L, Schotel R, Sohier J, de Wijn JR, van Blitterswijk CA. Polymer hollow fiber three-dimensional matrices with controllable cavity and shell thickness. Biomaterials. 2006; 27(35):5918-26.

112. Dai J, Rabie ABM. VEGF: an Essential Mediator of Both Angiogenesis and Endochondral Ossification. J Dent Res. 2007; 86(10):937-50.

113. Tarkka T, Sipola A, Jamsa T, Soini Y, Yla-Herttuala S, Tuukkanen J, et al. Adenoviral VEGF-A gene transfer induces angiogenesis and promotes bone formation in healing osseous tissues. J Gene Med. 2003; 5(7):560-6.

114. Chen RR, Silva EA, Yuen WW, Mooney DJ. Spatio-temporal VEGF and PDGF delivery patterns blood vessel formation and maturation. Pharmaceutical Research. 2007; 24(2):258-64.

115. Zisch AH, Lutolf MP, Hubbell JA. Biopolymeric delivery matrices for angiogenic growth factors. Cardiovasc Pathol. 2003; 12(6):295-310.

116. Takeshita S, Zheng LP, Brogi E, Kearney M, Pu LQ, Bunting S, et al. Therapeutic angiogenesis. A single intraarterial bolus of vascular endothelial growth factor augments revascularization in a rabbit ischemic hind limb model. J Clin Invest. 1994; 93(2):662-70.

117. Elcin YM, Dixit V, Gitnick G. Controlled release of endothelial cell growth factor from chitosan-albumin microspheres for localized angiogenesis: in vitro and in vivo studies. Artif Cells Blood Substit Immobil Biotechnol. 1996; 24(3):257-71.

118. Sakiyama-Elbert SE, Hubbell JA. Development of fibrin derivatives for controlled release of heparin-binding growth factors. Journal of Controlled Release. 2000; 65(3):389-402.

119. Tanihara M, Suzuki Y, Yamamoto E, Noguchi A, Mizushima Y. Sustained release of basic fibroblast growth factor and angiogenesis in a novel covalently crosslinked gel of heparin and alginate. J Biomed Mater Res. 2001; 56(2):216-21.

120. Pieper JS, Hafmans T, van Wachem PB, van Luyn MJ, Brouwer LA, Veerkamp JH, et al. Loading of collagen-heparan sulfate matrices with bFGF promotes angiogenesis and tissue generation in rats. J Biomed Mater Res. 2002; 62(2):185-94.

121. Lee JY, Nam SH, Im SY, Park YJ, Lee YM, Seol YJ, et al. Enhanced bone formation by controlled growth factor delivery from chitosan-based biomaterials. J Control Release. 2002; 78(1-3):187-97.

122. Silva GA, Coutinho OP, Ducheyne P, Shapiro IM, Reis RL. Starch-based microparticles as vehicles for the delivery of active platelet-derived growth factor. Tissue Engineering. 2007; 13(6):1259-68.

123. Malafaya PB, Silva GA, Reis RL. Natural-origin polymers as carriers and scaffolds for biomolecules and cell delivery in tissue engineering applications. Advanced Drug Delivery Reviews. 2007; 59(4-5):207-33.

124. Kaigler D, Wang Z, Horger K, Mooney DJ, Krebsbach PH. VEGF scaffolds enhance angiogenesis and bone regeneration in irradiated osseous defects. J Bone Miner Res. 2006; 21(5):735-44.

125. Silva GA, Costa FJ, Coutinho OP, Radin S, Ducheyne P, Reis RL. Synthesis and evaluation of novel bioactive composite starch/bioactive glass microparticles. J Biomed Mater Res A. 2004; 70A(3):442-9.

126. Murphy WL, Simmons CA, Kaigler D, Mooney DJ. Bone regeneration via a mineral substrate and induced angiogenesis. J Dent Res. 2004; 83(3):204-10.

127. Lerouxel E, Weiss P, Giumelli B, Moreau A, Pilet P, Guicheux J, et al. Injectable calcium phosphate scaffold and bone marrow graft for bone reconstruction in irradiated areas: an experimental study in rats. Biomaterials. 2006; 27(26):4566-72.

128. Li R, Stewart DJ, von Schroeder HP, Mackinnon ES, Schemitsch EH. Effect of cell-based VEGF gene therapy on healing of a segmental bone defect. J Orthop Res. 2008.

129. Davies N, Dobner S, Bezuidenhout D, Schmidt C, Beck M, Zisch AH, et al. The dosage dependence of VEGF stimulation on scaffold neovascularisation. Biomaterials. 2008.

130. Moldovan NI, Ferrari M. Prospects for microtechnology and nanotechnology in bioengineering of replacement microvessels. Arch Pathol Lab Med. 2002; 126(3):320-4.

131. Sefcik LS, Petrie Aronin CE, Wieghaus KA, Botchwey EA. Sustained release of sphingosine 1-phosphate for therapeutic arteriogenesis and bone tissue engineering. Biomaterials. 2008; 29(19):2869-77.

132. Kilian O, Alt V, Heiss C, Jonuleit T, Dingeldein E, Flesch I, et al. New blood vessel formation and expression of VEGF receptors after implantation of platelet growth factor-enriched biodegradable nanocrystalline hydroxyapatite. Growth Factors. 2005; 23(2):125-33.

133. Kilian O, Wenisch S, Karnati S, Baumgart-Vogt E, Hild A, Fuhrmann R, et al. Observations on the microvasculature of bone defects filled with biodegradable nanoparticulate hydroxyapatite. Biomaterials. 2008; 29(24-25):3429-37.

134. Nillesen ST, Geutjes PJ, Wismans R, Schalkwijk J, Daamen WF, van Kuppevelt TH. Increased angiogenesis and blood vessel maturation in acellular collagen-heparin scaffolds containing both FGF2 and VEGF. Biomaterials. 2007; 28(6):1123-31.

135. Huang YC, Kaigler D, Rice KG, Krebsbach PH, Mooney DJ. Combined angiogenic and osteogenic factor delivery enhances bone marrow stromal cell-driven bone regeneration. J Bone Miner Res. 2005; 20(5):848-57.

136. Richardson TP, Peters MC, Ennett AB, Mooney DJ. Polymeric system for dual growth factor delivery. Nat Biotechnol. 2001; 19(11):1029-34.

137. Jabbarzadeh E, Jiang T, Deng M, Nair LS, Khan YM, Laurencin CT. Human endothelial cell growth and phenotypic expression on three dimensional poly(lactide-co-glycolide) sintered microsphere scaffolds for bone tissue engineering. Biotechnol Bioeng. 2007; 98(5):1094-102.

138. Santos MI, Fuchs S, Gomes ME, Unger RE, Reis RL, Kirkpatrick CJ. Response of micro- and macrovascular endothelial cells to starch-based fiber meshes for bone tissue engineering. Biomaterials. 2007; 28(2):240-8.

139. Unger RE, Peters K, Huang Q, Funk A, Paul D, Kirkpatrick CJ. Vascularization and gene regulation of human endothelial cells growing on porous polyethersulfone (PES) hollow fiber membranes. Biomaterials. 2005; 26(17):3461-9.

140. Breithaupt-Faloppa AC, Kleinheinz J, Crivello O, Jr. Endothelial cell reaction on a biological material. J Biomed Mater Res B Appl Biomater. 2006; 76(1):49-55.

141. Unger RE, Peters K, Wolf M, Motta A, Migliaresi C, Kirkpatrick CJ. Endothelialization of a non-woven silk fibroin net for use in tissue engineering: growth and gene regulation of human endothelial cells. Biomaterials. 2004; 25(21):5137-46.

142. Choong CS, Hutmacher DW, Triffitt JT. Co-culture of Bone Marrow Fibroblasts and Endothelial Cells on Modified Polycaprolactone Substrates for Enhanced Potentials in Bone Tissue Engineering. Tissue Eng. 2006.

143. Chu CF, Lu A, Liszkowski M, Sipehia R. Enhanced growth of animal and human endothelial cells on biodegradable polymers. Biochim Biophys Acta. 1999; 1472(3):479-85.

144. Boura C, Muller S, Vautier D, Dumas D, Schaaf P, Claude Voegel J, et al. Endothelial cell--interactions with polyelectrolyte multilayer films. Biomaterials. 2005; 26(22):4568-75.

145. Unger RE, Huang Q, Peters K, Protzer D, Paul D, Kirkpatrick CJ. Growth of human cells on polyethersulfone (PES) hollow fiber membranes. Biomaterials. 2005; 26(14):1877-84.

146. Massia SP, Hubbell JA. Human endothelial cell interactions with surface-coupled adhesion peptides on a nonadhesive glass substrate and two polymeric biomaterials. J Biomed Mater Res. 1991; 25(2):223-42.

147. Santos M.I. PI, Alves C.M, Gomes M.E., Fuchs S, Unger R.E, Reis R.L., Kirkpatrick C.J. . Surface-Modified 3D Starch-based Scaffold for Improved Endothelialization for Bone Tissue Engineering. Journal of Materials Chemistry. 2008; Submitted.

148. Holder WD, Gruber HE, Roland WD, Moore AL, Culberson CR, Loebsack AB, et al. Increased vascularization and heterogeneity of vascular structures occurring in polyglycolide matrices containing aortic endothelial cells implanted in the rat. Tissue Engineering. 1997; 3(2):149-60.

149. Nor JE, Peters MC, Christensen JB, Sutorik MM, Linn S, Khan MK, et al. Engineering and characterization of functional human microvessels in immunodeficient mice. Laboratory Investigation. 2001; 81(4):453-63.

150. Schechner JS, Nath AK, Zheng L, Kluger MS, Hughes CC, Sierra-Honigmann MR, et al. In vivo formation of complex microvessels lined by human endothelial cells in an immunodeficient mouse. Proc Natl Acad Sci U S A. 2000; 97(16):9191-6.

151. Kim S, von Recum H. Endothelial stem cells and precursors for tissue engineering: cell source, differentiation, selection, and application. Tissue Eng Part B Rev. 2008; 14(1):133-47.

152. Laurens N. Isolation, purification and culture of human micro- and macrovascular endothelial cells. In: Augustin HG, editor. Methods in endothelial cell biology. Heidelberg: Springer Lab manual; 2004. p. 3.

153. Chi JT, Chang HY, Haraldsen G, Jahnsen FL, Troyanskaya OG, Chang DS, et al. Endothelial cell diversity revealed by global expression profiling. P Natl Acad Sci USA. 2003; 100(19):10623-8.

154. Luttun A, Carmeliet G, Carmeliet P. Vascular progenitors: from biology to treatment. Trends Cardiovasc Med. 2002; 12(2):88-96.

155. Hristov M, Erl W, Weber PC. Endothelial progenitor cells: isolation and characterization. Trends Cardiovasc Med. 2003; 13(5):201-6.

156. Wu X, Rabkin-Aikawa E, Guleserian KJ, Perry TE, Masuda Y, Sutherland FWH, et al. Tissue-engineered microvessels on three-dimensional biodegradable scaffolds using human endothelial progenitor cells. American Journal of Physiology-Heart and Circulatory Physiology. 2004; 287(2):H480-H7.

157. Veleva AN, Heath DE, Cooper SL, Patterson C. Selective endothelial cell attachment to peptide-modified terpolymers. Biomaterials. 2008; 29(27):3656-61.

158. Fuchs S, Hermanns MI, Kirkpatrick CJ. Retention of a differentiated endothelial phenotype by outgrowth endothelial cells isolated from human peripheral blood and expanded in long-term cultures. Cell and Tissue Research. 2006; 326(1):79-92.

159. Yoon CH, Hur J, Park KW, Kim JH, Lee CS, Oh IY, et al. Synergistic neovascularization by mixed transplantation of early endothelial progenitor cells and late outgrowth endothelial cells: the role of angiogenic cytokines and matrix metalloproteinases. Circulation. 2005; 112(11):1618-27.

160. Fuchs S, Motta A, Migliaresi C, Kirkpatrick CJ. Outgrowth endothelial cells isolated and expanded from human peripheral blood progenitor cells cells for endothelialization as a potential source of autologous of silk fibroin biomaterials. Biomaterials. 2006; 27(31):5399-408.

161. Matsumoto T, Kawamoto A, Kuroda R, Ishikawa M, Mifune Y, Iwasaki H, et al. Therapeutic potential of vasculogenesis and osteogenesis promoted by peripheral blood CD34-positive cells for functional bone healing. Am J Pathol. 2006; 169(4):1440-57.

162. Matsumoto T, Kuroda R, Mifune Y, Kawamoto A, Shoji T, Miwa M, et al. Circulating endothelial/skeletal progenitor cells for bone regeneration and healing. Bone. 2008; 43(3):434-9.

163. Mifune Y, Matsumoto T, Kawamoto A, Kuroda R, Shoji T, Iwasaki H, et al. Local delivery of granulocyte colony stimulating factor-mobilized CD34-positive progenitor cells using bioscaffold for modality of unhealing bone fracture. Stem Cells. 2008; 26(6):1395-405.

164. Melero-Martin JM, Khan ZA, Picard A, Wu X, Paruchuri S, Bischoff J. In vivo vasculogenic potential of human blood-derived endothelial progenitor cells. Blood. 2007; 109(11):4761-8.

165. Au P, Daheron LM, Duda DG, Cohen KS, Tyrrell JA, Lanning RM, et al. Differential in vivo potential of endothelial progenitor cells from human umbilical cord blood and adult peripheral blood to form functional long-lasting vessels. Blood. 2008; 111(3):1302-5.

166. Melero-Martin JM, De Obaldia ME, Kang SY, Khan ZA, Yuan L, Oettgen P, et al. Engineering robust and functional vascular networks in vivo with human adult and cord blood-derived progenitor cells. Circulation Research. 2008; 103(2):194-202.

167. Fuchs S, Ghanaati S, Orth C, Barbeck M, Kolbe M, Hofmann A, et al. Contribution of outgrowth endothelial cells from human peripheral blood on in vivo vascularization of bone tissue engineered constructs based on starch polycaprolactone scaffolds. Biomaterials. 2009; 30(4):526-34.

168. Rouwkema J, De Boer J, Van Blitterswijk CA. Endothelial cells assemble into a 3-dimensional prevascular network in a bone tissue engineering construct. Tissue Engineering. 2006; 12(9):2685-93.

169. Fuchs S, Hofmann A, Kirkpatrick CJ. Microvessel-like structures from outgrowth endothelial cells from human peripheral blood in 2-dimensional and 3-dimensional co-cultures with osteoblastic lineage cells. Tissue Eng. 2007; 13(10):2577-88.

170. Unger RE, Sartoris A, Peters K, Motta A, Migliaresi C, Kunkel M, et al. Tissue-like self-assembly in cocultures of endothelial cells and osteoblasts and the formation of microcapillary-like structures on three-dimensional porous biomaterials. Biomaterials. 2007; 28(27):3965-76.

171. Fuchs S, Hofmann A, James Kirkpatrick C. Microvessel-Like Structures from Outgrowth Endothelial Cells from Human Peripheral Blood in 2-Dimensional and 3-Dimensional Co-Cultures with Osteoblastic Lineage Cells. Tissue Eng. 2007.

172. Hofmann A, Ritz U, Verrier S, Eglin D, Alini M, Fuchs S, et al. The effect of human osteoblasts on proliferation and neo-vessel formation of human umbilical vein endothelial cells in a long-term 3D co-culture on polyurethane scaffolds. Biomaterials. 2008; 29(31):4217-26.

173. Yu H, Vandevord PJ, Gong W, Wu B, Song Z, Matthew HW, et al. Promotion of osteogenesis in tissue-engineered bone by pre-seeding endothelial progenitor cells-derived endothelial cells. J Orthop Res. 2008; 26(8):1147-52.

174. Scherberich A, Galli R, Jaquiery C, Farhadi J, Martin I. Three-dimensional perfusion culture of human adipose tissue-derived endothelial and osteoblastic progenitors generates osteogenic constructs with intrinsic vascularization capacity. Stem Cells. 2007; 25(7):1823-9.

175. Steffens L, Wenger A, Stark GB, Finkenzeller G. In vivo engineering of a human vasculature for bone tissue engineering applications. J Cell Mol Med. 2008.

176. Choong CS, Hutmacher DW, Triffitt JT. Co-culture of bone marrow fibroblasts and endothelial cells on modified polycaprolactone substrates for enhanced potentials in bone tissue engineering. Tissue Eng. 2006; 12(9):2521-31.

177. Santos MI, Unger R, Sousa RA, Reis RL, Kirkpatrick CJ. Co-culture system of osteoblasts and endothelial cells, an in vitro strategy to enhance vascularization in bone regeneration. Tissue Engineering Part A. 2008; 14(5):712-.

178. Wenger A, Stahl A, Weber H, Finkenzeller G, Augustin HG, Stark GB, et al. Modulation of in vitro angiogenesis in a three-dimensional spheroidal coculture model for bone tissue engineering. Tissue Eng. 2004; 10(9-10):1536-47.

179. Sun H, Qu Z, Guo Y, Zang G, Yang B. In vitro and in vivo effects of rat kidney vascular endothelial cells on osteogenesis of rat bone marrow mesenchymal stem cells growing on polylactide-glycoli acid (PLGA) scaffolds. Biomed Eng Online. 2007; 6:41.

180. Kaigler D, Krebsbach PH, Polverini PJ, Mooney DJ. Role of vascular endothelial growth factor in bone marrow stromal cell modulation of endothelial cells. Tissue Eng. 2003; 9(1):95-103.

181. Fuchs S, Jiang X, Schmidt H, Dohle E, Ghanaati S, Orth C, et al. Dynamic processes involved in the pre-vascularization of silk fibroin constructs for bone regeneration using outgrowth endothelial cells. Biomaterials. In Press, Corrected Proof.

182. Stahl A, Wenger A, Weber H, Stark GB, Augustin HG, Finkenzeller G. Bi-directional cell contact-dependent regulation of gene expression between endothelial cells and osteoblasts in a three-dimensional spheroidal coculture model. Biochem Bioph Res Co. 2004; 322(2):684-92.

183. Finkenzeller G, Arabatzis G, Geyer M, Wenger A, Bannasch H, Stark GB. Gene expression profiling reveals platelet-derived growth factor receptor alpha as a target of cell contact-dependent gene regulation in an endothelial cell-osteoblast co-culture model. Tissue Eng. 2006; 12(10):2889-903.

184. Kneser U, Schaefer DJ, Polykandriotis E, Horch RE. Tissue engineering of bone: the reconstructive surgeon's point of view. Journal of Cellular and Molecular Medicine. 2006; 10(1):7-19.

185. Ren LL, Ma DY, Feng X, Mao TQ, Liu YP, Ding Y. A novel strategy for prefabrication of large and axially vascularized tissue engineered bone by using an arteriovenous loop. Med Hypotheses. 2008.

186. Polykandriotis E, Arkudas A, Horch RE, Sturzl M, Kneser U. Autonomously vascularized cellular constructs in tissue engineering: opening a new perspective for biomedical science. J Cell Mol Med. 2007; 11(1):6-20.

187. Casabona F, Martin I, Muraglia A, Berrino P, Santi P, Cancedda R, et al. Prefabricated engineered bone flaps: an experimental model of tissue reconstruction in plastic surgery. Plast Reconstr Surg. 1998; 101(3):577-81.

188. Pelissier P, Villars F, Mathoulin-Pelissier S, Bareille R, Lafage-Proust MH, Vilamitjana-Amedee J. Influences of vascularization and osteogenic cells on heterotopic bone formation within a madreporic ceramic in rats. Plast Reconstr Surg. 2003; 111(6):1932-41.

189. Scheufler O, Schaefer DJ, Jaquiery C, Braccini A, Wendt DJ, J.A. G, et al. Spatial and temporal patterns of bone formation in ectopically prefabricated, autologous cell-based engineered bone flaps in rabbits. Journal of Cellular and Molecular Medicine. 2007; 12(4):1238-49.

190. Kneser U, Polykandriotis E, Ohnolz J, Heidner K, Grabinger L, Euler S, et al. Engineering of vascularized transplantable bone tissues: induction of axial vascularization in an osteoconductive matrix using an arteriovenous loop. Tissue Eng. 2006; 12(7):1721-31.

191. Kneser U, Polykandriotis E, Ohnolz J, Heidner K, Grabinger L, Euler S, et al. Engineering of vascularized transplantable bone tissues: Induction of axial vascularization in an osteoconductive matrix using an arteriovenous loop. Tissue Engineering. 2006; 12(7):1721-31.

192. Lokmic Z, Stillaert F, Morrison WA, Thompson EW, Mitchell GM. An arteriovenous loop in a protected space generates a permanent, highly vascular, tissue-engineered construct. Faseb J. 2007; 21(2):511-22.

CHAPTER II

Materials and Methods

CHAPTER II.

Materials and Methods

This chapter is aimed to provide a general overview of the methodologies, materials and cells used in the experimental plan of the thesis.

1. SCAFFOLDS

1.1. Starch polycaprolactone (SPCL) fiber-mesh scaffolds

SPCL fiber-mesh scaffolds were produced from a polymeric blend (30/70 wt%) of corn starch with the synthetic polymer PCL. Starch is one of the most abundant naturally occurring polymers, that present excellent characteristics for applications in biomaterials field, such as low toxicity, biodegradability and biocompatibility [1]. PCL, on the other hand is a Food and Drug Administration (FDA)-approved biodegradable polyester [2]. The combination of these two polymers in a blend confers increased biodegradability to PCL and improves the processability and mechanical properties of starch [3].

Two different methodologies were used in the production of SPCL fiber-mesh scaffolds: melt spinning and fiber-bonding. First, by a process of melt spinning the polymeric blend is melted for extrusion through a spinneret and directly solidified by cooling. The obtained fbers with diameter in the range of 160-260 μm were processed into fiber-mesh scaffolds by a fiber-bonding methodology consisting in cutting and sintering. The samples were cut into discs of approximately 8 mm diameter and 1.5-2 high mm and were sterilized by ethylene oxide.

Our group has proposed and extensively studied SPCL fiber-mesh scaffold as a biodegradable natural-based material aimed for bone regeneration. Thus, within

these years a great amount of knowledge has been accumulated about SPCL fiber-mesh scaffolds. Next it will be reviewed the most relevant studies related with theme of this thesis.

SPCL is a biodegradable polymer susceptive to be degraded by hydrolysis mainly catalysed by the enzymes lipase and α-amylase [4]. The first catalyses he hydrolysis of PCL, whereas the second catalyses the hydrolysis of α-1,4-glycosidic linkages of starch. Among other sources, both lipase and α-amylase exists in serum [1, 5]. Degradation studies of SPCL fiber-mesh scaffolds have been performed in solutions contanining the hydrolytic enzymes lipase and α-amylase in physiological concentrations [6]. The results have shown that after 12 weeks of immersion the scaffolds were completely degraded. Furthermore, the products resultant from degration are non toxic and are either metabolized via the tricarboxylic acid cycle or eliminated by direct renal secretion [4, 7].

The great advantage of fiber-mesh design is the large surface area for cell attachment which also enables rapid diffusion of nutrients enhancing cell survival and growth [6]. As determined by micro computed tomography (μCT) analysis the SPCL scaffolds used in this thesis have a porosity ranging 66-75 % [8, 9]. Nevertheless, regarding the application of these scaffolds in hard-tissue replacement the mechanical properties are also an important aspect to have in consideration. The mechanical properties evaluated in compression tests in the dry and wet state are 2.1±0.40 and 1.82±0.40 MPa, respectively [6]. Hence, these mechanical properties suggest the application of SPCL fiber-mesh scaffold in the regeneration of non-load bearing defects [10].

An additional advantage of SPCL fiber-mesh scaffold architecture and specially pore interconnectivity is its application in tissue-engineering strategies that involve the use of bioreactor cultures. The work of Gomes et al with flow perfusion bioreactors [8, 11] has shown that SPCL fiber-mesh scaffold was an appropriate matrice for the proliferation and osteogenic differentiation of rat bone marrow cells. It was also reported the production of several growth factors with osteogenic and angiogenic activity by the seeded cells [11]. Furthermore, the fiber-mesh structure allowed a homogenous distribution of the cells and throughout deposition of mineralized matrix [8]. A complementary work investigated the influence of porosity of these scaffolds in

a flow perfusion bioreactor and concluded that the best outcome was obtained with SPCL fiber-mesh scaffolds with a porosity of 75%, rather than 50% [12].
SPCL fiber-mesh scaffold is the common denominator to all remaining five chapters. This thesis deals not only with the interaction between cells (ECs and osteoblasts) and SPCL fiber-mesh scaffolds but also with improvements in the architecture and surface of the scaffold towards the final aim of vascularization.

1.2. Plasma-modified SPCL fiber-mesh scaffolds

Plasma treatment is one of the main techniques of modifying polymer surfaces to improve cell adhesion while maintaining the desirable properties of the bulk material. Chapter IV deals with the surface modification of SPCL fiber-mesh scaffold by means of Ar plasma to improve ECs adhesion and proliferation. In this study it was used the plasma reactor PlasmaPrep$_5$ (Gala Instrument GmbH, Germany) that allowed a fully automated process and had a control reactor with a chamber size of 15 cm diameter and 31 cm length (5L). Ar was the working gas and the air present in the system was first displaced with Ar, by flushing it through the reactor. Then, the outlet was closed, and the reactor was filled with Ar with a controlled pressure of 0.18 mbar. A radio frequency source (13.56MHz) and a power of 30 W were used, and the scaffolds were exposed to plasma for 15 minutes. The samples were kept at air atmosphere after being removed from the reactor.

1.3. Nano/micro fiber-combined scaffolds

Nano/micro fiber-combined scaffold is an architectural upgrade of SPCL fiber-mesh scaffold, inspired in the physical structure of the ECM. The interaction of ECs with this combined structure and its influence in several biological functions are evaluated in the scope of chapter V.
Electrospinning is an electrostatic processing methodology used to fabricate fibers with diameters that can do down to 3 nm [13]. Due to its ability to produce fibers in

the nano-range, electrospinning was the selected methodology to produce the nano-fibers of the starch-based scaffold. In electrospinning a high voltage is applied to create electrically charged jets of a polymer solution or melt [14]. These jets dry to form nanofibers, which are collected on a target. The final diameter of the fibers are easily changed by manipulating the polymer concentration, the used solvent and various process parameters [15]. This technique was used to produce

Nano/micro fiber-combined scaffolds previously developed by Tuzkoglu were obtained by a two-step methodology. First, it was produced the micro support, i.e., SPCL fiber-mesh scaffold by melt-spinning and fiber-bonding, as previously described. Then, this scaffold was impregnated with electrospun nano-fibers. The solution used in the electrospinning experiments was prepared by dissolving 1g of SPCL in 7 ml chloroform. After dissolution was completed, 3 ml of dimethylformamide (DMF) which has a high dielectric constant was added to the solution to enhance electrospinning of the solution. A syringe filled with the polymer solution was placed on a syringe pump and SPCL fiber-mesh scaffolds were stationed in a special designed collector that allowed the movement of the samples through the electrospun polymeric jets. Collector and syringe needle were distanced by 10 cm. A high power supply provided a 15 KV voltage and the scaffolds were electrospun for 10 s. This procedure was applied to both sides of SPCL fiber-mesh scaffolds. In the final structure nano-fibers had an average diameter of 400 nm.

1.4. Collagen-nano and SPCL-micro fiber-combined scaffolds

Collagen-nano and SPCL-micro fiber-combined scaffold is a structure that aims to recreate not only the physical but the chemical structural of ECM. This construct combines in the same structure electrospun type I collagen nano-fibers with starch-based micro-fibers. In chapter VI it will be provided a more detailed description of the production of this combined structure.

As macrosupport of the combined structure were used SPCL fiber-meshes obtained by wet-spinning. For this, SPCL was dissolved in chloroform at a concentration of 40% (W/V) and the solution was extruded with a syringe pump (World Precision

Instruments, UK) into a coagulation bath of methanol. The fiber-mesh structure was formed during the processing by moving the coagulation bath randomly. Following an overnight dry at room temperature (RT) to remove solvent traces, fiber-meshes were impregnated with collagen nanofibers obtained by electrospinning. The collagen used in this process was isolated from Wistar rat tails according to a typical cid extraction procedure [16]. For electrospinning a syringe placed in a syringe pump was filled with a solution of 0.85 mg of collagen dissolved in 1 mL of 1,1,1,3,3,3-hexafluoro-2-propanoll (HFP, Sigma-Aldrich, Germany). Fiber-meshes were placed in the collector and it was applied a voltage of 20 KV for 10 seconds. The fiber-meshes were turned and the procedure repeated. The final structures were dried overnight at RT to eliminate solvent residuals. Finally, in order to maintain the structural and mechanical integrity of collagen nano-fibers the scaffolds were crosslinked with saturated gluteraldehyde vapour at RT for 48 hrs. After crosslinking, the constructs were subsequently immersed in 0.02 M glycine solution for 4 hrs in order to remove unreacted glutaraldehyde. The structures were washed several times with distilled water, dried and stored in desiccators until use.

Additionally, it was also produced thicker scaffolds exploring the proposed concept of layer by layer. SPCL fiber-meshes scaffolds with nano-fibers on one side were stacked together by heating at 60ºC, the melting point of SPCL.

2. STRUCTURAL/CHEMICAL CHARACTERIZATION

2.1. Optical and scanning electron microscopy (SEM)

The overall organization of collagen-nano and SPCL-micro fiber-combined structures was visualized by optical microscopy (chapter VI). Scanning electron microscopy (SEM, Leica Cambridge S360) on the other hand, was used to assess the morphology of the collagen nano-fibers. Previously to SEM analysis samples surfaces were gold sputtered (Fisons Instruments, Suptter Coater SC502, UK).

On chapter IV the surface morphology of SPCL fibers was analyzed by SEM before and after plasma treatment.

2.2. Confocal laser scanning microscopy (CLSM)

To confirm the collagenous nature and to reveal the architecture of the nano-network on the combined structures the samples were stained with antibody against type I collagen and visualized by confocal laser scanning microscopy (CLSM, Olimpus IX81). The samples were incubated for 1 h at RT with the primary antibody mouse anti-bovine (1:100, Sigma-Aldrich, Germany), followed by incubation with secondary antibody anti-mouse Alexa Fluor 488 (1:1000, Invitrogen, USA) also for 1 h at RT. Phosphate buffered saline (PBS) washing was performed between each step and for CLSM observation the samples were covered with mounting medium (Vectashield, UK).

2.3. Optical profilometry

When the surface of a polymer is exposed to plasma treatment it might occur etching of the superficial layers, thus changing the roughness and topography of the material [17]. The roughness of a surface can be measured by atomic force microscopy (AFM) or in the case of a 3D structure by optical profilometry. This last technique allows roughness analysis of 3D structures with high resolution from subnanometer to millimetre-high steps.

In chapter IV using optical profilometry it was measured the topographical changes in SPCL fiber-mesh scaffolds surface after Ar plasma treatment. It was used an optical profiler Wyko NT 3300 from Veeco Instruments Inc and measurements were performed in Vertical Scanning Interferometry (VSI) mode. An area of 2 mm with vertical resolution of 3 nm was analyzed.

2.4. Surface chemical analysis

X-Ray photoelectron spectroscopy (XPS) and time-of-flight secondary ion mass spectrometry (TOF-SIMS) are two surface chemical analysis techniques that measure

the elemental composition of a material surface. TOF-SIMS is complementary to XPS, owing to its molecular information, high sensitivity and selectivity to the uppermost surface layers [18]. In chapter IV these two techniques were used to assess the effect of plasma treatment on surface chemistry of SPCL fiber-mesh scaffolds. The XPS analysis was carried out using the instrument VG Escalab 250 iXL (VG Scientific, UK) and TOF-SIMS with a TOF-SIMS IV instrument (Ion-TOF GmbH, Germany); further details of the analysis are provided in the respective chapter.

2.5. Contact angle

Contact angle is a technique that characterizes the wettability of a surface by measuring the surface tension of a water droplet at its interface with a homogenous surface [19]. In order to determine the effect of Ar plasma treatment on the wettability of SPCL, static angle measurements were performed on two dimensional (2D) samples (chapter IV). These samples were prepared by a similar procedure to that used for the scaffolds, i.e., by polymer melting with subsequent injection into a mould. The surface of SPCL 2D samples was treated using the same conditions as described in section 1.2 for the 3D scaffolds. The values were obtained by sessile drop method using a contact angle meter OCA15+ with a high-performance image processing system from DataPhysics Instruments, Germany.

3. PROTEIN ADSORPTION

Protein adsorption is one of the first events to occur upon implantation of a graft and is a critical modulator of several cellular mechanisms [20]. In turn, protein adsorption is dependent on the chemical and physical properties of the underlying substrate [21]. Thus, in chapter IV it was evaluated in which extent Ar plasma treatment of SPCL fiber-mesh scaffolds affected the adsorption profile of two adhesive proteins fibronectin (Fn) and vitronectin (Vn). For that, untreated and plasma-modified SPCL fiber-mesh scaffolds were immersed for 1 h at 37 ºC in a multi-protein solution that

was basically constituted by M199 culture medium (Sigma-Aldrich, Germany) supplemented with 20% (v/v) of fetal calf serum (FCS, Sigma-Aldrich, Germany). As blanks were used samples immersed in PBS. For immunostainning samples were fixed in 2.5 % formalin solution, washed and incubated for 1 h with the primary antibody mouse anti-human Fn with goat cross-reactivity (1:50, Sigma-Aldrich, Germany) or mouse anti-bovine anti-Vn (1:50, Santa Cruz, USA). Finally, samples were incubated with the secondary antibody goat anti-mouse Alexa Fluor 488 for 1h at RT and analysed by CLSM

4. CELLS

4.1. Endothelial cells (ECs)

ECs line in the lumen of all blood vessels and play important roles in angiogenesis, i.e., in the formation of new blood vessels from existing ones [22]. Furthermore, ECs also participate in inflammation trough the recruitment of circulating lymphocytes to the inflammatory focus [23]. Regarding the vascularization topic addressed in this thesis, and the relevance of ECs for this phenomenon, the use of ECs cultures was the common element to all the chapters of the present thesis. In the experimental plan it was used the endothelial cell line HPMEC-ST1 and primary cultures of HUVECs and HDMECs.

4.1.1. Cell line HPMEC-ST1

The microvascular cell line HPMEC-ST1 was developed from human pulmonary microvascular ECs. This cell line was generated by transfection and displays the major constitutively expressed and inducible endothelial phenotypic markers [24]. HPMEC-ST.6R were propagated in the conditions summarized in table II.1. Geneticin was added to the medium as the selective agent for selection of the transfected HPMEC-ST1 cells. Other supplements also common to the culture of HUVEC and

HDMEC are: endothelial cell growth supplement (ECGS) that contains a mixture of growth factors aimed to improve proliferation; sodium heparin, stabilize the growth factors in culture and Glutamax I is a direct substitute for L-glutamine that aims to improve growth efficiency and performance of mammalian cell culture systems.
Expanded cells were cultured in culture flasks coated with gelatine 0.2% (Sigma-Aldrich, Germany). This a common procedure in ECs culture because previous studies have shown that coating culture dishes with components of ECM potentiate the FGF-2 activity and that the absence of this coating did not support the growth of low seed density HUVEC in the presence of 20% FCS [25, 26]. Cells were cultured under standard conditions (37 ºC, 5 % CO_2) and medium was changed every 3 days.

Table II.1 – Conditions for endothelial cells culture

Cells	Culture medium	Supplement (type, amount and supplier)
HPMEC-ST1	M199 (Sigma-Aldrich, Germany)	FCS - 20% (Life technologies, Germany) Glutamax I – 2mM (Life technologies, Germany) Pen/strep – 100U/100µg/mL (Sigma-Aldrich,Germany) Sodium heparin – 50 µg/mL (Sigma-Aldrich, ECGS – 25 µg/mL (BD Biosciences, USA) Geneticin 418 – 50 µg/mL (Life technologies, Germany)
HUVEC	M199	FCS - 10% (Life technologies, Germany) FCS - 10% (PAA Laboratories, Germany) Pen/strep – 100U/100µg/mL (Sigma-Aldrich, Germany) Glutamax I – 2mM (Life technologies, Germany) Sodium heparin – 25 µg/mL (Sigma-Aldrich, Germany) ECGS – 25 µg/mL (BD Biosciences, USA)
HDMEC	Endothelial Basal Medium MV (PromoCell,Germany)	FCS – 15 % (Invitrogen, Germany) Pen/strep – 100U/100µg/mL (Sigma-Aldrich, Germany) FGF-2 – 2.5 ng/mL (Sigma-Aldrich, Germany) Sodium heparin – 25 µg/mL (Sigma-Aldrich, Germany)

4.1.2. Human umbilical vein endothelial cells (HUVEC)

HUVECs were isolated from the umbilical cord vein by collagenase digestion [27]. Briefly, the umbilical vein was cannulated and with the help of a syringe perfused and

washed with HEPPES buffer. Following perfusing the vein with a solution of pre-heated collagenase (22 U/100 mL HEPES, (Worthington Biochemical Corporation, USA) it was incubated for 20 min at 37ºC. After incubation the cells were mechanically loose and the vein was flushed with complete medium (table II.1). The collected cells were then centrifuged 5 min at 1500 rpm, the medium discarded and ECs resuspended in fresh culture medium. The cells were cultured in gelatine coated flasks and cell were used until fourth passage.

4.1.3. Human dermal microvascular endothelial cell (HDMEC)

HDMECs were isolated from juvenile foreskin by enzymatic diggestion. The foreskin was cut into small pieces, washed with PBS and incubated in 3–5 ml dispase (depending on the amount of tissue; 2.5 U/ml PBS; Sigma Chemicals, Germany) overnight (12–18 h) at 4ºC. This enzymatic digestion assisted in the removal of the epidermis. Epidermis-free dermal pieces were incubated in 5ml versene (0.02% EDTA in PBS; Gibco, Germany) with trypsin (0.04%; Seromed, Germany) at 37ºC for 2 h. Enzymatic digestion was stopped by the addition of 2ml FCS, then the tissue pieces were placed into culture medium (table II.1) and pressed with the back of a scalpel to loosen the individual cells from the tissue. The resulting cell suspension (containing HDMEC and other contaminating cell types) was centrifuged at 300g for 5 min. The cell pellet was resuspended in culture medium and seeded into a 75 cm^2 tissue culture flask (gelatin-coated). Culture medium was changed every 2–3 days. Before the cultures were confluent (normally 3 days upon seeding) the HDMEC were separated from the other cells in culture by immunomagnetic isolation with CD31-Dynabeads following the manufacturer's instructions (Invitrogen, USA). For the experiments were used purified HDMEC expanded until passage four.

4.2. Osteoblasts

In the present studies it was used the osteoblast cell line SaOs-2 and human primary osteoblasts (hOBs) isolated from human femoral head explants. SaOs-2, a non-transformed cell line derived from a primary osteosarcoma was used in chapter VI for monoculture studies with collagen-nano and SPCL-micro fiber-combined scaffolds. hOBs on the other hand, were used in co-culture systems (chapter VII) and were obtained by sequential enzymatic digestion of bone chips as will be briefly described. Table II.2 compiles the culture conditions for SaOs-2 and hOBs. Bone chips were scraped from the femoral head, and washed thoroughly several times with calcium-free PBS to remove erythrocytes, bone marrow and tissue debris. The bone chips were then grown in a complete osteoblast medium (Table II.2) and digested with a collagenase (100 U/mL)/trypsin (300 U/mL) (Sigma-Aldrich, Germany) mixture buffered with 0.01 m HEPES to prepare a single cell suspension. The cells were then expanded in culture and cultured under standard conditions.

Table II.2 – Conditions for osteoblast cell culture

Cells	Culture medium	Supplement (type, amount and supplier)
Cell line SaOs-2	DMEM low glucose (Sigma-Aldrich, Germany)	10% Foetal Bovine Serum (Sigma-Aldrich, Germany) Pen/strep – 100U/100µg/mL (Sigma-Aldrich, Germany)
hOBs	DMEM low glucose (Sigma-Aldrich, Germany)	10 % FCS (Sigma-Aldrich, Germany) Pen/strep – 100U/100µg/mL (Sigma-Aldrich, Germany) 300 µg/mL ascorbic acid (Sigma-Aldrich, Germany) 100 nM dexamethasone (Sigma-Aldrich, Germany) 2 mM Glutamax (Life Technologies, Germany).

5. CELL CULTURE

5.1. Scaffolds seeding

Prior to cell seeding scaffolds were immersed overnight in serum-free culture medium. For ECs culture the scaffolds were previously coated with Fn. As afore mentioned, in order to sustain ECs adhesion and growth the majority of the substrates require a pre-coating with an adhesive protein such as Fn. For that, the samples were coated with 10μg/mL Fn in PBS (Roche, Germany) for 1 hour at 37ºC. Plasma-treated SPCL fiber-mesh scaffolds once were modified aiming to the avoid Fn coating did not receive this treatment. Confluent ECs in culture flasks were trypsinized and a cell suspension (0.5 mL) was added to each scaffold. The number of cells added to each scaffold is specified in each chapter. Regarding osteoblast seeding, apart from Fn pre-coating, the procedure was the same. The scaffolds were incubated under standard conditions and medium was changed every 3 days.

5.2. Co-culture

For the co-culture studies described in chapter VII, HDMECs and hOBs were mixed in a proportion of 4:1 and cultured in HDMEC medium. One day prior to co-culture, hOBs medium was changed to the one used in co-culture. Then, Fn-coated SPCL fiber-mesh scaffolds were seeded with 1.5 x 10^5 cells of the mixed cell suspension and cultured for up to 35 days. Scaffolds were also cultured with HDMECs (1.30 x 10^5 cells/scaffold) or hOBs (2 x 10^4 cells/scaffold) alone to be used as monoculture controls. All experiments involving HDMECs:hOBs co-culture were performed with at least three different HDMEC and hOBs donors.

6. BIOLOGICAL CHARACTERIZATION

6.1. Morphology

The morphological analysis of cells growing on the scaffolds under study was performed by SEM. After each time interval, cells/scaffold constructs were fixed with 2.5% glutaraldehyde for 30 min in 0.1 M sodium cacodylate buffer, dehydrated in increasing concentrations of acetone and dried with hexamethyldisilane. Before the analysis all the samples were sputtered coated with gold.

On chapter V the ultrastructure of HDMECs that migrate from nano/micro fiber-combined scaffold onto a collagen gel was evaluated by transmission electron microscopy (TEM). Scaffolds plus collagen gel were fixed in 2.5 % glutaraldehyde in cacodylate buffer, post-fixed in 1% osmium tetroxide for 2 h and dehydrated in increasing ethanol concentration. Samples were embedded in agar resin 100 (PLANO, Germany) with ethanol as solvent for transition state and subjected to polymerization at 60ºC for 48 hrs. Ultrathin sections were cut, placed onto copper grids and examined by transmission electron microscope (Philips EM 410).

6.2. Viability

The viable cells growing on the developed scaffolds were visualized by CLSM (Leica TCSN, Germany) after incubating the samples with medium supplemented with 0.1 M calcein-AM (Invitrogen, USA) for 10 min. Calcein-AM is a non-fluorescent membrane-permeant compound that in viable cells by the action of active intracellular esterases is converted into the green fluorescent and impermeable calcein. Viable cell are identifiable by the green fluorescent cytoplasma.

6.3. Proliferation

The proliferation of cells growing on the scaffolds was assessed with the metabolic assay Cell Titer 96® Aqueous One Solution Cell Proliferation (Promega, USA) or the DNA quantification assay PicoGreen (Invitrogen, USA).

The principle of the first assay is based on MTS (3-(4,5-dimethylthiazol-2-yl)-5-(3-carboxymetyhoxyphenyl)-2(4-sulfophenyl)- 2H tetrazolium), a substrate that is converted by nicotinamide adenosine dinucleotide phosphate (NADPH) or NADP which are produced by dehydrogenase enzymes in metabolically active cells, thus yielding a brown formazan product . The intensity of the color is directly related to the number of viable cells, and thus to their proliferation *in vitro.* Cell viability on the scaffolds after different time intervals was determined by using Cell Titer 96® Aqueous One Solution Cell Proliferation Assay kit according to the standard procedure. Briefly, the samples were transfered to new culture wells with fresh medium without phenol red and MTS reagent in 5/1 ratio. Following an incubation 3h at 37°C, 100 µl of incubated medium was transferred to 96-well plate and optical density was read at 490nm in a micro-plate reader (Synergy HT, Bio-tek). The results were expressed as the average absorbance of triplicate samples.

In PicoGreen assay a fluorophore specific for double-stranded DNA allows to quantify the amount of DNA per scaffold. Knowing that each cell type has a certain amount of DNA is possible, trough a calibration curve, to relate DNA content with cell number. For the assay the samples were prepared by rinsing with sterile PBS and incubated with sterile ultra pure water at 37°C for 1h. Then, they were frozen at - 80°C and thawed. Before starting the assay, they were sonicated 15min in an ultrasonic bath. An aliquot of each sample was transferred to the 96-well plate. A certain ratio of Tris-EDTA buffer and PicoGreen reagent prepared in the same buffer was added to the each well. The fluorescence was read at 485nm and 528nm excitation and emission, respectively. The number of cells in each scaffold was then calculated by correlation with the DNA of a known amount of cells.

7. PROTEIN ANALYSIS

7.1. Immunofluorescence

By immunofluorescence it was assessed at the single cell level the expression of the endothelial cell markers: platelet endothelial cell adhesion molecule-1 (PECAM-1) and Von Willebrand factor (vWF); of the pro-inflammatory molecule E-selectin; and of the gap junction protein Cx43. The E-selectin staining was performed on ECs growing on SPCL fiber-mesh scaffolds and on culture plastic in the presence or absence of 1.0 μg/mL of lipopolysaccharide (LPS) for 4 hrs (Sigma-Aldrich, Germany).

At different time points the constructs seeded with ECs cultured alone or with osteoblasts were fixed in 2% paraformaldehyde for 30 min. Samples were then permeabilized with 0.1% Triton for 5 min at RT. After washing with PBS the samples were incubated for 1 hr at RT with the respective primary antibody (table II.3). Under the same conditions a second incubation was performed with the secondary antibody (table II.3). The nuclei were counterstaining with 1 μg/mL Hoechst. Between all the steps the samples were washed with PBS. Finally, the samples were mounted with Gel/Mount (Natutec, Germany) and visualized by CLSM.

Table II.3 – Primary and secondary antibodies used in immunofluorescence

Primary antibody (anti-human) (dilution, supplier)	Secondary antibody (dilution, supplier)
Mouse PECAM-1; 1:50; (Dako, Denmark)	Anti-mouse Alexa Fluor 488 (Invitrogen, USA) Anti-mouse Alexa Fluor 594 (Invitrogen, USA)
Rabbit vWF; 1:8000; (Dako, Denmark)	Anti-rabbit Alexa Fluor 488 (Invitrogen, USA)
Mouse E-selectin; 1:100;(Monosan)	Anti-mouse Alexa Fluor 488 (Invitrogen, USA)
Rabbit Cx43; 1:50; (Cell Signalling, USA)	Anti-rabbit Alexa Fluor 488 (Invitrogen, USA)

7.2. Immunohistochemistry

The expression of PECAM-1, collagen I and IV was assessed on co-cultures of HDMEC:hOBs on SPCL fiber-mesh by immunohistochemistry. At several time points the samples were fixed with 3.7% glutaraldehyde for 30 min, dehydrated in ascending alcohol concentrations, changed to xylene substitute and finally transferred to liquid paraffin. Parafin blocks were cut in transversal cross-section (5 μm thick), deparaffinised and rehydrated. Sections were blocked with serum for unspecific binding and then the sections were incubated first with primary antibody for 1h at RT, followed by a second incubation with secondary antibody biotin-labeled (table II.4). This was followed by a 30 min incubation with horseradish peroxide-conjugated streptavidin complex (ABC kit, Vector). Peroxidase staining was performed using 3,3′-diaminobenzidine (DAB) as a chromogen (Vector). The nuclei were counterstained with Mayer's haematoxylin and the sections were examined under a light microscope. Between all the steps it was performed at least one PBS washing.

Table II.4 – Primary and secondary antibodies used in immunohistochemistry

Primary antibody (anti-human) (dilution, supplier)	Secondary antibody (dilution, supplier)
Mouse PECAM-1; 1:50; (Dako, Denmark)	Anti-mouse biotin-labeled; 1:200 (Vector,USA)
Rabbit collagen type I; 1:100 (Biodesign Inter., USA)	Anti-rabbit biotin-labeled; 1:200 (Vector,USA)
Mouse collagen IV; 1:50 (Dako, Denmark)	Anti-mouse biotin-labeled; 1:200 (Vector,USA)

7.3. Enzyme-Linked Immunosorbent Assay (ELISA)

Enzyme-linked immunosorbent assay (ELISA) is a biochemical technique used to detect and quantify an antibody or antigen in a fluid. In the scope of chapter VII it was

used a sandwich ELISA to quantify the VEGF released in the supernatant of HDMEC:hOBs co-culture and monocultures (HDMEC and hOBs) on SPCL fiber-mesh scaffolds. The supernatant from these cultures was collected every 7 days and stored at -80ºC. VEGF was quantified using the human VEGF DuoSet (R&D Systems, Germany) and following manufacturer's instructions. Briefly, a capture antibody anti-VEGF was bound to a microtiter plate to create the solid phase. Unbound antibody was removed by washing the plate and a blocking reagent was added. Following a wash, samples, standards and blank (culture medium) were then incubated with the solid phase antibody, which captures VEGF present in the supernatant. After washing away unbound analyte, biotin-conjugated detection antibody was added. This detection antibody binds to a different epitope of immobilized VEGF, completing the sandwich. Following a wash to remove unbound detection antibody, the detection reagent streptavidin-horseradish peroxidase was added. The plate was washed, hydrogen peroxidase was added as substrate solution and color developed in proportion to the amount of bound analyte. Color development was stopped with an acid solution and the intensity of the color was measured at 450 nm in a micro-plate reader

8. GENE EXPRESSION

8.1. mRNA isolation and cDNA synthesis

In the present thesis different aspects of cell-substrate and cell-cell interaction were evaluated at the gene level. In chapter III and V it was assessed the ability of ECs growing on SPCL fiber-mesh scaffolds to express pro-inflammatory genes upon stimulation with LPS; in chapter IV it was evaluated the effect of plasma treatment on the expression of endothelial cell markers; and in chapter VII it was studied the expression of a set of osteogenesis-related genes in co-culture relatively to monocultures. For the assessment of pro-inflammatory genes the samples were cultured on the scaffolding material and on 2D tissue culture polystyrene (TCPs) in the presence and absence of LPS, as previously described in section 7.1.

Total RNA was extracted from the constructs using the RNeasy Micro Kit (Qiagen, Germany). Total RNA (0.5 µg) was then reverse transcribed into cDNA using Omniscript RT Kit (Qiagen, Germany).

8.2. Semi-quantitative polymerase chain reaction (PCR)

Using gene-specific primer sets the genes of interest were amplified by semi-quantitative polymerase chain reaction (PCR). Equal amounts of cDNA (1µg), measured by NanoDrop microspectrophotometer, were amplified by PCR with Taq DNA Polymerase Kit (Qiagen) and with gene-specific primer sets shown in Table II.5. Thirty five cycles were used for all genes, each one consisting of 2 min of denaturation at 94ºC, 30s of annealing (Table II.5) and 30s of chain elongation at 72ºC, followed by a final 10 min extension at 72ºC. Amplification products were separated by electrophoresis on an agarose gel (0.8%) and stained with ethidium bromide staining. The housekeeping gene β-actin was used as internal standard.

Table II.5 – Genes amplified by semi-quantitative PCR

Name of gene	Product size (bp)	Annealing Temperature (ºC)	Primer pair sequences
β-actin	574	65	5'AGCATTTGCGGTGGACGATGGAG-3' 5'-GACCTGACTGACTACCTCATGA-3'
E-selectin	304	62	5'-ATCAACATGAGCTGCAGTGG-3' 5'-AGCTTCCGTCTGATTCAAGG-3'
ICAM	395	57	5'-TATTCAAACTGCCCTGATGG-3' 5'-CAGTGCGGCACGAGAAATTGG-3'
VCAM	282	62	5'-TCTCATTGACTTGCAGCACC-3' 5'-ACTTGACTGTGATCGGCTTCC-3'
PECAM-1	280	57	5'- CAACAGACATGGCAACAAGG-3' 5'- TTCTGGATGGTGAAGTTG GC-3'
VE-cadherin	452	57	5'-GCTGAAGGAAAACCAGAAGAAGC-3' 5'-TCGTGATTATCCGTGAGGGTAAAG-3'
VEGF-R1	665	55	5'- TCTCCTTAGGTGGGTCTCC - 3' 5'- CAGCTCAGCGTGGTCGTAG - 3'

8.3. Real time PCR

In opposition to semi-quantitative PCR, real time PCR enables the quantification of the amplified gene-product, thus giving a relative or absolute quantification of gene expression.

The amplification of pro-inflammatory genes E-selectin and intercellular adhesion molecule-1 (ICAM-1) plus the housekeeping gene glyceraldehyde-3-phosphate dehydrogenase (GAPDH) was performed using Applied Biosystems 7300 Real-Time PCR System (Applera Deutschland GmbH, Germany). The number of cycles and annealing temperature were selected according to the manufacturer's instructions. Real time PCR was performed with 2.5 ng cDNA and 12.5 µL of 2x-master mix, primers (0.25 µL forward and 0.25 µL reverse primer) in a final volume of 25 µL. Table II.6 lists the gene-specific primer sets that were used. Gene expression was normalized to the expression of the housekeeping gene GAPDH. Relative quantification of gene expression was calculated in stimulated samples (+LPS) compared to samples cultured in the absence of pro-inflammatory stimulus (-LPS).

Table II.6 – Pro-inflammatory genes and housekeeping gene amplified by real time-PCR

Name of gene	Primer pair sequences
E-selectin	5'-CCCGTGTTTGGCACTGTGT-3' 5' -GCCATTGAGCGTCCATCCT-3'
ICAM-1	5' -CGGCTGACGTGTGCAGTAAT-3' 5' -CACCTCGGTCCCTTCTGAGA-3'
GAPDH	5'- ATGGGGAAGGTGAAGGTCG-3' 5' -TAAAAGCAGCCCTGGTGACC-3'

In chapter VII it was used a human osteogenesis RT^2 Profiler PCR array (Superarray, USA) to profile the expression of 84 genes related to osteogenesis plus housekeeping and control genes (table II.7). Equal amounts of cDNA (1.25 ng) plus master mix RT^2 SYBR Green/ROX qPCR (12.5 µL) were added in a final volume of 25 µL to each well of the human osteogenesis RT^2 Profiler PCR array for quantitative PCR. The number of cycles and annealing temperature were selected according to the manufacturer's

instructions. For these experiments three different donors for both OBs and ECs were used. In each sample the mRNA level expression of each gene was normalized to the average expression of the housekeeping genes GAPDH and ribosomal protein L13A (RPL13A). Gene fold change was calculated in comparison with HDMEC or hOBs as control samples. The statistic treatment of the results and their plot in the form of a volcano plot are explained in greater detail in the respective chapter.

Table II.7 – Osteogenesis-related genes amplified by real-time PCR

Gene name	Description	Gene bank Accession no.
AHSG	Alpha-2-HS-glycoprotein	NM_001622
ALPL	Alkaline phosphatase, liver/bone/kidney	NM_000478
AMBN	Ameloblastin	NM_016519
AMELY	Amelogenin, Y-linked	NM_001143
ANXA5	Annexin A5	NM_001154
BGLAP	Bone gamma-carboxyglutamate protein (osteocalcin)	NM_199173
BGN	Biglycan	NM_001711
BMP1	Bone morphogenetic protein 1	NM_006129
BMP2	Bone morphogenetic protein 2	NM_001200
BMP3	Bone morphogenetic protein	NM_001201
BMP4	Bone morphogenetic protein 4	NM_130851
BMP5	Bone morphogenetic protein 5	NM_021073
BMP6	Bone morphogenetic protein 6	NM_001718
CALCR	CALCITONIN RECEPTOR	NM_001742
CD36	CD36 molecule	NM_000072
CDH11	Cadherin 11, type 2	NM_001797
COL10A1	Collagen, type X, alpha	NM_000493
COL11A1	Collagen, type XI, alpha 1	NM_080629
COL12A1	Collagen, type XII, alpha 1	NM_004370
COL14A1	Collagen, type XIV, alpha 1	NM_021110
COL15A1	Collagen, type XV, alpha 1	NM_001855
COL1A1	Collagen, type I, alpha 1	NM_000088
COL1A2	Collagen, type I, alpha 2	NM_000089
COL2A1	Collagen, type II, alpha 1	NM_001844
COL3A1	Collagen, type III, alpha 1	NM_000090
COL4A3	Collagen, type IV, alpha 3	NM_000091
COL5A1	Collagen, type V, alpha 1	NM_000093
COMP	Cartilage oligomeric matrix protein	NM_000095
CSF2	Colony stimulating factor 2	NM_000758
CSF3	Colony stimulating factor 3	NM_000759
CTSK	Cathepsin K	NM_000396
DMP1	Dentin matrix acidic phosphoprotein	NM_004407
DSPP	Dentin sialophosphoprotein	NM_014208
EGF	Epidermal growth factor	NM_001963
EGFR	Epidermal growth factor receptor	NM_005228
ENAM	Enamelin	NM_031889
FGF1	Fibroblast growth factor 1 (acidic)	NM_000800
FGF2	Fibroblast growth factor 2 (basic)	NM_002006
FGF3	Fibroblast growth factor 3	NM_005247
FGFR1	Fibroblast growth factor receptor 1	NM_015850
FGFR2	Fibroblast growth factor receptor 2	NM_00014

Table II.7 - (*Continued*)

Gene name	Description	Gene bank Accession no.
FLT1	Fms-related tyrosine kinase 1	NM_002019
FN1	Fibronectin 1	NM_002026
GDF10	Growth differentiation factor 10	NM_004962
ICAM1	Intercellular adhesion molecule 1	NM_000201
IGF1	Insulin-like growth factor 1	NM_000618
IGF1R	Insulin-like growth factor 1 receptor	NM_000875
IGF2	Insulin-like growth factor 2	NM_000612
ITGA1	Integrin, alpha 1	NM_181501
ITGA2	Integrin, alpha 2	NM_002203
ITGA3	Integrin, alpha 3	NM_002204
ITGAM	Integrin, alpha M	NM_000632
ITGB1	Integrin, beta 1	NM_002211
MINPP1	Multiple inositol polyphosphate histidine phosphatase, 1	NM_004897
MMP10	Matrix metallopeptidase 10	NM_002425
MMP2	Matrix metallopeptidase 2	NM_004530
MMP8	Matrix metallopeptidase 8	NM_002424
MMP9	Matrix metallopeptidase 9	NM_004994
MSX1	Msh homeobox 1	NM_002448
NFKB1	Nuclear factor of kappa polypeptide gene enhancer B1 cells	NM_003998
PDGFA	Platelet-derived growth factor alpha polypeptide	NM_002607
PHEX	Phosphate regulating endopeptidase homolog	NM_000444
RUNX2	Runt-related transcription factor 2	NM_004348
SCARB1	Scavenger receptor class B, member 1	NM_005505
SERPINH1	Serpin peptidase inhibitor	NM_001235
SMAD1	SMAD family member 1	NM_005900
SMAD2	SMAD family member 2	NM_005901
SMAD3	SMAD family member 3	NM_005902
SMAD4	SMAD family member 4	NM_005359
SOX9	Sex determining region Y	NM_000346
STATH	Statherin	NM_003154
TFIP11	Tuftelin interacting protein 11	NM_012143
TGFB1	Transforming growth factor, beta 1	NM_000660
TGFB2	Transforming growth factor, beta 2	NM_003238
TGFB3	Transforming growth factor, beta 3	NM_003239
TGFBR1	Transforming growth factor, beta receptor I	NM_004612
TGFBR2	Transforming growth factor, beta receptor II	NM_003242
TNF	Tumor necrosis factor	NM_000594
TUFT1	Tuftelin 1	NM_020127
TWIST1	Twist homolog 1	NM_000474
VCAM1	Vascular cell adhesion molecule 1	NM_001078
VDR	Vitamin D (1,25- dihydroxyvitamin D3) receptor	NM_000376

Table II.7- (*Continued)*

Gene name	Description	Gene bank Accession no.
VEGFA	Vascular endothelial growth factor A	NM_003376
VEGFB	Vascular endothelial growth factor B	NM_003377
B2M	Beta-2-microglobulin	NM_004048
HPRT1	Hypoxanthine phosphoribosyltransferase 1 syndrome)	NM_000194
RPL13A	Ribosomal protein L13a	NM_012423
GAPDH	Glyceraldehyde-3-phosphate dehydrogenase	NM_002046
ACTB	Actin, beta	NM_001101

9. IN VITRO ANGIOGENESIS

The angiogenic potential of HDMEC growing on nano/micro fiber-combined scaffold and control scaffolds (without nano-fibers) was assessed by observing the cell migration from the scaffold into a collagen type I gel that mimics the in vivo microenvironment. Scaffolds with confluent HDMECs were transferred to a Petri dish, covered by a solution of collagen type I and when solidified into a gel culture medium supplemented with angiogenic growth factors 50 ng/mL VEGF (Biomol, Germany) and 10 ng/mL FGF-2 was added. After an additional 7 days in culture, the migration of ECs the samples was assessed by incubation with calcein-AM live-staining and visualization by CLSM. Furthermore, the obtained confocal image stacks were post-processed with the image processing software ITK-SNAP [28] to provide a better perception of the spatial distribution of capillary-like structures and micro-fibers.

REFERENCES

1. Martins AM, Santos MI, Azevedo HS, Malafaya PB, Reis RL. Natural origin scaffolds with in situ pore forming capability for bone tissue engineering applications. Acta Biomater. 2008.

2. Petrie Aronin CE, Cooper Jr JA, Sefcik LS, Tholpady SS, Ogle RC, Botchwey EA. Osteogenic differentiation of dura mater stem cells cultured in vitro on three-dimensional

porous scaffolds of poly([epsilon]-caprolactone) fabricated via co-extrusion and gas foaming. Acta Biomaterialia. 2008; 4(5):1187-97.

3. Pashkuleva I, Azevedo HS, Reis RL. Surface structural investigation of starch-based biomaterials. Macromol Biosci. 2008; 8(2):210-9.

4. Azevedo HS, Gama FM, Reis RL. In vitro assessment of the enzymatic degradation of several starch based biomaterials. Biomacromolecules. 2003; 4(6):1703-12.

5. Tietz NW, Shuey DF. Lipase in serum--the elusive enzyme: an overview. Clin Chem. 1993; 39(5):746-56.

6. Gomes ME, Azevedo HS, Moreira AR, Ella V, Kellomaki M, Reis RL. Starch-poly(epsilon-caprolactone) and starch-poly(lactic acid) fibre-mesh scaffolds for bone tissue engineering applications: structure, mechanical properties and degradation behaviour. J Tissue Eng Regen Med. 2008; 2(5):243-52.

7. Kweon H, Yoo MK, Park IK, Kim TH, Lee HC, Lee HS, et al. A novel degradable polycaprolactone networks for tissue engineering. Biomaterials. 2003; 24(5):801-8.

8. Gomes ME, Sikavitsas VI, Behravesh E, Reis RL, Mikos AG. Effect of flow perfusion on the osteogenic differentiation of bone marrow stromal cells cultured on starch-based three-dimensional scaffolds. J Biomed Mater Res. 2003; 67A(1):87-95.

9. Santos MI, Unger R, Sousa RA, Reis RL, Kirkpatrick CJ. Co-culture system of osteoblasts and endothelial cells, an in vitro strategy to enhance vascularization in bone regeneration. Tissue Engineering Part A. 2008; 14(5):712-.

10. Dietmar Werner Hutmacher JTSCXFLKCTTCL. State of the art and future directions of scaffold-based bone engineering from a biomaterials perspective. Journal of Tissue Engineering and Regenerative Medicine. 2007; 1(4):245-60.

11. Gomes ME, Bossano CM, Johnston CM, Reis RL, Mikos AG. In vitro localization of bone growth factors in constructs of biodegradable scaffolds seeded with marrow stromal cells and cultured in a flow perfusion bioreactor. Tissue Eng. 2006; 12(1):177-88.

12. Gomes ME, Holtorf HL, Reis RL, Mikos AG. Influence of the porosity of starch-based fiber mesh scaffolds on the proliferation and osteogenic differentiation of bone marrow stromal cells cultured in a flow perfusion bioreactor. Tissue Eng. 2006; 12(4):801-9.

13. Matthews JA, Wnek GE, Simpson DG, Bowlin GL. Electrospinning of collagen nanofibers. Biomacromolecules. 2002; 3(2):232-8.

14. Min BM, Lee G, Kim SH, Nam YS, Lee TS, Park WH. Electrospinning of silk fibroin nanofibers and its effect on the adhesion and spreading of normal human keratinocytes and fibroblasts in vitro. Biomaterials. 2004; 25(7-8):1289-97.

15. D. Li YX. Electrospinning of Nanofibers: Reinventing the Wheel? Advanced Materials. 2004; 16(14):1151-70.

16. Piez K, Eigner E, Lewis M. The chomatographic separation and amino acid composition of the subunits of several collagens. Biomechistry. 1962; 2(1):58-66.

17. Chu PK, Chen JY, Wang LP, Huang N. Plasma-surface modification of biomaterials. Materials Science & Engineering R-Reports. 2002; 36(5-6):143-206.

18. D. Léonard, P. Bertrand Y, Khairallah-Abdelnour, F. Arefi-Khonsari, Amouroux J. Time-of-flight secondary ion mass spectrometry (ToF-SIMS) study of SF6 and SF6-CF4 plasma-treated low-density polyethylene films. Surface and Interface Analysis. 1995; 23(7-8):467-76.

19. Macagnano A, Zampetti E, Pistillo BR, Pantalei S, Sgreccia E, Paolesse R, et al. Double layer sensors mimic olfactive perception: A case study. Thin Solid Films. 2008; 516(21):7857-65.

20. Alves CM, Reis RL, Hunt JA. Preliminary study on human protein adsorption and leukocyte adhesion to starch-based biomaterials. J Mater Sci Mater Med. 2003; 14(2):157-65.

21. Lord MS, Cousins BG, Doherty PJ, Whitelock JM, Simmons A, Williams RL, et al. The effect of silica nanoparticulate coatings on serum protein adsorption and cellular response. Biomaterials. 2006; 27(28):4856-62.

22. Sumpio BE, Riley JT, Dardik A. Cells in focus: endothelial cell. Int J Biochem Cell Biol. 2002; 34(12):1508-12.

23. Muller WA. Leukocyte-endothelial cell interactions in the inflammatory response. Laboratory Investigation. 2002; 82(5):521-33.

24. Krump-Konvalinkova V, Bittinger F, Unger RE, Peters K, Lehr HA, Kirkpatrick CJ. Generation of human pulmonary microvascular endothelial cell lines. Lab Invest. 2001; 81(12):1717-27.

25. Relou IAM, Damen CA, van der Schaft DWJ, Groenewegen G, Griffioen AW. Effect of culture conditions on endothelial cell growth and responsiveness. Tissue and Cell. 1998; 30(5):525-30.

26. Maciag T, Hoover GA, Stemerman MB, Weinstein R. Serial propagation of human endothelial cells in vitro. J Cell Biol. 1981; 91(2):420-6.

27. Jaffe EA, Nachman RL, Becker CG, Minick CR. Culture of Human Endothelial Cells Derived from Umbilical Veins - Identification by Morphologic and Immunological Criteria. Journal of Clinical Investigation. 1973; 52(11):2745-56.

28. Yushkevich PA, Piven J, Hazlett HC, Smith RG, Ho S, Gee JC, et al. User-guided 3D active contour segmentation of anatomical structures: Significantly improved efficiency and reliability. Neuroimage. 2006; 31(3):1116-28.

CHAPTER III

Response of micro- and macrovascular endothelial cells to starch-based fiber meshes for bone tissue engineering

CHAPTER III

Response of micro- and macrovascular endothelial cells to starch-based fiber meshes for bone tissue engineering *

ABSTRACT

The establishment of a functional vasculature is as yet an unrealized milestone in bone reconstruction therapy. For this study, fiber-mesh scaffolds obtained from a SPCL, that have previously been shown to be an excellent material for the proliferation and differentiation of bone marrow cells and thereby represent a great potential as constructs for bone regeneration, were examined for EC compatibility. To be successfully applied *in vivo*, this tissue engineered construct should also be able to support the growth of ECs in order to facilitate vascularization and therefore assure the viability of the construct upon implantation. The main goal of this study was to examine the interactions between ECs and SPCL fiber-meshes. Primary cultures of HUVEC cells were selected as a model of macrovascular cells and the cell line HPMEC-ST1 as a model for microvascular endothelial cells.

Both macro and microvascular ECs adhered to SPCL fiber-mesh scaffolds and grew to cover much of the available surface area of the scaffold. In addition, endothelial cells growing on the SPCL fibers exhibited a typical morphology, maintained important functional properties, such as the expression of the intercellular junction proteins, PECAM-1 and vascular endothelial-cadherin (VE-cadherin), the expression of the most typical endothelial marker vWF and sensitivity to pro-inflammatory stimuli, as shown by induction of the expression of cell adhesion molecules by LPS. These data indicate that ECs growing on SPCL fiber-mesh scaffolds maintain a normal expression of EC-specific genes/proteins, indicating a cell compatibility and potential suitability of these scaffolds for the vascularization process in bone tissue engineering *in vivo*.

* This chapter is based on the following publication:

M. I. Santos, S. Fuchs, M.E. Gomes, R.E. Unger, R.L Reis, C.J. Kirkpatrick. Response of micro- and macrovascular endothelial cells to starch-based fiber meshes for bone tissue engineering. Biomaterials. (2007). 28: 240-248.

1. INTRODUCTION

A critical obstacle in tissue engineering approaches based on the *in vitro* culture of cell-scaffold constructs prior to implantation is the ability to maintain large masses of living cells upon transfer from the *in vitro* culture conditions into the host [1]. *In vivo* most cells are no more than 100μm away from the nearest capillary, which serves to supply oxygen and nutrients, remove waste products and transport biochemical signals [2]. Insufficient vascularization results in hypoxic cell death of engineered tissues [3] and consequently in implant failure [4]. Considering that the infiltration of blood vessels into a macroporous scaffold is a process that occurs at a rate of < 1 mm per day and that it typically takes 1-2 weeks for the vascular structure to complete the penetration into relatively thin (3 mm thick) scaffolds [1], the need for the development of new approaches to increase the rate or augment vascularization is evident.

In the particular case of bone grafts the lack of a successful blood supply is implicated as one of the major factors responsible for implant failure. In bone, angiogenesis is a fundamental process for both osseous formation and repair [3]. Thus, for example, in intramembranous bone formation extensive vascularization is observed at the transition of pre-osteoblasts to osteoblasts [5]. In endochondral bone formation, an avascular cartilage template is replaced by highly vascularized bone tissue [6]. In the repair of fractures by callus production the formation of soft callus is accompanied by strong angiogenic activity [7]. Accordingly, strategies that enhance angiogenesis should have positive effects on bone repair [3]. Several approaches have emerged to solve the lack of vascularization in bone grafts, such as incorporation of angiogenic factors in the scaffold to stimulate the endogenous angiogenic response [8-10], deposition of an angiogenic extracellular matrix on the surface of the implant by a tumorigenic cell line [11, 12], vector delivery of genes encoding angiogenic factors [13-15], bulk culturing of EC as a homogenous population [13] or combined with osteoblasts [16]. These approaches all have in

common the focus on ECs because these are the primary cells making up the vasculature.

Previous studies [17, 18] have demonstrated that fiber-meshes obtained from a blend of starch and polycaprolactone constitute an excellent scaffolding material for rat bone marrow stromal cells, allowing for their proliferation and differentiation into osteoblasts. Bioreactor studies have also shown the expression of an array of bone growth factors by marrow stromal cells growing on SPCL fiber-mesh scaffolds [19]. However, for a bone cell-scaffold construct to be successful after implantation it should also elicit an adequate response of ECs. The scope of this work was to examine the ability of SPCL fiber-meshes, a scaffold for bone repair, to serve as an appropriate substrate for ECs. For this purpose two types of ECs, HUVEC and HPMEC-ST1 were cultured with SPCL fiber-mesh scaffolds and several functional and structural features of cells were analysed such as: viability, morphology, expression of EC markers and EC responsiveness to a pro-inflammatory stimulus.

2. MATERIALS AND METHODS

2.1. Scaffolds

The fiber-mesh scaffolds used in this study were based on SPLC (a polymeric blend of corn starch with polycaprolactone, 30/70% wt) and were obtained by a fiber bonding process, as described elsewhere [20]. The fiber-meshes scaffolds had a porosity of about 75% and for these experiments were cut into discs of approximately 8 mm diameter and 2 mm height. The scaffolds were sterilized by ethylene oxide and prior to cell seeding were immersed overnight in serum-free culture medium.

2.2. Cells and culture conditions

In this study primary cultures of human endothelial cells derived from umbilical vein (HUVEC) and the microvascular cell line HPMEC-ST1 developed from human pulmonary microvascular endothelial cells were used. HUVEC were isolated from umbilical vein by collagenase digestion according to a published method [21]. HUVECs were cultured in M199 medium (Sigma-Aldrich, Germany) supplemented with 10% FCS (Life Technologies, Germany), 10% FCS (PAA Laboratories, Germany), 100 U/100 µg/mL Pen/Strep (Sigma-Aldrich, Germany), 2mM Glutamax I (Life Technologies, Germany), 25 µg/mL sodium heparin (Sigma-Aldrich, Germany) and 25 µg/mL ECGS (BD Biosciences, USA). Cells were used until the fourth passage. The HPMEC-ST1 cell line was generated by transfection and displays the major constitutively expressed and inducible endothelial phenotypic markers [22]. HPMEC-ST1 was propagated in M199 culture medium supplemented with 20% FCS (Life Technologies, Germany), 2mM Glutamax I, 100 U/100 µg/mL Pen/Strep (Sigma-Aldrich, Germany), 50 µg/mL sodium heparin, 25 µg/mL ECGS and 50 µg/mL geneticin 418 (Life Technologies, Germany) for selection of transfected cells. Both cells were cultured until confluence in culture flasks cultured with 0.2% gelatin (Sigma-Aldrich, Germany).

2.3. Endothelial cell culture on SPCL fiber-mesh scaffolds

SPCL fiber-meshes were placed in 48 well plates and coated with 10µg/mL Fn in PBS (Roche, Germany) for 1 hour at 37ºC. A control in PBS without Fn was performed under the same conditions. Confluent HPMEC-ST1 and HUVEC cells were trypsinized and a suspension of $1{,}5x10^5$ HPMEC-ST1 cells or $2{,}5x10^5$ HUVEC cells was added per scaffold. The culture plate was placed in the incubator for 2 hours and then the cell-seeded SPCL fiber-meshes were transferred to a new 24 well plate with 1.5 ml of fresh culture medium. Cells from the same donor grown on cell culture polystyrene

were used as controls. The scaffolds were incubated under standard culture conditions (37ºC, 5% CO_2) for 3 and 7 days.

2.4. Endothelial cell imaging

The viability and morphology of endothelial cells on SPCL fiber-meshes was assessed, after 3 and 7 days, by CLSM following calcein-AM staining and by SEM. For CLSM visualization, SPCL fiber-meshes were incubated in culture medium with 0.1μM calcein-AM (Molecular Probes, Netherlands) for 10 min. Calcein-AM is a non-fluorescent permeable compound that once inside viable cells is converted by intracellular esterases into a fluorescent cell impermeable form. The calcein-AM stained scaffold was placed on a microscope slide and observed by CLSM (Leica TCS NT). In order to examine the growth and morphology of ECs on SPCL fiber-meshes the samples were treated for SEM observation. Samples were fixed with 2% glutaraldehyde in 0.1M sodium cacodylate buffer for 30 min, postfixed in 1% osmium tetroxide for 1 h, dehydrated in increasing concentrations of acetone, critical point dried and sputter coated with gold prior to SEM observation.

2.5. DNA quantification

The DNA content of each scaffold was measured using the PicoGreen DNA quantification assay (Molecular Probes). The samples were allowed to thaw at room temperature and then were sonicated for roughly 15 min. A description of the assay can be found elsewhere [23]. The number of cells on each scaffold was then calculated by correlation with the DNA of a known amount of ECs. Results are presented as means ± standard deviation (n=3).

2.6. Immunostaining of endothelial cell markers

The expression and localization of the endothelial cell markers PECAM-1, vWF and E-selectin was assessed by immunocytochemistry. The expression of PECAM-1 and vWF was assessed after growing HUVECs on SPCL fiber-mesh scaffolds for 7 days. The E-selectin staining was performed on HUVECs growing on SPCL fiber-mesh scaffolds and on cell culture plastic in the presence or absence of LPS. HUVEC cells on the scaffold and on plasticware were rinsed briefly with PBS and then fixed with 2% paraformaldehyde for 30 min. Samples were then rinsed in PBS and treated with 0.1% Triton for 5 min at RT. After washing with PBS the samples were incubated for 45 min at RT with the primary antibodies: mouse anti-human PECAM-1 (1:50, Dako, Denmark), rabbit anti-human vWF (1:8000, Dako, Denmark) and mouse anti-human E-selectin (1:100, Monosan). Following PBS washing, a second incubation was performed for 45 min at RT with the secondary antibodies: anti-mouse Alexa Fluor 488 for PECAM and E-selectin staining and anti-rabbit Alexa Fluor 488 for vWF (Molecular Probes, Netherlands). The nuclei were counterstained with 1μg/mL Hoechst in PBS for 5 min. SPCL fiber-meshes were then washed with PBS, mounted with Gel/Mount (Natutec, Germany) and visualized by CLSM (Leica TCS SP2).

2.7. Molecular analysis of proinflammatory genes

For assessment of cell adhesion molecules expression on HUVEC seeded on to SPCL fiber-meshes, these samples were cultured in the presence or absence of 1.0 μg/mL of LPS for 4 hours (Sigma-Aldrich, Germany). HUVEC cells grown on plasticware with and without LPS were used as controls. The cell adhesion molecules under analysis were E-selectin, ICAM, vascular cell adhesion molecule (VCAM) and the housekeeping gene β-actin was used as internal standard. Total RNA from HUVEC cells was extracted using the RNeasy Mini Kit (Qiagen, Germany) according to the manufacturer's protocol. Afterwards, the extracted RNA was reverse transcribed into

cDNA, (Omniscript RT Kit, Qiagen) and used for PCR analysis. Equal amounts of cDNA (1μg), measured by NanoDrop microspectrophotometer, were amplified by PCR with Taq DNA Polymerase Kit (Qiagen) and with gene-specific primer sets shown in Table III.1. Thirty five cycles were used for all genes, each one consisting of 2 min of denaturation at 94ºC, 30s of annealing (Table III.1) and 30s of chain elongation at 72ºC, followed by a final 10 min extension at 72ºC. Amplification products were separated by electrophoresis on an agarose gel (0.8%) and stained with ethidium bromide staining.

Table III.1 – Amplified genes, specific primer pair sequences and annealing temperature and product size

Name of gene (GenBank Accession no.)	Product size (bp)	Annealing Temperature (ºC)	Primer Pair sequences
β-actin (AB004047)	574	65	5'AGCATTTGCGGTGGACGATGGAG-3' 5'-GACCTGACTGACTACCTCATGA-3'
E-selectin (NM 000450)	304	62	5'-ATCAACATGAGCTGCAGTGG-3' 5'-AGCTTCCGTCTGATTCAAGG-3'
ICAM (J03132)	395	57	5'-TATTCAAACTGCCCTGATGG-3' 5'-CAGTGCGGCACGAGAAATTGG-3'
VCAM (X53051)	282	62	5'-TCTCATTGACTTGCAGCACC-3' 5'-ACTTGACTGTGATCGGCTTCC-3'

3. RESULTS

3.1. Micro- and macrovascular endothelial cell adhesion to SPCL fiber-mesh scaffolds

Endothelial cells of micro- (HPMEC-ST1) and macrovascular (HUVEC) origin were both able to attach and proliferate on Fn-coated SPCL fiber-meshes (Fig. III.1). However, in the absence of Fn coating, very few cells adhered, cells remained in a rounded-up

shape and with time, no cells were detected on SPCL fiber-meshes (data not shown). CLSM micrographs showed an increase in the cell number of HPMEC-ST1 (Fig. III.1A, C) and HUVEC (Fig. III.1B, D) cells, on the surface of SPCL fiber-meshes, between 3 and 7 days. Also, EC remained viable on SPCL fiber-meshes as shown by their ability to convert calcein-AM into a green fluorescent compound. To further confirm that cell numbers increased with time, cell DNA was isolated and quantified at two different time points, day 3 and 7 after addition of cells. As depicted in 1E, both HUVEC and HPMEC-ST1 cell numbers increased with time. Concerning cell morphology, SEM analysis showed that both micro- and macrovascular cells spread along the fibers, exhibited a typical flattened morphology and established contact with adjacent EC (Fig. III.2).

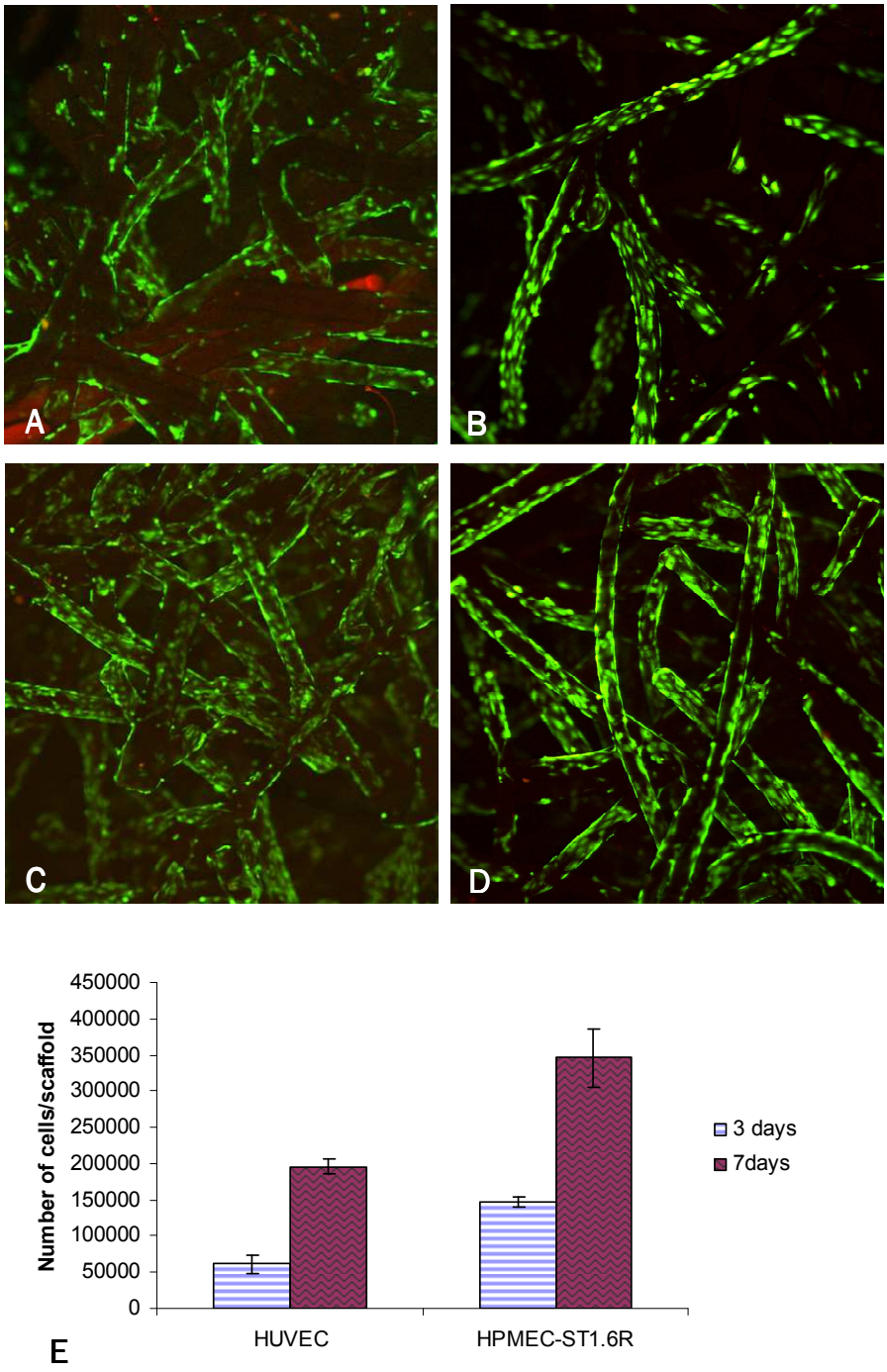

Figure III.1. Confocal micrographs of HPMEC-ST1 cells (A, C) and HUVEC (B, D) seeded on Fn-coated SPCL fiber-meshes stained by calcein-AM after 3 (A, B) and 7 days of culture (C, D). Magnification (100x). Number of cells on SPCL fiber-mesh scaffolds after 3 and 7 days of culture based on DNA quantification (as described in Materials and Methods) (E).

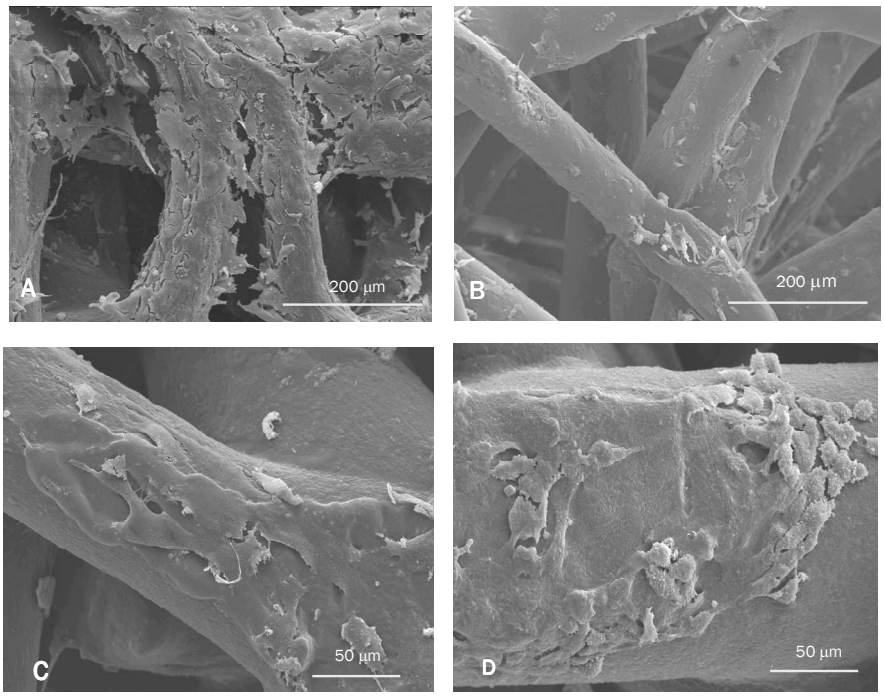

Figure III.2. SEM micrographs of HPMEC-ST1 (A, C) and HUVEC cells (B, D) on Fn-coated SPCL fiber-meshes, after 3 (A, B) and 7 days of culture (C, D).

3.2. Immunohistochemistry of endothelial cell markers

The expression of the endothelial cell markers vWF, PECAM and VE-cadherin was examined by immunohistochemistry. Immunostaining data showed vWF in a small dotted pattern surrounding the nuclei, and represented storage in Weibel-Palade bodies (Fig. III.3A-B). Strong PECAM-1 staining was observed at the cell-cell interface typical of endothelial cells on cell culture plastic and *in vivo* (Fig. III.4A-B). Immunostaining of VE-cadherin exhibited labelling at the intercellular junctions between adjacent EC, similar to cells grown on cell culture plastic (data not shown). Thus, the labelling pattern and localization of the endothelial cell structural markers for cells growing on SPCL fiber-mesh materials exhibited a similar pattern to that observed for HUVEC cells grown on normal cell culture plastic (data not shown).

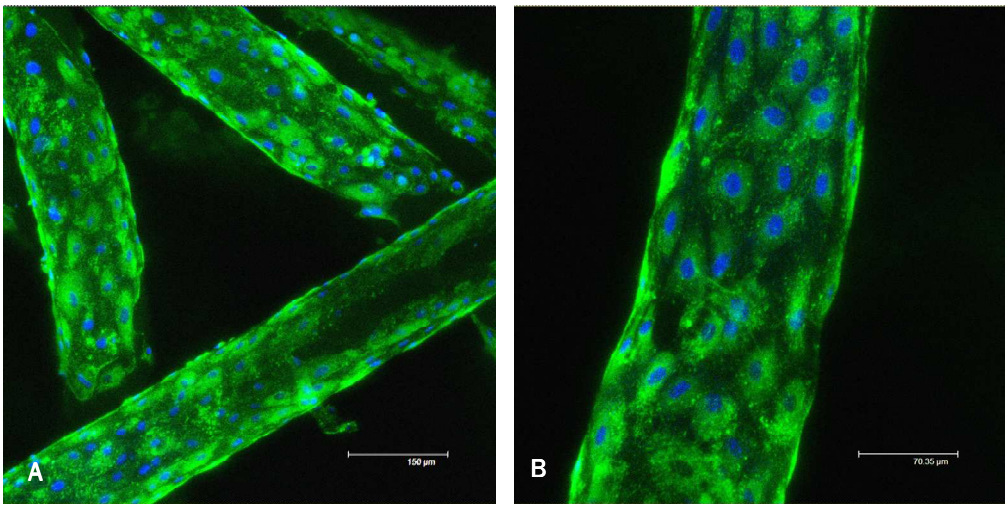

Figure III.3. Immunofluorescent micrographs of HUVEC cells grown for one week on Fn-coated SPCL fiber-meshes and stained for vWF (green fluorescence) and with Hoechst for nuclear staining (blue fluorescence).

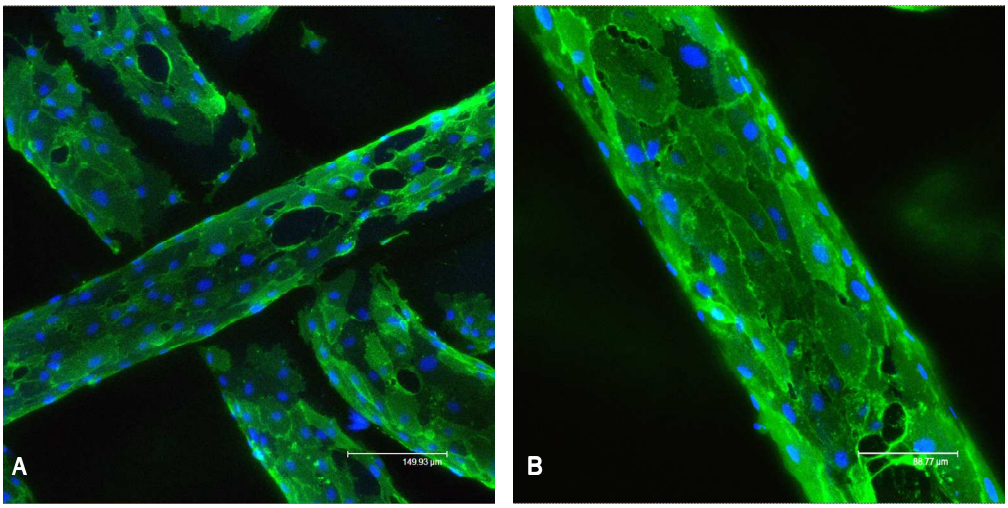

Figure III.4. Immunofluorescent micrographs of HUVEC cells grown for one week on Fn-coated SPCL fiber-meshes and stained for PECAM-1 (green fluorescence) and with Hoechst for nuclear staining (blue fluorescence).

3.3. Expression of pro-inflammatory genes

Endothelial cells are involved in the inflammatory response *in vivo* through the expression of cell adhesion molecules. These molecules are expressed by the inflamed endothelium in a sequential manner and in response to inflammatory

stimuli such as cytokines and endotoxins [24]. Fig. III.5 shows the mRNA expression of genes encoding cell adhesion molecules of HUVECs grown on plastic wells and on SPCL fiber-meshes, in the absence and in the presence of the pro-inflammatory stimulus. LPS, an endotoxin present in the cell wall of Gram-negative bacteria, was the selected stimulus. HUVEC grown on plastic wells in the absence of LPS expressed little or no levels of the cell adhesion molecules. However, in the presence of LPS an induction of cell adhesion molecules expression was observed. Under non-inflammatory conditions, HUVEC on the SPCL fiber-mesh scaffold had a low basal expression of ICAM, VCAM and E-selectin. In response to LPS, the expression of cell adhesion molecules increased.

Since RT-PCR analysis examines the RNA of the entire population and does not give an indication of the gene expression at the single-cell level, we also carried out an E-selectin staining of cells growing on the SPCL fiber-mesh scaffolds in the presence and absence of LPS and compared the expression to the same cell type growing on normal cell culture plastic. As depicted in Fig. III.6, a few HUVEC growing on both cell culture plastic and SPCL fiber-meshes exhibited an expression of E-Selectin in the absence of LPS. We generally observe this for primary endothelial cells in culture and between 1-5% of cells may exhibit expression of E-selectin in the absence of LPS stimulation (data not shown). However, after a 4 hour stimulation with LPS, a large number of cells were observed on both materials exhibiting E-selectin expression (Fig. III.6). Thus, endothelial cells grown on the SPCL fiber-meshes exhibited a similar pattern of expression and induction of E-selectin compared to cells growing on plastic.

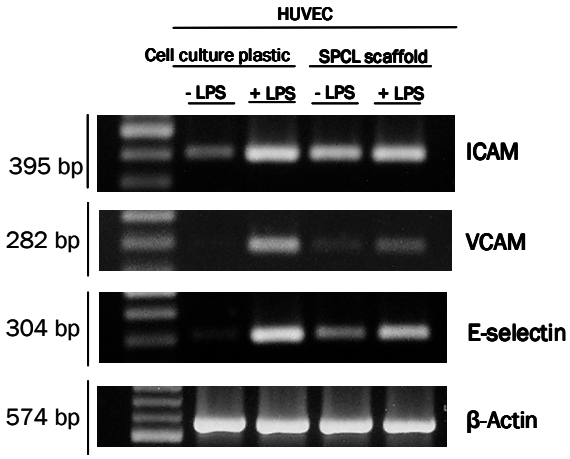

Figure III.5. PCR analysis of the genes that encode cell adhesion molecules on HUVEC cells grown on SPCL fiber-meshes for 7 days. cell adhesion molecule expression was assessed in the absence and in the presence of pro-inflammatory stimulus (LPS 1.0 μg/m for 4 h). β-actin was the selected housekeeping gene.

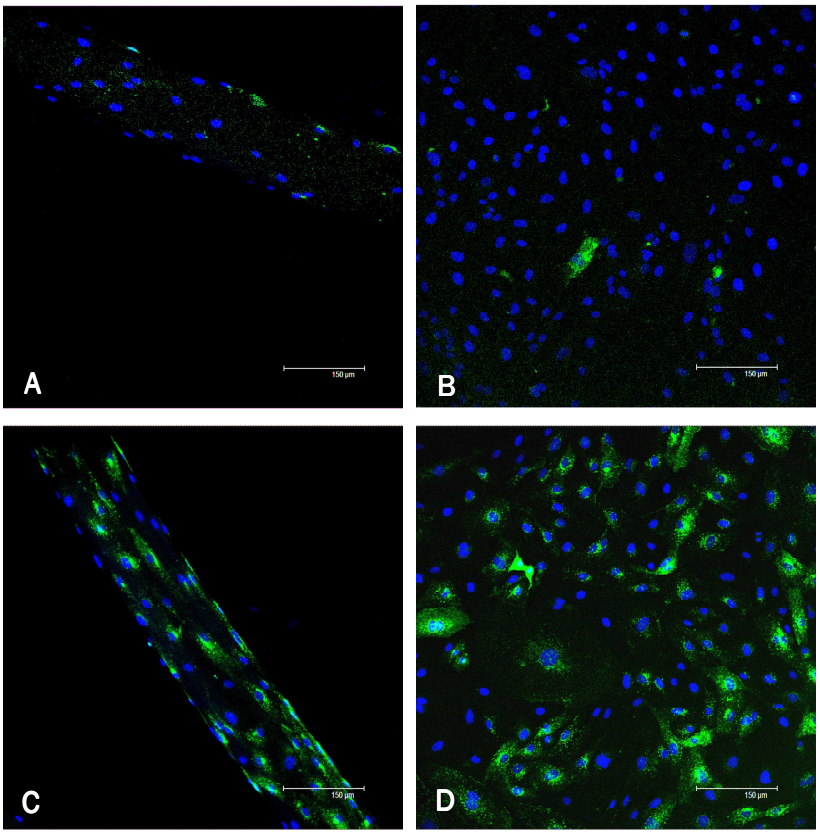

Figure III.6. Immunofluorescent images of E-selectin-stained HUVEC cells grown on Fn-coated SPCL fiber-meshes (A and C) and on cell culture plastic (B and D) with and without LPS for 4h. Figures A-B correspond to cells grown in the absence of LPS and C-D in its presence.

4. DISCUSSION

After implantation of a biomaterial, a neovascularization process begins with the formation and outgrowth of microvasculature from the host tissue. For this reason, the ability of a tissue engineering scaffold to illicit an appropriate response from the host endothelial cells is crucial for a successful vascularization of the implant. We have formerly described the SPCL fiber-mesh scaffold as a biomaterial for bone regeneration. Previous work has shown that this is an excellent scaffolding material for rat bone marrow stromal cells, allowing for their proliferation and differentiation into osteoblasts [17]. A successful implant not only requires the growth and function of the cells for a functioning tissue or organ replacement but also needs an intact vasculature to supply these cells with oxygen and nutrients and also to remove metabolites. Therefore, in this study the growth, morphology and gene expression of human endothelial cells on the SPCL fiber-mesh scaffolds were examined. HUVEC and the human microvascular endothelial cell line, HPMEC-ST1, were used to assess endothelial cell interaction with the biomaterial since these cells maintain the endothelial cell phenotype *in vitro* and have been validated on many biomaterials [25-27].

Calcein-AM staining (Fig. III.1) and SEM analysis (Fig. III.2) of HPMEC-ST1 and HUVEC cells on SPCL fiber-meshes showed that with time these cells covered much of the available surface area of the fiber-meshes. Cells grew to various depths in the fiber meshes and were also observed on the side opposite to that to which the cells were added (data not shown). An increase in cell number measured by DNA quantification was also observed for both cell types between day 3 and 7 (Fig. III.1E). In addition, cells remained viable and retained the typical flattened morphology for the tested periods. However, this behaviour was only shown on Fn-coated fiber meshes. This is not a surprising result, since it has been extensively reported in the literature [28, 29] that ECs show little adhesion and no proliferation on several kind of materials without prior coating with some form of extracellular matrix. Considering the relevance of the interactions of EC with extracellular matrix molecules for cell adhesion and proliferation [30, 31], a common way to improve this behaviour is

accomplished by coating the material with cell adhesion proteins, such as Fn, prior to the cell seeding. Plasma treatment of the surface of SPCL fiber-mesh scaffold may also be a way to improve the adhesion of endothelial cells without requiring the addition of extracellular matrix molecules [32] and we are currently examining this possibility. In addition to depending on the tight adhesion of the cells to the underlying basement membrane, the integrity of the endothelial layer is also strongly dependent on the junctions established between adjacent EC [33]. Such cell-cell adhesion is also crucial for vessels to sprout and the elongation process is mediated by a distinct series of cell surface receptors that includes PECAM-1 and VE-cadherin [34]. PECAM-1, or Platelet Endothelial Cell Adhesion Molecule-1, occurs on the endothelial cell membrane, close to the intercellular junctions, and regulates the adhesion of endothelial cells to other cells of the same type and to leukocytes [35]. VE-cadherin is an adhesion molecule that mediates cell-cell contact between ECs and plays a relevant role in the maintenance of vascular integrity [36]. Immunocytochemical data revealed the typical localization of the endothelial cell markers vWF, around the nuclei and PECAM-1 and VE-cadherin at the intercellular junctions between adjacent cells (Fig. III.3 and III.4). The maintenance of the expression of PECAM-1, VE-cadherin and vWF, by HUVEC cells on SPCL fiber-meshes is a good indicator of the interactions between EC and SPCL fiber-meshes.

In addition to participating in angiogenesis EC also play an important role in the inflammatory response. During the inflammatory response to endotoxins or cytokines a cross-talk between the endothelium and immune cells occurs resulting in the up-regulation of cell adhesion molecules. These molecules are expressed on the inflamed endothelium in a sequential manner. These cells are involved in the steps leading to the adherence of circulating leukocytes from the blood flow and in their transmigration to the inflammatory focus. Thus, for example, E-selectin induces a prolonged contact between circulating leukocytes, resulting in a decelerated rolling along the endothelium [24]. VCAM-1 favours the adhesion and transendothelial migration especially of lymphocytes where they find the specific ligand [35]. ICAM-1 is constitutively expressed at a low level on EC and during inflammation is up-regulated several fold to facilitate EC-leukocyte adhesion, especially neutrophils and monocytes [37, 38]. In contrast, E-selectin and VCAM are not usually expressed

under physiological conditions, indicating that they require induction, a process involving *de novo* mRNA synthesis, resulting ultimately in the expression of the gene product, which then appears on the EC plasma membrane [38]. Analysis of expression of cell adhesion molecules by RT-PCR and immunofluorescent staining of HUVEC cells grown on SPCL fiber-meshes compared with HUVEC cells on plastic provided information regarding the ability of these cells to participate in the inflammatory response through the expression of cell adhesion molecules in response to pro-inflammatory stimulus (Fig. III.5 and III.6). HUVEC cells growing on plastic wells were used as control and RT-PCR analysis of their mRNA revealed that little or none of the analyzed cell adhesion molecules was expressed in unstimulated cells. In the presence of LPS the cells responded by rapidly inducing the synthesis of mRNA of ICAM, VCAM and E-selectin. The intensity of the bands for the three cell adhesion molecules was higher than that detected in the absence of LPS. A similar result was observed by HUVEC growing on SPCL fiber-meshes in the presence and absence of LPS. Little or no expression of E-selectin, VCAM and ICAM by HUVEC cells was observed in the absence of LPS, and in the presence of LPS, a clear increase was observed. This indicates that growth on SPCL fiber-meshes does not effect the expression of the inflammatory genes, but after an inflammatory-stimulating event, a normal induction of gene expression occurs. This was also confirmed through the immunofluorescent staining of the cells for E-selectin. Under non-inflammatory conditions, only a few cells exhibited E-selectin staining. Upon LPS-stimulation, most of the cells exhibited some degree of E-selectin expression. Interestingly, the few cells expressing E-selectin in the absence of LPS also confirmed the results observed in the RT-PCR analysis (slight bands for E-selectin in the unstimulated cells, Fig. III.5). We routinely see that up to 5% of freshly isolated human endothelial cells may express cell adhesion molecules (unpublished data). However, in all cases, after the addition of LPS, an increase in the expression of cell adhesion molecules was observed, indicating normal cell behaviour when growing on the SPCL fiber-meshes.

5. CONCLUSIONS

It was found that endothelial cells from both macro and microvascular origin adhered to SPCL fiber-meshes and grew over much of the surface area of the scaffold and cells, with viability being maintained up to at least 7 days after addition to the scaffold. Moreover, SPCL fiber-mesh scaffolds supported the maintenance of EC morphological structure. Important functions such as endothelial integrity were maintained as shown by the expression of the endothelial intercellular junction proteins, PECAM-1 and VE-cadherin. The expression of the most typical endothelial marker vWF was also detected at single cell level. Furthermore, ECs cultures onto SPCL fiber-meshes were sensitive to a pro-inflammatory stimulus as was shown by the enhancement in the expression of cell adhesion molecules induced by LPS. The results obtained demonstrate that SPCL fiber-meshes are an excellent substrate for the growth of human endothelial cells required for the vascularization process. Our findings, coupled with those previously reported for bone marrow cells, suggest that SPCL fiber-meshes may have a potential for use as a scaffold material for bone tissue engineering applications.

REFERENCES

1. Nomi M, Atala A, Coppi PD, Soker S. Principals of neovascularization for tissue engineering. Mol Aspects Med. 2002; 23(6):463-83.

2. Freed LE, Vunjak-Novakovic G. Culture of organized cell communities. Advanced Drug Delivery Reviews. 1998; 33(1-2):15-30.

3. Stahl A, Wenger A, Weber H, Stark GB, Augustin HG, Finkenzeller G. Bi-directional cell contact-dependent regulation of gene expression between endothelial cells and osteoblasts in a three-dimensional spheroidal coculture model. Biochem Bioph Res Co. 2004; 322(2):684-92.

4. Cassell OC, Hofer SO, Morrison WA, Knight KR. Vascularisation of tissue-engineered grafts: the regulation of angiogenesis in reconstructive surgery and in disease states. Br J Plast Surg. 2002; 55(8):603-10.

5. Deckers MM, van Bezooijen RL, van der Horst G, Hoogendam J, van Der Bent C, Papapoulos SE, et al. Bone morphogenetic proteins stimulate angiogenesis through osteoblast-derived vascular endothelial growth factor A. Endocrinology. 2002; 143(4):1545-53.

6. Maes C, Carmeliet P, Moermans K, Stockmans I, Smets N, Collen D, et al. Impaired angiogenesis and endochondral bone formation in mice lacking the vascular endothelial growth factor isoforms VEGF164 and VEGF188. Mech Dev. 2002; 111(1-2):61-73.

7. Carano RA, Filvaroff EH. Angiogenesis and bone repair. Drug Discov Today. 2003; 8(21):980-9.

8. Huang YC, Kaigler D, Rice KG, Krebsbach PH, Mooney DJ. Combined angiogenic and osteogenic factor delivery enhances bone marrow stromal cell-driven bone regeneration. J Bone Miner Res. 2005; 20(5):848-57.

9. Kent Leach J, Kaigler D, Wang Z, Krebsbach PH, Mooney DJ. Coating of VEGF-releasing scaffolds with bioactive glass for angiogenesis and bone regeneration. Biomaterials. 2006; 27(17):3249-55.

10. Murphy WL, Simmons CA, Kaigler D, Mooney DJ. Bone regeneration via a mineral substrate and induced angiogenesis. J Dent Res. 2004; 83(3):204-10.

11. Kidd KR, Nagle RB, Williams SK. Angiogenesis and neovascularization associated with extracellular matrix-modified porous implants. J Biomed Mater Res. 2002; 59(2):366-77.

12. Kidd KR, Williams SK. Laminin-5-enriched extracellular matrix accelerates angiogenesis and neovascularization in association with ePTFE. J Biomed Mater Res A. 2004; 69(2):294-304.

13. Moldovan NI, Ferrari M. Prospects for microtechnology and nanotechnology in bioengineering of replacement microvessels. Arch Pathol Lab Med. 2002; 126(3):320-4.

14. Soker S, Machado M, Atala A. Systems for therapeutic angiogenesis in tissue engineering. World J Urol. 2000; 18(1):10-8.

15. Alessandri G, Emanueli C, Madeddu P. Genetically engineered stem cell therapy for tissue regeneration. Ann N Y Acad Sci. 2004; 1015:271-84.

16. Wenger A, Stahl A, Weber H, Finkenzeller G, Augustin HG, Stark GB, et al. Modulation of in vitro angiogenesis in a three-dimensional spheroidal coculture model for bone tissue engineering. Tissue Eng. 2004; 10(9-10):1536-47.

17. Gomes ME, Sikavitsas VI, Behravesh E, Reis RL, Mikos AG. Effect of flow perfusion on the osteogenic differentiation of bone marrow stromal cells cultured on starch-based three-dimensional scaffolds. J Biomed Mater Res. 2003; 67A(1):87-95.

18. Tuzlakoglu K, Bolgen N, Salgado AJ, Gomes ME, Piskin E, Reis RL. Nano- and micro-fiber combined scaffolds: a new architecture for bone tissue engineering. J Mater Sci Mater Med. 2005; 16(12):1099-104.

19. Gomes ME, Bossano CM, Johnston CM, Reis RL, Mikos AG. In vitro localization of bone growth factors in constructs of biodegradable scaffolds seeded with marrow stromal cells and cultured in a flow perfusion bioreactor. Tissue Eng. 2006; 12(1):177-88.

20. Gomes ME, Godinho JS, Tchalamov D, Cunha AM, Reis RL. Alternative tissue engineering scaffolds based on starch: processing methodologies, morphology, degradation and mechanical properties. Materials Science & Engineering C-Biomimetic and Supramolecular Systems. 2002; 20(1-2):19-26.

21. Jaffe EA, Nachman RL, Becker CG, Minick CR. Culture of Human Endothelial Cells Derived from Umbilical Veins - Identification by Morphologic and Immunological Criteria. Journal of Clinical Investigation. 1973; 52(11):2745-56.

22. Krump-Konvalinkova V, Bittinger F, Unger RE, Peters K, Lehr HA, Kirkpatrick CJ. Generation of human pulmonary microvascular endothelial cell lines. Lab Invest. 2001; 81(12):1717-27.

23. Punshon G, Vara DS, Sales KM, Kidane AG, Salacinski HJ, Seifalian AM. Interactions between endothelial cells and a poly(carbonate-silsesquioxane-bridge-urea) urethane. Biomaterials. 2005; 26(32):6271-9.

24. Muller AM, Hermanns MI, Cronen C, Kirkpatrick CJ. Comparative study of adhesion molecule expression in cultured human macro- and microvascular endothelial cells. Exp Mol Pathol. 2002; 73(3):171-80.

25. Unger RE, Huang Q, Peters K, Protzer D, Paul D, Kirkpatrick CJ. Growth of human cells on polyethersulfone (PES) hollow fiber membranes. Biomaterials. 2005; 26(14):1877-84.

26. Unger RE, Peters K, Wolf M, Motta A, Migliaresi C, Kirkpatrick CJ. Endothelialization of a non-woven silk fibroin net for use in tissue engineering: growth and gene regulation of human endothelial cells. Biomaterials. 2004; 25(21):5137-46.

27. Unger RE, Peters K, Huang Q, Funk A, Paul D, Kirkpatrick CJ. Vascularization and gene regulation of human endothelial cells growing on porous polyethersulfone (PES) hollow fiber membranes. Biomaterials. 2005; 26(17):3461-9.

28. Chu CF, Lu A, Liszkowski M, Sipehia R. Enhanced growth of animal and human endothelial cells on biodegradable polymers. Biochim Biophys Acta. 1999; 1472(3):479-85.

29. Boura C, Muller S, Vautier D, Dumas D, Schaaf P, Claude Voegel J, et al. Endothelial cell--interactions with polyelectrolyte multilayer films. Biomaterials. 2005; 26(22):4568-75.

30. Pompe T, Markowski M, Werner C. Modulated fibronectin anchorage at polymer substrates controls angiogenesis. Tissue Engineering. 2004; 10(5-6):841-8.

31. Marin V, Kaplanski G, Gres S, Farnarier C, Bongrand P. Endothelial cell culture: protocol to obtain and cultivate human umbilical endothelial cells. J Immunol Methods. 2001; 254(1-2):183-90.

32. Pu FR, Williams RL, Markkula TK, Hunt JA. Effects of plasma treated PET and PTFE on expression of adhesion molecules by human endothelial cells in vitro. Biomaterials. 2002; 23(11):2411-28.

33. Ayalon O, Sabanai H, Lampugnani MG, Dejana E, Geiger B. Spatial and Temporal Relationships between Cadherins and Pecam-1 in Cell-Cell Junctions of Human Endothelial-Cells. J Cell Biol. 1994; 126(1):247-58.

34. Cines DB, Pollak ES, Buck CA, Loscalzo J, Zimmerman GA, McEver RP, et al. Endothelial cells in physiology and in the pathophysiology of vascular disorders. Blood. 1998; 91(10):3527-61.

35. Cenni E, Granchi D, Ciapetti G, Verri E, Cavedagna D, Gamberini S, et al. Expression of adhesion molecules on endothelial cells after contact with knitted Dacron. Biomaterials. 1997; 18(6):489-94.

36. Nachtigal P, Gojova A, Semecky V. The role of epithelial and vascular-endothelial cadherin in the differentiation and maintenance of tissue integrity. Acta Medica (Hradec Kralove). 2001; 44(3):83-7.

37. Remy M, Valli N, Brethes D, Labrugere C, Porte-Durrieu MC, Dobrova NB, et al. In vitro and in situ intercellular adhesion molecule-1 (ICAM-1) expression by endothelial cells lining a polyester fabric. Biomaterials. 1999; 20(3):241-51.

38. Kirkpatrick CJ, Wagner M, Kohler H, Bittinger F, Otto M, Klein CL. The cell and molecular biological approach to biomaterial research: A perspective. J Mater Sci-Mater M. 1997; 8(3):131-41.

CHAPTER IV

Surface-Modified 3D Starch-based Scaffold for Improved Endothelialization for Bone Tissue Engineering

CHAPTER IV

Surface-Modified 3D Starch-based Scaffold for Improved Endothelialization for Bone Tissue Engineering *

ABSTRACT

Providing adequate vascularization is one of the main hurdles to the widespread clinical application of bone tissue engineering approaches. Due to their unique role in blood vessel formation, EC play a key role in the establishment of successful vascularization strategies. However, currently available polymeric materials do not generally support EC growth without coating with adhesive proteins. In this work we present Ar plasma treatment as a suitable method to render the surface of a 3D starch-based scaffold compatible for ECs, this way obviating the need for protein pre-coating. To this end we studied the effect of plasma modification on surface properties, protein adsorption and ultimately on several aspects regarding EC behavior. Characterization of surface properties revealed increased surface roughness and change in topography, while at the chemical level a higher oxygen content was demonstrated. The increased surface roughness of the material, together with the changed surface chemistry modulated protein adsorption as indicated by the different adsorption profile observed for Vn. *In vitro* studies showed that human umbilical vein ECs (HUVECs) seeded on plasma-modified scaffolds adhered, remained viable, proliferated, and maintained the typical cobblestone morphology, as observed for positive controls (scaffold pre-coated with adhesive proteins). Furthermore, genotypic expression of endothelial markers was maintained and neighbouring cells expressed PECAM-1 at the single-cell-level. These results indicate that Ar plasma modification is an effective methodology with potential to be incorporated in biomaterial strategies to promote the formation of vascularized engineered bone.

* This chapter is based on the following publication:

Santos M. I., Pashkuleva I., Alves C.M., Gomes M.E., Fuchs S., Unger R.E., Reis R.L., Kirkpatrick C.J. Surface-Modified 3D Stach-based Scaffold for Improved Endothelialization for Bone Tissue Engineering. (2008). *Submitted*.

1. INTRODUCTION

During its 15 years of existence the tissue engineering field has evolved greatly and important milestones have been achieved [1]. However, despite the major advances this field has brought, the lack of vascular supply remains the holy grail and the main hurdle to the clinical application of large constructs. When *in vitro* engineered cellular constructs are transferred *in vivo*, they have to rely on processes, such as interstitial fluid diffusion and blood perfusion to cover their metabolic demands [2]. Theoretical modeling studies predict hypoxia and central necrosis in almost any graft site with a diffusion distance of more than 500 to 1000 μm [3]. Therefore, a successful engineered-construct must be supported by a dense capillary network connected to the microcirculation at the implantation site, supplying perfusion for adequate oxygenation and nutrition, as well as removal of waste products from the corresponding tissues.

In the particular case of bone, a functional vascular network is more than just simple conduits that ensure cellular metabolic requirements. Its importance is already manifest in bone ontogeny, where angiogenesis precedes osteogenesis and continues during bone process repair [4]. Furthermore, initial vascularization may be essential for enhanced engraftment and prevention of infections [2]. For these reasons, induction of vascularization is an integral element of any successful bone tissue engineering concept. Several strategies have been proposed to accelerate vascularization in engineered bone. Hybrid approaches, combining tissue engineering with microvascular surgical techniques such as free bone flap [5] and pedicle bone flap transplantation [6], have been described. Nevertheless, these methods are associated with several major drawbacks such as the need for a donor site, creation of a soft-tissue donor-site defect and the consequent patient inconvenience in the clinical setting [5, 7]. The localized or systemic application of angiogenic growth factors has also been one of the most popular strategies [8]. Delivery systems releasing a single angiogenic growth factor [9] have been upgraded into multi-phasic delivery systems [10], able to promote the formation of more stable vessels. However, these systems can only be regarded as an adjuvant of vascularization

orchestration. As ECs are the main cellular mediator of neovascular growth several approaches for vascularized engineered-bone involving this cell type have been explored. Strategies involving bulk culturing of mature ECs [11], progenitor cells [12] or ECs combined with other cell types such as osteoblasts [13] can be found in the literature. It is expected that in the *in vivo* environment ECs migrate out from the tissue-engineered construct into the implantation site, form networks of capillaries and gain access to the recipient's circulation [2, 7]. Hence, whether relying on an extrinsic or intrinsic blood supply, the adopted neovascularization approach will always have, directly or indirectly, ECs as target cell type. Therefore, it is of ultimate importance that the 3D construct is compatible with this cell type.

It is rare that a biomaterial with adequate bulk properties also possesses the surface characteristics suitable for clinical application [14] and this is particularly true for ECs because most of the proposed polymeric substrates do not support their adhesion and growth. A common approach is to fabricate biomaterials with appropriate bulk properties and to modify those by specific treatments resulting in enhanced surface properties [15]. Surface modification techniques for 3D polymeric structures include different wet chemical treatments such as grafting, attaching cell-recognizing ligands or more aggressive methods as soaking in oxidative or hydrolytic baths. However, lack of reactive groups on the polymer backbones and/or interactions between the solvents and the modified materials, also leading to bulk modification, are very often obstacles to the use of these methods. Hence, some research has been focused on coating of scaffolds with extracellular matrix proteins in order to increase cell adhesion to the surface [16, 17]. Although this approach overcomes the difficulties related with the wet-based treatments, protein adsorption is a difficult process to control and its stability with time is problematic [18]. Plasma surface modification has only recently been considered as an alternative route to enhance the surface biocompatibility of 3D polymer-based structures [19, 20]. The difficulties in modification of scaffolds by plasma are enhanced by the requirement for highly porous and interconnected samples. Therefore, application of different plasma surface modification has been limited to various polymer membranes and 2D bulk structures.

In this work, fiber-mesh scaffolds made from SPCL and previously proposed for bone engineering scaffolding [21-24], have been modified by means of Ar plasma treatment. This method was applied to tailor the surface of this type of scaffold to promote EC adhesion and proliferation, and thus obviate the need for protein pre-coating. To our knowledge this is the first report on a efficient plasma surface modification of a 3D natural-based construct for tissue engineering applications. The effect of plasma treatment at the surface properties level and its influence on the adsorption of adhesive proteins were assessed. Furthermore, the ultimate benefits of plasma-modified SPCL fiber-mesh scaffolds were evaluated by assessing EC biological responses, namely adhesion, proliferation profile and genotypical/phenotypical expression of endothelial markers.

2. MATERIALS AND METHODS

2.1. Scaffolds

Scaffolds produced from a blend of starch with polycaprolactone (SPCL, 30/70 wt%) were used for this study. SPCL fiber-mesh scaffolds were obtained by a fiber-bonding process consisting of spinning, cutting and sintering melt-spun fibers, as previously described [21, 22, 25]. The samples were cut into discs with 8 mm diameter and 2 mm height and sterilized by ethylene oxide.

2.2. Plasma Surface Modification

The surface treatment was performed using a plasma reactor PlasmaPrep$_5$ (Gala Instrument GmbH, Germany) with a fully automated process control. Ar was used as a working gas and the pressure in the reactor was controlled (0.18 mbar) by adjusting flow rate. Prior the treatment, the chamber was pursuit with Ar five times. A radio frequency source (13.56MHz) was used and a power of 30 W was applied for

15 minutes. The samples were kept at air atmosphere after being removed from the reactor.

2.3. Surface characterization and protein adsorption

2.3.1. Scanning electron microscopy (SEM)

The surface morphology of SPCL fibers was analysed by SEM (Leica Cambridge S360, UK) before and after plasma treatment. The samples were previously sputter-coated with gold in an ion sputter chamber (JEOL JFC 1100). Microphotographs at the surface were taken at various magnifications.

2.3.2. Optical profiler analysis

Optical profilometry is a non-contact method which allows roughness analysis of 3D structures with high resolution from subnanometer to millimeter step□height. In this study an optical profiler Wyko NT 3300 from Veeco Instruments Inc. was used. The measurements were performed in VSI mode and an area of 2 mm was analysed with vertical resolution of 3 nm.

2.3.3. X-Ray photoelectron spectroscopy (XPS)

XPS was used to determine the elemental surface composition of treated and untreated samples. The analysis was carried out using the instrument VG Escalab 250 iXL (VG Scientific, UK). The measurements were performed with monochromatic Al-Kα radiation (hv=1486.6 eV) in a constant analyzer energy mode (CAE) with 100 eV pass energy for survey spectra and 20 eV pass energy for high-resolution spectra. Photoelectrons were collected from a take-off angle of 90° relative to the sample surface. Charge referencing was adjusted by setting the lower binding energy C1s

hydrocarbon (CH_x) peak at 285.0 eV. Surface elemental composition was determined by standard Scofield photoemission cross sections. The identification of the chemical functional groups was obtained from the high-resolution peak analysis of C1s envelopes by XPSPEAK 4.1 software.

2.3.4. Time-of-Flight Secondary Ion Mass Spectrometry (TOF-SIMS)

Detailed quantitative analysis of the surface composition before and after plasma modification was obtained by TOF-SIMS. The mass spectra of the samples were recorded on a TOF-SIMS IV instrument from Ion-TOF GmbH Germany. The samples were bombarded with a pulsed bismuth ion beam (25 keV) at 45º incidence over an area with size 100 mm^2. The generated secondary ions were extracted with a 10 kV voltage and their time of flight from the sample to the detector was measured in a reflection mass spectrometer.

2.3.5. Contact angle measurements

Surface wettability was evaluated by static contact angle measurements on 2D samples prepared by a procedure similar to the one used for the scaffolds, i.e. by polymer melting with subsequent injection into a mould. Prior measurements, the samples were plasma modified at the same conditions used for the scaffolds. The values were obtained by sessile drop method using a contact angle meter OCA15+ with a high-performance image processing system from DataPhysics Instruments, Germany. The used liquid (H_2O, 1 mL, HPLC grade) was added by a motor driven syringe at room temperature. Five samples of each material were used and six measurements per sample were carried out. The normality of the data was checked by applying the Shapiro-Wilk's W-test. Since all the samples followed a normal distribution, Student's t-tests for independent samples were performed to test differences. Throughout the following discussion differences were considered

significant if $p<0.05$, and highly significant if $p<0.01$. The statistical analysis was performed with the package Statistica 6.0 (StatSoft, USA).

2.3.6. Protein adsorption: Immunolabelling and Confocal Laser Scanning Microscopy (CLSM)

The effect of plasma treatment on the adsorption of Fn and Vn from the cell culture media was investigated using CLSM in combination with fluorescent immunolabelling methodology. The protein system used in this study was a multi-protein solution of 20% (v/v) of FCS (Sigma, Germany) in of M199 medium (Sigma, Germany). Untreated and plasma treated SPCL scaffolds were immersed in this solution and incubated for 1h at RT. Samples immersed in PBS were used as blanks. Then, samples were fixed in 2.5 % formalin solution for 5 min and washed with PBS solution. Afterwards, samples were incubated with primary antibody mouse anti-human Fn with calf cross-reactivity (1:50, Sigma, Germany) or mouse anti-bovine anti-vitronectin (1:50, Santa Cruz, USA). After washing with PBS, materials were incubated with goat anti-mouse Alexa Fluor 488 secondary antibody (Invitrogen, USA), for 1 h at RT. Labelled samples were analysed by CLSM (Olimpus IX81).

2.4. Cell culture and scaffold seeding

Primary endothelial cells (ECs) derived from the umbilical cord vein (HUVECs) were used for cell culture studies. The cells were isolated from the umbilical vein by collagenase solution. Further details about the procedure can be found elsewhere [26]. HUVECs were cultured in M199 medium supplemented with 20 % FCS, 1% penicillin/streptomycin, 25 µg/mL ECGS (BD Bioscience, USA) and 2 mM Glutamax I (Gibco, Germany). Cells were cultured in culture flask previously coated with 0,2 % gelatine (Sigma, Germany).

Prior to cell seeding SPCL fiber-mesh scaffolds were soaked overnight in culture medium without serum. Untreated scaffolds pre-coated with 10 µg/mL Fn in PBS

(Roche, Germany) for 1 h at 37 ºC were used as positive control since this is a standard procedure to improve ECs adhesion to a certain substrate. As negative control non-coated untreated scaffolds were used. Plasma-modified SPCL fiber-mesh scaffolds were also not coated with any protein. Confluent HUVECs were trypsinized and a suspension of 2 x 10^5 cells was added per scaffold. The samples were incubated under standard culture conditions (37 ºC, 5 % CO_2) for up to 7 days.

2.5. Characterization of cell viability, growth and morphology

Cell growth and viability were assessed by staining with the fluorochrome dye calcein-AM and samples were visualized by CLSM. HUVECs were cultured for 4 hrs, 3 days and 7 days on the three materials studied: i) Ar plasma-modified SPCL fiber-mesh scaffold; ii) positive control (untreated and Fn-coated scaffold); and iii) negative control (untreated and non-coated scaffold). After each time point, the samples were incubated in culture medium with 0.1 μM calcein-AM (Invitrogen, USA) for 10 min under standard culture conditions. For CLSM (Leica TCS NT), and samples were prepared in mounting medium (Natutec, Germany). SEM was used to evaluate cellular morphology. Thus, after 7 days of culture samples were fixed with 2 % glutaraldehyde in 0.1 M sodium cacodylate buffer for 30 min and postfixed in 1 % osmium tetroxide for 1 h. Subsequently, samples were dehydrated with increasing ethanol concentrations, dried with hexamethyldisilasane and sputter coated with gold.

2.6. Cell proliferation assay

The DNA content in the scaffolds lysate was determined using the fluorescent picoGreen dsDNA quantification assay (Invitrogen, USA). The samples were thawed at RT and sonicated for 15 min. A detailed description of the assay is published elsewhere [27]. The number of cells was calculated by correlation with the DNA content of a known number of ECs. Triplicates were prepared for all materials and results were presented as means ± standard deviations. All the values were analysed

by a two-tailed student's *t*-test. Throughout the following discussion, the differences were considered significant if $p<0.05$.

2.7. Gene and protein expression

The expression of markers related with ECs and angiogenesis, namely PECAM-1 (CD31), (vascular endothelial growth factor receptor 1) VEGFR1 and VE-cadherin, was assessed at the mRNA level by semi-quantitative PCR. Total RNA was extracted from HUVECs cultured for 7 days on Ar plasma-modified SPCL scaffold, on the positive control and on 2D tissue culture polystyrene (TCPs), using the RNeasy Micro Kit (Qiagen, Germany). Equal amounts of RNA (1 μg), measured by the NanoDrop microspectrophotometer, were reverse transcribed into cDNA (Omniscript RT Kit, Qiagen, Germany). Afterwards, using gene-specific primer sets (Table IV.1) the genes of interest were amplified by PCR with Taq DNA polymerase Kit (Qiagen). The procedure for all the genes included 35 cycles, consisting of an initial stage of 2 min of denaturation at 94ºC, followed by 30 s of annealing (Table IV.1), 30 s of chain elongation at 72 ºC and a final 10 min extension at 72 ºC. Amplification products were separated by electrophoresis on an agarose gel (0.8 %) and stained with ethidium bromide. β-actin was selected as the housekeeping gene.

Table IV.1. Genes under evaluation, primers and PCR conditions

Name of gene (GenBank Accession no.)	Product size (bp)	Annealing Temperature (ºC)	Primer Pair sequences
β-actin (AB004047)	574	65	5'AGCATTTGCGGTGGACGATGGAG-3' 5'-GACCTGACTGACTACCTCATGA-3'
PECAM-1	280	57	5'- CAACAGACATGGCAACAAGG-3' 5'- TTCTGGATGGTGAAGTTG GC-3'
VE-cadherin	452	57	5'-GCTGAAGGAAAACCAGAAGAAGC-3' 5'-TCGTGATTATCCGTGAGGGTAAAG-3'
VEGF-R1	665	55	5' – TCTCCTTAGGTGGGTCTCC – 3' 5' – CAGCTCAGCGTGGTCGTAG – 3'

The expression of PECAM-1, a major endothelial hallmark, was evaluated at the cell-cell level by immunocytochemistry. Hence, after 7 days of culture, the samples were fixed with a solution of 2 % paraformaldehyde for 30 min and washed with PBS. Then, the cells were permeabilized with 0.1 % Triton for 5 min and incubated with mouse anti-human PECAM-1 (1:50, Dako, Denmark) for 1 h. After PBS washing, the secondary antibody goat anti-mouse Alexa Fluor 488 (Invitrogen, USA) was added and incubated for 1 h. Nuclei were counterstained with 1 µg/mL Hoechst in PBS for 5 min. For CLSM observation SPCL fiber-mesh scaffolds were covered with mounting medium. All immunostainning procedures were performed at RT.

3. RESULTS

3.1. Physical and chemical characterization of Ar plasma modified SPCL fiber-mesh scaffolds

During the contact of plasma with the biomaterial surface different physical and chemical processes occur. These processes can provoke changes in surface morphology and composition, which in turn can affect protein and cell behaviour on the modified material. Untreated materials presented a smooth surface with minor irregularities (Figs. IV.1A and IV.2A), typically observed for melt-processed polymers. Although the SEM analysis did not show different morphology or surface texture after the applied plasma treatment (pictures not shown) the results from optical profiler demonstrated (Figs. IV.1B and IV.2B) a strong increase of the surface roughness for the modified samples. An average roughness of Ra= 144.5±6.5 nm was measured for the untreated samples, while this value was almost double for the modified ones (Ra=236.5±18.5 nm). Moreover, not only roughness but also a topography change was observed for the modified samples and the characteristic signal for the untreated samples' laminated structure was markedly reduced (Fig. IV.2).

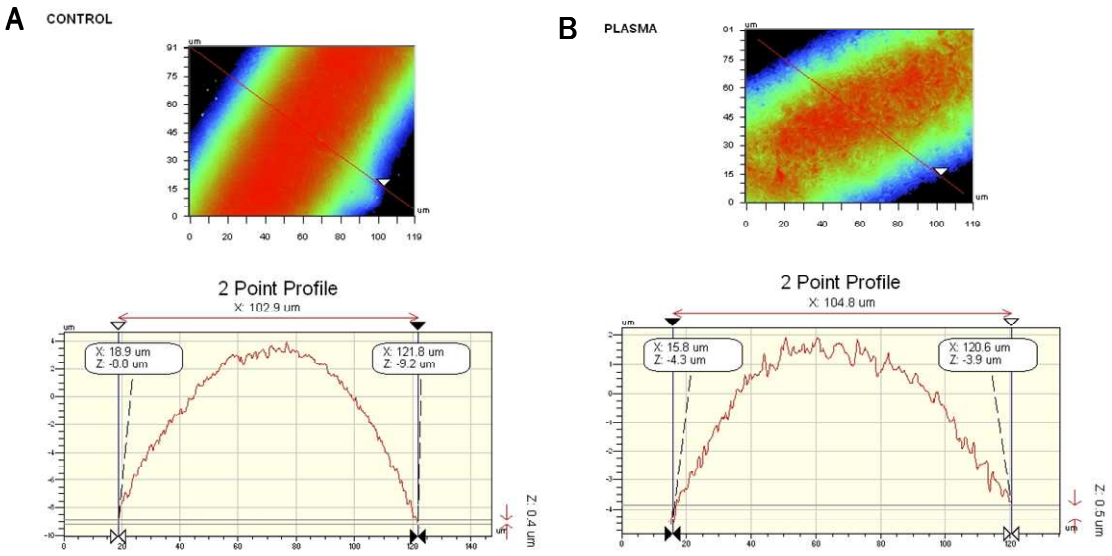

Figure IV.1. Two-points line profile analysis for untreated (A) and plasma modified (B) SPCL

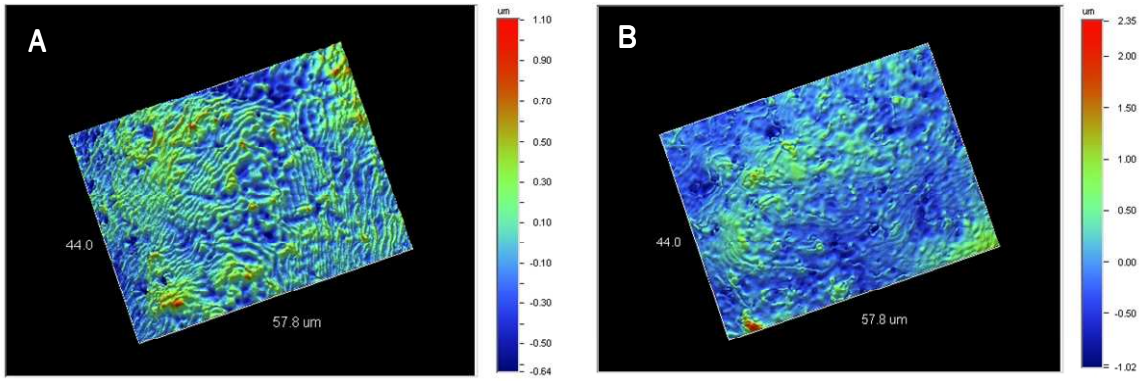

Figure IV.2. Optical profiler micrographs for SPCL fibers before (A) and after (B) surface modification by Ar plasma (Mode: VSI, Mag: 107x)

On the other hand, the surface chemistry was also affected by the applied treatment and significantly higher oxygen content was measured for the modified surface compared to the untreated one (Table IV.2). The measured C:O ratio together with the TOF-SIMS spectrum (Fig. IV.3A) of the untreated material, shows predominant

presence of the synthetic component (PCL) on the surface. Prominent peaks characteristic for the low mass hydrocarbon fragments derived from the linear back bone of PCL [28] were detected at m/z 41, 55, 69, 97 as well as the monomer $(M+H)^+$ at m/z 115. The applied treatment by plasma was confirmed by SIMS and less intensive peaks were detected in the positive mass spectrum of modified samples (Fig. IV.3B). The decrease of these peaks intensities for the treated material reflects the attack of the aliphatic sites and the subsequent loss/modification of these groups. The change in the general appearance of the negative mass spectra (Fig. IV.4) as a result of the treatment is typical [29] for plasma-treated polymers. The original polymer gives rise to a limited number of intense peaks (Fig. IV.4A), referring to structural ions while plasma treatment produces complex patterns with an intense peak on almost every m/z (Fig. IV.4B), although the signal-to-noise ratio of individual peaks remains good.

The contact angle values did not show any significant changes in the hydrophilicity of the studied materials. The value of 83.56±5.34 measured for untreated material was almost the same as that (81.76±2.09) measured after the applied treatment by plasma. However, it must be noticed that because of the changes in the surface roughness the effect of Cassie [30] must be present and influences the measured values, especially those after modification.

Table IV.2. Calculated atomic concentrations of the building elements (carbon and oxygen) of the studied materials

Material	%C	%O	C:O ratio
Theoretical PCL	75.0	25.0	3.00
Theoretical SPCL	68.9	31.1	2.20
Untreated SPCL scaffolds	77.0	23.0	3.35
Plasma-modified SPCL scaffolds	72.2	27.8	2.60

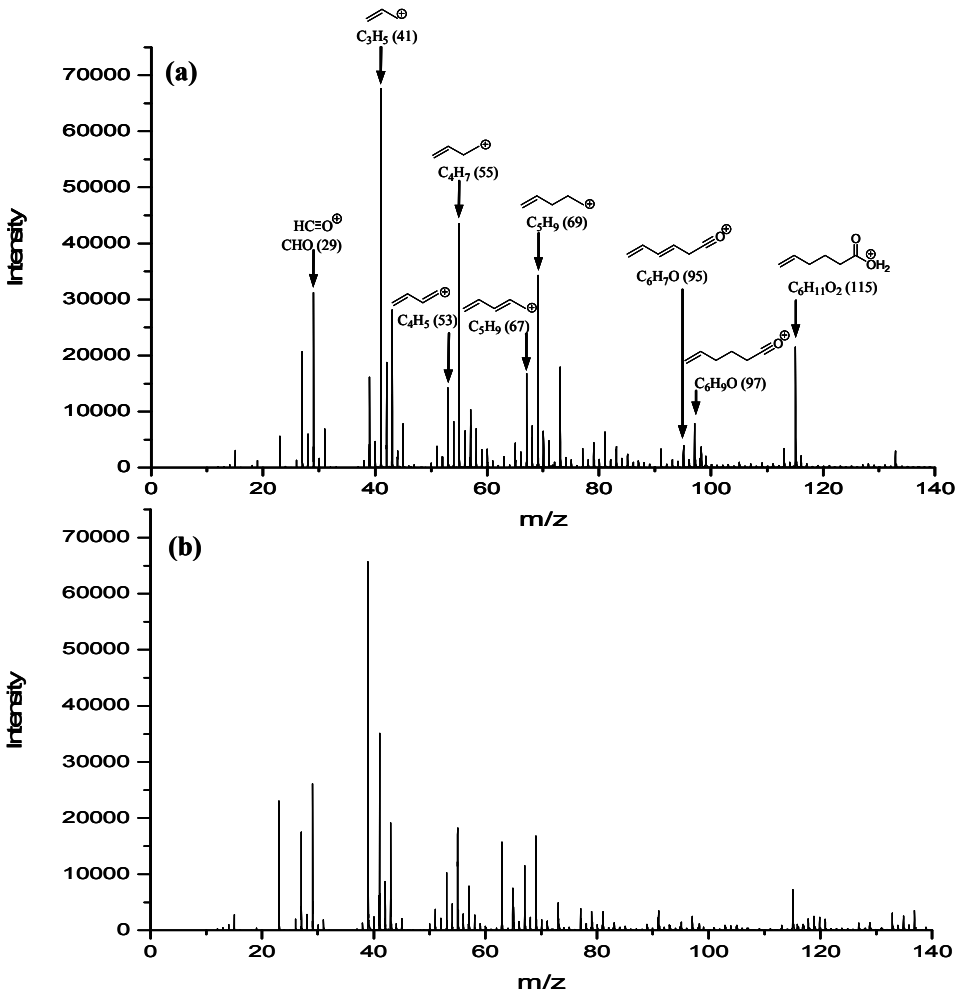

Figure IV.3. Positive ion TOF-SIMS spectra of SPCL fiber mesh before (A) and after (B) plasma modification. The PCL peaks are marked.

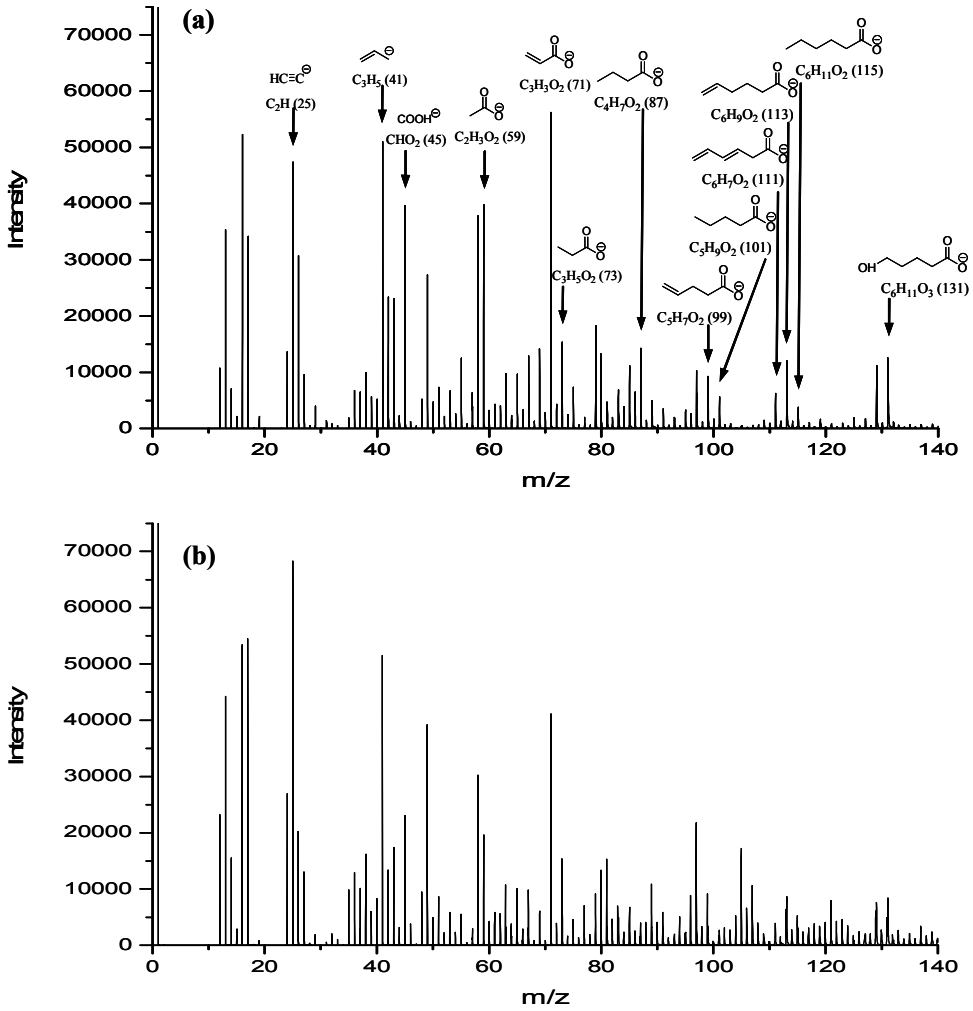

Figure IV.4. Negative ion TOF-SIMS spectra of SPCL fiber mesh before (A) and after (B) plasma modification. More characteristic PCL peaks are marked.

3.2. Protein adsorption on treated and untreated SPCL fiber-mesh scaffolds

Two different adhesive proteins, Fn and Vn, were taken for the studied materials. Fn was chosen for this study because it is commonly used as a standard procedure, applied to improve the adhesion of ECs. Vn is known for its ability to modulate HUVEC spreading and migration. Moreover, a previous study [31] on 2-dimensional starch-based materials has shown higher adsorption affinity of Vn than Fn or albumin using unitary or complex protein solutions. The micrographs presented on Figure IV.5

confirmed the results obtained for 2D samples and higher staining intensities for Vn can be observed in comparison with those for Fn. Homogeneous protein distribution was simliar for both Fn-labelled untreated (Figure IV.5A) and treated (Figure IV.5B) samples. In contrast, different protein distribution patterns were observed for Vn adsorbed onto non-treated (Figure IV.5c) and plasma-modified scaffolds (Figure IV.5d). In the latter case, Vn presented a heterogeneous distribution on the SPCL fiber surface, with foci of high fluorescent signal on the Ar plasma-treated scaffolds.

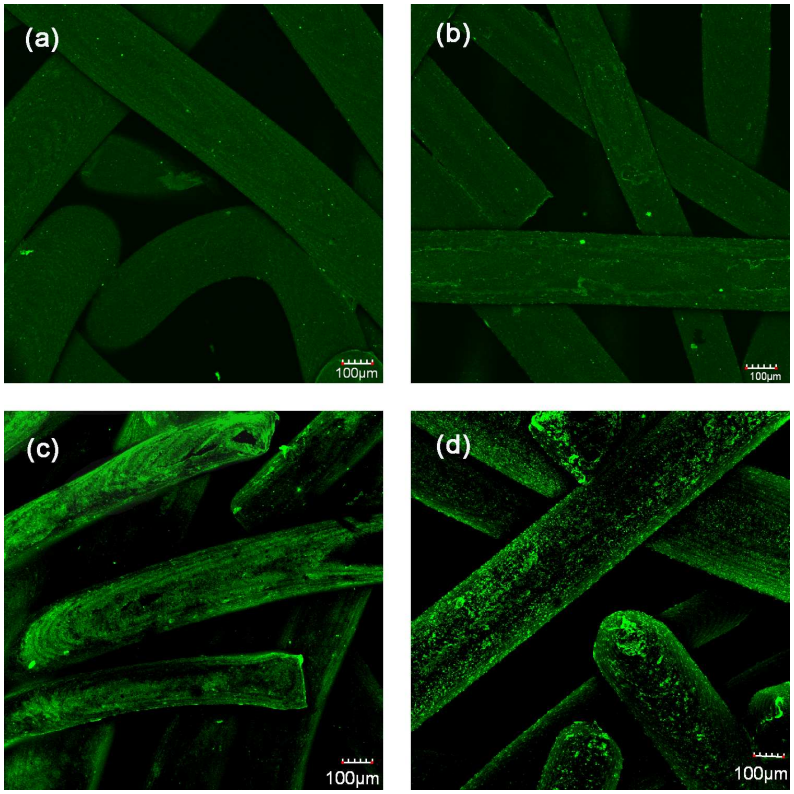

Figure IV.5. Untreated (a, c) and plasma-modified (b, d) SPCL fiber meshes immunolabeled for Fn (a-b) and Vn (c-d) after 1h immersion in culture medium supplemented with 20 % serum. Note the markedly increased adsorption of Vn compared to Fn.

3.3. Influence of Ar plasma treatment on cell adhesion, viability and morphology

Viable ECs were detected on the surface of Ar plasma-modified scaffolds after 4 hours of cell seeding (Fig. IV.6A). The cells were homogenously distributed on the scaffold and presented a morphology that reflects an early stage of attachment. On

the positive control, i.e., untreated scaffolds pre-coated with Fn, viable ECs had also adhered on the surface and the cells exhibited a well-developed spread morphology (Fig. IV.6b). In contrast, only a few cells exhibiting a rounded-up morphology were observed on the negative control (Fig. IV.6c). After 7 days of culture, ECs formed a complete monolayer on the surface of the plasma-modified scaffolds, as well as on the positive control (Figs. IV.6d and IV.6e). In addition, the morphological differences observed for these two samples at the earlier time points vanished after 7 days of culture. On the other hand, on the negative control, only a few cells were detectable on the scaffold surface (Fig. IV.6f). Figure IV.7 reveals further details of EC morphology on the plasma-modified scaffold and on the positive control after 7 days of culture. ECs exhibited the typical flattened and well-spread morphology in both samples. Moreover, the intimate contact established between neighbouring cells led to a compact and uniform cell distribution that covered the individual fibers of the scaffolds.

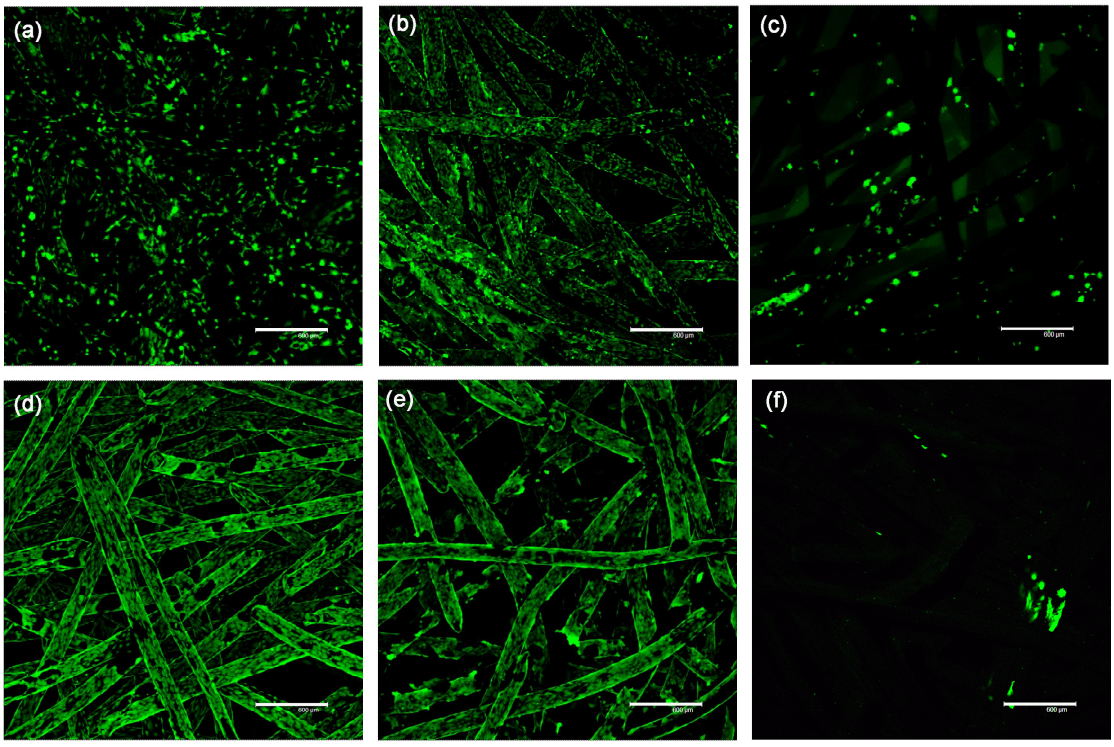

Figure IV.6. Calcein-AM viability assay of HUVEC grown on plasma-modified (a, d), Fn-coated (b, e) and untreated (c, f) scaffolds for 4 hours (left column) and 7 days (right column). The value of the scale bars is 600 μm.

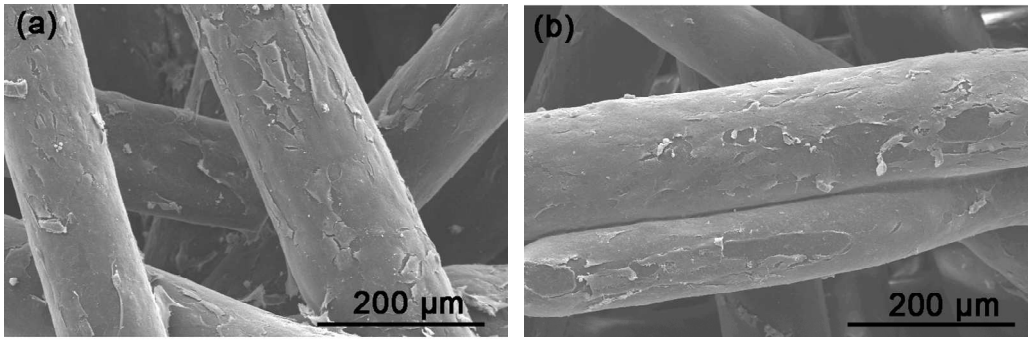

Figure IV.7. SEM micrographs of HUVEC grown on plasma-modified scaffolds (a) and on the positive (Fn-coated scaffolds) control (b) for 7 days.

3.4. EC proliferation profile on the SPCL fiber mesh scaffolds

DNA quantification (Fig. IV.8) showed that HUVECs were able to proliferate when they were cultured on plasma-modified or Fn-coated fiber meshes. From day 3 to 7 increased cell proliferation was observed for these two materials and this difference was significant for the plasma-modified material. On the contrary, the negative control sustained the growth of very few cells, and after 7 days of culture this value dropped below the method's detection limit. It must be noted that the highest number of cells was observed on the plasma-modified scaffolds. This pattern was more apparent after longer culture times when the proliferation rate on plasma-treated scaffolds was significantly higher as compared to the positive control.

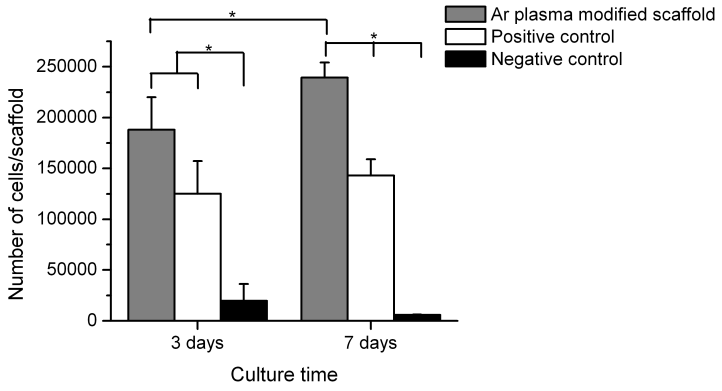

Figure IV.8. Cell proliferation of HUVEC growing on plasma-modified scaffold, positive and negative control. The number of cells was determined by DNA quantification. Error bars represent means ± SD. *Significantly different t-Test, $p<0.05$.

3.5. Expression of endothelial markers

To confirm the maintenance of the endothelial phenotype and of markers involved in angiogenesis, total RNA was extracted from EC-seeded scaffolds and assayed by RT-PCR. The expression of important cell adhesion molecules such as PECAM-1 and VE-cadherin was retained in both plasma-treated and positive control scaffolds (Fig. IV.9). Furthermore, RT-PCR revealed the expression of the receptor for the most potent angiogenic growth factor, vascular endothelial growth factor (VEGFR1). On TCP, the optimal surface for tissue culture, used as 2D control, ECs were also capable of producing mRNA that encodes for the three markers under study.

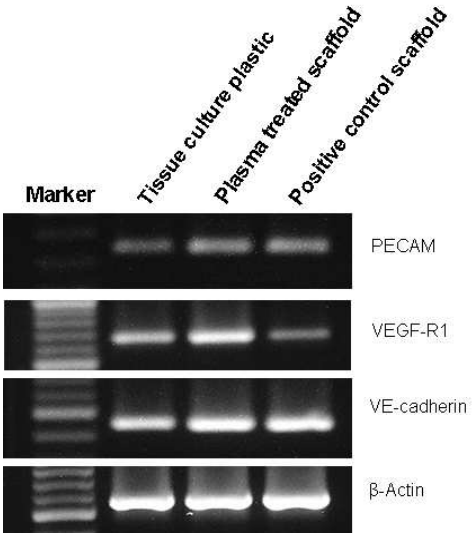

Figure IV.9. Expression of endothelial markers at the mRNA level (RT-PCR) for HUVEC grown on tissue culture polystyrene, plasma-treated, and Fn-coated SPCL scaffolds.

PECAM-1 expression was also assessed at the single-cell level by immunocytochemistry. This marker was depicted as a well-defined green ring around neighbouring cells on the surface of plasma-treated and on positive control SPCL fiber-mesh scaffolds (Fig. IV.10). In fact, the expression of this adhesion molecule involved in endothelial cell-cell interaction was similar for these two materials and represents the distribution pattern for physiologically quiescent, that is, non-activated ECs.

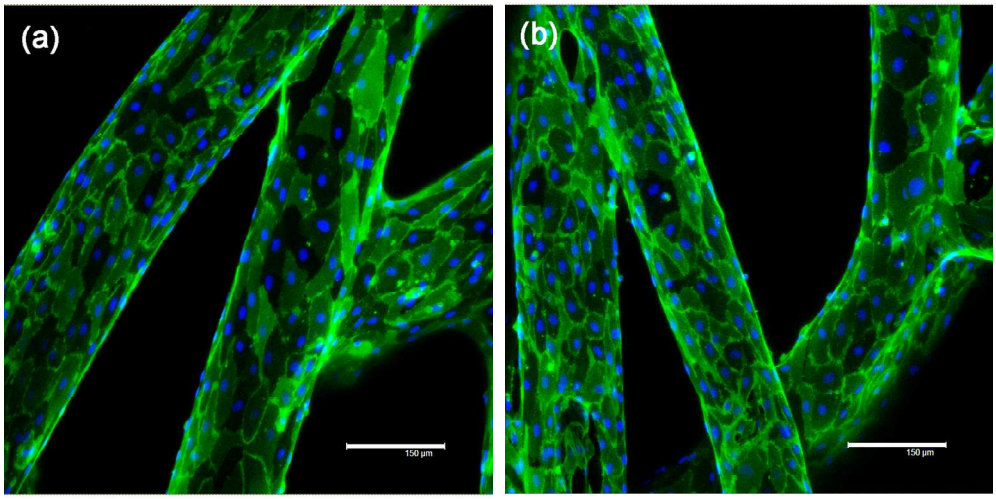

Figure IV.10. PECAM-1 staining (green fluorescence) of ECs on plasma-modified SPCL scaffold (a) and on positive control (b) cultured for 7 days. Nuclei were counterstained with Hoechst (blue fluorescence). The value of the scale bars is 150 µm.

4. DISCUSSION

In a simplistic way, bone can be described as a three-component tissue: i) a mineralized matrix, supplied by ii) a complex vascular network and orchestrated by iii) several cell types that release a multitude of growth factors. Therefore, in a strategy aimed at regeneration of bone tissue, these components must be considered. The bulk structure of the scaffold must take into account the mechanical function of the tissue, while the architecture must allow the penetration of a functional vascular plexus and the scaffold's surface must be compatible with the different cells that build up the tissue. SPCL fiber-mesh structures have been proposed as a scaffolding material for bone tissue engineering [21, 22, 32]. Previous studies have shown the ability of these scaffolds to promote adhesion of bone marrow cells, their differentiation into an osteoblast lineage accompanied by the deposition of a mineralized matrix and production of several growth factors involved in osteogenesis and angiogenesis [21, 23, 33]. Moreover, regarding the importance of ECs in angiogenesis, other work from our group demonstrates the ability of this material to

support the adhesion, proliferation and maintenance of the phenotypic expression of ECs [24]. The surface of SPCL fiber-mesh scaffold requires a pre-coating with an adhesive protein in order to sustain EC adhesion similar to that observed by a large number of other polymeric substrates [34-36] However, protein adsorption is a process difficult to control and several obstacles such as low stability to sterilization processes, heat treatment and pH variation, storage and conformation shifting [37, 38] are associated with its application. Therefore, based on the results of our studies, we propose that plasma surface modification of SPCL fiber-mesh scaffolds can be used as an alternative approach to render the surface compatible for EC adhesion. The described methodology has the advantage that it obviates the need for protein pre-coating and can be simultaneously used as a cost-effective method for sterilization.

The interplay between the surface features changed by plasma modification and the adsorption of proteins may subsequently affect cell behaviour via:

i) Increasing the surface area available for protein adsorption by etching processes, typically ongoing during the plasma treatment;

ii) Modulation of the surface chemistry, i.e. the physical bonds on the surface/proteins. Although a straightforward relation can not always be established, EC adhesion is often associated with groups such as hydroxyl (-OH) or carboxyl (-COOH) [39, 40]. Furthermore, enhanced EC proliferation and spreading in response to increased oxygen content has also been shown in previous studies [41, 42] on 2D samples prepared from synthetic polymers.

iii) Alternation of the surface charge. Negatively charged groups have shown[43-46] positive effects on cell adhesion and growth and this is attributed to the favourable protein conformation on these surfaces. The polarity of these groups allows formation of additional hydrogen bonds with the proteins, which will keep them fixed onto the surface. From the oxygen containing functional groups, COOH are the ones that influence mostly the growth of ECs [47, 48]

When physical plasma becomes into contact with the biomaterial surface, the activated species are accelerated towards the substrate by the applied electrical field. Since some parts of the surfaces are exposed to energies higher than the bonding energy of polymers, these parts undergo chain scission [49, 50]. Chain

scission processes will then initiate various events. Surface degradation or so-called etching is one of the effects that can be observed. This effect depends on the used power, which determines the acceleration of the active species toward the material surface, as well as on the time during which the material is exposed to this bombarding with active species. Surface etching was observed at the used conditions for SPCL fiber-mesh scaffolds. Both roughness and topography were altered by the applied treatment as shown by optical profilometry. Hence, alterations in cellular/protein behaviour could be expected as a response to the introduced changes of the surface morphology. The higher roughness is associated with a higher surface area and therefore an increased quantity of adsorbed proteins as well as ahigher number of cells on the modified surface must be observed. On the other hand, the chain scission was confirmed by TOF-SIMS, were the intensity of the characteristic polymer peaks decreased for the plasma treated material. Chain scission results in the formation of highly reactive radicals on the surface. Those radicals can recombine (e.g. crosslinking reactions) or react with the other species such as oxygen from the air. Those processes were confirmed by both XPS and TOF-SIMS analyses of the surface chemical composition of the studied materials. XPS showed higher oxygen concentration for the modified materials. Additionally, the negative mass spectrum of plasma treated scaffolds was abundant in new, low intensity peaks, which also reveal ongoing functionalisation. Changing of the surface chemistry in turn is expected to modulate protein adsorption. Depending on the nature of the established protein-surface interactions, surfaces can modulate adhesion and cell biochemical mechanisms such as those involved in cell differentiation. Protein-containing solutions can be used as a source of biomolecules that will further bridge and affect cell adhesion. The analysis of the adsorption of the cell-adhesive molecules, Fn and Vn, showed some differences in their comparative adsorption ability as well for the comparison of modified and untreated samples. Although a different affinity of Fn and Vn to 2-dimensional SPCL surfaces was previously observed [31], the analysis of the adsorption of these molecules on 3D starch-based scaffolds following Ar surface modification has not been demonstrated. An important result of the present study is the indication that Vn distribution follows the surface morphology of the studied fibers and can be altered by changing of their

surface pattern. Before treatment, a laminated distribution of Fn was observed. This same morphology was also shown by optical profiler for the untreated scaffolds. After plasma treatment the laminated structure was lost and in turn the Vn distribution pattern was affected, analogous to the changed morphology of SPCL scaffolds. Vn is a biomolecule known to control and modulate EC spreading and migration and is well-characterized as a modulator of the cytoskeleton.[51, 52] On the other hand, no difference was observed for Fn. However, this is not surprising, as it is reported that in complex protein solutions Fn interacts with the available cell non-adhesive molecules[53], which reduces its competitiveness and explains its failure to adsorb on to the substrate in the presence of other serum proteins[54]. As a result, in bovine plasma and fresh serum higher cell activity is associated with Vn but not with Fn.

Cell adhesion is the ultimate functional result of both the material's surface physicochemical properties and its protein adsorption. The changed physicochemical properties of the underlying substrate can modulate the EC behaviour by affecting the proteins' conformation and orientation and hence enhancing the anchorage strength to the substrate. Additionally, the surface properties of treated scaffolds might also stabilize the proteins secreted and deposited by ECs aimed to constitute the basement membrane [48, 55]. *In vitro* studies with human ECs revealed that uncoated and non-modified SPCL fiber-mesh scaffolds displayed substantially reduced cellular adhesion. However, cell attachment to SPCL scaffolds was significantly enhanced when physically adsorbed Fn, a standard procedure in endothelial culture, was used. Moreover, ECs on the positive controls remained viable and also proliferated during the 7 days of culture. When the SPCL surface was treated by Ar plasma the surface was tailored for EC adhesion, obviating the need for protein pre-coating. Furthermore, the proliferation level of ECs on Ar plasma-treated scaffolds was significantly higher than on the positive control. Hence, plasma treatment not only promoted the initial stages of cell attachment but also triggered the EC metabolic activity.

Protein-mediated interactions established between cells and substrate not only provide anchorage sites for cell adhesion but also dictate important cell parameters such as morphology, proliferation, migration, differentiation and responsiveness [56]. Therefore, the effect of the performed modification on the morphology and

phenotypic/genotypic expression of ECs was assessed. Morphology mirrors cell-substrate interactions in so far as altered orientation of adsorbed proteins will modulate cellular integrin receptor binding and consequently this will be reflected in cytoskeletal re-arrangement. Changing the surface of SPCL fiber-mesh scaffolds by Ar plasma did not affect the typical flattened EC morphology. This is a positive indicator of cellular mechanical coupling to the underlying substrate. Regarding endothelial markers, the expression of VEFGR-1 at the gene level was confirmed for plasma-treated scaffolds as well as on positive and TCP controls. VEGFR1 is a key gene not only involved in angiogenesis but also associated with monocyte chemotaxis and with recruitment of bone marrow-derived progenitor cells [57]. Another gene whose expression was maintained on the modified scaffold was VE-cadherin, an essential cell adhesion molecule in establishing and maintaining endothelial integrity. The anchorage of cadherins to the cytoskeleton and their clustering are indispensable for the development of strong and rigid cell-cell adhesions [58]. Additionally, PECAM-1, one of the hallmarks of the endothelium is a crucial molecule for homotypic adhesion involved in the maintenance of endothelial integrity [59]. The expression of PECAM-1 was observed on plasma-modified and Fn-coated scaffolds at both mRNA and single-cell protein level. Furthermore, cell-cell adhesion was detected at the cell borders, which is a good indication of the non-activated status of interactions between neighbouring cells. These overall results indicate that ECs maintained their differentiated phenotype and the integrity of endothelial monolayer on plasma-modified scaffolds.

5. CONCLUSIONS

Ar plasma treatment was shown to be an effective method to modify the surface of a 3D starch-based scaffold for EC adhesion. Cell attachment and expression of endothelial markers on plasma-treated SPCL fiber-mesh scaffolds was comparable to the scaffold pre-coated with Fn, used as positive control. However, higher proliferation rates were observed on plasma-modified scaffolds. This improved

overall biological outcome is the result of novel protein-surface interactions generated by plasma treatment. Increased surface roughness, altered surface pattern and changed surface chemistry were the main physicochemical changes demonstrated on the SPCL fiber-mesh scaffold surface. Consequently, these properties modulate protein adsorption as indicated by the different adsorption profile of the adhesive protein Vn.

Finally, Ar plasma treatment renders the surface compatible for ECs and this is a significant step forward towards the improvement of constructs for vascularization. Furthermore, in addition to eliminating the need for pre-coating with proteins and the respective drawbacks associated with this methodology, plasma treatment does not affect the scaffold's bulk structure and can simultaneously be used as an effective sterilization method. Starch-based scaffolds treated by Ar plasma were shown to be a good support to use on bone tissue engineering, where vascularization is a main requirement.

REFERENCES

1. Fauza DO. Tissue engineering: Current state of clinical application. Current Opinion in Pediatrics. 2003; 15(3):267-71.

2. Kneser U, Schaefer DJ, Polykandriotis E, Horch RE. Tissue engineering of bone: the reconstructive surgeon's point of view. Journal of Cellular and Molecular Medicine. 2006; 10(1):7-19.

3. Muschler GF, Nakamoto C, Griffith LG. Engineering principles of clinical cell-based tissue engineering. J Bone Joint Surg Am. 2004; 86-A(7):1541-58.

4. McCarthy I. The physiology of bone blood flow: a review. J Bone Joint Surg Am. 2006; 88 Suppl 3:4-9.

5. Warnke PH, Springer IN, Wiltfang J, Acil Y, Eufinger H, Wehmoller M, et al. Growth and transplantation of a custom vascularised bone graft in a man. Lancet. 2004; 364(9436):766-70.

6. Kneser U, Polykandriotis E, Ohnolz J, Heidner K, Grabinger L, Euler S, et al. Engineering of vascularized transplantable bone tissues: induction of axial vascularization in an osteoconductive matrix using an arteriovenous loop. Tissue Eng. 2006; 12(7):1721-31.

7. Cassell OC, Hofer SO, Morrison WA, Knight KR. Vascularisation of tissue-engineered grafts: the regulation of angiogenesis in reconstructive surgery and in disease states. Br J Plast Surg. 2002; 55(8):603-10.

8. Patel ZS, Mikos AG. Angiogenesis with biomaterial-based drug- and cell-delivery systems. J Biomater Sci Polym Ed. 2004; 15(6):701-26.

9. Yamashita H, Shimizu A, Kato M, Nishitoh H, Ichijo H, Hanyu A, et al. Growth/differentiation factor-5 induces angiogenesis in vivo. Experimental Cell Research. 1997; 235(1):218-26.

10. Chen RR, Silva EA, Yuen WW, Mooney DJ. Spatio-temporal VEGF and PDGF delivery patterns blood vessel formation and maturation. Pharmaceutical Research. 2007; 24(2):258-64.

11. Moldovan NI, Ferrari M. Prospects for microtechnology and nanotechnology in bioengineering of replacement microvessels. Arch Pathol Lab Med. 2002; 126(3):320-4.

12. Masuda H, Asahara T. Post-natal endothelial progenitor cells for neovascularization in tissue regeneration. Cardiovasc Res. 2003; 58(2):390-8.

13. Unger RE, Sartoris A, Peters K, Motta A, Migliaresi C, Kunkel M, et al. Tissue-like self-assembly in cocultures of endothelial cells and osteoblasts and the formation of microcapillary-like structures on three-dimensional porous biomaterials. Biomaterials. 2007; 28(27):3965-76.

14. Chu PK, Chen JY, Wang LP, Huang N. Plasma-surface modification of biomaterials. Materials Science & Engineering R-Reports. 2002; 36(5-6):143-206.

15. Liu X, Ma PX. Polymeric scaffolds for bone tissue engineering. Ann Biomed Eng. 2004; 32(3):477-86.

16. Douglas T, Hempel U, Mietrach C, Heinemann S, Scharnweber D, Worch H. Fibrils of different collagen types containing immobilised proteoglycans (PGs) as coatings: characterisation and influence on osteoblast behaviour. Biomol Eng. 2007; 24(5):455-8.

17. Bhati RS, Mukherjee DP, McCarthy KJ, Rogers SH, Smith DF, Shalaby SW. The growth of chondrocytes into a fibronectin-coated biodegradable scaffold. J Biomed Mater Res. 2001; 56(1):74-82.

18. Massia SP, Hubbell JA. Human endothelial cell interactions with surface-coupled adhesion peptides on a nonadhesive glass substrate and two polymeric biomaterials. J Biomed Mater Res. 1991; 25(2):223-42.

19. Chim H, Ong JL, Schantz JT, Hutmacher DW, Agrawal CM. Efficacy of glow discharge gas plasma treatment as a surface modification process for three-dimensional poly (D,L-lactide) scaffolds. J Biomed Mater Res A. 2003; 65A(3):327-35.

20. Lin J, Lindsey ML, Zhu B, Agrawal CM, Bailey SR. Effects of surface-modified scaffolds on the growth and differentiation of mouse adipose-derived stromal cells. J Tissue Eng Regen Med. 2007; 1(3):211-7.

21. Gomes ME, Sikavitsas VI, Behravesh E, Reis RL, Mikos AG. Effect of flow perfusion on the osteogenic differentiation of bone marrow stromal cells cultured on starch-based three-dimensional scaffolds. J Biomed Mater Res. 2003; 67A(1):87-95.

22. Pavlov MP, Mano JF, Neves NM, Reis RL. Fibers and 3D mesh scaffolds from biodegradable starch-based blends: production and characterization. Macromol Biosci. 2004; 4(8):776-84.

23. Gomes ME, Holtorf HL, Reis RL, Mikos AG. Influence of the porosity of starch-based fiber mesh scaffolds on the proliferation and osteogenic differentiation of bone marrow stromal cells cultured in a flow perfusion bioreactor. Tissue Eng. 2006; 12(4):801-9.

24. Santos MI, Fuchs S, Gomes ME, Unger RE, Reis RL, Kirkpatrick CJ. Response of micro- and macrovascular endothelial cells to starch-based fiber meshes for bone tissue engineering. Biomaterials. 2007; 28(2):240-8.

25. Gomes ME, Azevedo HS, Moreira AR, Ella V, Kellomaki M, Reis RL. Starch-poly(epsilon-caprolactone) and starch-poly(lactic acid) fibre-mesh scaffolds for bone tissue engineering applications: structure, mechanical properties and degradation behaviour. J Tissue Eng Regen Med. 2008; 2(5):243-52.

26. Marin V, Kaplanski G, Gres S, Farnarier C, Bongrand P. Endothelial cell culture: protocol to obtain and cultivate human umbilical endothelial cells. J Immunol Methods. 2001; 254(1-2):183-90.

27. Punshon G, Vara DS, Sales KM, Kidane AG, Salacinski HJ, Seifalian AM. Interactions between endothelial cells and a poly(carbonate-silsesquioxane-bridge-urea) urethane. Biomaterials. 2005; 26(32):6271-9.

28. Ogaki R, Green FM, Vert SLM, Alexander MR, Gilmore IS, Davies MC. A comparison of the static SIMS and G-SIMS spectra of biodegradable homo-polyesters. Surface and Interface Analysis. 2008; 40(8):1202-8.

29. Adriaens A, Van Vaeck L, Adams F. Static secondary ion mass spectrometry (S-SIMS) Part 2: Material science applications. Mass Spectrometry Reviews. 1999; 18(1):48-81.

30. Cassie ABD, Baxter S. Wettability of porous surfaces. Transactions of the Faraday Society. 1944; 40:0546-50.

31. Alves CM, Reis RL, Hunt JA. Preliminary study on human protein adsorption and leukocyte adhesion to starch-based biomaterials. J Mater Sci Mater Med. 2003; 14(2):157-65.

32. Oliveira AL, Reis RL. Pre-mineralisation of starch/polycrapolactone bone tissue engineering scaffolds by a calcium-silicate-based process. J Mater Sci Mater Med. 2004; 15(4):533-40.

33. Gomes ME, Bossano CM, Johnston CM, Reis RL, Mikos AG. In vitro localization of bone growth factors in constructs of biodegradable scaffolds seeded with marrow stromal cells and cultured in a flow perfusion bioreactor. Tissue Eng. 2006; 12(1):177-88.

34. Unger RE, Peters K, Wolf M, Motta A, Migliaresi C, Kirkpatrick CJ. Endothelialization of a non-woven silk fibroin net for use in tissue engineering: growth and gene regulation of human endothelial cells. Biomaterials. 2004; 25(21):5137-46.

35. Pompe T, Keller K, Mothes G, Nitschke M, Teese M, Zimmermann R, et al. Surface modification of poly(hydroxybutyrate) films to control cell-matrix adhesion. Biomaterials. 2007; 28(1):28-37.

36. Sanborn SL, Murugesan G, Marchant RE, Kottke-Marchant K. Endothelial cell formation of focal adhesions on hydrophilic plasma polymers. Biomaterials. 2002; 23(1):1-8.

37. Hersel U, Dahmen C, Kessler H. RGD modified polymers: biomaterials for stimulated cell adhesion and beyond. Biomaterials. 2003; 24(24):4385-415.

38. Alves CM, Yang Y, Carnesc DL, Ong JL, Sylvia VL, Dean DD, et al. Modulating bone cells response onto starch-based biomaterials by surface plasma treatment and protein adsorption. Biomaterials. 2007; 28:307-15.

39. Ruardy TG, Moorlag HE, Schakenraad JM, VanderMei HC, Busscher HJ. Growth of fibroblasts and endothelial cells on wettability gradient surfaces. Journal of Colloid and Interface Science. 1997; 188(1):209-17.

40. KottkeMarchant K, Veenstra AA, Marchant RE. Human endothelial cell growth and coagulant function varies with respect to interfacial properties of polymeric substrates. J Biomed Mater Res. 1996; 30(2):209-20.

41. Tajima S, Chu JS, Li S, Komvopoulos K. Differential regulation of endothelial cell adhesion, spreading, and cytoskeleton on low-density polyethylene by nanotopography and surface chemistry modification induced by argon plasma treatment. J Biomed Mater Res A. 2007; 84A(3):828-36.

42. Ertel SI, Ratner BD, Horbett TA. Radiofrequency plasma deposition of oxygen-containing films on polystyrene and poly(ethylene terephthalate) substrates improves endothelial cell growth. J Biomed Mater Res. 1990; 24(12):1637-59.

43. Lee MH, Ducheyne P, Lynch L, Boettiger D, Composto RJ. Effect of biomaterial surface properties on fibronectin-alpha5beta1 integrin interaction and cellular attachment. Biomaterials. 2006; 27(9):1907-16.

44. Keselowsky BG, Collard DM, Garcia AJ. Surface chemistry modulates fibronectin conformation and directs integrin binding and specificity to control cell adhesion. J Biomed Mater Res A. 2003; 66(2):247-59.

45. Keselowsky BG, Collard DM, Garcia AJ. Surface chemistry modulates focal adhesion composition and signaling through changes in integrin binding. Biomaterials. 2004; 25(28):5947-54.

46. Faucheux N, Tzoneva R, Nagel MD, Groth T. The dependence of fibrillar adhesions in human fibroblasts on substratum chemistry. Biomaterials. 2006; 27(2):234-45.

47. Wang YX, Robertson JL, Spillman WB, Jr., Claus RO. Effects of the chemical structure and the surface properties of polymeric biomaterials on their biocompatibility. Pharm Res. 2004; 21(8):1362-73.

48. Tidwell CD, Ertel SI, Ratner BD, Tarasevich BJ, Atre S, Allara DL. Endothelial cell growth and protein adsorption on terminally functionalized, self-assembled monolayers of alkanethiolates on gold. Langmuir. 1997; 13(13):3404-13.

49. Inagaki N. Plasma surface modification and plasma polymerization. Basel, Switzerland: Technomic Publishing AG; 1996.

50. Oehr C. Plasma surface modification of polymers for biomedical use. NIM B. 2003; 208:40-7.

51. Schwartz MA. Spreading of human endothelial cells on fibronectin or vitronectin triggers elevation of intracellular free calcium. J Cell Biol %R 101083/jcb12041003. 1993; 120(4):1003-10.

52. Leavesley DI, Schwartz MA, Rosenfeld M, Cheresh DA. Integrin beta 1- and beta 3-mediated endothelial cell migration is triggered through distinct signaling mechanisms. J Cell Biol. 1993; 121(1):163-70.

53. P. B. van Wachem BWLMADTBJFABJPDWGvA. Adsorption of fibronectin derived from serum and from human endothelial cells onto tissue culture polystyrene. Journal of Biomedical Materials Research. 1987; 21(11):1317-27.

54. Underwood PA, Bennett FA. A comparison of the biological activities of the cell-adhesive proteins vitronectin and fibronectin. J Cell Sci. 1989; 93 (Pt 4):641-9.

55. Chu CFL, Lu A, Liszkowski M, Sipehia R. Enhanced growth of animal and human endothelial cells on biodegradable polymers. Biochimica Et Biophysica Acta-General Subjects. 1999; 1472(3):479-85.

56. Davies PF, Robotewskyj A, Griem ML. Endothelial cell adhesion in real time. Measurements in vitro by tandem scanning confocal image analysis. J Clin Invest. 1993; 91(6):2640-52.

57. Roy H, Bhardwaj S, Yla-Herttuala S. Biology of vascular endothelial growth factors. Febs Letters. 2006; 580(12):2879-87.

58. Tzoneva R, Faucheux N, Groth T. Wettability of substrata controls cell-substrate and cell-cell adhesions. Biochimica et Biophysica Acta (BBA) - General Subjects. 2007; 1770(11):1538-47.

59. Pu FR, Williams RL, Markkula TK, Hunt JA. Effects of plasma treated PET and PTFE on expression of adhesion molecules by human endothelial cells in vitro. Biomaterials. 2002; 23(11):2411-28.

CHAPTER V

Endothelial Cell Colonization and Angiogenic Potential of Combined Nano- and Micro-fibrous Scaffolds for Bone Tissue Engineering

CHAPTER V

Endothelial Cell Colonization and Angiogenic Potential of Combined Nano- and Micro-fibrous Scaffolds for Bone Tissue Engineering *

ABSTRACT

Presently the majority of tissue engineering approaches aimed at regenerating bone rely only on post-implantation vascularization. Strategies that include seeding ECs on biomaterials and promoting their adhesion, migration and functionality might be a solution for the formation of vascularized bone. Nano/micro fiber-combined scaffolds have an innovative structure, inspired by ECM that combines a nano-network, aimed to promote cell adhesion, with a micro-fiber mesh that provides the mechanical support. In this work we addressed the influence of this nano-network on growth pattern, morphology, inflammatory expression profile, expression of structural proteins, homotypic interactions and angiogenic potential of human EC cultured on a scaffold made of a blend of starch and poly(caprolactone). The nano-network allowed cells to span between individual micro-fibers and influenced cell morphology. Furthermore, on nano-fibers as well as on micro-fibers ECs maintained the physiological expression pattern of the structural protein vimentin and PECAM-1 between adjacent cells. In addition, ECs growing on the nano/micro fiber-combined scaffold were sensitive to pro-inflammatory stimulus. Under pro-angiogenic conditions *in vitro*, the ECM-like nano-network provided the structural and organizational stability for ECs migration and organization into capillary-like structures. The architecture of nano/micro- fiber-combined scaffolds elicited and guided the 3D distribution of ECs without compromising the structural requirements for bone regeneration.

* This chapter is based in the following publication:

M. I. Santos, K. Tuzlakoglu, S. Fuchs, M.E. Gomes, K. Peters, R.E. Unger, E. Piskin, R.L Reis, C.J. Kirkpatrick. Endothelial Cell Colonization and Angiogenic Potential of Combined Nano- and Micro-fibrous Scaffolds for Bone Tissue Engineering. Biomaterials (2008). 29:4306-4313.

1. INTRODUCTION

To become widely used in clinical practice tissue engineering products must overcome a series of major challenges, the vascularization of the biomaterial constructs being one of the major current limitations [1-3]. To date, most approaches in tissue engineering have relied on postimplantation neovascularization from the host, but for large and metabolically demanding organs, which rely on blood vessel ingrowth, this is clearly insufficient to meet the implant's demand for oxygen and nutrients [4-6].

In vascularized tissues/organs such as bone a complex network of blood vessels is more than just simple conduits that provide nutrients and oxygen and simultaneously remove by-products. They also have important metabolic and rheological functions which are organ-specific [7-9]. In bone, the intraosseous circulation allows traffic of minerals between the blood and bone tissue, and transmit the blood cells produced within the bone marrow into the systemic circulation [9, 10]. New blood vessels are intimately involved in osteogenesis (intramembranous and endochondral) and, furthermore, cytokines and growth factors that regulate intraosseous angiogenesis also regulate bone remodelling [7, 9]. In addition, vascularization is also vital for the survival of the implanted cells on the carrier material after implantation [6].

Many approaches have been proposed to increase vascularization in bone such as gene and/or protein delivery of angiogenenic growth factors [11, 12], provision of a vascularized bone-flap [13, 14] and *ex vivo* culturing of scaffolds with ECs alone or in combination with other cell types [6, 15]. Recently the work of Levenberg et al on skeletal muscle showed that pre-vascularization of constructs improved *in vivo* performance of the tissue construct, shedding light into *ex vivo* use of ECs to accelerate vascularization [16]. Thus, the scaffold design must not only take into consideration the structural and mechanical properties of bone but also ECs adhesion, migration and blood vessel formation and ingrowth. In blood vessels ECs are attached as a monolayer to a basement membrane composed of protein fibers in the nanoscale, such as type IV collagen and laminin fibers, embedded in heparin

sulfate proteoglycan hydrogels [17, 18]. This natural ECM provides structural and organizational stability to ECs and during angiogenesis EC migration is dependent on the adhesion to this matrix [19].

In this present work we evaluate the interaction of ECs with a scaffold made from SPCL with an innovative structure, inspired by the ECM, and combining polymeric micro- and nano-fibers in the same construct. This architecture was designed for bone regeneration to simultaneously provide mechanical support and to mimic the physical structure of ECM. We hypothesized that the presence of a nano-network might favour the adhesion of ECs and increase the density of cell colonization between micro-fibers, and might thus accelerate vascularization of the implanted scaffold. Previous work demonstrated favourable activity and differentiation of bone-like cells on this nano/micro- fiber-combined scaffold [20]. In this paper we addressed several important biological questions, such as whether this nano-network favours the growth pattern of ECs on the scaffold, cell morphology, inflammatory gene expression profile, expression of structural proteins and finally the angiogenic potential.

2. MATERIALS AND METHODS

2.1. Scaffolds

The scaffolds used in this study were based on a blend of starch with poly(caprolactone). Nano/micro-fiber-combined scaffolds resulted from a two step methodology. First by a fiber bonding methodology an SPCL fiber-mesh scaffold composed of micro-fibers (Φ 160 μm) with 70% porosity was obtained and second, by electrospinning the scaffold was impregnated with nano-fibers (Φ 400nm). SPCL fiber-mesh scaffold without the nano-network were used as control. Further details concerning scaffold production have been published elsewhere [20-22]. Samples were cut into discs of 8 mm diameter and 2 mm height and sterilized by ethylene oxide. Prior to cell seeding scaffolds were soaked overnight in medium without serum.

2.2. Cells, culture conditions and scaffolds seeding

Primary cultures of human ECs isolated from umbilical cord (HUVEC) and from human dermis (HDMEC) were used. HUVECs were isolated from umbilical vein by collagenase digestion according to a published method [21]. HDMECs were obtained from enzymatic digestion of juvenile foreskin as previously described [22]. HUVEC were cultured in M199 medium (Sigma-Aldrich, Germany) supplemented with 20% FCS (Gibco, Germany), 100U/100µg/mL Pen/Strep (Sigma-Aldrich, Germany), 2 mM glutamax I (Life Technologies, Germany), 25 µg/mL sodium heparin (Sigma-Aldrich, Germany) and 25 µg/mL ECGS (BD Biosciences, USA). HDMEC were cultivated in Endothelial Basal Medium MV (PromoCell, Germany) supplemented with 15 % FCS (Invitrogen, Germany), 100 U/100 µg/mL Pen/Strep (Sigma-Aldrich, Germany), 2.5 ng/mL, FGF-2 (Sigma-Aldrich, Germany), 10 µg/mL sodium heparin and 100 U/100 µg/mL Pen/Strep. In order to promote better cell adhesion, ECs were seeded into culture flasks previously coated with gelatine. All assays were conducted with cells until passage 4.

Prior to cell seeding scaffolds were coated with a Fn solution (10 µg/mL PBS, Roche, Germany) for 1 hr at 37 ºC. Confluent HUVECs and HDMECs were trypsinized and a suspension of 2 x 10^5 cells was added to each scaffold. The scaffolds were incubated under standard culture conditions (37 ºC, 5 % CO_2, humidified atmosphere).

2.3. ECs imaging

The viability, phenotype and growth of ECs on nano/micro fiber-combined scaffolds and on SPCL fiber-mesh scaffolds were analysed by scanning electron microscopy [23] and by CLSM after 3 and 7 days. For viability assessment, the ECs-seeded scaffolds were incubated for 10 min in medium supplemented with 0.1 µM calcein-

AM. Viable cells convert the non-fluorescence and membrane permeable calcein-AM due to the presence of active intracellular esterases into the green fluorescent and impermeable calcein. Viable cells are identifiable by the green fluorescent cytoplasm when viewed with CLSM (Leica TCSN NT). For SEM analysis the samples were fixed for 30 min with 2.5 % glutaraldehyde in 0,1 M sodium cacodylate buffer, dehydrated in increasing concentrations of acetone, dried with hexamethyldisilasane and sputter coated with gold prior to SEM observation (Leica Cambridge S360).

2.4. Gene analysis of pro-inflammatory genes

The gene analysis of two pro-inflammatory cell adhesion molecules E-selectin and ICAM-1 were analysed by Real Time PCR. The mRNA expression of cell adhesion molecules as well as the house keeping gene GAPDH were analyzed in HUVECs growing for 7 days on SPCL fiber-mesh scaffold and on nano/micro fiber-combined scaffold. As control HUVECs were grown on cell-culture plastic. Furthermore, as positive control, gene expression was analyzed when the samples were cultured in the presence of 1.0 µg/mL of LPS for 4 hours (Sigma-Adrich, Germany). Total mRNA from HUVEC cells was extracted using the RNeasy Mini Kit (Qiagen, Germany) according to the manufacturer's protocol. Afterwards, total RNA (0.5 µg) was reverse transcribed using Omniscript RT Kit (Qiagen, Germany). Gene amplification was performed using Applied Biosystems 7300 Real-Time PCR System (Applera Deutschland GmbH, Germany). The number of cycles and annealing temperature were selected according to the manufacturer's instructions. Real time PCR was performed with 2.5 ng cDNA and 12.5 µL of 2x-master mix, primers (0.25 µL forward and 0.25 µL reverse primer) in a final volume of 25 µL. The following gene-specific primer sets were used: (1) E-selectin, sense 5`-CCCGTGTTTGGCACTGTGT-3', antisense 5`-GCCATTGAGCGTCCATCCT-3; (2) ICAM-1, sense 5'-CGGCTGACGTGTGCAGTAAT-3', antisense 5`-CACCTCGGTCCCTTCTGAGA-3` (3) GAPDH, sense 5'- ATGGGGAAGGTGAAGGTCG-3', antisense 5`-TAAAAGCAGCCCTGGTGACC-3.`Gene expression was normalized to the expression of

the housekeeping gene GAPDH. Relative quantification of gene expression was calculated in stimulated samples (+LPS) compared to samples cultured in the absence of pro-inflammatory stimulus (-LPS).

2.5. Immunocytochemistry

The expression pattern of the structural protein vimentin and of PECAM-1 (also known as CD31) was examined by immunocytochemistry. After 7 days in culture, EC-confluent SPCL scaffolds were fixed with a solution of 2 % paraformaldehyde for 30 min at RT. Samples were rinsed in PBS and then treated with PBS-buffered 0.1 % Triton X-100 for 5 min at RT to permeabilize the cell membranes for the antibody reactions. The samples were incubated for 45 min at RT with the primary antibodies: mouse anti-human PECAM-1 (1:50, Dako, Denmark) or mouse anti-human vimentin (1:200, Sigma-Aldrich, Germany). Following PBS washing, a second incubation was performed for 45 min at RT with the secondary antibody anti-mouse Alexa Fluor 488 (Invitrogen, Germany). The nuclei were counterstained with 1µg/mL Hoechst in PBS for 5 min. SPCL fiber-meshes were then washed with PBS, mounted with Gel/Mount (Natutec, Germany) and visualized by CLSM.

2.6. Induction of angiogenesis in vitro

The angiogenic potential of HDMEC growing on SPCL fiber-mesh scaffolds was assessed by observing the cell migration from the scaffold into a collagen type I gel that mimics the in vivo microenvironment. When HDMECs reached confluence on the scaffolds the scaffolds were transferred to a Petri dish and covered with a 1.5 mg/mL solution of collagen type I in M199 medium containing 2% sodium bicarbonate, 0.05 M NaOH and 200 nM HEPES. As soon as the solution solidified into a gel, culture medium supplemented with angiogenic growth factors 50 ng/mL VEGF (Biomol, Germany) and 10 ng/mL FGF-2 was added. After an additional 7 days in culture, materials were examined for the migration of ECs and organization into

capillary-like structures after calcein-AM live-staining and visualization by CLSM. All the above referred reagents were from Sigma-Aldrich, Germany.

In order to have a better perception of the spatial distribution of capillary-like structures and micro-fibers the confocal images were post-processed using the image processing software ITK-SNAP [24]. Individual confocal image stacks from nano/micro fiber combined scaffold composed of 99 sections were examined. Capillary-like structures were identified and labelled in green and red, respectively, using the manual segmentation tool and the segmented elements were processed into a final 3D image.

Aimed at the evaluation of EC ultrastructure, transmission electron microscopy (TEM) of collagen gel ultrathin sections was performed. Scaffolds plus collagen gel were fixed in 2.5 % glutaraldehyde in cacodylate buffer, post-fixed in 1% osmium tetroxide for 2 h and dehydrated in increasing ethanol concentration. Samples were embedded in agar resin 100 (PLANO, Germany) with ethanol as solvent for transition state and subjected to polymerization at 60°C for 48 hrs. Ultrathin sections were cut, placed onto copper grids and examined by transmission electron microscope (Philips EM 410).

3. RESULTS

3.1. Growth, viability and phenotype of ECs on starch-based scaffolds

ECs of microvascular origin, HDMECs as well the macrovascular HUVECs grew on both Fn-coated nano/micro fiber-combined scaffolds and on SPCL micro-mesh scaffolds. Growth was observed on both micro- and nano-fibers (Fig. V.1). The requirement of a pre-coating with Fn or other ECM molecule for EC adhesion to several substrates has been widely reported [25-27]. On nano/micro fiber-combined scaffolds, after 3 days of culture HDMEC spanned between adjacent micro-fibers using the nanobridges formed by the nano-fibers, thus yielding a high density of adherent ECs (Fig. V.1A). After 7 days, nearly complete growth on the surface areas

of the scaffold was observed (Fig. V.1B). HDMEC were found on both micro- and nano-fibers and remained viable as proven by the ability to convert calcein-AM into a green fluorescent compound. On the other hand, on the scaffold without the nano-network, cells were detected on the micro-fibers after 3 days as well as after 7 days, but no cells were seen to span between the fibers (Fig. V.1D and V.1E).

Cell adhesion studies were also performed with primary cultures of macrovascular ECs, HUVECs. HUVECs seeded onto nano/micro fiber-combined scaffolds rapidly covered the entire surface of the nano-network without significantly impairing the scaffold porosity (day 3, Fig. V.1C). On the other hand, viable HUVECs adhered to the individual fibers on SPCL micro-fiber mesh scaffold (Fig. V.1F).

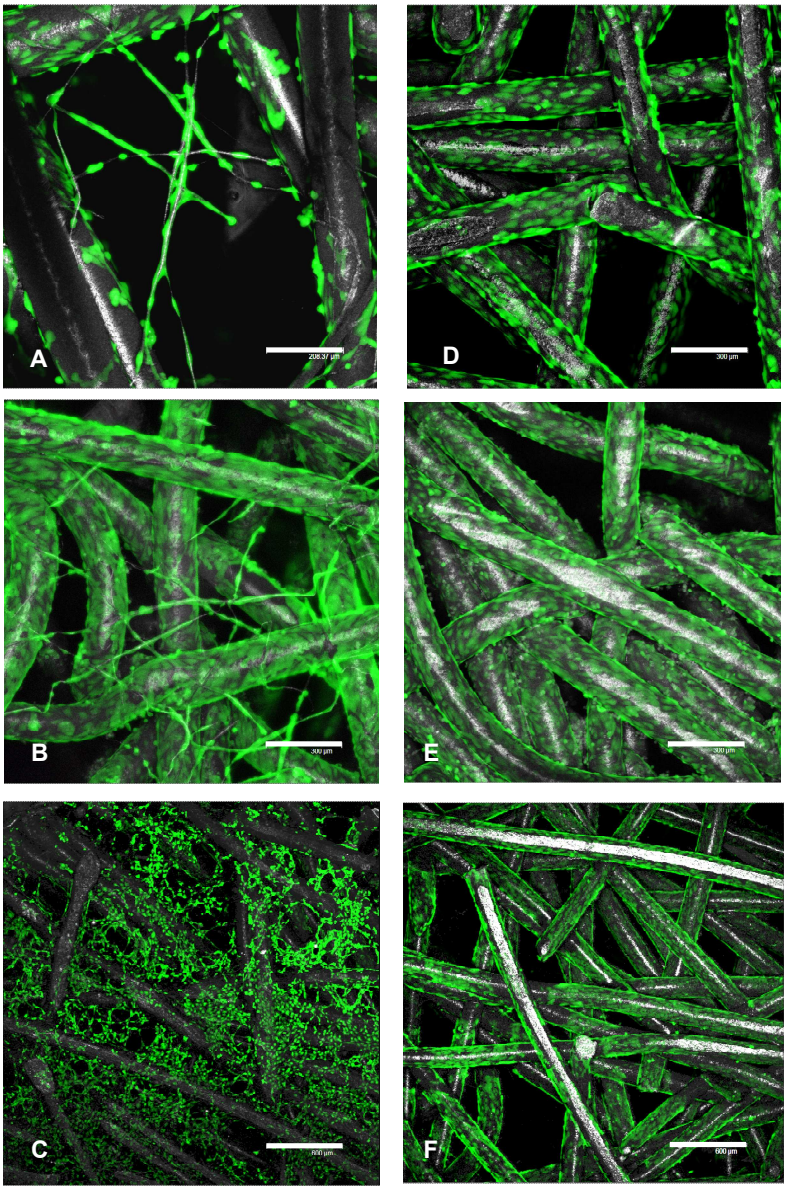

Figure V.1. Confocal fluorescent micrographs of viable HDMECs (A, B, D, E) and HUVECs (C & F) growing on Fn-coated nano/micro fiber combined scaffolds (left column) and on micro-fibre scaffold (right column) after 3 (A, D, C, F) and 7 days (B, E). Cells were stained with the vital fluorochrome calcein-AM. Good cell growth is seen for both EC types on both nano- and micro-fibres. The values of the scale bars are: (A) 208 μm, (B, D, E) 300 μm, (C, F) 600μm.

Phenotype of HUVECs was assessed by SEM after 3 days of culture. ECs adhered to the randomly electrospun nano-network as well as to microfibers and cells used the nano-fibers to bridge empty spaces in the micro-fiber mesh (Fig. V.2A). In contrast, the SPCL micro-fiber mesh scaffold did not induce cell-spanning across the construct

(Fig. V.2C). Morphologically, ECs on micro-fibers exhibited the typical flattened phenotype of ECs (Fig. V.2C) whereas the nano-network induced a different cytoskeletal arrangement reflected in the stretched shape and numerous cellular protrusions (Fig. V.2A). Besides improving the interconnectivity in the scaffold, nano/micro fiber-combined scaffolds also provided a unique physical support that allows the growth of ECs into circular arrangements that resemble the morphology of capillary-like structures (Fig. V.2B).

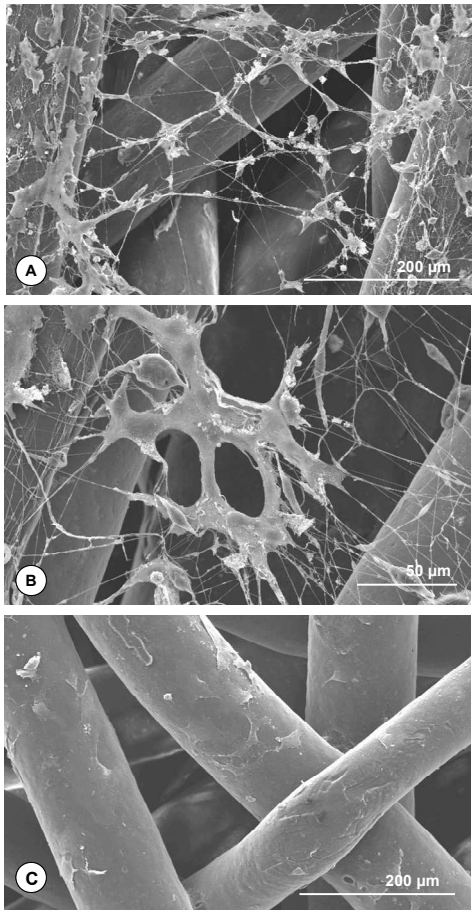

Figure V.2. SEM micrographs of HUVEC cells on Fn-coated SPCL scaffolds: (A, B) nano/micro fiber-combined scaffold and (C) micro-fibre scaffold after 3 days of culture. Note the ability of the EC to use the nanofibres to span across the microfibre structure.

3.2. Expression of genes involved in the inflammatory response

In blood vessels the endothelium functions as a dynamic and actively transporting barrier, which under special conditions, such as inflammation, mediates leukocyte

recruitment by the expression of different cell adhesion molecules like ICAM-1 and selectins. Utilizing Real Time PCR the expression of two cell adhesion molecules E-selectin and ICAM-1 on HUVECs growing on nano/micro fiber-combined scaffolds was analyzed and compared with the expression on control scaffolds (SPCL micro-fiber mesh scaffold without nano-fibers). HUVECs grown on tissue culture plastic served as control (Fig. V.3). ECs growing on the three substrates reacted in a similar way when exposed to the pro-inflammatory stimulus LPS, increasing the levels of mRNA that code for ICAM-1 and E-selectin. As a common pattern it was observed that the up-regulation of E-selectin was higher than ICAM-1 in response to LPS. This lower level of up-regulation of ICAM-1 relatively to E-selectin is probably due to the constitutive expression of this cell adhesion molecule on ECs and consequently to a minor difference between the basal and stimulated state. With respect to the combined scaffold, the presence in the same construct of micro- and nanometric fiber size did not affect the ability of ECs to properly respond to pro-inflammatory stimuli through the up-regulation of these genes related to the capture of circulating leukocyte, this representing an essential stage in the physiological inflammatory reaction.

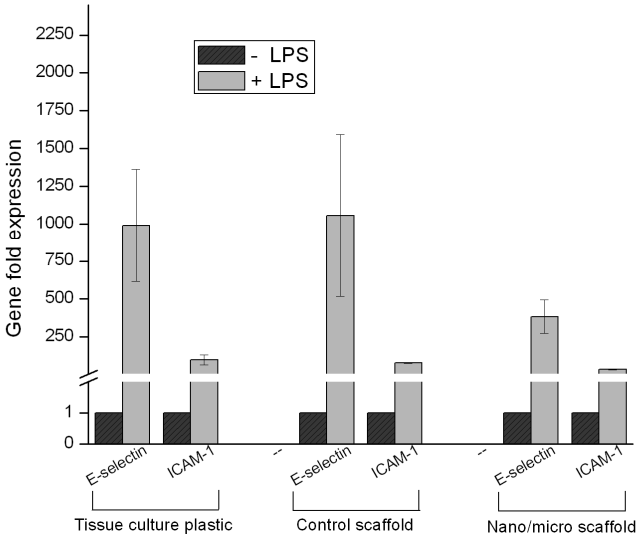

Figure V.3. Relative quantification of E-selectin and ICAM-1 mRNA in HUVECs grown on nano/micro fiber scaffolds and on micro-fibre scaffolds in the presence of LPS (+LPS) compared with the growth in the absence of pro-inflammatory stimulus (-LPS). As a control the expression of these inflammatory genes was assessed on HUVECs growing on cell culture plastic.

3.3. Expression of the structural protein vimentin and of the cell-cell adhesion molecule PECAM-1

Cell structure and the interactions with neighbouring cells are important aspects to take into consideration in studying cell functionality. Thus, the expression of vimentin, an intermediate filament protein present in mesenchymal cells and of PECAM-1 (CD 31), a cell adhesion molecule present predominantly at the intercellular junctions was assessed by immunocytochemical staining. Figure V.4A shows that on nano-fibers, endothelial vimentin filaments are more stretched, but no disruption of this structural protein was observed. Elongated, vimentin-stained cells populated the entire scaffold and grew along both nano- and micro-fibers.

A typical PECAM-1 expression pattern (a peripheral ring surrounding cells at cell-cell interfaces) was observed on both nano-micro fiber-combined scaffolds and on control scaffolds (Fig. V.4B and V.4C). ECs on nano-fibers as well as on micro-fibers continued to express this major cell adhesion molecule. This indicates that despite the differences in the dimensions of the underlying substratum ECs can still establish contact with adjacent cells.

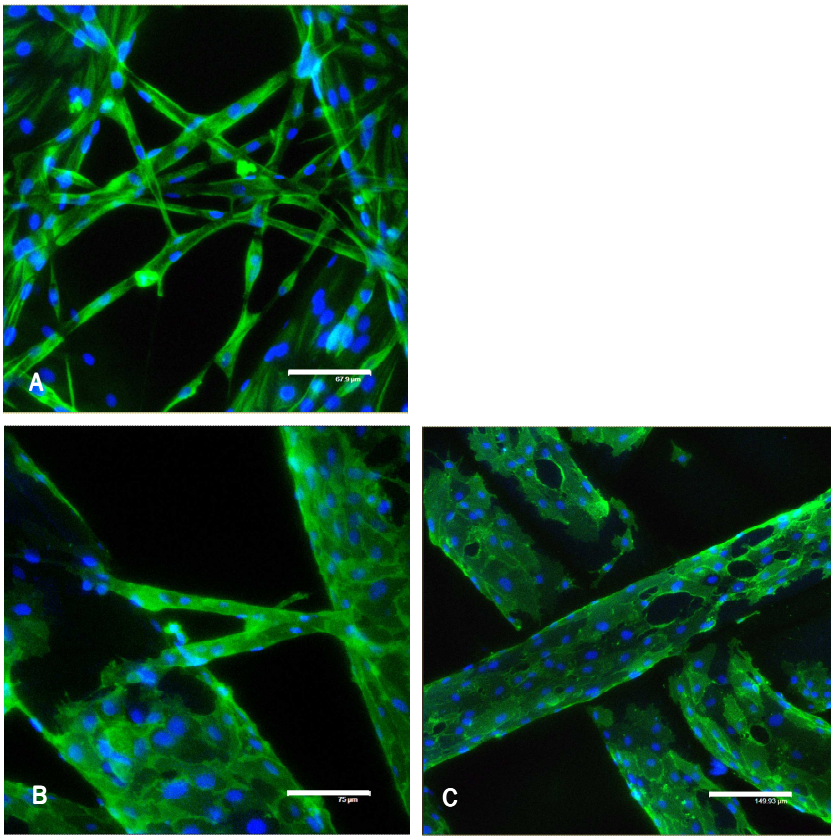

Figure V.4. Immunofluorescence micrographs of vimentin (A) and PECAM-1 staining (B, C) (green fluorescence) in HUVEC cells grown on nano/micro fiber combined scaffold (A, B) and on micro-fibre scaffold (C). Nuclei were counterstained with Hoechst (blue fluorescence). The values of the scale bars are: (A) 68 μm, (B) 75 μm, (C) 150 μm.

3.4. Angiogenic potential of ECs on starch-based scaffolds

In a more complex in vitro assay, the ability of ECs in contact to the scaffolds to invade into and to form capillary-like structures within a 3D-gel of collagen in response to angiogenic factors was assayed. To visualize the cells within the 3D-matrix a calcein-AM staining was necessary. This staining revealed that ECs were able to migrate from the scaffold and invade into the collagen gel on both nano/micro fiber-combined scaffolds as well as in control scaffolds, after 7 days of culture (Fig. V.5). However, a different behaviour between the two scaffolds was observed. On the micro/nano fiber combined scaffold, ECs formed more capillary structures with branching (Fig. V.5A). In contrast, on the scaffolds without the nano-network, ECs formed fewer capillary-like structures with less branching (Fig. V.5C).

The 3D reconstitution of the segmented micro-fibers and capillary-like structures from the confocal stack images of nano/micro fiber-combined scaffold (Fig. V.5A is the projection) provided further information. It was shown that the tubular structures formed by ECs were present at different depths, and that there was a spatial separation between the capillary-like structures and the micro-fibers along the Z axis (Fig. V.5D). Thus, this further reinforces the ability of ECs to migrate out of the scaffold into the collagen matrix and to organize into capillary-like structures.

The ultrastructure of ECs assessed by TEM revealed the existence of adherent junctions between ECs, denoting the intimate contact between angiogenesis-stimulated cells (Fig. V.6A). At a higher magnification numerous vesicles were visible, indicative of the highly active state of the ECs (Fig. V.6B).

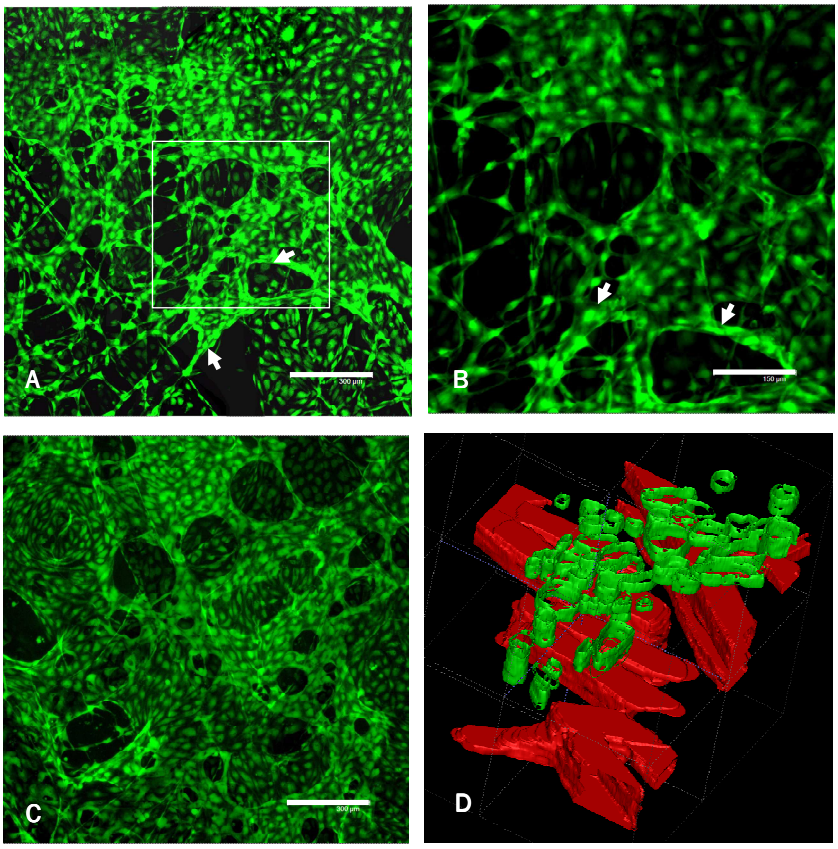

Figure V.5. CLSM of capillary-like structures formed by angiogenesis-stimulated HDMECs from nano/micro fiber combined scaffold (A, B, D) and from micro-fibre scaffold (C). Fig. B is the higher magnification of the square highlighted in Fig. A. Fig. D is the 3D reconstruction from the manual segmentation of micro-fibers and capillary-like structures on the sections that make up Fig.. A. Scaffolds were cultured for 7 days with HDMECs and then covered with a type I collagen gel and cultured for a further 7 days. White arrows indicate some of the capillary-like structures. The values of the scale bars are: (A) 300 μm, (B) 150 μm, (C) 300μm.

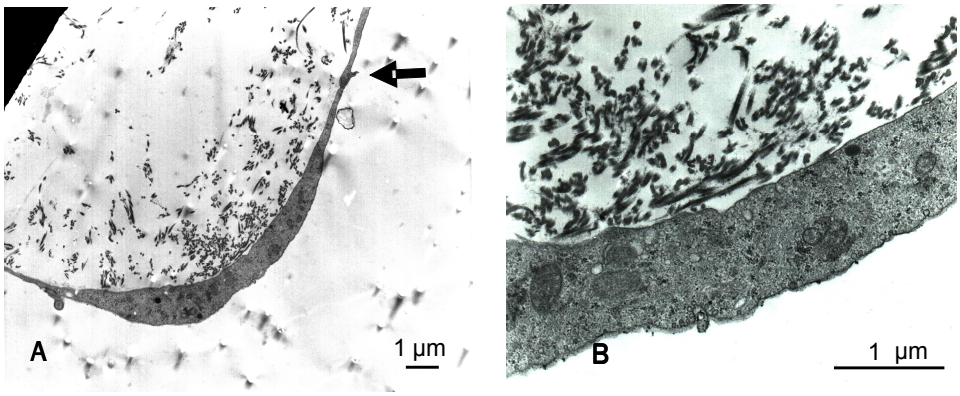

Figure 6. Transmission electron micrograph of migrating ECs from nano/micro combined scaffold to collagen gel, in a pro-angiogenic environment. The black arrow indicates the intimate contact between two ECs.

4. DISCUSSION

Tissue engineering scaffolds should function as temporary ECMs and until repair or regeneration occurs they should aim to mimic native ECM both architecturally and functionality [28]. In physiological tissue re-organization (e.g. during wound healing) the bidirectional flow of information exchanged between cells and ECM steers important cell functions such as adhesion, differentiation and migration [29]. Thus, it can be suggested that the more a scaffold can resemble ECM, the more successful the scaffold can be. To date, electrospinning has been one of the main processing techniques used in the fabrication of structures in the nanometer range. This fiber spinning technique produces polymer fibers with diameters down to a few nanometers and nano-fibers obtained by electrospinning have been proposed for engineering many different tissues [30]. However electrospun scaffolds retain several problems such as three-dimensional cell growth restricted to a depth of 100 µm, lack of control of pore diameter and distribution, as well as low stiffness [31].

Tuzlakoglu et al proposed nano/micro fiber-combined scaffolds, a matrix that combines two structures (i) a nano-network produced by electrospining, that mimics ECM and aims to increase cell adhesion and motility; with (ii) a microfiber-mesh produced by fiber-bonding aimed to give the mechanical support required during repair [20]. This latter structure, an SPCL fiber-mesh scaffold, was used in this work

as a control and it was previously described by our group as a promising biomaterial for bone regeneration [21, 32, 33]. Studies with bone marrow cells cultured under dynamic conditions on SPCL fiber-mesh scaffolds showed that cells differentiated into osteoblasts, deposited a mineralized matrix and produced several bone growth factors [21, 32, 33]. Furthermore, previous work with ECs revealed that they maintained their genotypic and phenotypic patterns when growing on SPCL fiber-mesh scaffolds [34].

Based on the previous studies that have proven the suitability of nano/micro fiber-combined scaffold for osteoblast differentiation and activity [20], the present work deals with the influence this ECM-like architecture has on EC growth pattern, homo- and heterotypic interactions and on angiogenic potential.

Cell adhesion studies with HDMECs and HUVECs revealed that both cell types adhere and remain viable on fibers in the nano- as well as in the micrometer-range. In fact, in the nano/micro fiber-combined scaffold the existence of a structure that resembles the physical structure of ECM furnishes the physical points required for ECs to span between the bulk structure of the scaffold without compromising the porosity and interconnectivity of the structure. Moreover, these nanometer dimensions are reflected in individual cell phenotype and overall cellular rearrangement. On the micro-fibers the cells exhibit the same flattened morphology characteristic of their location inside larger blood vessels. By contrast, on the nano-network ECs present an extremely stretched shape reminiscent of the angiogenic phenotype, with multiple cellular protrusions anchoring them to several nano-fibers. This stretched phenotype might be beneficial as it was reported that ECs spreading or elongating show increased sensitivity to specific growth factors such as FGF-2 [35]. Furthermore, the nano-fibers allow a more comprehensive arrangement of ECs positioned within the scaffolds when compared with the scaffolds without nano-fibers. Thus, ECs could be easier available for blood vessel formation after implantation of constructs. Of special interest is the capability of the adherent cells to use the physical support provided by the nano-network to adhere and spread into circular arrangements that morphologically resemble capillary-like structures.

Bone tissue-engineered constructs should not only induce good phenotypic properties in ECs such as spreading morphology, cell viability, and cell attachment

but also encourage ECs cell functions, which can be assessed through the expression of cell-cell adhesion molecules involved in heterotypic (cell adhesion molecules such as ICAM-1) and homotypic (PECAM-1) interactions as well as in migration studies. Concerning the heterotypic interactions, ECs play a key role during the inflammatory response through the sequential expression of cell adhesion molecules [36]. These molecules recognize specific ligands on circulating leukocytes and help them to transmigrate across the endothelium towards the pro-inflammatory stimuli, thus enabling inflammation. In a scaffold for tissue regeneration it is necessary that in the presence of a pro-inflammatory stimulus, such as cytokines like TNF-α or bacterial compounds like endotoxins, ECs possess the potential to participate through the expression of adhesion molecules for leukocytes. That means that scaffolds must allow ECs to participate adequately during an inflammatory response but in the absence of an inflammatory stimulus should not induce up-regulation of cell adhesion molecules. This last situation could lead to a continuously inflammatory activated endothelium and consequently to a massive recruitment of leukocytes and increased vascular permeability. To this end, the possible interference of the nano/micro fiber-combined scaffold on gene expression of two cell adhesion molecules characteristic for pro-inflammatory activation of ECs, E-selectin and ICAM-1, was analyzed by Real Time PCR. The results showed the ability of ECs on nano/micro fiber-combined scaffold to up-regulate the expression of ICAM-1 and E-selectin in response to the pro-inflammatory stimulus LPS, following the same pattern observed for the scaffold- and tissue culture plastic controls. This not only suggests the capacity of cells growing on nano/micro combined scaffolds and on control scaffolds to participate in the inflammatory response through the expression of pro-inflammatory genes, but also indicates that under normal conditions (absence of LPS) the growth of ECs on these scaffolds does not appear to affect the expression of these genes.

The interendothelial interactions of endothelial cells on the scaffolds were evaluated by PECAM-1 distribution pattern. When studying the interaction of tissue engineered scaffolds with ECs it is important to assess PECAM-1 distribution pattern, not only because it is a major endothelial marker but also due to the key role this protein plays in endothelial barrier integrity and in leukocyte transmigration during the

inflammatory response [37]. On SPCL fibers in the nano- and micro-range, PECAM-1 is present predominantly in the contact sites at cell-cell borders. These cell-cell contact sites are a positive indication of the adequate interendothelial contacts established between adjacent cells when growing and are typical of a quiescent (non-stimulated) endothelium. This is particularly relevant for the nano-network as the effects of electrospun nano-fibers on the phenotypic behavior of a variety of cell types has been previously reported [28]. In order to examine endothelial cell structure we performed immunostaining for vimentin on cells growing on fibers. Vimentin is an intermediate filament protein responsible for maintaining cell shape, integrity of the cytoplasm, and stabilizing cytoskeletal interactions [38]. Vimentin filaments in the cells growing on the nano-network were more stretched than those on micro-fibers but exhibited no apparent disruption of cell structural integrity.

A successful scaffold for bone regeneration must not only promote osteogenesis but also promote the development of a vascular network. Post-natal vascularization occurs mainly by angiogenesis, which is a multi-stage process characterized by an orderly sequence of events including matrix degradation, EC migration, proliferation and formation of new basement membrane components [39]. Migration is driven chemotactically via gradients of cytokines or other agonists but it is the fibrillar structure of ECM in the nanometer-range of dimensions that provides the physical cues to proliferating and migrating ECs to organize and form new 3D capillary networks [19]. The angiogenic potential of ECs on the scaffold with ECM-like structure under a pro-angiogenic environment was examined in order to determine if nano-structures affected this process. ECs migrated from both scaffolds into the collagen gel, but there appeared to be an elevation in migration and 3D organization into capillary-like structures in the nano/micro combined scaffold. This achievement in the later scaffold could be due to the increased surface area, the ECM-like structure and to the elongated cell morphology. Folkman et al reported that confluent ECs are refractory to growth factors, whereas stretched or elongated ECs have increased sensitivity to growth factors, such as FGF-2 [35]. These findings might indicate that stretched cells on nano-fibers are more responsive to angiogenic growth factors thus organizing more easily into capillary-like structures, than confluent and

less sensitive cells on micro-fibers. Whether this is the case, needs to be investigated in further studies which quantitate the complex three-dimensional reaction.

5. CONCLUSION

The incorporation of structures that physically mimic the ECM, *i.e.*, nano-networks on micro-fiber meshes, not only increased the adhesion surface area and interconnectivity in the constructs but also provided structural and organizational stability for ECs. Using nano-fibers as bridges both human micro- and macrovascular ECs spanned between micro-fibers, exhibited a more stretched phenotype when compared with the scaffold without nano-fibers. Furthermore, once the nano-fibers allowed a comprehensive arrangement of ECs in the in vitro constructs, ECs could be easier available for blood vessel formation after implantation of constructs. Furthermore, ECs on nano- as well on micro-fibers maintained their structural integrity (vimentin) and their intercellular contacts (PECAM-1). Moreover, ECs growing on nano/micro combined scaffolds exhibited a marked angiogenic potential as shown by their ability to form extensive networks of capillary-like structures.

REFERENCES

1. Shastri VP. Future of regenerative medicine: challenges and hurdles. Artif Organs. 2006; 30(10):828-34.

2. Laschke MW, Harder Y, Amon M, Martin I, Farhadi J, Ring A, et al. Angiogenesis in tissue engineering: Breathing life into constructed tissue substitutes. Tissue Engineering. 2006; 12(8):2093-104.

3. Zhu YB, Gao CY, He T, Shen JC. Endothelium regeneration on luminal surface of polyurethane vascular scaffold modified with diamine and covalently grafted with gelatin. Biomaterials. 2004; 25(3):423-30.

4. Jain RK, Au P, Tam J, Duda DG, Fukumura D. Engineering vascularized tissue. 2005; 23(7):821-3.

5. Kneser U, Polykandriotis E, Ohnolz J, Heidner K, Grabinger L, Euler S, et al. Engineering of vascularized transplantable bone tissues: Induction of axial vascularization in an osteoconductive matrix using an arteriovenous loop. Tissue Engineering. 2006; 12(7):1721-31.

6. Rouwkema J, De Boer J, Van Blitterswijk CA. Endothelial cells assemble into a 3-dimensional prevascular network in a bone tissue engineering construct. Tissue Engineering. 2006; 12(9):2685-93.

7. Parfitt AM. The mechanism of coupling: a role for the vasculature. Bone. 2000; 26(4):319-23.

8. Brey EM, Uriel S, Greisler HP, McIntire LV. Therapeutic neovascularization: contributions from bioengineering. Tissue Eng. 2005; 11(3-4):567-84.

9. Laroche M. Intraosseous circulation from physiology to disease. Joint Bone Spine. 2002; 69(3):262-9.

10. Mikos AG, Herring SW, Ochareon P, Elisseeff J, Lu HH, Kandel R, et al. Engineering complex tissues. Tissue Eng. 2006; 12(12):3307-39.

11. Koch S, Yao C, Grieb G, Prevel P, Noah EM, Steffens GCM. Enhancing angiogenesis in collagen matrices by covalent incorporation of VEGF. J Mater Sci-Mater M. 2006; 17(8):735-41.

12. Richardson TP, Peters MC, Ennett AB, Mooney DJ. Polymeric system for dual growth factor delivery. Nat Biotechnol. 2001; 19(11):1029-34.

13. Warnke PH, Springer IN, Wiltfang J, Acil Y, Eufinger H, Wehmoller M, et al. Growth and transplantation of a custom vascularised bone graft in a man. Lancet. 2004; 364(9436):766-70.

14. Warnke PH, Wiltfang J, Springer I, Acil Y, Bolte H, Kosmahl M, et al. Man as living bioreactor: Fate of an exogenously prepared customized tissue-engineered mandible. Biomaterials. 2006; 27(17):3163-7.

15. Choong CS, Hutmacher DW, Triffitt JT. Co-culture of Bone Marrow Fibroblasts and Endothelial Cells on Modified Polycaprolactone Substrates for Enhanced Potentials in Bone Tissue Engineering. Tissue Eng. 2006.

16. Levenberg S, Rouwkema J, Macdonald M, Garfein ES, Kohane DS, Darland DC, et al. Engineering vascularized skeletal muscle tissue. Nat Biotechnol. 2005; 23(7):879-84.

17. Ma Z, Kotaki M, Yong T, He W, Ramakrishna S. Surface engineering of electrospun polyethylene terephthalate (PET) nanofibers towards development of a new material for blood vessel engineering. Biomaterials. 2005; 26(15):2527-36.

18. Li CM, Vepari C, Jin HJ, Kim HJ, Kaplan DL. Electrospun silk-BMP-2 scaffolds for bone tissue engineering. Biomaterials. 2006; 27(16):3115-24.

19. Davis GE, Senger DR. Endothelial extracellular matrix: biosynthesis, remodeling, and functions during vascular morphogenesis and neovessel stabilization. Circ Res. 2005; 97(11):1093-107.

20. Tuzlakoglu K, Bolgen N, Salgado AJ, Gomes ME, Piskin E, Reis RL. Nano- and micro-fiber combined scaffolds: a new architecture for bone tissue engineering. J Mater Sci Mater Med. 2005; 16(12):1099-104.

21. Gomes ME, Sikavitsas VI, Behravesh E, Reis RL, Mikos AG. Effect of flow perfusion on the osteogenic differentiation of bone marrow stromal cells cultured on starch-based three-dimensional scaffolds. J Biomed Mater Res. 2003; 67A(1):87-95.

22. Gomes ME, Azevedo HS, Moreira AR, Ella V, Kellomaki M, Reis RL. Starch-poly(epsilon-caprolactone) and starch-poly(lactic acid) fibre-mesh scaffolds for bone tissue engineering applications: structure, mechanical properties and degradation behaviour. J Tissue Eng Regen Med. 2008; 2(5):243-52.

23. Nachtigal P, Gojova A, Semecky V. The role of epithelial and vascular-endothelial cadherin in the differentiation and maintenance of tissue integrity. Acta Medica (Hradec Kralove). 2001; 44(3):83-7.

24. Yushkevich PA, Piven J, Hazlett HC, Smith RG, Ho S, Gee JC, et al. User-guided 3D active contour segmentation of anatomical structures: Significantly improved efficiency and reliability. Neuroimage. 2006; 31(3):1116-28.

25. Unger RE, Huang Q, Peters K, Protzer D, Paul D, Kirkpatrick CJ. Growth of human cells on polyethersulfone (PES) hollow fiber membranes. Biomaterials. 2005; 26(14):1877-84.

26. Unger RE, Peters K, Wolf M, Motta A, Migliaresi C, Kirkpatrick CJ. Endothelialization of a non-woven silk fibroin net for use in tissue engineering: growth and gene regulation of human endothelial cells. Biomaterials. 2004; 25(21):5137-46.

27. Boura C, Muller S, Vautier D, Dumas D, Schaaf P, Claude Voegel J, et al. Endothelial cell--interactions with polyelectrolyte multilayer films. Biomaterials. 2005; 26(22):4568-75.

28. Pham QP, Sharma U, Mikos AG. Electrospinning of polymeric nanofibers for tissue engineering applications: a review. Tissue Eng. 2006; 12(5):1197-211.

29. Lutolf MP, Hubbell JA. Synthetic biomaterials as instructive extracellular microenvironments for morphogenesis in tissue engineering. Nat Biotechnol. 2005; 23(1):47-55.

30. Kwon IK, Kidoaki S, Matsuda T. Electrospun nano- to microfiber fabrics made of biodegradable copolyesters: structural characteristics, mechanical properties and cell adhesion potential. Biomaterials. 2005; 26(18):3929-39.

31. Boudriot U, Dersch R, Greiner A, Wendorff JH. Electrospinning approaches toward scaffold engineering--a brief overview. Artif Organs. 2006; 30(10):785-92.

32. Gomes ME, Bossano CM, Johnston CM, Reis RL, Mikos AG. In vitro localization of bone growth factors in constructs of biodegradable scaffolds seeded with marrow stromal cells and cultured in a flow perfusion bioreactor. Tissue Eng. 2006; 12(1):177-88.

33. Gomes ME, Holtorf HL, Reis RL, Mikos AG. Influence of the porosity of starch-based fiber mesh scaffolds on the proliferation and osteogenic differentiation of bone marrow stromal cells cultured in a flow perfusion bioreactor. Tissue Eng. 2006; 12(4):801-9.

34. Santos MI, Fuchs S, Gomes ME, Unger RE, Reis RL, Kirkpatrick CJ. Response of micro- and macrovascular endothelial cells to starch-based fiber meshes for bone tissue engineering. Biomaterials. 2007; 28(2):240-8.

35. Folkman J, Shing Y. Angiogenesis. J Biol Chem. 1992; 267(16):10931-4.

36. Muller AM, Hermanns MI, Cronen C, Kirkpatrick CJ. Comparative study of adhesion molecule expression in cultured human macro- and microvascular endothelial cells. Exp Mol Pathol. 2002; 73(3):171-80.

37. Peters K, Unger R, Stumpf S, Schäfer J, Tsaryk R, Hoffmann B, et al. Cell type-specific aspects in biocompatibility testing: the intercellular contact in vitro as an indicator for endothelial cell compatibility. Journal of Materials Science: Materials in Medicine. 2008; 19(4):1637-44.

38. Goldman RD, Khuon S, Chou YH, Opal P, Steinert PM. The function of intermediate filaments in cell shape and cytoskeletal integrity. J Cell Biol. 1996; 134(4):971-83.

39. Cassell OC, Hofer SO, Morrison WA, Knight KR. Vascularisation of tissue-engineered grafts: the regulation of angiogenesis in reconstructive surgery and in disease states. Br J Plast Surg. 2002; 55(8):603-10.

CHAPTER VI

Design of Nano- and Micro-fiber Combined Scaffolds by Electrospinning of Collagen onto Starch-based Fiber Meshes: A Man-made Equivalent of Natural ECM

CHAPTER VI

Design of Nano- and Micro-fiber Combined Scaffolds by Electrospinning of Collagen onto Starch-based Fiber Meshes: A Man-made Equivalent of Natural ECM *

ABSTRACT

Mimicking the structural organization and biologic function of ECM has been one of the main goals of tissue engineering. Nevertheless, the majority of scaffolding materials for bone regeneration highlights biochemical functionality typically in detriment of mechanical properties. In this work we present a rather innovative construct that combines in the same structure electrospun type I collagen nano-fibers with starch-based micro-fibers. These combined structures were obtained by a two step methodology and structurally consist in a type I collagen nano-network incorporated on a macro starch-based support. The morphology of the developed structures was assessed by several microscopy techniques and the collagenous nature of the nano-network was confirmed by immunohistochemistry. In addition, and especially regarding the requirements of large bone defects, we also successfully introduce the concept of layer-by-layer as a way to produce thicker structures.

In an attempt to recreate bone microenvironment the design and biochemical composition of the combined structures was also envisioning bone forming cells and ECs. The inclusion of a type I collagen nano-network induced a stretched morphology and improved metabolic activity of osteoblasts. Regarding ECs, the presence of type I collagen on the combined structures provided adhesive support and obviated the need of pre-coating with Fn. It was also importantly observed that ECs on the nano-network were organized into circular structures in a 3D arrangement distinct from that observed for osteoblasts. These self-organized structures resembled the microcappillary-like organizations formed during angiogenesis. By providing simultaneously physical and chemical cues for cells, the herein proposed combined structures hold a great potential in bone regeneration as a man-made equivalent of extracellular matrix.

* This chapter is based on the following publication:

K. Tuzlakoglu#, M. I. Santos#, Nuno Neves, R. L. Reis. Design of Nano- and Micro-fiber Combined Scaffolds by Electrospinning of Collagen onto Starch-based Fiber Meshes: A Man-made Equivalent of Natural ECM. (2008). *Submitted*.

# These two authors contributed equally to this work

1. INTRODUCTION

In bone tissue engineering, the material selection lies at the very heart of the scaffold design. Up to date, various alternatives, such as metals, ceramics and polymers, have been proposed to be used as scaffold materials. Nowadays, scaffolds are typically fashioned from biodegradable materials of natural origin proteins like collagen [1], silk fibroin [2], and polymers like chitosan [3], starch [4], poly(3-hydroxybutyrate) [5] and also from synthetic polymers such as poly(lactide) [6], PLGA [7], PCL [8]. Although synthetic polymers appear to be a good choice regarding processing, critical problems in biocompatibility, degradation products, and numerous other issues still remain to be solved. Conversely, naturally derived materials offer some advantages in terms of biocompatibility, as well as biochemical functionality by showing similarity to structures in animal tissues. The use of collagen as a scaffold is distinct from other polymers mainly in its role in the formation of tissue and organs. It is the most abundant mammalian protein accounting for about 20–30% of total body proteins [9]. Collagen assembles into different supramolecular structures in natural ECM of tissues and has exceptional functional diversity.

ECM is a complex composite of various proteins in fibrillar form and glycosaminoglycans chains [10] and provides an important model for scaffold design. This network structure serves as a scaffold which can support tensile and compressive stresses by the fibrils and hydrated networks. Besides providing an appropriate microenvironment for cells, ECM is responsible for transmitting signals to cell membrane receptors that reach nucleus via intracellular signaling cascades. Therefore, the fibrillar and porous structure of ECM have a great influence on cell functionality, mainly on cell adhesion and migration.

The development of suitable scaffolds, man-made systems that can mimic the structural organization and biologic function of natural ECM, remains a major aim for tissue engineers. In recent years, the electrospinning processes have received substantial attention as a way to mimic the structure of natural ECM by means of producing fibers down to 3nm [11]. This is due to architectural similarity of the nonwoven mats, composed of electrospun nanofibers, to collagen structure of ECM.

However, the pore sizes of electrospun mats, which are smaller than a cellular diameter, can not allow for cell migration within the structure and results in a scaffold surface covered as a film by cells. Such type of systems can not be used for tissue engineering of 3D tissues. Furthermore, the small size of the fibers tends not to maximize the points of cell attachment which is a negative effect on the expression of several factors and on cell spreading and differentiation.

When trying to engineer of bone, the scaffold must meet the mechanical properties of the tissue while it should also ideally imitate the biological task of ECM. Bone tissue is composed of a heterogeneous mixture of cell types embedded within a mineralized ECM [12]. In order to assure the requirements of this metabolic active tissue, bone microenvironment is supplied by a complex intraosseous circulation composed by an intricate network of arteries, capillaries and veins [13]. Type I collagen is the major organic component of the osseous ECM. Besides its structural role, this ECM protein also promotes cell adhesion in an integrin-mediated fashion [14]. In addition, type I collagen modulates cell-specific functions. It has been reported that in the osteogenic lineage it promotes osteogenic differentiation, proliferation and mineralization [12, 15]. ECs are pivotal cells in blood vessel formation, and it is known that interstitial type I collagen induces the directional migration and lumen formation during angiogenesis [16, 17].

In fact osteogenesis and angiogenesis are two phenomena that can not be dissociated during skeletal development, fracture repair as well as in bone tissue engineering [18]. It is well-known that prompt revascularization favors osteoblastic differentiation, whereas prolonged hypoxia favors formation of cartilage or fibrous tissue [19]. In bone tissue engineering, vascularization is not only necessary for new bone formation but it is also vital for the survival of the implanted cells on the carrier material after implantation [20]. Accordingly, strategies that enhance angiogenesis should have positive effects on bone repair [21].

Most approaches to engineering new tissue relied on the host for vascularization but this is clearly not successful in thick and highly vascularized tissues such as bone [22]. Hence, the need for proper vascularization, which involves the creation of a microvascular network and a macroscopic circulation, remains one of the major problems for larger tissue-engineered structures [23]. To create a vascularized

scaffold, a number of methods have been proposed [24, 25]. One approach involves the transplantation of ECs in an effort to engineer a vascular network from these cells, rather than waiting for host-blood-vessel ingrowth [26]. However, independently of the adopted approach to accelerate vascularization all of them will involve directly or indirectly ECs. Therefore, the key success for vascularized bone is the development of a structure that includes not only bone forming cells but also ECs.

We herein propose for the first time the use of combined structures as a man-made equivalent of natural ECM for bone tissue engineering. These constructs combine a macro support, made from SPCL microfibers meshes, with a nano-network of electrospun type I collagen, these structures were designed envisioning formation of a mineralized matrix supplied by a vascular network. Therefore, in this work we have characterized the developed structures from the chemical and structural point of view, and assessed the cellular responses of bone forming cells and ECs.

2. MATERIALS AND METHODS

2.1. Materials

The material used in the production of fiber meshes was a SPCL blend. More details on this material can be found elsewhere [4, 27]

Collagen was isolated from Wistar rat tails according to a typical acid extraction procedure. Briefly, the rat tails from sacrificed animals were cut off and soaked in 70% ethanol for 1 min. The tendons were then pull out and dissolved in 0.5M sterile acetic acid. The resulted solution were filtered through a sterile muslin gauze and freeze dried. All the reagents used were analytical grade unless specified otherwise.

2.2. Production of nano- and micro-fiber combined structures

2.2.1. Wet spinning

Starch-based fiber meshes were fabricated by wet spinning methodology as described elsewhere [4]. In a typical procedure, a viscous polymer solution was obtained by dissolving SPCL in chloroform at a concentration of 40% (w/v). Methanol was used as a coagulant. A syringe pump (World Precision Instruments, UK) was used to extrude a certain amount of polymer into a coagulation bath. The fiber mesh structure was formed during the processing by moving of the coagulation bath randomly. The fiber meshes were then dried at room temperature overnight in order to remove remaining solvents.

2.2.2. Electrospinning

To obtain collagen nanofibers on the wet-spun SPCL fiber meshes, an electrospinning method was used. A 0.85mg of collagen was dissolved in 1ml of HFP and thoroughly mixed until the dissolution completed. The polymer solution was put into a syringe and placed in a syringe pump. A positive high-voltage supplier was used to maintain the voltage at 20kV. The voltage was applied between the syringe tip and a ground plate, where the fiber mesh membranes were placed, during 10 seconds. Both sides of the membranes were impregnated with collagen nanofibers. The final structures were then dried overnight at room temperature to eliminate solvent residuals.

2.2.3. Crosslinking of the combined structures

The developed constructs were crosslinked with saturated gluteraldehyde vapor at room temperature for 48h. The samples were placed on a metal mesh and put inside a vacuum oven containing an aqueous glutaraldehyde solution with a concentration of 30% (v/v). After crosslinking, the constructs were subsequently immersed in 0.02 M glycine solution for 4h in order to remove unreacted glutaraldehyde. They were

then washed several times with distilled water, dried and stored at desiccator until use.

2.2.4. Design of thicker scaffolds using a layer by layer concept

Although the thickness of the prepared membrane allows to impregnate the micro fiber meshes with nanofibers, it would be more difficult to obtain a homogenous structure when the thickness of the fiber meshes increases. In order to overcome this problem, we propose in this work the use of a layer by layer concept in order to design a thick scaffold with a homogenous nanofiber distribution, even in the interior part of the scaffold. In this method, SPCL fiber mesh membranes with one side deposited with collagen nanofibers were stack together by simply heating at 60°C, which is the melting point of SPCL. The schematic illustration of this process presented in figure VI.2.

2.3. Morphology of nano/micro combined scaffold

The morphology of the developed structures was visualized by SEM (Leica Cambridge S360) and an optical microscope. The samples were further examined by SEM in order to evaluate the influence of crosslinking in the fiber morphology and overall structure.

Furthermore and in a way to complement SEM data, the 3D architecture of the collagen nanonetwork was assessed by CLSM (Olympus IX81, Japan) after staining with antibody against type I collagen. The scaffolds were incubated for 1 h at RT with the primary antibody mouse anti-bovine (1:100, Sigma-Aldrich, Germany). Following PBS washing a second incubation was performed for 1 h at RT with secondary antibody anti-mouse Alexa Fluor 488 (1:100, Invitrogen, USA). The constructs were washed with PBS, mounted with mounting medium (Vectashield, UK) and visualized by CLSM.

2.4. Cells, culture conditions and scaffolds seeding

A human osteoblast cell line (SaOs-2) was selected to test the developed structures. The cells were cultured in completed medium (DMEM low glucose (Sigma-Aldrich, Germany) supplemented with 10% Foetal Bovine Serum (Sigma, Germany), 1% antibiotics/antimicotics (Sigma-Aldrich, Germany)) until they reached the confluency. They were then trypsinized and seeded onto the samples using the density of $2x10^5$ cells/scaffold. The cells on the combined structures were allowed to grow for 7 days under standard conditions (37 ºC, 5 % CO_2).

Primary cultures of human ECs (HUVEC) were isolated from the umbilical vein by collagenase digestion according to a previously published method [28]. HUVECs were cultured in M199 medium (Sigma-Aldrich, Germany) supplemented with 20 % FCS (Gibco, USA), 1% antibiotics/antimicotics, 2 mM glutamax I (Gibco, USA) , 25 µg/mL sodium heparin (Sigma-Aldrich, Germany) and 25 µg/mL ECGS (BD Biosciences, USA). Some of the combined structures were pre-coated with a Fn solution (10 µg/mL PBS, Sigma-Aldrich, Germany) for 1 hr at 37ºC. Confluent HUVECs were trypsinized and a suspension of $7.5x10^4$cells was added to each sample. The cell/sample constructs were incubated under standard culture conditions for 3 and 7 days.

2.5. Cells imaging

SEM was the chosen technique for an initial evaluation of the morphology of the cells growing on the developed scaffolds. Samples were fixed with 2,5 % glutaraldehyde in PBS for 30 min, dehydrated in increasing concentrations of alcohol, air-dried and sputter coated with gold prior to SEM observation (Leica Cambridge S360).

The cellular viability was assessed through the vital dye calcein-AM. Both osteoblasts- and HUVECs-seeded combined structures were incubated for 10 min in medium supplemented with 0,1µM calcein-AM. This vital dye is internalized by viable cells that due to the action of active intracellular esterases is converted into a green

fluorescent impermeable dye. Then samples were mounted in mounting medium Vectorshield (Vector, UK) and visualized by CLSM (Olimpus IX81).

2.6. PECAM-1 and phalloidin expression

Samples were fixed with a solution of 3.7% formalin (Sigma, Germany) and permeabilized with 0.1 % Triton for 5 min at RT. The scaffolds cultured with HUVECs were stained for the cell-cell adhesion molecule PECAM-1. For that ECs-seeded scaffolds were incubated for 45 min at RT with the primary antibody mouse anti-human PECAM-1 (1:50, Dako, Denmark). A second incubation was performed with the secondary antibody anti-mouse Alexa Fluor 488 for 45 min at RT.

Actin fibres of both HUVECs and SaOs cells growing on the scaffolds under analysis were visualized by fluorescent phalloidin. Fixed and permeabilized samples were incubated for 20 min with Alexa Fluor conjugated phalloidin (1:80, Sigma, Germany) at RT.

In both PECAM-1 and phalloidin staining experiments, the nuclei were counterstained with DAPI (1:1000, Sigma, Germany) for 5 min at RT. To remove the excess of reagents between each step, a washing with PBS was always performed.

2.7. Cell proliferation assay

After 3 and 7 days of culture, cell proliferation was assessed by means of measuring mitochondrial dehydrogenase activity using Cell Titer 96 Aqueous One Solution Cell Proliferation Assay kit (Promega, USA), according to the manufacturer's protocol. This assay is based on the bioreduction of the substrate MTS into a brown formazan product by NADPH or NADP produced by dehydrogenase enzyme in metabolically active cells. According to the standard procedure, the triplicates of the samples were washed with sterile PBS and placed in new culture wells. Fresh medium without phenol red and MTS reagent were added to each well in 5/1 ratio. The reaction was carried out by incubating the cell/scaffold constructs with this medium for 3h at 37°C

in a humidified atmosphere containing 5% of CO_2. In the end of the reaction, 100 µl of incubated medium was transferred to 96-well plate and optical density was read at 490nm in a micro-plate reader (Synergy HT, Bio-tek). The results are expressed as the average absorbance of triplicate samples.

2.8. Statistical Analysis

All data related to MTS assay were reported means ± SD for n=3 for each sample. Values were analyzed by using a two-tailed student's *t*-test and *p*-values less than 0.05 were considered significant.

3. RESULTS

3.1. Morphology of the developed structures

Optical microscope image demonstrates the structural organization of both nano and microfiber networks in a combined structure (Fig. VI.1A). SPCL microfibers with a diameter of 100 µm create a nonwoven mesh structure while collagen nanofibers laid onto them with a random orientation. This structural organization can be seen more clearly by SEM in Figure VI.1B. The average diameter of collagen nanofibers was measured to be around 400nm. In addition, there was no bead formation on the nanofibers which indicates that optimum experimental parameters for electrospinning were used for this particular study.

The collagenous nature of the nanofibers in the combined structures was assessed by immunohistochemistry with antibody raised against type I collagen (Fig. VI.1C). CLSM confirmed the type I collagen nature of the nanofibers and disclosed their spatial distribution on the combined structures. On the combined structures type I collagen nanofibers were found on top of the microfibers and spanning between them. Nanofibers covering SPCL microfibers provided them with a type I collagen

coating. Between microfibers, randomly electrospun nanofibers originated a branched network of type I collagen.

To maintain the structural and mechanical integrity, scaffolds made of collagen should be crosslinked. There are several methods that can be used for collagen crosslinking. Herein, we applied chemical crosslinking strategy based on the application of glutaraldehyde vapor. Using glutaraldeyhde in the vapor form would not only allow the crosslinker to penetrate into the deepest part of the samples, but also will minimize the toxic effect of this reaction. It is also important to note that glycine is used to remove unreacted glutaraldehyde. It has been reported that amino groups of glycine can react easily with the aldehyde groups that are coming from unreacted gluteraldeyde [29]. After crosslinking, it is important to analyze the effect of the reaction on the morphology of the collagen nanofibers, as well as on the integrity of the overall scaffold structure. As it is presented in Figure VI.1D, crosslinking process had no side effect on the nanofiber morphology and the combined structures retained their structural integrity as before crosslinking.

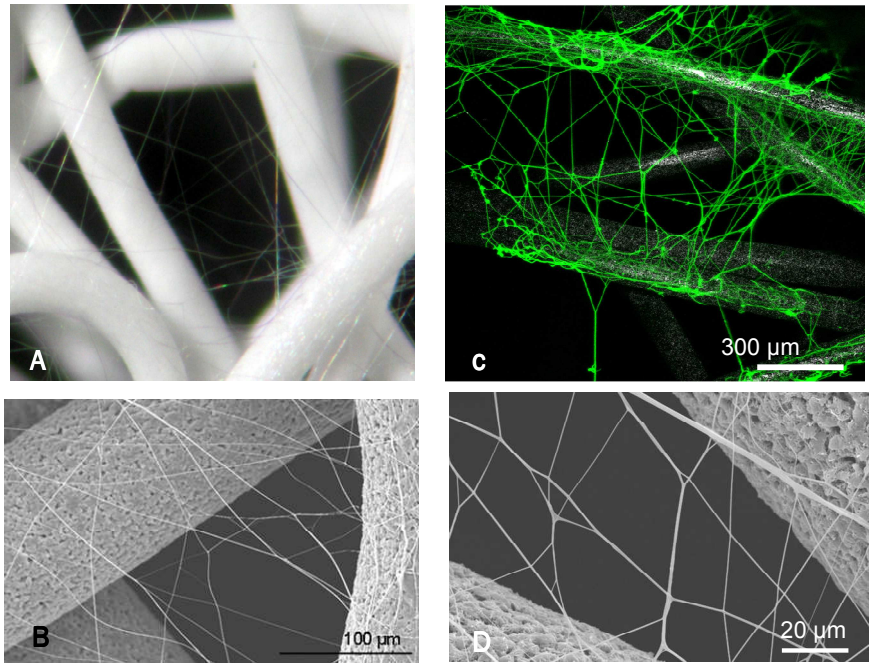

Figure VI.1. Structural organization of the combined constructs observed by; A) Optical microscopy, 50X, B) SEM. C) Immunostaining with antibody against type I collagen, D) Morphology of the structures after crosslinking with glutaraldehyde.

Figure VI.2 shows a schematic illustration of thick combined scaffolds prepared by means of using the layer by layer concept. SEM analysis indicated that collagen nanofibers distributed homogenously overall scaffold, including the interior part. Moreover, both micro and nanofiber meshes were able to maintain their original structural organizations in the same construct even after the mild heating process and create a thicker scaffold.

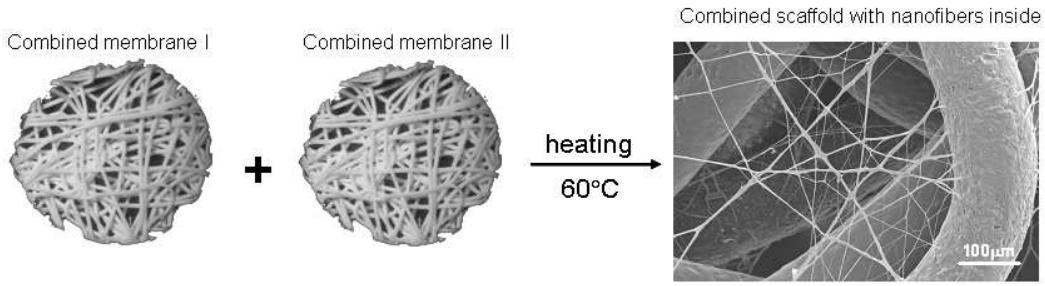

Figure VI.2. Schematic illustration of layer-by-layer concept (thickness of the fiber mesh membranes are about 500μm).

3.2. Osteoblast cell attachment and proliferation

The viability of the osteoblasts seeded on the combined structures was visually determined by Calcein-AM staining, a vital dye, in the medium and by its conversion into a green fluorescent and impermeable product by esterases of viable cells. After 3 days of culture, cells could attach and cover both nano and micro fibers of the combined structures (Fig. VI.3A). They were able to bridge between SPCL microfibers by using collagen nanofibers. The influence of nanofibers on the cell morphology can be seen better in the SEM image (Fig. VI.3B). In the presence of nanofibers, osteoblast were stretching themselves along the nanofibers and making bridges between microfibers. This morphological change of the cells led a cytoskeleton rearrangement as it was observed by phalloidin staining (Fig. VI.3C). The difference between the cytoskeletons of osteoblasts growing on nano and micro fibers were clearly observed by the difference in the formation of actin filaments (please see the arrows in Fig. VI.3C)

Cell proliferation was followed by a MTS assay during 7 days. Cell proliferation increased form days 3 to 7 for both control (samples without collagen nanofibers) and combined scaffolds. Compared to the cell proliferation in the presence of nanofibers, metabolic activity of the cells was significantly ($p<0.05$) higher for all time period tested.

3.3. Endothelial cell attachment and proliferation

On what concerns to Calcein-AM staining, after 3 days of culture non-coated combined structures were covered by viable ECs (Fig. VI.4A). On the nano-network ECs were organizing in circular structures, an arrangement quite distinct from that observed for the osteoblasts (Fig. VI.3A). SEM data revealed flat and spread ECs on the nanonetwork and arranged in circular structures (Fig. VI.3C). A higher magnification unveils that ECs are not only growing on top of type I collagen nano-fibers but also that these nano-fibers are being integrated into the cellular cytoplasma (Fig. VI.4D). When analysing the effect of pre-coating (or not) the scaffold with Fn, it was observed the same cell adhesion pattern and cell morphology, in both situations, non-coated and Fn pre-coated (Fig. VI.4B, E). MTS data further support these finding insofar as after 3 and 7 days there was not observed any significative difference in the proliferation of ECs growing on Fn- and non-coated combined structures (Fig. VI.4E).

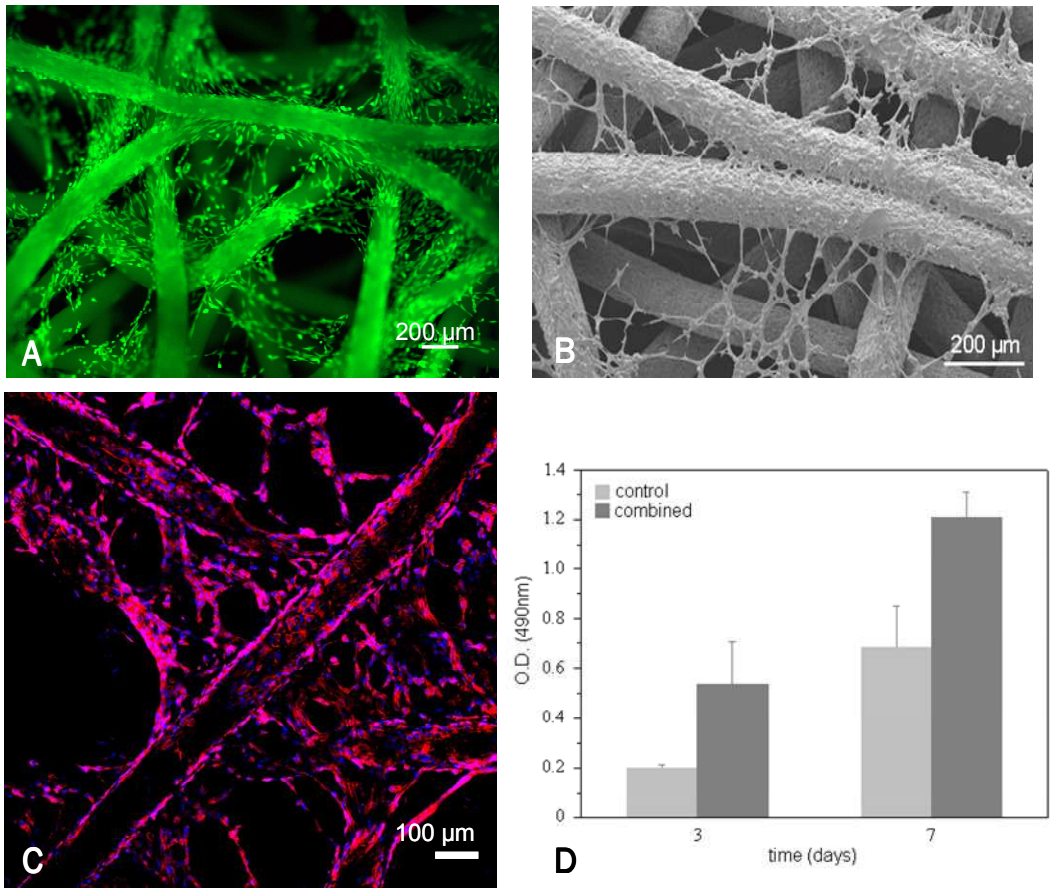

Figure VI.3 – Osteoblast-like cells on the combined structures after 3 days of culture. A) Confocal microscopy of HUVECs after staining with the vital dye calcein-AM. B) SEM images of HUVECs on the developed structures. C) Phalloidin of osteoblasts seeded on combined structures. Nuclei were counterstained with DAPI and the immunofluorescent micrographs were obtained by confocal microscopy. Original magnification: X100 D)Proliferation of HUVEs was determined by MTS assay (F). The values of scale bars are: (A, B) 200 µm.

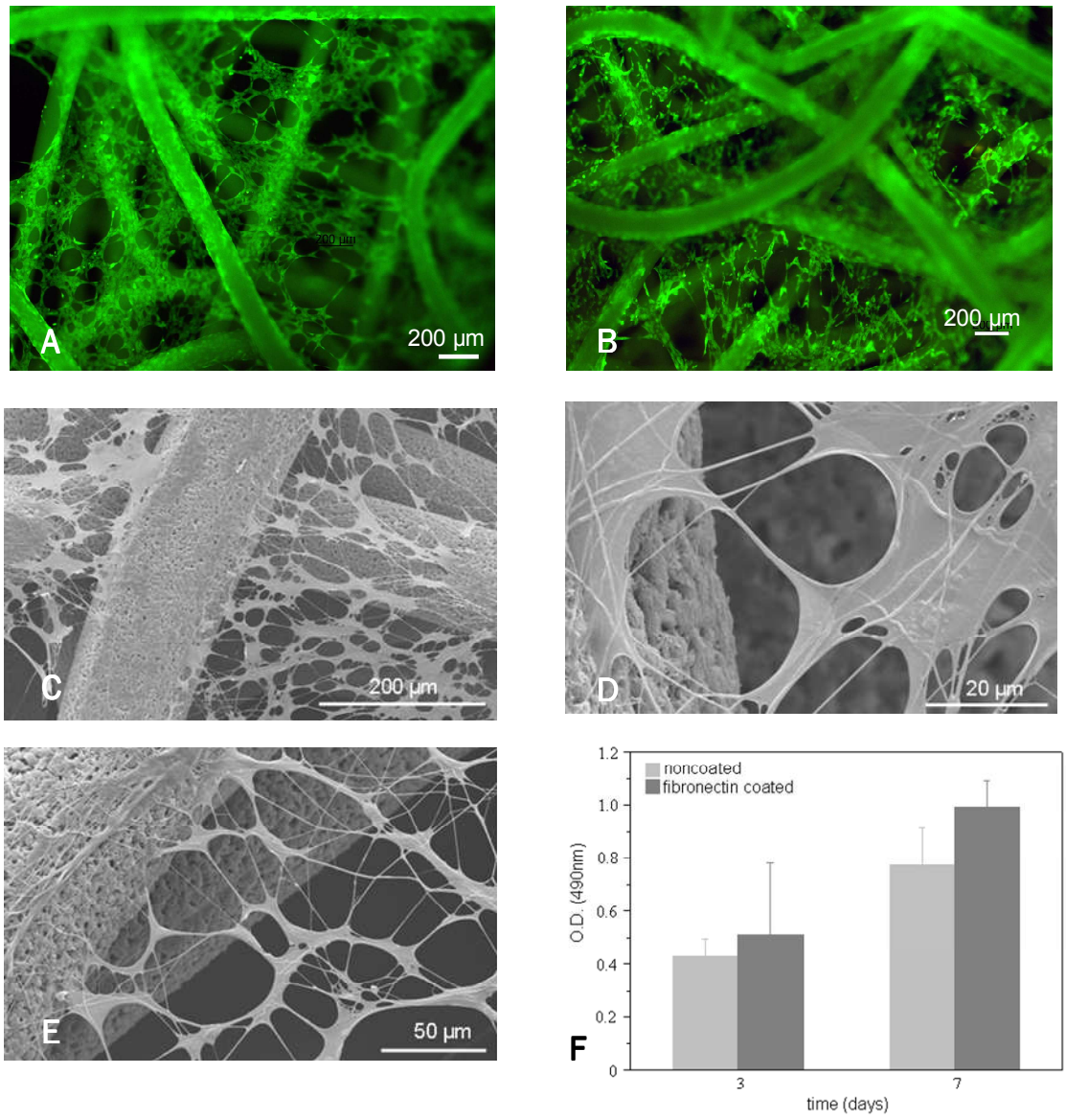

Figure VI.4. HUVEC cells on the combined structures after 3 days of culture and the influence of Fn pre-coating in viability, morphology and proliferation; (A, C, D) non-coated constructs and (B, E) pre-coated with Fn. Confocal microscopy of HUVECs after staining with the vital dye calcein-AM (A-B). SEM images of HUVECs on the developed structures (C, D, E). Proliferation of HUVEs was determined by MTS assay (F). The values of scale bars are: (A, B) 200 µm.

Cell morphology of ECs growing on non-coated and Fn-coated combined structures was further unveiled after actin cytoskeleton staining with phalloidin. On the nano-network ECs' cytoskeleton arrangement followed the alignment dictated by type I

collagen nano-fibers (Fig. VI.5A). One should particularly note that there are single cells growing on the individual nano-fibers with their actin filaments directed in a unidirectional way. When looking at the positive control, scaffolds pre-coated with Fn, no difference was observed in the pattern of cytoskeleton arrangement in relation to nano/micro-fiber combined scaffold without coating (Fig. VI.5B).

The expression of the cell junction PECAM-1, the major hallmark of the endothelia, was assessed by immunohistochemistry and visualized by CLSM. ECs growing on the combined structures were able to express PECAM-1 at cell-cell borders (Fig. VI.5C). The expression of this important molecule was observed both on micro- and nano-fibers. Once more, Fn-coating did not influenced ECs behaviour on the developed combined structures and the same PECAM-1 staining between adjacent cells was also observed for the positive control (Fig. VI.5D).

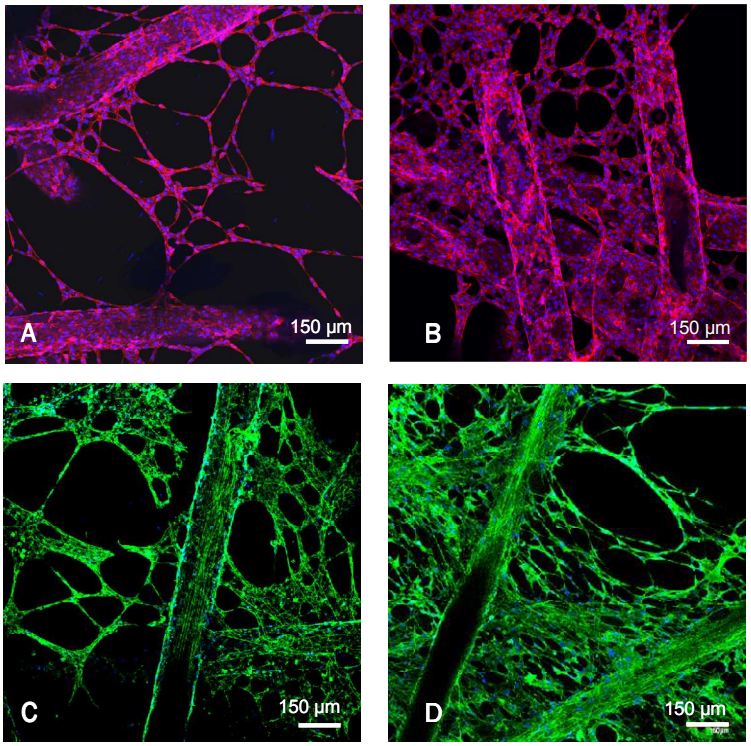

Figure VI.5. Phalloidin (A, B) and PECAM-1 staining (C, D) of HUVECs seeded on combined structures non-coated (A, C) and Fn-coated (B, D). Nuclei were counterstained with DAPI and the immunofluorescent micrographs were obtained by confocal microscopy. Original magnification: X100.

4. DISCUSSION

Wet-spun microfiber meshes made of SPCL polymeric blend and electrospun nanofibers from collagen were joined into the same construct, giving rise to combined structures. For that, it was used a two step methodology, a concept and technology previously developed and reported by Tuzlakoglu et al. [30]. This new construct is proposed as a man-made equivalent of natural ECM, which could mimic the physical and chemical structure of it. SPCL microfiber meshes mainly constitute the macro support for the cells, while collagen nanofibers laid on them are able to in some way mimic the collagen fibrils of natural ECM. The role of long and stiff collagen fibrils in ECM is to serve structural support as well as connecting and recognition function between cells and the matrix [10]. Collagen has maintained a highly conserved aminoacids sequence that provides binding sites for integrins presented in cell membranes. In fact, integrin binding is a key factor for the necessary cell-ECM communication that is lacking when synthetic polymers are used [31]. Besides the above mentioned importance, the choice of collagen relay in the fact that is the most abundant protein within the natural ECM.

In order to evaluate the structural similarity of the developed combined structures to natural ECM, we used optical and scanning electron microscopy observation. Furthermore, confocal microscopy was selected to assess and visualize collagen nanofibers which were supposed to play a role in chemically mimicking besides the structural one. Structures prepared from micro- and nanofibers demonstrated an architecture with randomly distributed nanofibers that matches the one in the natural ECM [10]. In electrospinning experiments, processing conditions, particularly processing time, were optimized to create nanofibers in appropriate deposition amount and size. The optimum used conditions were resulted in a random deposition of nanofibers on the microfiber meshes. The average diameter of nanofibers was around 400 nm which coincides well with the collagen fiber bundle diameter characteristic of the natural ECM [32].

Depending on tissue, collagen is present in different types in ECM, and each one of them plays different roles, such as type VII is an important component of the anchoring fibrils of keratinocytes, while type VI acts as a connector of functional

proteins and GAGs to larger structural proteins [33]. Type I is the primary structural collagen that exits in most of the tissues including bone. Taking this in consideration, we used collagen Type I to try to mimic the chemical structure of natural ECM. Immunohistochemistry results confirmed the collagenous nature of nanofibers which were deposited on SPCL microfiber meshes.

The herein introduced a layer by layer concept is a novel approach that we have developed in order to be able to design a closer structure to natural ECM, simultaneously taking in account the needs for real clinical applications. This rather simple method allowed us to create a construct with a requested thickness for an implantation, by means of combining micro fiber meshes with homogenously distributed nanofibers incorporated into the all bulk of the micro-structure..

The structural merits of developed constructs were evaluated by assessing cellular responses of two important cell types in bone repair, *i.e.* osteoblasts and endothelial, and their proliferation profiles, cytoskeleton arrangement and expression markers. Data published in this study clearly demonstrated that osteoblast-like cells cultured on the combined structures were able to stretch themselves along the nanofibers, while maintaining their typical spindle-like morphology on the microfibers. It is worth to mention that the surface of SPCL micro fibers were also covered by collagen nanofibers as it was observed by SEM analysis. With respect to this indication, we can that claim the morphological changes of osteoblasts were not only influenced by the chemical nature of the material but also by its the structural organization.

The effect of nano/micro fiber combination on cell viability and proliferation was screened using a MTS assay. The presence of collagen nanofibers in the structure resulted in an increase of metabolic activity and growth rate when directly compared to a scaffold one without nanofibers. A closely similar results were previously reported with SaOs-2 and rat bone marrow stromal cells in culture on nano- and micro combined structure made of SPCL [30]. Previous reports have demonstrated that Type I collagen enhances bone cell viability and growth [34, 35]. It has been used to coat metallic implant to enhance osteoblast spreading that results in a more rapid formation of focal adhesions and their associated stress fibers [36, 37]. Our results suggest that the presence of type I collagen nanofibers appears to influence the cell viability of the osteoblast-like cells cultured on the developed structures.

Besides the chemical influence of collagen, the previously deposited nanofibers reduce large void spaces between microfibers and create larger surface area that the cells can adhere from the very beginning. With respect to this phenomena, the presence of collagen nanofibers in the constructs initially clearly increases the cell seeding efficiency and later on results in a higher cell proliferation.

Cellular adhesion, spreading and migration is known to be dependent on its cytoskeleton system, including actin filaments [38]. The cytoskeletal organization of the cells also ordinates the morphological organization of ECM. Therefore, we performed fluorescent phalloidin staining to visualize actin filaments in the cytoskeleton of the cells. A clear difference in actin filaments was observed between the cells growing on the microfibers and the nanofibers. Due to the effect of collagen nanofibers, cytoskeleton of the cells growing on nanofibers showed more elongated shape than the one growing on microfibers. Since the cell shape is modulated by polymerization of actin filaments, these results can explain the morphological changes of osteoblast growing on nanofibers, which was observed by SEM.

Presently, one of the major hurdles in the clinical application of tissue engineering to repair of metabolically demanding tissues (*e.g.* bone) is the absence of a capillary bed linking the construct to the host blood system [39]. Due to their active role in angiogenesis, ECs are a key cell type [40]. Besides that, ECs are pivotal members of a complex interactive communication network in bone [41]. Therefore, the chemical composition as well as architecture of combined structures was designed envisioning not only bone forming cells but also ECs. Type I collagen, that together with SPCL is one the building blocks of this scaffold, is the major constituent of the extracellular matrices to which proliferating ECs are exposed in injured tissue [42]. Moreover, collagen also provides adhesive support as for osteoblasts as it has been discussed above [43]. Therefore, one of the objectives of including a nano-network of type I collagen was not only to supply a nano-range physical support for cells but also to provide a cell adhesion promoter. This last aspect is especially important for ECs once they are very demanding and dependent in terms of substrate adhesion. Normally, a very common procedure to improve EC adhesion to the substrate is a pre-coating with molecules from ECM such as Fn [44-46]. In this work we evaluated the ability of the combined structures to support the growth on ECs without the

requirement of any additional pre-coating. As a positive control the scaffolds were pre-coated with Fn. ECs adhered to uncoated combined structures, remained viable and exhibited a flat and stretch morphology. The same cell adhesion pattern and cellular morphology were observed for combined structures with Fn coating. Metabolic activity quantification of ECs further supported the fact that no significant difference was observed between the positive control and uncoated combined structures. These overall results indicate that pre-coating with Fn did not further improve cell adhesion, proliferation or influenced cell morphology.

Angiogenesis is a complex phenomenon with multiple progressive steps towards the end point of new blood vessels formation. It starts with cell adhesion to the new substratum, passing by migration, proliferation, organization in tube-like structures and deposition of new basement membrane; all these steps have as a common denominator type I collagen [43, 47]. On the nano-network of the developed constructs ECs organized into circular structures resembling the microcapillary-like structures formed during angiogenesis. Also, of particular interest is the intimate contact that was established between ECs and collagen nano-fibers. As observed by SEM, nano-fibers were integrated within cellular cytoplasma. It has long been recognized that 3D interstitial collagen type I provokes ECs in culture to undergo marked shape changes that closely imitate the cord-like structures observed during adult angiogenesis [43]. This behaviour is ECs-specific and this may explain why osteoblasts did not exhibit the same morphology and 3D arrangement on the combined structures.

Regarding ECs cytoskeleton, phalloidin staining revealed different arrangements on the combined structures. On nano-fibers the cells were more stretched and with actin filaments aligned in an un-directional way, in contrast to microfibers where cells exhibit a more disperse conformation of actin fibrils. These differences reflex the distinct biochemical and physiochemical natures of the substrata on the combined structures, which ultimately will dictate diverse cell functions such as migration, proliferation, among others [10].

ECs migration is an important factor for angiogenesis, particularly during sprouting of new blood vessels from the existing vasculature [43]. The inclusion of the nano-network was also designed to increment ECs' motility. This was based on data

indicating that ECs are most motile in sparse culture in which they establish few contacts with their neighbours, in opposition to cells incorporated into a confluent monolayer that reveal reduced movements [48, 49]. Therefore, it is expected that when exposed to an angiogenic environment, ECs on the different fiber-size of the combined structure will behave differently; Sparse ECs on nanofibers will be more motile than confluent cells lying down on micro-fibers. Also, the collagenous nature of the nano-network will probably contribute to this motility. This assumption is in keeping with *in vitro* studies that have shown that type I collagen not only support chemotactic migration of ECs but is also responsible for haptotactic migration [43].

For vessel formation, networking and remodelling cell-cell adhesion are particularly important [49]. PECAM-1 is a cell adhesion molecule, concentrated at the lateral junctions of adjacent ECs and is a major hallmark of the endothelium. On the combined structures ECs contacted with their neighbour cells and expressed PECAM-1 at the borders. PECAM-1 staining was present on the overall structure indicating that the effect of micro- and nanometric fibre size did not affect cell-cell communication. These findings confirm the normal endothelial phenotype, being also a good indicator of the interactions between ECs and the novel combined structures.

5. CONCLUSIONS

In conclusion, we developed combined structures as a new construct nature-inspired that recreates the physical and chemical environment of bone matrix. These structures were obtained by a two step methodology where nano-fibers of type I collagen, with an average size of 400 nm, electrospun on the macro support made from SPCL fiber mesh. The collagenous nature of the nanonetwork was confirmed by immunhistochemistry and its 3D architecture characterized by several microscopy techniques. Furthermore, it was proved the efficacy of the concept layer-by-layer as an approach to create thicker scaffolds.

Regarding cellular interactions, combined structures were able to support the adhesion and growth of both osteoblasts and ECs. About osteoblasts, the presence of type I nanofibers increased metabolic activity and the surface area available for

cell spanning. In the particular case of ECs, the inclusion of type I collagen obviated the need of pre-coating with Fn and cells organized into circular structures resembling angiogenic organization.

Our findings indicate that combined structures are an appropriate man-equivalent of natural ECM for bone tissue engineering.

REFERENCES

1. Saadeh PB, Khosla RK, Mehrara BJ, Steinbrech DS, McCormick SA, DeVore DP, et al. Repair of a critical size defect in the rat mandible using allogenic type I collagen. J Craniofac Surg. 2001; 12(6):573-9.

2. Unger RE, Wolf M, Peters K, Motta A, Migliaresi C, Kirkpatrick CJ. Growth of human cells on a non-woven silk fibroin net: a potential for use in tissue engineering. Biomaterials. 2004; 25(6):1069-75.

3. Seol YJ, Lee JY, Park YJ, Lee YM, Young-Ku, Rhyu IC, et al. Chitosan sponges as tissue engineering scaffolds for bone formation. Biotechnol Lett. 2004; 26(13):1037-41.

4. Tuzlakoglu K, Pashkuleva, I., Rodrigues, M. R., Gomes, van Lenthe, G. H., Müller, R., Reis, R. L. A New Route to Produce Starch-based Fiber Mesh Scaffolds by Wet Spinning and the Improvement in Cell Attachment and Proliferation by Tailoring Their Surface Properties J Biomed Mater Res :Part A. 2008; submitted.

5. Sombatmankhong K, Sanchavanakit N, Pavasant P, Supaphol P. Bone scaffolds from electrospun fiber mats of poly (3-hydroxybutyrate), poly(3-hydroxybutyrate-co-3-hydroxyvalerate) and their blend. Polymer. 2007; 48(5):1419-27.

6. Gugala Z, Gogolewski S. The in vitro growth and activity of sheep osteoblasts on three-dimensional scaffolds from poly(L/DL-lactide) 80/20%. J Biomed Mater Res A. 2005; 75A(3):702-9.

7. Ren TB, Ren J, Jia XZ, Pan KF. The bone formation in vitro and mandibular defect repair using PLGA porous scaffolds. J Biomed Mater Res A. 2005; 74A(4):562-9.

8. Zhou YF, Hutmacher DW, Varawan SL, Lim TM. In vitro bone engineering based on polycaprolactone and polycaprolactone-tricalcium phosphate composites. Polym Int. 2007; 56(3):333-42.

9. Harkness RD. Biological Functions of Collagen. Biol Rev. 1961; 36(4):399-&.

10. Lutolf MP, Hubbell JA. Synthetic biomaterials as instructive extracellular microenvironments for morphogenesis in tissue engineering. Nat Biotechnol. 2005; 23(1):47-55.

11. Huang ZM, Zhang YZ, Kotaki M, Ramakrishna S. A review on polymer nanofibers by electrospinning and their applications in nanocomposites. Compos Sci Technol. 2003; 63(15):2223-53.

12. Heng BC, Cao T, Stanton LW, Robson P, Olsen B. Strategies for Directing the Differentiation of Stem Cells Into the Osteogenic Lineage In Vitro doi:10.1359/JBMR.040714. Journal of Bone and Mineral Research. 2004; 19(9):1379-94.

13. Laroche M. Intraosseous circulation from physiology to disease. Joint Bone Spine. 2002; 69(3):262-9.

14. Garcia AJ, Reyes CD. Bio-adhesive surfaces to promote osteoblast differentiation and bone formation. J Dent Res. 2005; 84(5):407-13.

15. Ignatius A, Blessing H, Liedert A, Schmidt C, Neidlinger-Wilke C, Kaspar D, et al. Tissue engineering of bone: effects of mechanical strain on osteoblastic cells in type I collagen matrices. Biomaterials. 2005; 26(3):311-8.

16. Deroanne CF, Lapiere CM, Nusgens BV. In vitro tubulogenesis of endothelial cells by relaxation of the coupling extracellular matrix-cytoskeleton. Cardiovasc Res. 2001; 49(3):647-58.

17. Palmieri D, Camardella L, Ulivi V, Guasco G, Manduca P. Trimer Carboxyl Propeptide of Collagen I Produced by Mature Osteoblasts Is Chemotactic for Endothelial Cells 10.1074/jbc.M002698200. J Biol Chem. 2000; 275(42):32658-63.

18. Wenger A, Stahl A, Weber H, Finkenzeller G, Augustin HG, Stark GB, et al. Modulation of in vitro angiogenesis in a three-dimensional spheroidal coculture model for bone tissue engineering. Tissue Engineering. 2004; 10(9-10):1536-47.

19. Muschler GF, Nakamoto C, Griffith LG. Engineering principles of clinical cell-based tissue engineering. J Bone Joint Surg Am. 2004; 86-A(7):1541-58.

20. Rouwkema J, De Boer J, Van Blitterswijk CA. Endothelial cells assemble into a 3-dimensional prevascular network in a bone tissue engineering construct. Tissue Engineering. 2006; 12(9):2685-93.

21. Stahl A, Wenger A, Weber H, Stark GB, Augustin HG, Finkenzeller G. Bi-directional cell contact-dependent regulation of gene expression between endothelial cells and osteoblasts in a three-dimensional spheroidal coculture model. Biochem Bioph Res Co. 2004; 322(2):684-92.

22. Levenberg S, Rouwkema J, Macdonald M, Garfein ES, Kohane DS, Darland DC, et al. Engineering vascularized skeletal muscle tissue. Nat Biotechnol. 2005; 23(7):879-84.

23. Choong CS, Hutmacher DW, Triffitt JT. Co-culture of Bone Marrow Fibroblasts and Endothelial Cells on Modified Polycaprolactone Substrates for Enhanced Potentials in Bone Tissue Engineering. Tissue Eng. 2006.

24. Cassell OC, Hofer SO, Morrison WA, Knight KR. Vascularisation of tissue-engineered grafts: the regulation of angiogenesis in reconstructive surgery and in disease states. Br J Plast Surg. 2002; 55(8):603-10.

25. Soker S, Machado M, Atala A. Systems for therapeutic angiogenesis in tissue engineering. World J Urol. 2000; 18(1):10-8.

26. Kim BS, Mooney DJ. Development of biocompatible synthetic extracellular matrices for tissue engineering. Trends Biotechnol. 1998; 16(5):224-30.

27. Gomes ME, Godinho JS, Tchalamov D, Cunha AM, Reis RL. Alternative tissue engineering scaffolds based on starch: processing methodologies, morphology, degradation and mechanical properties. Mat Sci Eng C-Bio S. 2002; 20(1-2):19-26.

28. Jaffe EA, Nachman RL, Becker CG, Minick CR. Culture of human endothelial cells derived from umbilical veins. Identification by morphologic and immunologic criteria. J Clin Invest. 1973; 52(11):2745-56.

29. Hermanson GT. Bioconjugate Techniques. California: Academic Press, Inc; 1996.

30. Tuzlakoglu K, Bolgen N, Salgado AJ, Gomes ME, Piskin E, Reis RL. Nano- and micro-fiber combined scaffolds: A new architecture for bone tissue engineering. J Mater Sci-Mater M. 2005; 16(12):1099-104.

31. Bowlin GL. A new spin on scaffolds. Materials Today. 2004:64.

32. Sell S, Barnes C, Smith M, McClure M, Madurantakam P, Grant J, et al. Extracellular matrix regenerated: tissue engineering via electrospun biomimetic nanofibers. Polym Int. 2007; 56(11):1349-60.

33. Badylak SE. The extracellular matrix as a scaffold for tissue reconstruction. Semin Cell Dev Biol. 2002; 13(5):377-83.

34. Tesema Y, Raghavan D, Stubbs J. Bone cell viability on collagen immobilized poly (3-hydroxybutrate-co-3-hydroxyvalerate) membrane: Effect of surface chemistry. J Appl Polym Sci. 2004; 93(5):2445-53.

35. Morra M, Cassinelli C, Cascardo G, Cahalan P, Cahalan L, Fini M, et al. Surface engineering of titanium by collagen immobilization. Surface characterization and in vitro and in vivo studies. Biomaterials. 2003; 24(25):4639-54.

36. Geissler U, Hempel U, Wolf C, Scharnweber D, Worch H, Wenzel KW. Collagen type I-coating of Ti6Al4V promotes adhesion of osteoblasts. J Biomed Mater Res. 2000; 51(4):752-60.

37. Roehlecke C, Witt M, Kasper M, Schulze E, Wolf C, Hofer A, et al. Synergistic effect of titanium alloy and collagen type I on cell adhesion, proliferation and differentiation of osteoblast-like cells. Cells Tissues Organs. 2001; 168(3):178-87.

38. Li CY, Gao SY, Terashita T, Shimokawa T, Kawahara H, Matsuda S, et al. In vitro assays for adhesion and migration of osteoblastic cells (Saos-2) on titanium surfaces. Cell Tissue Res. 2006; 324(3):369-75.

39. Kannan RY, Salacinski HJ, Sales K, Butler P, Seifalian AM. The roles of tissue engineering and vascularisation in the development of micro-vascular networks: a review. Biomaterials. 2005; 26(14):1857-75.

40. Ucuzian AA, Greisler HP. In vitro models of angiogenesis. World J Surg. 2007; 31(4):654-63.

41. Guillotin B, Bourget C, Remy-Zolgadri M, Bareille R, Fernandez P, Conrad V, et al. Human primary endothelial cells stimulate human osteoprogenitor cell differentiation. Cell Physiol Biochem. 2004; 14(4-6):325-32.

42. Seandel M, Noack-Kunnmann K, Zhu D, Aimes RT, Quigley JP. Growth factor-induced angiogenesis in vivo requires specific cleavage of fibrillar type I collagen. Blood. 2001; 97(8):2323-32.

43. Davis GE, Senger DR. Endothelial extracellular matrix: biosynthesis, remodeling, and functions during vascular morphogenesis and neovessel stabilization. Circ Res. 2005; 97(11):1093-107.

44. S. Tajima JSFC, S. Li, K. Komvopoulos,. Differential regulation of endothelial cell adhesion, spreading, and cytoskeleton on low-density polyethylene by nanotopography and surface chemistry modification induced by argon plasma treatment. J Biomed Mater Res A. 2007; 9999(9999):NA.

45. Santos MI, Fuchs S, Gomes ME, Unger RE, Reis RL, Kirkpatrick CJ. Response of micro- and macrovascular endothelial cells to starch-based fiber meshes for bone tissue engineering. Biomaterials. 2007; 28(2):240-8.

46. Unger RE, Peters K, Wolf M, Motta A, Migliaresi C, Kirkpatrick CJ. Endothelialization of a non-woven silk fibroin net for use in tissue engineering: growth and gene regulation of human endothelial cells. Biomaterials. 2004; 25(21):5137-46.

47. Breithaupt-Faloppa AC, Kleinheinz J, Crivello O, Jr. Endothelial cell reaction on a biological material. J Biomed Mater Res B Appl Biomater. 2006; 76(1):49-55.

48. Osborn EA, Rabodzey A, Dewey CF, Jr., Hartwig JH. Endothelial actin cytoskeleton remodeling during mechanostimulation with fluid shear stress. Am J Physiol Cell Physiol. 2006; 290(2):C444-52.

49. Liebner S, Cavallaro U, Dejana E. The multiple languages of endothelial cell-to-cell communication. Arterioscler Thromb Vasc Biol. 2006; 26(7):1431-8.

CHAPTER VII

Cellular Crosstalk on Biomaterials as a Strategy for Bone Vascularization: Co-culture on a Starch-based Scaffold

CHAPTER VII

Cellular Crosstalk on Biomaterials as a Strategy for Bone Vascularization: Co-culture on a Starch-based Scaffold *

ABSTRACT

The reconstruction of bone defects based on cell-seeded constructs requires a functional microvasculature that meets the metabolic demands of the engineered-tissue. Solely relying on post-implantation vascularization will jeopardize the implant. Therefore, strategies that augment neovascularization need to be identified. We propose an *in vitro* strategy consisting of the simultaneous culture of osteoblasts and ECs on a starch-based scaffold for the formation of pre-vascular structures, with the final aim of accelerating the establishment of a vascular bed in the implanted construct. HDMECs were co-cultured with primary human osteoblasts (hOBs) on a 3D starch-based scaffold and after 21 days of culture HDMEC aligned and organized into microcapillary-like structures. With increased culture time these vascular-like structures evolved from a cord-like configuration to a more complex branched morphology. Of special importance is the observation that microcapillary-like structures had a patent lumen and stained in the perivascular region for type IV collagen, the major constituent of endothelial basement membrane. Genetic profiling of 84 osteogenesis-related genes was performed on co-culture versus monoculture. Osteoblasts in co-culture showed a significant up-regulation of collagen type I (6.8 ± 2.6 fold). Immunohistochemistry revealed that the scaffold was filled with a dense matrix that stained for collagen type I, thus corroborating the molecular data. In direct contact with HDMEC, hOBs secreted higher amounts of VEGF in relation to monoculture and the highest peak in the release profile correlated with the formation of microcapillary-like structures. The heterotypic communication between the two cell types was also assured by direct cell-cell contact as shown by the expression of the gap junction Cx43. In summary, this co-culture system is a strategy to form vascular-like structures *in vitro* on a 3D scaffold, making use of heterotypic cellular crosstalk without the requirement for exogenous growth factor supply.

*This chapter is based on the following publication:

Santos M.I, Unger R.E., Sousa R.A., Reis R.L., Kirkpatrick C.J. Cellular Crosstalk on Biomaterials as a Strategy for Bone Vascularization : Co-culture on a Starch-based Scaffold (2008). *Submitted*

1. INTRODUCTION

The reconstruction of large skeletal defects, such as those resulting from resection of bone tumors or trauma, are still a major orthopedic challenge. Tissue engineering strategies often fail to regenerate these defects due to inadequate vascularization [1]. A functional microvasculature supplying the construct would guarantee the metabolic demand of the seeded cells, of the newly formed tissue, and could participate in other as yet unknown aspects of cellular cross-talk in orchestrating bone formation. Due to their unique role in angiogenesis, ECs have attracted most attention in strategies that seek to achieve bone vascularization. However, there is clear evidence that on their own these cells cannot do more than form incipient vascular structures that resemble early capillaries but which are not stable in the long-term [2, 3]. Therefore, ECs co-cultured with the cell characteristic of the tissue to be regenerated has been a proposed strategy. Hence, since bone is a tissue formed by several cell types, co-cultures of heterogenous cell types recreates more closely the *in vivo* microenvironment than single-cell cultures. Several studies have shown that there is a reciprocal regulation and functional relationship between ECs and osteoblasts during osteogenesis [4]. Numerous regulatory molecules (e.g. endothelins, prostaglandins) which exert major effects in controlling the differentiation and activity of bone-forming cells are secreted by ECs [5]. On the other hand, osteoblasts influence EC activity through the release of diverse angiogenic growth factors, such as VEGF and FGF-2 [6]. Furthermore, cell-cell interactions mediated by proteins at gap junctions is another communication strategy used between these two cell types [7].

Previously, our group [8] showed that co-culturing ECs derived from the microvasculature (HDMECs) with hOBs resulted in the formation of microcapillary-like structures similar to those observed *in vivo*. Surprisingly, these two cell populations were able to "self-assemble" from a cell suspension mixture seeded on the three-dimensional biomaterials investigated. Other models of co-culture for bone tissue engineering have been also proposed, such as spheroidal co-culture of HUVECs and osteoblast co-culture as spheroids [9], co-culture of bone marrow fibroblasts and

human marrow endothelial cell line on polycaprolactone scaffold [10], spheroid co-culture of human mesenchymal stem cells with HUVECs [11], and OECs with an osteoblast cell line or with hOBs on 2D- and 3D-aggregate co-cultures [12]. Nevertheless, most of the co-culture systems proposed to date are mainly models to study heterotypic interactions and only few include the use of 3D scaffolds [8, 10]. Hence, the goal of this study was to use a human co-culture system directly on established 3D scaffolds to investigate more closely the cross-talk between osteoblasts and vascular cells in forming microvessels within the three-dimensionality of an innovative biomaterial HDMECs:hOBs were co-cultured on fiber-mesh scaffolds made from SPCL, a 3D support previously proposed and extensively studied for bone tissue engineering [13-19]. The co-culture system on starch-based scaffolds was evaluated as a strategy to unravel the mechanisms of formation of vascular-like structures in the context of biomaterials for bone regeneration. We do not rule out the possibility of a pre-seeding co-culture strategy, followed by implantation, but this was not the prime aim of our study, as the problem of rapidly connecting an *in vitro* formed microcirulatory network to the functional microcirculation *in vivo* has not yet been satisfactorily solved. In addition, specific questions related to cellular interactions were addressed: i) the 3D cellular distribution and the dynamics of the two cell populations in the scaffolding material; ii) gene expression profiling and iii) heterotypic communication in co-culture.

2. Materials and Methods

2.1. Scaffolds

A blend of corn starch with poly(ε-caprolactone) (30/70 %wt) was used to produce fiber-mesh scaffolds. In summary, SPCL fibers were produced by melt-spinning (mean fiber diameter of 213 ± 50 μm) and subsequently cut into 10 mm segments. Short fiber bundles were randomly displaced into the mould cavities and subjected to thermal treatment before compression and boding of the fibers into a porous mesh. Standardized scaffolds were finally obtained by cutting the fiber meshes with a

circular die (0.6 cm in diameter). Scaffolds obtained exhibited 67.9 ± 1.6 % of porosity as determined by μCT. All samples were subsequently sterilized by ethylene oxide and soaked overnight in medium without serum prior to cell seeding. More details about these scaffolds and their properties can be found elsewhere [13, 16, 20].

2.2. Cells and culture conditions

ECs were derived from juvenile foreskin (HDMECs) and human primary osteoblasts (hOBs) isolated from human femoral head explants were used in this study. The use of this biological material for research purposes was authorized by the responsible ethical committee and was based on informed consent. HDMECs were obtained by enzymatic digestion, as previously described [21], and were cultured in Endothelial Basal Medium MV (PromoCell, Germany) supplemented with 15 % FCS (Sigma-Aldrich, Germany), 100 U/100 μg/mL Pen/Strep (Sigma-Aldrich, Germany), 2.5 ng/mL, FGF-2 (Sigma-Aldrich, Germany), 10 μg/mL sodium heparin (Sigma-Aldrich, Germany) and 100 U/100 μg/mL Pen/Strep (Sigma-Aldrich, Germany). hOBs were obtained by sequential enzymatic digestion of bone chips as described [22] and cultured in DMEM medium 1000 mg/L (Sigma-Aldrich, Germany) supplemented with 10 % foetal calf serum, 100 U/100 μg/mL Pen/Strep, 300 μg/mL ascorbic acid (Sigma-Aldrich, Germany), 100 nM dexamethasone (Sigma-Aldrich, Germany) and 2 mM Glutamax (Life Technologies, Germany). The cells used in this study were between passage 3-4 and were incubated under standard culture conditions (37 ºC, 5 % CO_2, humidified atmosphere).

2.3. HDMECs:hOBs co-culture on SPCL fiber-mesh scaffolds

HDMECs and hOBs were mixed in a proportion of 4:1 and cultured in HDMEC medium. One day prior to co-culture, hOBs medium was changed to the one used in co-culture. Before cell seeding SPCL fiber-mesh scaffolds were pre-coated with Fn

(10 µg/mL PBS, Roche, Germany) for 1 hr at 37 °C. Subsequently, 1.5 x 10^5 cells of the mixed cell suspension was added to each scaffold and cultured for up to 35 days. Scaffolds were also cultured with HDMECs (1.30 x 10^5 cells/scaffold) or hOBs (2 x 10^4 cells/scaffold) alone to be used as monoculture controls. The medium was changed every 3 days. All experiments were performed with at least three different HDMEC and hOBs donors.

2.4. Immunostaining of PECAM-1 (CD31) and connexin 43 (Cx43)

In order to distinguish between cell populations and their distribution on the co-culture, the samples were stained for PECAM-1 (CD31, endothelial specific) and for nuclei (identifying both hOBs and ECs). Every 7 days of culture a co-culture sample and one sample from each monoculture control (HDMECs and hOBs) were fixed in a solution of 2 % paraformaldehyde for 30 min at RT. Samples were rinsed in PBS and then treated with 0.1 % Triton for 5 min at RT to permeate cell membrane for the reactions with antibodies. The samples were incubated for 45 min at RT with the primary antibody mouse anti-human PECAM-1 (1:50, Dako, Denmark). Following PBS washing, a second incubation was performed for 45 min at RT with the secondary antibody anti-mouse Alexa Fluor 488 (Invitrogen, Germany). The nuclei were counterstained with 1µg/mL Hoechst in PBS for 5 min.

For Cx43, a gap junction protein involved in direct cell-cell communication, a double staining with PECAM-1 was performed. The fixation and permeation procedure was the same as described above. The samples were incubated for 1 hr at RT with PECAM-1 antibody and with rabbit anti-human Cx43 (1:50, Cell Signalling, USA). This was followed by a washing step and then further incubation with secondary antibodies, goat anti-mouse Alexa Fluor 594 (for PECAM-1, red fluorescence) and anti-rabbit Alexa Fluor 488 (for Cx43, green fluorescence). After nuclei counterstaining samples were washed with PBS, mounted with Gel/Mount (Natutec, Germany) and visualized by CLSM (Leica TCSN NT).

2.5. Real time PCR

After 21 days of culture, total RNA was extracted from co-cultures and monocultures on SPCL fiber-mesh scaffolds using the RNeasy Micro Kit (Qiagen, Germany). Total RNA (0.5 µg) was reverse transcribed using Omniscript RT Kit (Qiagen, Germany). Equal amounts of cDNA (1.25 ng) plus master mix RT^2 SYBR Green/ROX qPCR (12.5 µL) were added in a final volume of 25 µL to each well of the human osteogenesis RT^2 Profiler PCR array for quantitative PCR (Superarray, USA). The human osteogenesis RT^2 Profiler PCR array profiles the expression of 84 genes related to osteogenesis besides housekeeping and control genes. Gene amplification was performed using Applied Biosystems 7300 Real-Time PCR System (Applera Deutschland GmbH, Germany). The number of cycles and annealing temperature were selected according to the manufacturer's instructions. For these experiments three different donors for both OBs and ECs were used. In each sample the mRNA level expression of each gene was normalized to the average expression of the housekeeping genes GAPDH and ribosomal protein L13A (RPL13A). Gene fold change was calculated in comparison with HDMEC or hOBs as control samples. For each individual gene, fold differences in co-culture/monoculture were plotted in $\log_2$ scale against the associated statistic probability (p-value in $\log_{10}$ scale). Two tailed Student's t-test was employed to detect significant differences in gene expression between co-culture and monoculture (OBs and ECs) experiments. Differences were considered statistically significant for $p<0.05$.

To verify the Superarray data obtained for collagen type I gene real time PCR was performed with primers synthesized commercially: (forward) 5`-CTGGCCTCGGAGGAAACTTT-3' and (reverse) 5'-CCTCCGGTTGATTTCTCATCA-3'. RNA was isolated from four different HDMECs and hOBs donors (three donors were the same as used for array analysis) and reverse transcribed into cDNA as previously described. Real time PCR was performed with 2.5 ng cDNA and 12.5 µL of 2x-master mix, primers (0.25 µL forward and 0.25 µL reverse primer) in a final volume of 25 µL. Gene expression was normalized to the expression of the housekeeping gene GAPDH and gene fold change was calculated as previously explained.

2.6. Immunohistochemical analysis

The assessment of vascular characteristics (PECAM-1 and type IV collagen staining) in microcapillary-like structures, as well as the collagenous nature of the matrix in the inner sections of the construct was performed by immunohistochemistry. Briefly, at several time points, HDMECs-hOBs cocultures on the biomaterial scaffold were fixed with 3.7 % glutaraldehyde for 30 min, dehydrated in ascending alcohol concentrations, changed to xylene substitute and finally transferred to liquid paraffin. Solidified paraffin blocks were cut in transversal cross-sections (5 μm thick) and prior to staining were deparaffinized and rehydrated. Sections were blocked with serum for unspecific binding and then incubated for 1 hr at RT with the primary antibodies: human anti-mouse PECAM-1, rabbit anti-human collagen type I (1:100, Biodesign International, USA) or mouse anti-human collagen IV(1:50, Dako, Denmark). After washing with PBS the biotin-labeled secondary antibody horse anti-mouse or goat anti-rabbit was added (1:200, Vector, USA) for 1 hr. This was followed by a 30 min incubation with horseradish peroxide-conjugated streptavidin complex (ABC kit, Vector). Peroxidase staining was performed using DAB as a chromogen (Vector). The nuclei were counterstained with Mayer's haematoxylin and the sections were examined under a light microscope.

2.7. Vascular endothelial growth factor (VEGF) quantification

For quantification of soluble factors the supernatant of co-culture and monocultures (hOBs and HDMEC) on SPCL fiber-mesh scaffolds was collected and stored at -80ºC every 7 days. From each condition, three samples were taken and VEGF was quantified by ELISA using the human VEGF DuoSet (R&D Systems, Germany) according to the manufacturer's protocol. The culture medium was used as blank.

3. RESULTS

3.1. Formation of microcapillary-like structures in co-culture

Although the two cell types were mixed and seeded as a single cell suspension, at the first CLSM observation made after 7 days, cellular segregation with HDMEC appearing as monolayer patches among the osteoblasts was clearly observed (fig. VII.1a). With increasing culture time the dynamics of the culture changed, resulting in a decrease in the ECs population balanced by an increase in the osteoblast population. Nevertheless, after 21 days of culture cords of microcapillary-like structures were formed by aligned PECAM-positive HDMECs on SPCL fiber-mesh scaffolds (fig. VII.1b). These vascular-like structures were established among osteoblasts, which deposited a dense matrix in such a manner that the microvessel-like cords were interwoven through the individual fibers of the scaffold. At day 35, microcapillary-like structures exhibited formations with several branching points, denoting a higher level of complexity (fig. VII.1c-d). In monocultures, HDMEC cultured alone grew as a monolayer and no vascular-like structures were observed, while hOBs grew extensively over the 35 days of culture, colonizing the entire scaffold surface and depositing matrix (fig. VII.1e-f).

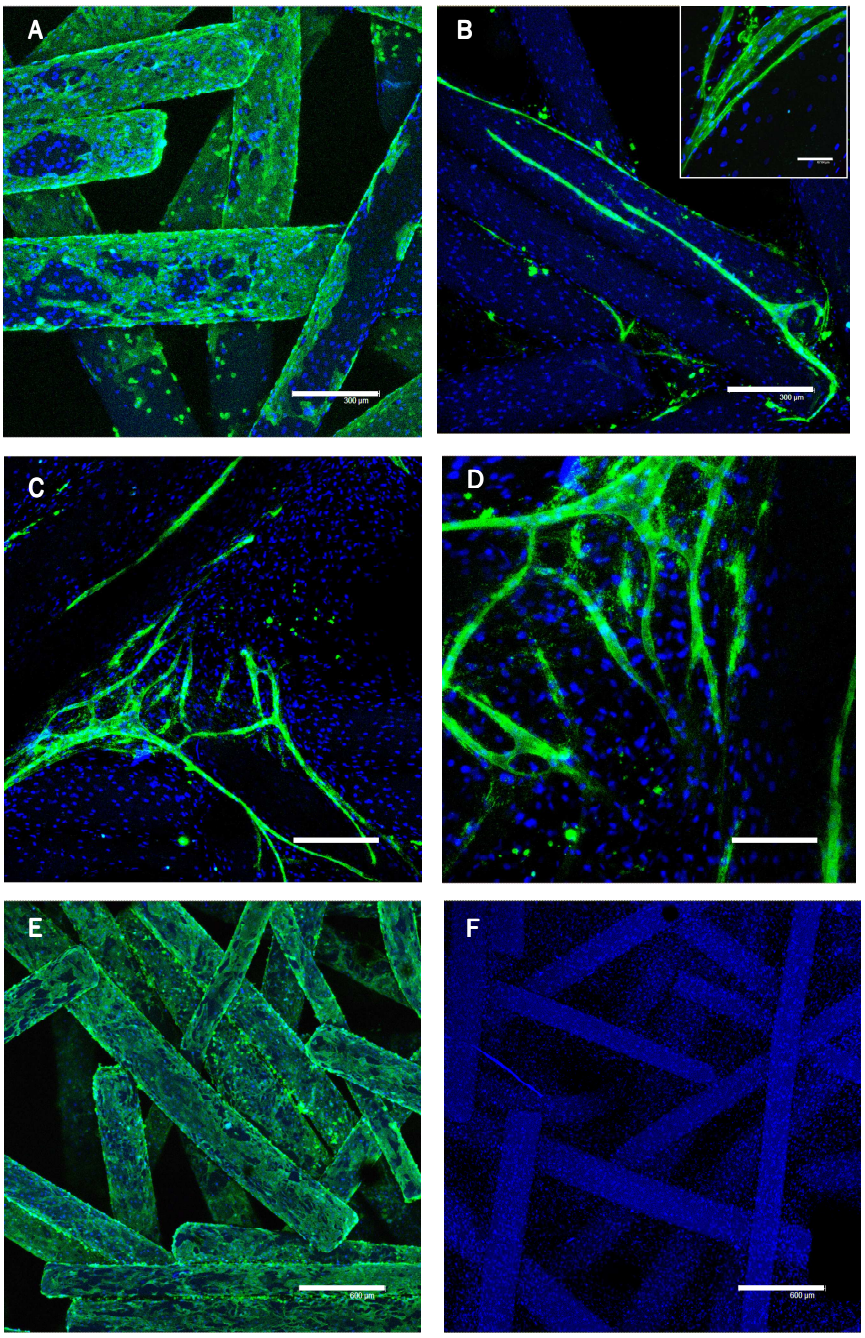

Figure VII.1. Distribution and organization of HDMECs and hOBs in co-culture (a-d) and monoculture (e-f) on SPCL fiber mesh scaffolds after 7 (a), 21 (b) and 35 (e-f) days of culture. In order to distinguish between the two cell populations samples were stained for PECAM-1 (CD31; green fluorescence, endothelial-specific) and nuclei (blue fluorescence, both hOBs and HDMECs). Note the formation of microcapillary-like structures after 21 days of co-culture, first as predominantly linear structures and then expansion to extensively branched forms after 35 days. As control HDMEC (e) and hOBs (f) were cultured in the scaffold for 35 days. The values of the scale bars are: (a, b, c) 300 μm; (d) 150 μm,; (e, f) 600 μm and 67 μm for the picture inserted in (b).

3.2. Expression profile of osteogenesis-related genes

Using the human osteogenesis PCR array the mRNA level of 84 osteogenesis-related genes was monitored in HDMECs:hOBs co-culture, HDMEC- and hOB-monoculture, all cultured on the SPCL fiber-mesh scaffolds. The assessment was performed after 21 days of culture, the time point when the first microcapillary-like structures were observed. Figure VII.2 summarizes in the form of a Volcano plot the expression of each individual gene in co-culture vs HDMEC-monoculture (fig. VII.2a) and co-culture vs. hOB-monoculture (fig. VII.2b), against the respective statistic significance (p value). Gene up-regulation was considered for a fold increase above 4 and considered statistically significant for $p<0,05$. In the case of co-culture vs. HDMEC-monoculture, 5 down-regulated and 21 up-regulated genes were identified (fig. VII.2a). Table VII.1 summarizes these genes grouped according to the biological processes they are involved in. The down-regulated genes are related with ECM and cell adhesion (MMP10, ITGA2), as well as with cell growth/differentiation (SMAD1, BMP-6, FLT1). In regard to up-regulated genes, there was a higher prevalence of genes that encode molecules related with ECM dynamics such as: structure (ex. col1A1), cell adhesion (FN1), degradation (ex. CTSK) and mineralization (ALPL). Furthermore, many other genes were related with skeletal development such as growth factors (e.g.. IGF-2, TGFβR1) and transcription factors (RUNX2, TWIST1). Genes such as Col1A1 and IGF-2, whose expression in co-culture increased 924- and 240-fold (respectively), had a very high threshold cycle (CT) value in the amplification plot of HDMEC-monoculture, near to real-time PCR detection limit. Thus, this indicates these genes are almost not expressed in HDMEC. In the case of co-culture vs. hOBs monoculture from the 84 genes under analysis only collagen type I had a significant up-regulation of 6.4-fold (fig. VII.2b). The remaining genes showed no significant difference between hOBs cultured alone or co-cultured with HDMEC. To validate this result the expression of collagen type I was assessed by real-time RT-PCR. For four different donors, collagen type I was significantly 6.8 ± 2.6 fold up-regulated for hOBs co-cultured with HDMEC on SPCL fiber-mesh scaffolds, thus validating array results.

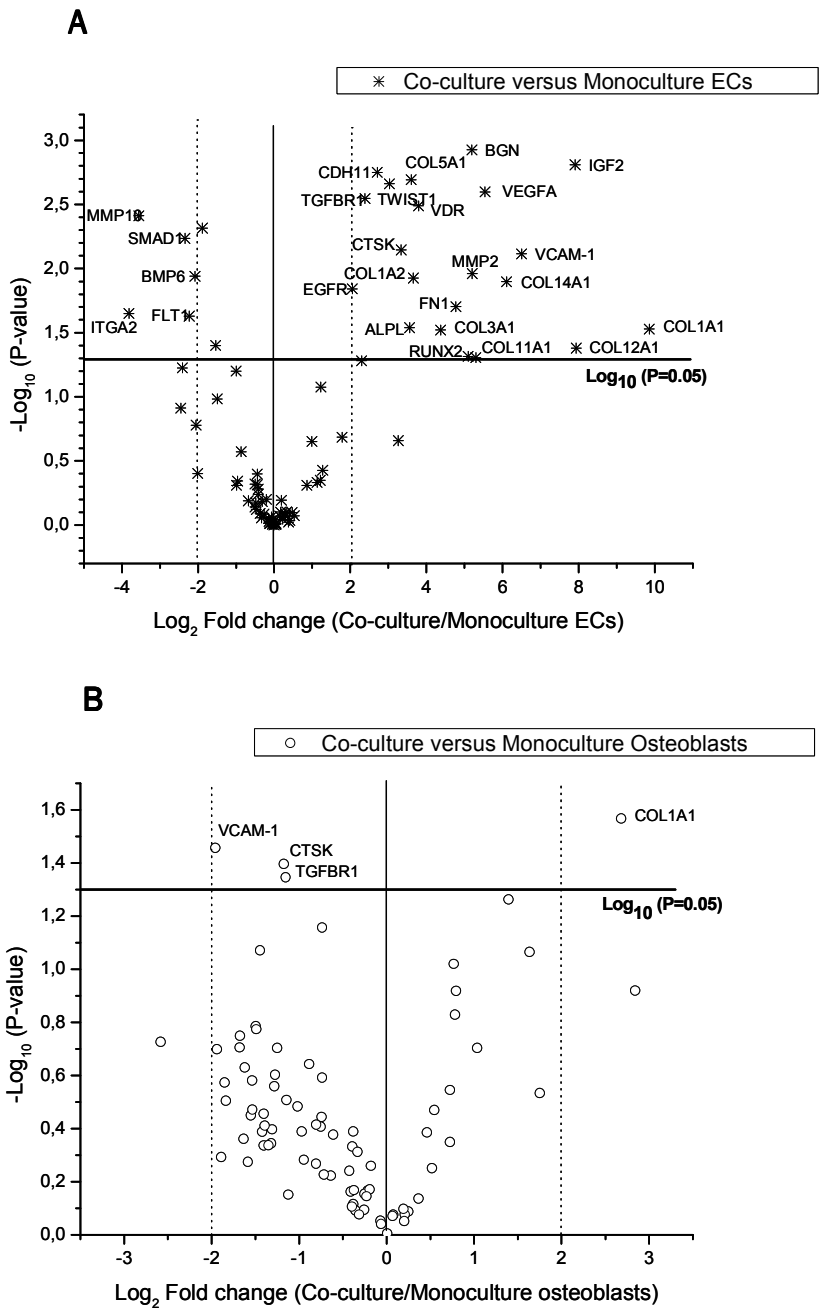

Figure VII.2. Changes in osteogenesis-related genes between co-culture and monocultures on SPCL fiber-mesh scaffolds, and the respective statistic probability. Fold changes are relative to differences between co-culture and HDMEC-monoculture (a) and between co-culture and hOB-monoculture (b). Values were plotted in the form of a volcano plot where the x axis is the $\log_2$ fold change and y axis is $-\log_{10}$ p-value. The figure shows the threshold for fold change (vertical lines, 4-fold) and for significant difference (horizontal line, $p<0.05$). Genes plotted farther from the central vertical axis have larger changes in gene expression (towards the left gene expression is down-regulated and towards the right gene expression is up-regulated). The genes above the horizontal line are statistically significant. This data represent results from three different donors (ECs and osteoblasts).

Table VII.1 – Genes regulated in co-culture relative to HDMEC-monoculture. The genes are grouped according to the final biological function of the protein that they code for.

Biological function	Symbol	Gene full name
Down-regulated genes		
Growth factors and receptors	BMP-6	Bone morphogenetic protein 6
	Flt1	Vascular endothelial growth factor receptor
ECM-related and cell adhesion molecules	MMP10	Matrix metalloproteinase 10
	ITGA2	Integrin alpha 2
Transcription factor	SMAD1	SMAD family member 1
Up-regulated genes		
Growth factors and receptors	VEGF	Vascular endothelial growth factor
	IGF-2	Insulin-like growth factor 2
	VDR	Vitamin D receptor
	EGFR	Epidermal growth factor receptor
	TGFβR1	Transforming growth factor β receptor 1
ECM-related and cell adhesion molecules	Col1A1	Collagen type I, alpha 1
	Col1A2	Collagen type I, alpha 2
	Col3A1	Collagen type III, alpha 1
	Col11A1	Collagen type XI, alpha 1
	Col12A1	Collagen type XII, alpha 1
	Col5A1	Collagen V, alpha 1
	Col14A1	Collagen type XIV, alpha 1
	CTSK	Cathepsin K
	MMP2	Matrix metalloproteinase 2
	FN1	Fibronectin 1
	BGN	Biglycan
	ALPL	Alkaline phosphatase
Cell-cell adhesion molecules	CDH11	Cadherin 11
	VCAM-1	Vascular cell adhesion molecule 1
Transcription factors	RUNX2	Runt-related transcription factor 2
	TWIST1	Twist transcription factor

3.3. Microcapillary-like structures with lumen formation and type I, IV collagen expression

Immunohistochemistry was performed on thin sections of SPCL fiber-mesh scaffolds after 35 days of co-culture. Cross-sections in both the outer and inner parts of the scaffold revealed a dense network matrix which stained for collagen type I and occupied all the void spaces between fibers (fig. VII.3a). A more intense collagen type

I-staining was detected in the immediate surroundings of the microcapillary-like structures, which demonstrated a definitive lumen containing degenerating cells (fig. VII.3b).

Sections were also stained for markers of the endothelial phenotype such as PECAM-1 and type IV collagen. Cells stained positively for the endothelial marker PECAM-1 were organized in microcapillary-like structures forming a lumen (fig. VII.3c, d). Furthermore, the areas corresponding to microcapillary-like structures were stained for collagen type IV, one of the hallmarks of the endothelial basement membrane (fig. VII.3e, f). The overall morphological impression given in figure VII.3 is that of a tissue-like self-assembly of the EC in a matrix in which the osteoblasts are embedded, reminiscent of a histological micrograph (fig. VII.3c).

3.4. Heterotypic communication in co-culture through VEGF and Cx43

The communication between HDMEC and hOBs was assessed at the indirect contact level through the release of VEGF growth factor and at the direct contact level by the expression of the gap junction protein Cx43. The concentration profile of VEGF produced in co-culture along the 35 days of culture was characterized by three distinct phases: i) from day 7 to 14 a steep increase in VEGF concentration; ii) between day 14 and day 28 a plateau phase and iii) from day 28 until day 35 a pronounced decrease of VEGF concentration (fig. VII.4). On the other hand, in hOB-monoculture, the VEGF concentration curve exhibited a steady increase (but at lower magnitude as compared to co-culture) until day 28 followed by a decrease. The VEGF concentration in co-culture supernatant was 4- to 2-times higher than in hOB-monoculture ($p<0.05$), while for HDMEC-monoculture no VEGF was detected. These results indicate that hOBs in co-culture are stimulated to secret higher amounts of VEGF.

In fig. VII.5 Cx43 is depicted as a punctuated bright green staining all over the co-culture section. Due to the co-staining of microcapillary-like structures (PECAM staining, red fluorescence) and Cx43 it is possible to observe the expression of this gap junction at HDMEC-hOB interfaces (arrows) and in the areas where osteoblasts

were depicted alone (only nuclear staining, blue fluorescence). Moreover, the osteoblasts also maintain a high expression of Cx43 in interaction with the scaffold material. These results indicate that on the SPCL fiber-mesh HDMECs and hOBs maintain a crosstalk communication mediated indirectly by VEGF and directly through the gap junction protein Cx43.

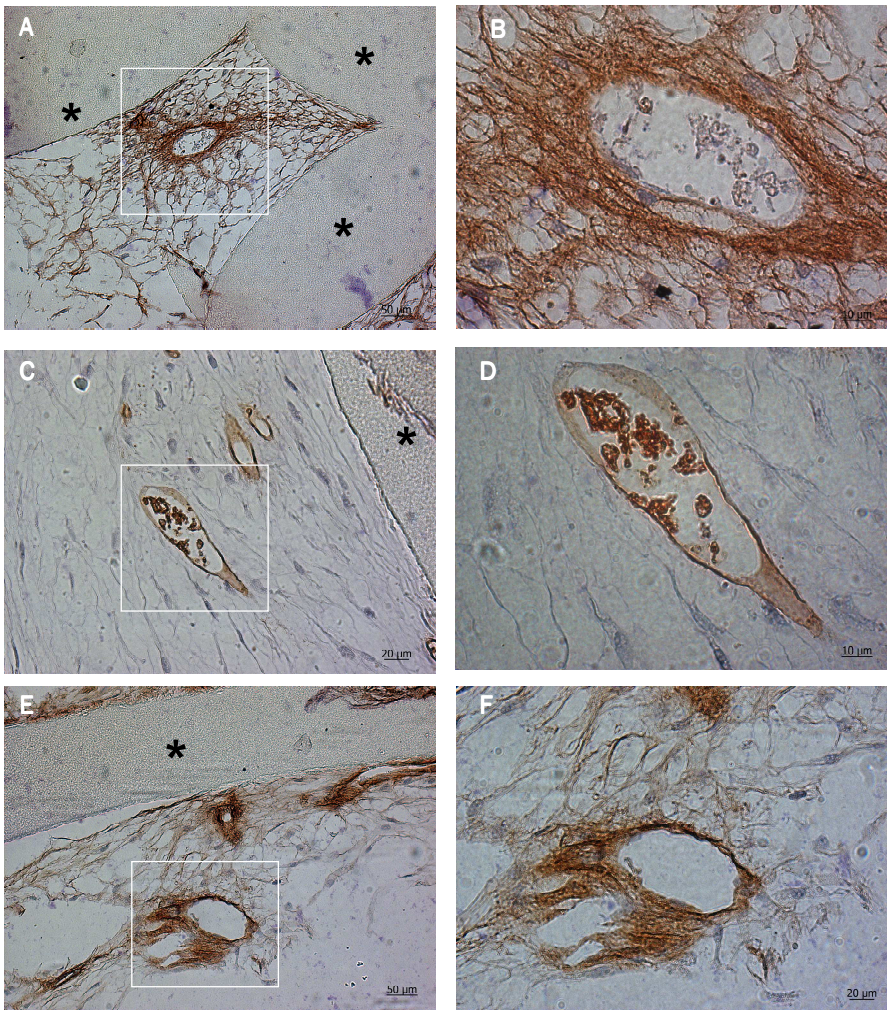

Figure VII.3. Immunohistochemical staining of thin-sections of HDMECs and hOBs in co-culture on SPCL fiber meshes after 35 days of culture. The sections were stained for the ECM macromolecule collagen type I (a, b), for the endothelial marker PECAM-1 (CD31) (c, d) and for the major element of the endothelial basement membrane collagen type IV (e, f). Nuclei were counterstained with Mayer's haematoxylin. "* " Identifies the scaffold material. Important observations: type I collagen fibers are closely associated with the biomaterial and concentrated around the vessel-like structures (a). In b. cell detritus in the lumen of the vessel-like structure, as well as numerous perivascular cells (hOBs) embedded in the type I collagen matrix. PECAM-1 staining confirms the endothelial nature of the lumen-forming cells as well as those cells degenerating in the lumen (c,d). The microvascular structures express a dense type IV collagen perivascular matrix (e,f).

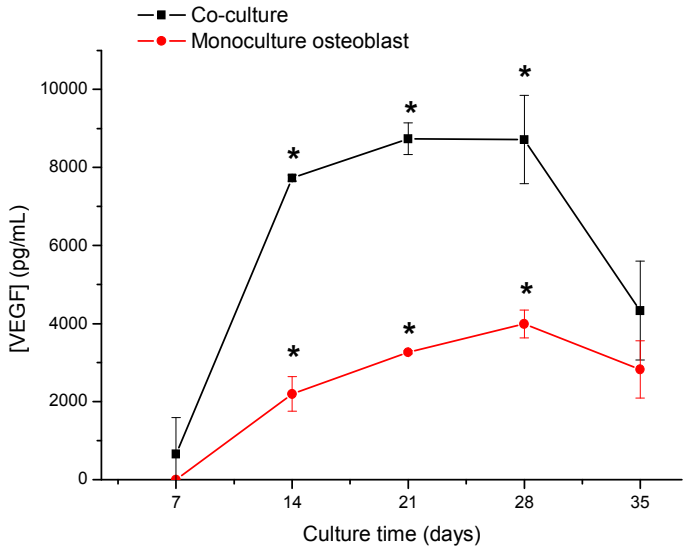

Figure VII.4. VEGF release profile in HDMECs:hOBs co-culture and hOBs-monoculture on SPCL fiber-mesh scaffold. VEGF was quantified in culture supernatant by ELISA. Triplicates were performed and the data are from a representative experiment. Error bars represent means ± SD and the values were considered significantly different (*) when $p<0.05$ (two tailed unpaired Student t-test). No line is shown for the EC synthesis as this was zero at all times. Marked upregulation of VEGF release in the co-cultures (black line) compared to the osteoblast monoculture (red line).

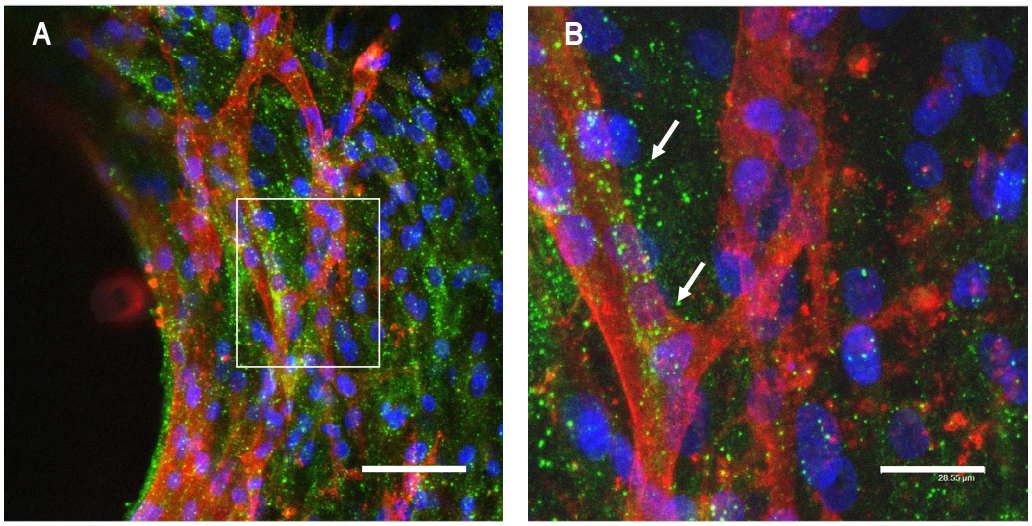

Figure VII.5. Heterotypic cell-cell communication as monitored by Cx43 expression on HDMECs:hOBs co-culture on SPCL fiber-mesh scaffolds. The co-staining of Cx43 (green fluorescence dots), PECAM-1 (red fluorescence, staining HDMECs aligned in microcapillary-like structures) and nuclei (blue fluorescence, marking both cell types was visualized by CLSM. Cx43 was detected at HDMEC-hOB interface (arrows) and also very strongly on hOBs. The values of the scale bars are: (a) 75 μm and (b) 29 μm.

4. DISCUSSION

This work assessed whether an *in vitro* strategy can be used to establish a pre-vascularization through the simultaneous culture of primary human microvascular ECs and mature human osteoblasts on a previously well characterized SPCL fiber-mesh scaffolds. A complex system such as this should not be regarded without first evaluating separately its respective single elements. Thus, previous studies [14, 16-18] focused on the interactions of osteoblast-like cells or ECs single-cell culture with SPCL fiber-mesh scaffolds. Rat bone marrow cells seeded on starch-based scaffold differentiated into osteoblasts, deposited a mineralized matrix and secreted several growth factors with osteogenic and angiogenic activity [16-18]. In endothelialization studies, SPCL fiber-mesh scaffolds revealed to be an adequate substrate for the formation and maintenance of a stable monolayer as well as for the preservation of normal endothelial phenotype profile, including the ability to respond to a pro-inflammatory stimulus [14]. Complementary work, involving surface modification of the scaffold by ar plasma demonstrated that this method is effective in promoting ECs adhesion and phenotype maintenance without the requirement of coating the scaffold with cell adhesion molecules [23].

In the co-culture system under evaluation, which started from a mixed cell suspension of hOBs and EC, the distribution of the two cell types in the scaffolding material reflected a heterotypic interaction variable through time and involving a cellular self-assembly phenomenon especially prominent in the case of the HDMEC. While early time points where characterized by cellular segregation of HDMECs-monolayer among hOBs, by 21 days of culture HDMECs aligned and organized into microcapillary-like structures. In these structures, cells established contact through the cell-cell adhesion molecule PECAM-1. Furthermore, microcapillary-like structures were present not only in the peripheral parts of the SPCL scaffold, but also in the innermost regions of the scaffold, evolved along time from a cord-like configuration to more complex branched structures, reminicent of capillaries *in vivo* Homotypic EC contact through PECAM-1 is crucial for vessel formation and maintenance [24]. Immunhistochemistry data further unveiled two important aspects of these vascular-like structures, such as lumen formation and collagen type IV deposition. Lumen

formation results from a complex molecular mechanism involving the up-regulation of over 1000 genes [25, 26]. Collagen IV provides the major structural support to basement membrane underlying ECs in blood vessels [27]. The formation of a structure with a lumen and the expression of the major constituent of the endothelial basement membrane, assures the vascular nature of the established structures. However, microvessel stability requires crosstalk between EC and mural cells, such as pericytes. Detailed studies in long-term culture are necessary to determine to what extent osteoblasts via a process of phenotypic change could adopt a pericyte and thus vessel stabilizing function. This is currently part of our further research activity.

The genetic profile of HDMECs:hOBs co-cultures compared to monocultures was also examined. From the comparative analysis of a panel of 84 genes osteogenesis-related between co-culture vs. HDMEC-monoculture, 21 genes with significant changes were observed. However, as the function of these genes is related with bone formation they are predominantly expressed in osteoblasts, which may be the reason for the high up-regulation in co-culture. Nevertheless, in co-culture there is a clear trend towards an increase of mRNAs related with ECM. On the other hand, when analysing co-culture vs. hOB-monoculture, only the up-regulation of collagen type I was observed. This 6.8 ± 2.6 fold up-regulation of collagen type I was reported for at least four different donors. Co-culture genetic profiling has also been explored by other authors. Finkenzeller et al [28] reported down-regulation of PDGFRα in osteoblasts upon co-cultivation on tissue culture plates, while spheroidal co-culture studies performed by Stahl el al [29] revealed an up-regulation of VEGFR2, alkaline phosphatase and downregulation of VEGF. Nevertheless, the co-culture systems were different in many aspects (for example, ECs derived from macro-/microvasculature, 2D/3D-cultures) and it is thus very difficult to compare such systems in a meaningful way, as multiple parameters vary.

The observation of a very high up-regulation of IGF-2 in the co-cultures was also worthy of deeper investigation, as this growth factor is highly relevant for both osteoblast differentiated function and the process of angiogenesis. This growth factor known to be produced by both ECs and osteoblasts exerts mitogenic effects on osteoblasts and it also has pro-angiogenic activity by mediating the induction of VEGF

[30-32]. Despite the up-regulation of the mRNA that codes for IGF-2, at the protein level the quantification of IGF-2 by ELISA in the supernatant of co-culture and mono-cultures revealed no results. Whether the IGF-2 mRNA is not being translated at all or whether the translated protein is unstable are questions that remain to be elucidated. Nevertheless, this dual function in both osteoblast proliferation and differentiation as well as angiogenesis makes IGF-2 a potentially useful growth factor for bone tissue engineering and regeneration and thus this subject will further studied.

Immunohistochemical studies revealed that spaces formed between the fibers of the micromesh scaffold were filled with a tissue-like dense network of collagen type I and this was consistent with the results of the molecular analysis. Thus, the co-culture of HDMECs with hOBs on SPCL fiber-mesh scaffold triggered collagen type I mRNA and protein synthesis. Collagen type I is a marker for bone formation and accomplishes different functions from mediating cell adhesion to contributing to the mature osteoblast phenotype as well as providing a template for mineralization [33-35]. Extracellular matrix-associated genes such as type I collagen are expressed during the proliferative period, whereas in heavily mineralized mature cultures (after 35 days) collagen mRNA level is present at low levels [36]. Hence, since after 21 days of co-culture high levels of mRNA collagen type I are still observed, most probably hOBs are still in the proliferative period. Moreover, mRNA coding for markers characteristic of other phases of bone cell differentiation such as osteonectin in ECM maturation and osteocalcin in mineralization are not being produced by hOBs at significant levels, otherwise their expression would be up-regulated on co-cultivation with ECs. Another aspect further supporting this proliferative phase hypothesis is the absence of a mineralized matrix as assessed by Von Kossa staining (data not shown). Collagen type I is known to drive EC migration by chemotaxis and haptotaxis [37]. The deposition of a very extensive network of collagen type I by hOBs in the scaffold creates an additional 3D support for ECs to migrate into and to organize into microcapillary-like structures. We believe that type I collagen is a key factor for successful neovascularization in this co-culture system insofar as it provides ECs with the chemical and physical cues for migration and proliferation.

Another major issue in co-culture is the heterotypic intercellular crosstalk. Independent of the co-culture system used, it appears that communication between ECs and osteoblast cells occurs via diffusible factors as well as direct cell-cell contact [8, 9, 28]. For indirect cell communication, VEGF was the soluble factor examined in this study since VEGF is a powerful pro-angiogenic factor with well established actions on ECs and it may have a direct effect on osteoblast functions [38, 39]. The results obtained for co-culture on SPCL fiber-mesh scaffolds were consistent with other reports as osteoblasts were the predominant source of VEGF [40] and osteoblasts in co-culture released higher amounts of VEGF [8]. Furthermore, the release profile of VEGF with culture time revealed that the highest concentration peak of VEGF in co-culture coincided with the first observations of microcapillary-like structures. Recent studies [40] shed some light on the mechanisms responsible for controlling VEGF-dependent OB:EC crosstalk. These studies suggest a paracrine mechanism in which VEGF-stimulated ECs release prostaglandins that strongly promote the VEGF release in osteoblasts.

For direct cell-cell contact the gap junction Cx43 was assessed in this co-culture system, due to its relevance in bone formation. Intercellular cross-talk between HDMECs and hOBs mediated by Cx43 occurred when cells were co-cultured on SPCL fiber-mesh scaffolds. The expression of this gap junction protein was depicted at the interface of hOBs with microcapillary-like structures formed by neighboring HDMECs. Previous work [8] has proven that direct cell-cell contact is necessary for the formation of microcapillary-like structures by HDMECs and that these structures are not seen in cultures with conditioned medium or co-cultures with indirect contact, that is separated by a porous synthetic membrane. Moreover, direct cell-cell contact is a critical aspect of co-culture as the the production of growth factors or gene expression are dependent on such contact [9, 29]. Cx43 expression was also observed between hOBs. This is not surprising since it is well described in the literature that Cx43 is the major gap junction present in osteoblasts and it is known to modulate the expression of genes pivotal to bone matrix formation and calcification, such as bone sialoprotein and osteocalcin [41, 42]. It is evident that further studies are necessary to investigate the time-related course of VEGF receptor

expression in the EC, as well as much more detailed investigation of connexin expression in osteoblast-endothelial interactions.

5. CONCLUSIONS

The co-cultivation of HDMEC with hOBs on SPCL fiber-mesh scaffolds proved to be an effective strategy for the *in vitro* formation of microcapillary-like structures containing a lumen and SPCL revealed to be an adequate 3D support for this type of co-culture. Furthermore, the expression of type IV collagen and the evolution from cord-like configuration to a branched morphology confirmed the vascular nature and the complexity of the established microcapillary-like structures. Regarding the underlying mechanisms, the up-regulation of mRNA collagen type I in co-culture and the deposition of a dense ECM led us to postulate that by providing chemical and physical cues for migrating ECs collagen type I is a key molecule and modulator in this system. Moreover, the VEGF produced by co-cultured hOBs and the expression of the gap junction Cx43 between the two cell types, indicated that heterotypic communication, a crucial aspect for co-culture orchestration, was assured. Therefore, this strategy is defined as self-sustainable insofar as on SPCL fiber-mesh scaffolds HDMECs and hOBs recreate the physical and chemical microenvironment favourable for the formation of vascular-like structures, thus obviating the need for an exogenous supply of pro-angiogenic stimuli.

REFERENCES

1. Klenke FM, Liu Y, Yuan H, Hunziker EB, Siebenrock KA, Hofstetter W. Impact of pore size on the vascularization and osseointegration of ceramic bone substitutes in vivo. J Biomed Mater Res A. 2007.

2. Koike N, Fukumura D, Gralla O, Au P, Schechner JS, Jain RK. Tissue engineering: creation of long-lasting blood vessels. Nature. 2004; 428(6979):138-9.

3. Beilmann M, Birk G, Lenter MC. Human primary co-culture angiogenesis assay reveals additive stimulation and different angiogenic properties of VEGF and HGF. Cytokine. 2004; 26(4):178-85.

4. Villars F, Bordenave L, Bareille R, Amedee J. Effect of human endothelial cells on human bone marrow stromal cell phenotype: role of VEGF? J Cell Biochem. 2000; 79(4):672-85.

5. Brandi ML, Collin-Osdoby P. Vascular biology and the skeleton. J Bone Miner Res. 2006; 21(2):183-92.

6. Deckers MML, van Bezooijen RL, van der Horst G, Hoogendam J, van der Bent C, Papapoulos SE, et al. Bone Morphogenetic Proteins Stimulate Angiogenesis through Osteoblast-Derived Vascular Endothelial Growth Factor A. Endocrinology. 2002; 143(4):1545-53.

7. Villars F, Guillotin B, Amedee T, Dutoya S, Bordenave L, Bareille R, et al. Effect of HUVEC on human osteoprogenitor cell differentiation needs heterotypic gap junction communication. Am J Physiol Cell Physiol. 2002; 282(4):C775-85.

8. Unger RE, Sartoris A, Peters K, Motta A, Migliaresi C, Kunkel M, et al. Tissue-like self-assembly in cocultures of endothelial cells and osteoblasts and the formation of microcapillary-like structures on three-dimensional porous biomaterials. Biomaterials. 2007; 28(27):3965-76.

9. Wenger A, Stahl A, Weber H, Finkenzeller G, Augustin HG, Stark GB, et al. Modulation of in vitro angiogenesis in a three-dimensional spheroidal coculture model for bone tissue engineering. Tissue Eng. 2004; 10(9-10):1536-47.

10. Choong CS, Hutmacher DW, Triffitt JT. Co-culture of Bone Marrow Fibroblasts and Endothelial Cells on Modified Polycaprolactone Substrates for Enhanced Potentials in Bone Tissue Engineering. Tissue Eng. 2006.

11. Rouwkema J, De Boer J, Van Blitterswijk CA. Endothelial cells assemble into a 3-dimensional prevascular network in a bone tissue engineering construct. Tissue Engineering. 2006; 12(9):2685-93.

12. Fuchs S, Hofmann A, James Kirkpatrick C. Microvessel-Like Structures from Outgrowth Endothelial Cells from Human Peripheral Blood in 2-Dimensional and 3-Dimensional Co-Cultures with Osteoblastic Lineage Cells. Tissue Eng. 2007.

13. Pavlov MP, Mano JF, Neves NM, Reis RL. Fibers and 3D mesh scaffolds from biodegradable starch-based blends: production and characterization. Macromol Biosci. 2004; 4(8):776-84.

14. Santos MI, Fuchs S, Gomes ME, Unger RE, Reis RL, Kirkpatrick CJ. Response of micro- and macrovascular endothelial cells to starch-based fiber meshes for bone tissue engineering. Biomaterials. 2007; 28(2):240-8.

15. Santos MI, Tuzlakoglu K, Fuchs S, Gomes ME, Peters K, Unger RE, et al. Endothelial cell colonization and angiogenic potential of combined nano- and micro-fibrous scaffolds for bone tissue engineering. Biomaterials. 2008.

16. Gomes ME, Sikavitsas VI, Behravesh E, Reis RL, Mikos AG. Effect of flow perfusion on the osteogenic differentiation of bone marrow stromal cells cultured on starch-based three-dimensional scaffolds. J Biomed Mater Res. 2003; 67A(1):87-95.

17. Gomes ME, Holtorf HL, Reis RL, Mikos AG. Influence of the porosity of starch-based fiber mesh scaffolds on the proliferation and osteogenic differentiation of bone marrow stromal cells cultured in a flow perfusion bioreactor. Tissue Eng. 2006; 12(4):801-9.

18. Gomes ME, Bossano CM, Johnston CM, Reis RL, Mikos AG. In vitro localization of bone growth factors in constructs of biodegradable scaffolds seeded with marrow stromal cells and cultured in a flow perfusion bioreactor. Tissue Eng. 2006; 12(1):177-88.

19. Tuzlakoglu K, Bolgen N, Salgado AJ, Gomes ME, Piskin E, Reis RL. Nano- and micro-fiber combined scaffolds: a new architecture for bone tissue engineering. J Mater Sci Mater Med. 2005; 16(12):1099-104.

20. Gomes ME, Azevedo HS, Moreira AR, Ella V, Kellomaki M, Reis RL. Starch-poly(epsilon-caprolactone) and starch-poly(lactic acid) fibre-mesh scaffolds for bone tissue engineering applications: structure, mechanical properties and degradation behaviour. J Tissue Eng Regen Med. 2008; 2(5):243-52.

21. Peters K, Schmidt H, Unger RE, Otto M, Kamp G, Kirkpatrick CJ. Software-supported image quantification of angiogenesis in an in vitro culture system: application to studies of biocompatibility. Biomaterials. 2002; 23(16):3413-9.

22. Annaz B, Hing KA, Kayser M, Buckland T, Di Silvio L. An ultrastructural study of cellular response to variation in porosity in phase-pure hydroxyapatite. J Microsc. 2004; 216(Pt 2):97-109.

23. Santos M.I. PI, Alves C.M, Gomes M.E., Fuchs S, Unger R.E, Reis R.L., Kirkpatrick C.J. . Surface-Modified 3D Starch-based Scaffold for Improved Endothelialization for Bone Tissue Engineering. Journal of Materials Chemistry. 2008; Submitted.

24. Simon AM, McWhorter AR. Vascular abnormalities in mice lacking the endothelial gap junction proteins connexin37 and connexin40. Dev Biol. 2002; 251(2):206-20.

25. Gerritsen ME, Soriano R, Yang SY, Zlot C, Ingle G, Toy K, et al. Branching out: A molecular fingerprint of endothelial differentiation into tube-like structures generated by affymetrix oligonucleotide arrays. Microcirculation. 2003; 10(1):63-81.

26. Bayless KJ, Salazar R, Davis GE. RGD-dependent vacuolation and lumen formation observed during endothelial cell morphogenesis in three-dimensional fibrin matrices involves the alpha(v)beta(3) and alpha(5)beta(1) integrins. Am J Pathol. 2000; 156(5):1673-83.

27. Kuhn K. Basement membrane (type IV) collagen. Matrix Biol. 1995; 14(6):439-45.

28. Finkenzeller G, Arabatzis G, Geyer M, Wenger A, Bannasch H, Stark GB. Gene expression profiling reveals platelet-derived growth factor receptor alpha as a target of cell contact-dependent gene regulation in an endothelial cell-osteoblast co-culture model. Tissue Eng. 2006; 12(10):2889-903.

29. Stahl A, Wenger A, Weber H, Stark GB, Augustin HG, Finkenzeller G. Bi-directional cell contact-dependent regulation of gene expression between endothelial cells and osteoblasts in a three-dimensional spheroidal coculture model. Biochem Bioph Res Co. 2004; 322(2):684-92.

30. Minuto F, Palermo C, Arvigo M, Barreca AM. The IGF system and bone. J Endocrinol Invest. 2005; 28(8 Suppl):8-10.

31. Andrew JG, Hoyland J, Freemont AJ, Marsh D. Insulinlike growth factor gene expression in human fracture callus. Calcif Tissue Int. 1993; 53(2):97-102.

32. Chao W, D'Amore PA. IGF2: epigenetic regulation and role in development and disease. Cytokine Growth Factor Rev. 2008; 19(2):111-20.

33. Watts NB. Clinical utility of biochemical markers of bone remodeling. Clin Chem. 1999; 45(8 Pt 2):1359-68.

34. Pham QP, Kurtis Kasper F, Scott Baggett L, Raphael RM, Jansen JA, Mikos AG. The influence of an in vitro generated bone-like extracellular matrix on osteoblastic gene expression of marrow stromal cells. Biomaterials. 2008.

35. Lynch MP, Stein JL, Stein GS, Lian JB. The influence of type I collagen on the development and maintenance of the osteoblast phenotype in primary and passaged rat calvarial osteoblasts: modification of expression of genes supporting cell growth, adhesion, and extracellular matrix mineralization. Exp Cell Res. 1995; 216(1):35-45.

36. Lian JB, Stein GS. Concepts of Osteoblast Growth and Differentiation - Basis for Modulation of Bone Cell-Development and Tissue Formation. Critical Reviews in Oral Biology & Medicine. 1992; 3(3):269-305.

37. Davis GE, Senger DR. Endothelial extracellular matrix: biosynthesis, remodeling, and functions during vascular morphogenesis and neovessel stabilization. Circ Res. 2005; 97(11):1093-107.

38. Li G, Cui YX, McIlmurray L, Allen WE, Wang HL. RhBMP-2, rhVEGF(165), rhPTN and thrombin-related peptide, TP508 induce chemotaxis of human osteoblasts and microvascular-endothelial cells. Journal of Orthopaedic Research. 2005; 23(3):680-5.

39. Roy H, Bhardwaj S, Yla-Herttuala S. Biology of vascular endothelial growth factors. Febs Letters. 2006; 580(12):2879-87.

40. Clarkin CE, Emery RJ, Pitsillides AA, Wheeler-Jones CP. Evaluation of VEGF-mediated signaling in primary human cells reveals a paracrine action for VEGF in osteoblast-mediated crosstalk to endothelial cells. J Cell Physiol. 2008; 214(2):537-44.

41. Lecanda F, Towler DA, Ziambaras K, Cheng SL, Koval M, Steinberg TH, et al. Gap junctional communication modulates gene expression in osteoblastic cells. Mol Biol Cell. 1998; 9(8):2249-58.

42. Lecanda F, Warlow PM, Sheikh S, Furlan F, Steinberg TH, Civitelli R. Connexin43 deficiency causes delayed ossification, craniofacial abnormalities, and osteoblast dysfunction. J Cell Biol. 2000; 151(4):931-44.

CHAPTER VIII

CONCLUSIONS

CHAPTER VIII

CONCLUSIONS

The main aim of this thesis was to address structural and cellular aspects that allow the design of vascularization strategies for 3D starch-based scaffolds. The first part of the work was devoted to the study of the interactions of endothelial cells (ECs) with fiber-mesh scaffolds made from a blend of starch with poly(ε-caprolactone) (SPCL) and to the development of surface and architectural upgrades of this scaffold towards the improvement of ECs adhesion and functionality. In the second part it was explored the existent communication between ECs and osteoblasts through the establishment of co-culture systems for the in vitro formation of vascular structures on SPCL fiber-mesh scaffolds.

Considering the void that existed on ECs compatibility of SPCL fiber-mesh scaffolds, chapter III addressed this subject and evaluated in which extent the scaffolding material affected ECs behaviour. Both human umbilical vein endothelial cells (HUVEC) and the human endothelial cell line HPMEC.ST1.6R used as a model of macro- and microvascular ECs (respectively) were able to adhere and proliferate on SPCL fiber-mesh scaffolds for the tested period. ECs growing on the scaffolding material exhibited the typical flattened morphology and the expression of the main endothelial markers platelet/endothelial cells adhesion molecule-1 (PECAM-1) and von Willebrand factor (vWF) was confirmed by immunofluorescence. Nevertheless, adhesion was only accomplished by means of pre-coating SPCL fiber-mesh scaffolds with the adhesive protein fibronectin, a treatment that is common to ECs cultures.
Beyond their key role in angiogenesis, ECs also participate in inflammation through the expression of cell adhesion molecules that recruit circulating leukocytes. Upon stimulation with the pro-inflammatory stimulus lipopolysaccharide, ECs on SPCL fiber-

mesh scaffolds retained the ability to up-regulate the expression of the cell adhesion molecules E-selectin, intercellular cell adhesion molecule-1 (ICAM-1) and vascular cell adhesion molecule-1 (VCAM-1). This is doubly important because not only the scaffolding material does not induce the inflammatory profile on adhered ECs but also when stimulated the cells are capable of inducing an adequate response.

Despite these results that point out to a positive interaction between ECs and SPCL fiber-mesh scaffolds, the fact is that ECs adhesion was dependent on coating with adhesive proteins. Hence, in chapter IV the surface of SPCL fiber-mesh scaffolds was modified by means of argon (Ar) plasma treatment in order to tailor it towards ECs adhesion and obviate the use of protein pre-coating. Plasma modified SPCL fiber-mesh scaffolds could successfully sustain HUVECs adhesion, proliferation, viability and the expression of the intercellular junction protein PECAM-1, similarly to what observed for scaffolds pre-coated with fibronectin. This outcome of plasma modified surface that it is not typical for other biodegradable type of substrates resulted from the interplay between surface properties and adsorbed proteins. The detailed characterization of the physical and chemical properties of the modified surface revealed an increased surface roughness, change in topography and higher oxygen content. Consequently, these properties modulated protein adsorption as indicated by the different adsorption profile of vitronectin and finally the adsorbed proteins controlled ECs cell behaviour.

Once identified the surface favourable to ECs biology, the next piece of work dealt with architectural upgrades of SPCL fiber-mesh scaffolds inspired in extracellular matrix (ECM). Chapter V focused on ECs interactions with nano/micro fiber-combined scaffold, a scaffolding material that integrates a nano-network mimicking the physical structure of ECM. One of the proposed strategies to accelerate vascularization consisted in seeding the scaffold with ECs and involves subsequent migration and interaction with host ECs. Due to the critical role of ECM in cell migration during angiogenesis it was hypothesized that the nano-network could provide the physical structure to elicit and guide ECs distribution. It was observed that the presence of nano-fibers allowed ECs to span in the bulk structure of the

scaffold without compromising the porosity and interconnectivity of the structure. ECs on nano-fibers exhibited a peculiar elongated morphology but retained the communication between neighbouring cells, as well as an inflammatory profile similar with control (scaffolds without nano-fibers). Of special attention is the fact that when exposed to an *in vitro* angiogenic environment ECs on the combined structure were able to migrate from the scaffolding material into the collagen gel and to organize into capillary-like structures. This very promising angiogenic potential of nano/micro fiber-combined scaffold was probably the result of the combined action of increased surface area, the ECM-like structure and the elongated cell morphology.

In chapter VI it was developed and tested collagen-nano and SPCL-micro fiber-combined scaffold, a structure inspired not only in the physical structure but also on the biochemical composition of ECM. This combined structure incorporates a type I collagen nano-network obtained by electrospinning and a fiber-mesh structure produced by wet-spinning. It was assessed the cellular response of the osteoblast-like cell line SaOs-2 and of HUVECs, and for SaOs-2 cells the inclusion of a type I collagen nano-network induced a stretched morphology and improved the metabolic activity. On the other hand, for HUVECs, besides inducing an elongated morphology this structure provided adhesive support, thus obviating the need of coating with an adhesive protein. Additionally, of special remark was the 3D arrangement of HUVECs on nano-network into circular structures that resemble microcapillary-like organization, a different configuration from that observed for osteoblast-like cells. Furthermore, it was successfully proven the concept of layer-by-layer, a methodology used to produce thicker structures.

After gathering valuable information regarding the interaction of ECs with 3D starch based scaffolds, chapter VII addressed a complex cellular strategy aimed for the *in vitro* formation of pre-vascular structures on the scaffolding material. This approach explored the heterotypic cross-talk existent between ECs and osteoblasts and consisted in the simultaneous culture of these two cell types on SPCL fiber-mesh scaffolds. The co-culture system of human dermal microvascular endothelial cells

(HDMEC) and primary human osteoblasts (hOBs) was successfully established on SPCL fiber-mesh scaffold and after 21 days of culture it was observed the formation of microcapillary-like structures. The complexity of these vascular structures positively-stained for PECAM-1 was patent in the branched morphology, in the existence of lumen and in the perivascular region stained for type IV collagen. Probably one of the key molecules in this system was type I collagen. Deposited by hOBs as a dense matrix, type I collagen provided the physical and chemical cues for migrating ECs. Furthermore, molecular data further supported this finding once in the genetic profile of 84 genes osteogenesis-related type I collagen was the only gene with a significant up-regulation in co-culture relatively to monoculture. Nevertheless, other mechanisms such as direct and indirect communication between ECs and hOBs might also being orchestrating the co-culture system. This hypothesis was corroborated by the higher production of VEGF in co-culture and by the cell-cell contact established by means of gap junction connexin 43.

In summary, the work described in this thesis is intended to generate the foundations and the knowledge that will support the development of more complex strategies that can actually lead to establishment of a functional vascular supply on bone tissue engineered constructs. Thus, it is expected that each individual piece of evidence generated in this thesis can be used as the building block for the construction of new 3D-scaffolds able to mimic the complexity and functionality of a vascularised bone tissue. Furthermore, it is envisioned that the established co-culture systems can be the starting point for the development of tri-culture systems encompassing a third element such as mural cells, to promote the formation of long-lasting blood-vessels.